U.S. DEPARTMENT OF COMMERCE
National Technical Information Service
PB80-142003

Surface and Subsurface Water Quality Hydrology in Surface Mined Watersheds
Part I: Text

Colorado State Univ, Fort Collins

Prepared for

Industrial Environmental Research Lab -Cincinnati, OH

Aug 79

PB80-142003

United States
Environmental Protection
Agency

Industrial Environmental Research
Laboratory
Cincinnati OH 45268

EPA-600/7-79-193a
August 1979

Research and Development

EPA

Surface and Subsurface Water Quality Hydrology in Surface Mined Watersheds

Part I: Text

Interagency Energy/Environment R&D Program Report

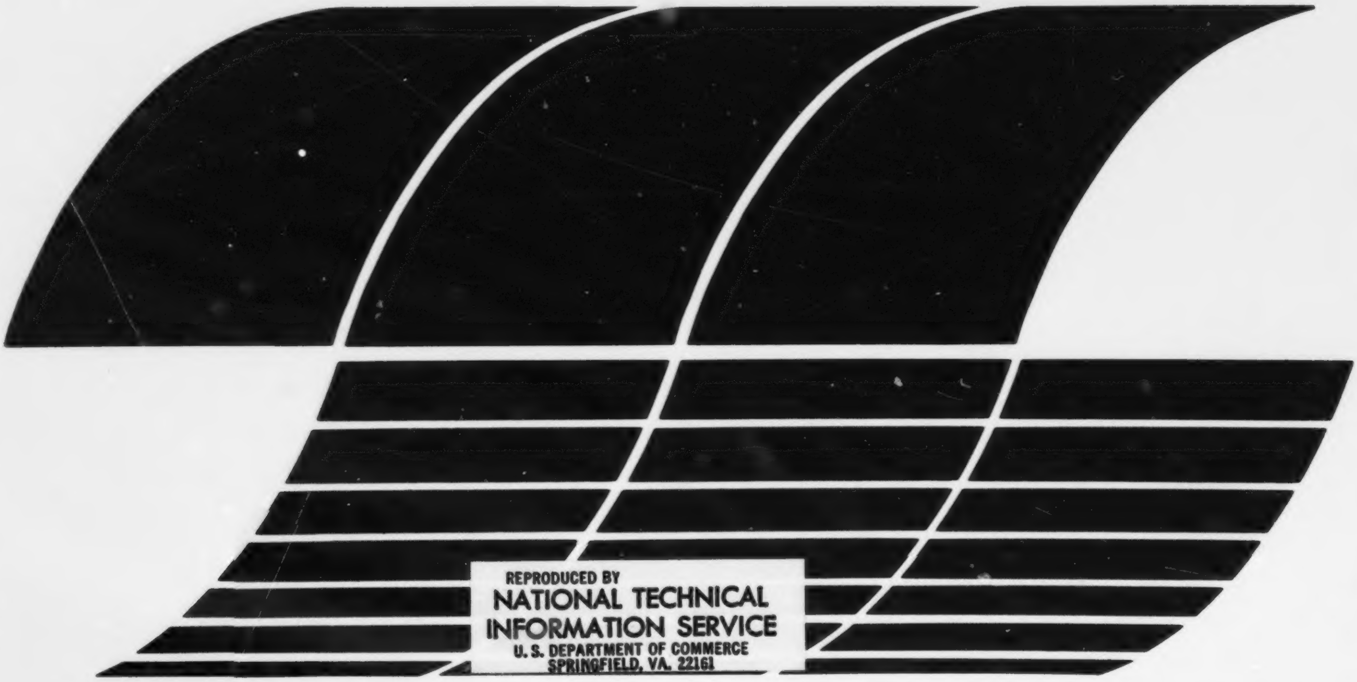

REPRODUCED BY
NATIONAL TECHNICAL
INFORMATION SERVICE
U. S. DEPARTMENT OF COMMERCE
SPRINGFIELD, VA. 22161

RESEARCH REPORTING SERIES

Research reports of the Office of Research and Development, U.S. Environmental Protection Agency, have been grouped into nine series. These nine broad categories were established to facilitate further development and application of environmental technology. Elimination of traditional grouping was consciously planned to foster technology transfer and a maximum interface in related fields. The nine series are:

1. Environmental Health Effects Research
2. Environmental Protection Technology
3. Ecological Research
4. Environmental Monitoring
5. Socioeconomic Environmental Studies
6. Scientific and Technical Assessment Reports (STAR)
7. Interagency Energy-Environment Research and Development
8. "Special" Reports
9. Miscellaneous Reports

This report has been assigned to the INTERAGENCY ENERGY-ENVIRONMENT RESEARCH AND DEVELOPMENT series. Reports in this series result from the effort funded under the 17-agency Federal Energy/Environment Research and Development Program. These studies relate to EPA's mission to protect the public health and welfare from adverse effects of pollutants associated with energy systems. The goal of the Program is to assure the rapid development of domestic energy supplies in an environmentally-compatible manner by providing the necessary environmental data and control technology. Investigations include analyses of the transport of energy-related pollutants and their health and ecological effects; assessments of, and development of, control technologies for energy systems; and integrated assessments of a wide range of energy-related environmental issues.

This document is available to the public through the National Technical Information Service, Springfield, Virginia 22161.

EPA-600/7-79-193a
August 1979

SURFACE AND SUBSURFACE WATER QUALITY HYDROLOGY IN SURFACE MINED WATERSHEDS
PART I. TEXT

by

D. B. McWhorter, J. W. Rowe, M. W. Van Liew,
R. L. Chandler, R. K. Skogerboe, D. K. Sunada, G. V. Skogerboe
Agricultural Engineering and Chemistry Departments
Colorado State University
Fort Collins, Colorado 80523

Grant No. R803175

Project Officer

Eugene Harris
Extraction Technology Branch
Industrial Environmental Research Laboratory
Cincinnati, Ohio 45268

INDUSTRIAL ENVIRONMENTAL RESEARCH LABORATORY
OFFICE OF RESEARCH AND DEVELOPMENT
U.S. ENVIRONMENTAL PROTECTION AGENCY
CINCINNATI, OHIO 45268

1a

DISCLAIMER

This report has been reviewed by the Industrial Environmental Research Laboratory-Cincinnati, U.S. Environmental Protection Agency, and approved for publication. Approval does not signify that the contents necessarily reflect the views and policies of the U.S. Environmental Protection Agency, nor does mention of trade names or commercial products constitute endorsement or recommendation for use.

FOREWORD

When energy and material resources are extracted, processed, converted, and used, the related pollutional impacts on our environment and even on our health often require that new and increasingly more efficient pollution control methods be used. The Industrial Environmental Research Laboratory-Cincinnati (IERL-Ci) assists in developing and demonstrating new and improved methodologies that will meet these needs both efficiently and economically.

This report contains the observations and conclusions from an intensive field and mathematical study of the inorganic water quality hydrology on surface mined watersheds. A portion of the material constitutes a step toward the development of practical procedures whereby the effect of surface mining in the Western United States upon the water quality hydrology can be assessed. The field data provide a background for study and comparison by other workers as well as establishing a quantitative case history for a western mine. Thus, many of the methods, results, and conclusions should be useful to industrial, State, and Federal personnel charged with the preparation and review of analyses of the effect of surface mining upon water quality hydrology. Data and computer requirements limit the routine usability of some components of the models developed in this study, but they should be found useful to other researchers concerned with organizing, assessing, and generalizing the great amount of site specific data that is rapidly being developed. Further information can be obtained from the Extraction Technology Branch.

David G. Stephan
Director
Industrial Environmental Research Laboratory
Cincinnati

ABSTRACT

Surface mining disturbs the natural sequence of geologic strata and, therefore, potentially modifies the quantity and quality of watershed drainage. The quantity and quality of water on a watershed disturbed by surface mining were monitored in Colorado. In addition, surface runoff, subsurface drainage, and sediment production were studied on a plot scale in the field. The most significant effect of mining on water quality was an increase in dissolved solids. Water and dissolved solids balance equations were used to derive a simple algebraic equation relating the annual average dissolved solids pickup rate to the dissolved solids content of overland flow runoff, the dissolved solids content of subsurface runoff, the distribution of total runoff, and the mined fraction of the watershed. The equation was used to analyze hydrologic observations and to estimate the contribution of the mined area to the total salt load.

The effect of surface mining on water quality and flow patterns in aquifers were estimated. Simple analytic calculations suggest that maximum effect can be estimated without knowledge of hydraulic parameters of aquifers or of disturbed portions. A detailed finite difference model is presented that can be used to refine estimates of post-mining flow patterns and water quality in disrupted aquifers when data warrant such refinement.

A model for the flow and chemical composition of soil solution in the zone between spoil surface and water table is presented. Predicted and measured dissolved solids concentrations in subsurface drainage agreed excellently; measured and calculated infiltration into the spoil also agreed well. The rate of subsurface drainage as computed for a shallow water table is extremely sensitive to hydraulic properties of the spoil. A hydraulic gradient of unity can be used when the water table is well below the surface and the calculated subsurface flow rate is much less sensitive to the spoil hydraulic properties.

A model for calculation of spoil sediment production is presented. Poor agreement between measured and calculated instantaneous rates of sediment production was obtained, particularly with respect to bed load. There was satisfactory agreement between calculated and measured total bed load sediment and between calculated and measured total wash load sediment.

This report was submitted in fulfillment of Grant No. R803175 by Colorado State University under the sponsorship of the U. S. Environmental Protection Agency. This report covers a period from May, 1974 through December, 1976 and work was completed as of January 31, 1977.

CONTENTS

Foreword iii

Abstract iv

Figures ix

Tables xii

Symbols xiv

Acknowledgment xx

1. Introduction 1
2. Conclusions 4
3. Recommendations 9
4. Watershed Studies 10
   - Physical profile 10
   - Method and procedure 20
   - Water quality and its relationship to spoil characteristics 32
   - Analysis of factors contributing to salt load 62
5. Some Limiting Effects of Aquifer Disruption 77
   - Steady flow patterns in disrupted aquifers 77
   - Water quality in disrupted aquifers 82
6. Experimental Studies 85
   - Materials and methods 85
   - Water quality and quantity 112
   - Hydraulic properties of the spoil 123
7. Sediment Modeling 130
   - Background description of soil erosion processes . . 130
   - Water routing model for overland flow 133
   - Sediment routing for overland flow 137
   - Model verification and application 144
   - Spoil erodibility 153

8. Water Quality Modeling 159
    Flow in partially saturated zone 159
    Flow in the saturated zone 162
    Inorganic chemistry model 165
    Chemical transport calculations 171
9. Results of Water Quality Modeling 174
    Flow in the partially saturated zone 174
    Predicted chemistry of drainage waters 180
    Example calculation for saturated zone 182
    Summary comments on water quality monitoring 184
References 186
Bibliography 191
Part II. Appendices (EPA-600/7-79-193b)

FIGURES

Number		Page
1	Location of the Edna Mine	11
2	Geologic map of Edna Mine and surrounding area	13
3	Stratigraphic column of exposed strata found in parts of northwestern Colorado	14
4	Individual watersheds on the Edna Mine and discharge monitoring stations	17
5	Schematic east-west cross-section near Station C6	19
6	Location of water quality monitoring stations	22
7	Supplementary water sample locations	24
8	Stage-discharge rating curves for Trout Creek at Station C2	26
9	Stage-discharge rating curves for Trout Creek at Station C6	27
10	Location of soil and spoil samples taken in May, 1976 . .	29
11	Factors for adjusting specific conductance of water . . .	30
12	Ionic composition of water in January, 1975	37
13	Ionic composition of water in May, 1975	38
14	Ionic composition of water in September, 1975	39
15	Average concentrations of major ions in water from stations shown	41
16	Sources of dissolved solids in the hydrologic system of a mined watershed	45
17	Discharge and water quality hydrograph for Station C2, 1975	46
18	Discharge and water quality hydrograph for Station C6, 1975	46
19	Discharge and water quality hydrograph for Station C3, 1975	48
20	Discharge and water quality hydrograph for Station C9, 1975	48
21	Discharge and water quality hydrograph for Station C10, 1975	49
22	Results of leaching test with aeration of sample to produce weathering	52

23 Plot of specific conductance versus total dissolved solids for water at the Edna Mine with line of best fit 54
24 Average monthly dissolved solids concentrations for Stations C2 and C6 on Trout Creek 60
25 Comparison of actual and estimated average monthly dissolved solids concentrations 61
26 Plot of R versus P_t with best fit curve found for K=1.04, f_s=0.06 69
27 Linear regression line 72
28 Plot of R versus P_t for various values of K and f_s 75
29 Coordinate system and geometry used to calculate the pattern of flow in a disturbed aquifer 78
30a Flow pattern in a disrupted aquifer, K_i/K_o = 0.5 81
30b Flow pattern in a disrupted aquifer, K_i/K_o = 5 81
31 Field plot layout at the Colorado site 87
32 Diagram of experimental test plot 89
33 Photograph of a lysimeter installation at the Colorado site 90
34 Photograph of a lysimeter before backfilling - Montana site 90
35 Calibration curve for the neutron-moisture-meter 93
36 Rainfall sprinkler riser design 96
37 Sprinkler design layout for test plots 97
38 Runoff and sediment discharge for run 6 99
39 Time-dependent wash load erosion rate for experiments on 1 and 3 percent bed slopes 101
40 Time-dependent wash load erosion rate for experiments on 5 and 7 percent bed slopes 102
41 Definition sketch for concave, uniform, and convex shapes on the 7 percent bed slope 106
42 Runoff and sediment discharge for run 14 107
43 Runoff and sediment discharge for run 15 107
44 Runoff and sediment discharge for run 16 108
45 Runoff and sediment discharge for run 17 108
46 Runoff and sediment discharge for run 18 109
47 Runoff and sediment discharge for run 19 109

48 Time-dependent wash load erosion rate for experiments with simulated rainfall on 1 and 7 percent bed slopes 111

49 Size distribution for composite samples of wash load and bed-material load sediments 113

50 Cumulative drainout for run 2 116

51 Drain discharge for run 2 117

52 Correlation of EC of drainage with EC of spoils 119

53 Apparatus for measuring the relationship between soil moisture content and suction 125

54 Desaturation curve for spoil from the Colorado site . . . 126

55 A constant head permeameter 128

56 Flow chart for water and sediment routing model 143

57 Comparison of simulated and measured sediment discharges for run 15 152

58 Comparison of simulated and measured sediment discharges for run 18 152

59 Comparison of measured and simulated bed-material sediment yields 154

60 Comparison of measured and simulated wash load sediment yields 155

61 Volumes of subsurface drainage 178

62 Comparison of calculated and measured dissolved-solids concentrations 181

63 Plan and cross-section views of confined aquifer disturbed by mining 183

64 Induced flow streamlines 360 days after beginning of flow. 184

TABLES

Number		Page
1	Watershed Areas	18
2	Description of Water Quality and Discharge Monitoring Stations	21
3	Average Ion Concentrations of Monthly Water Samples Taken October 1973 to November 1975	33
4	Maximum Ion Concentrations of Monthly Water Samples Taken October 1973 to November 1975	34
5	Heavy Metals Standards and Number of Times Exceeded at Stations C3, C5, and C7	36
6	Comparison of Electrical Conductivity of Spoil, Overburden, and Subsurface Water	42
7	Comparison of Common Ion Contents in Extracts and Mine Drainage	43
8	Monthly Discharge Volumes, Salt Loads and Average Dissolved Solids Concentrations	57
9	Total Yearly Runoff (Centimeters)	58
10	Summary of Data Used in Application of Model to Study Area	70
11	Comparison of Measured and Calculated Concentrations of Dissolved Solids in Watershed Drainage	71
12	Effect of Mining on Salt Pickup Between C2 and C6 in 1975.	73
13	Effect of Increasing Overland Flow From 6 to 40 Percent on the Disturbed Ground at the Edna Mine	74
14	Summary of Overland Flow Runoff Experiments Conducted During 1975	98
15	Summary of Sediment Discharge Data Collected From Overland Flow Runoff Experiments	104
16	Summary of Simulated Rainfall Experiments Conducted During 1976	104

17 Summary of Sediment Discharge Data Collected From Simulated Rainfall Experiments 112
18 Water Balance for Experimental Plots - Colorado Site . . . 115
19 Spoil Chemistry as Measured in 1:1 Extracts - Plot With 1% Slope - Colorado Site 115
20 Quality of Applied Water - Plot 1% Slope - Colorado Site . 118
21 Quality of Surface Runoff From Plot With 1% Slope - Colorado Site 119
22 Quality of Subsurface Drainage From Plot With 1% Slope - Colorado Site 120
23 Spoil Chemistry as Measured in Saturation Extracts - Montana Site 121
24 Quality of Applied Water - Montana Site 122
25 Quality of Surface Water - Montana Site 122
26 Quality of Subsurface Drainage - Montana Site 123
27 Input Data Required for the Simulation Model 145
28 Summary of Experimental Plot Dimensions and Percentages of Bed-Material Load Size Sediment at the Edna Mine Field Site 145
29 Summary of Regression Results for Sediment Transport Equations 149
30 Summary of Experimental Field Data Collected Under Simulated Rainfall and Computed Terms in the Universal Soil Loss Equation 157
31 Initial Moisture Distribution and Water Application Schedule 175
32 Comparison of Flow Model With Experimental Data 176
33 Measured and Calculated Composition of Drainage Waters . . 182

SYMBOLS

Symbol	Definition	Unit
SECTION A		
A_m	Area of watershed disturbed by mining	L^2
A_n	Area of watershed undisturbed by mining	L^2
A_t	Total area of watershed	L^2
EC	Electrical conductivity	µmohs/cm
ET	Evapotranspiration	L^3/L^2
f_{dm}	Fraction of precipitation lost through deep percolation on mined land	
f_{dn}	Fraction of precipitation lost through deep percolation on natural land	
f_{em}	Fraction of precipitation lost through evapotranspiration on mined land	
f_{en}	Fraction of precipitation lost through evapotranspiration on natural land	
F_m	Fraction of watershed mined	
f_s	Fraction of combined runoff from entire watershed occurring as overland flow	
f_{sm}	Fraction of combined runoff from mined portion of watershed occurring as overland flow	
f_{sn}	Fraction of combined runoff from natural portion of watershed occurring as overland flow	
I	Inflow between Stations C2 and C6	L^3/T
K	Model parameter	
K'	Model parameter including deep percolation	
m	Subscript indicating mean value	
P	TDS concentration	
P_{gm}	Average TDS concentration of subsurface water on mined land	mg/ℓ
P_{gn}	Average TDS concentration of subsurface water on natural land	mg/ℓ

P_m	Average TDS concentration of waters on mined land	mg/ℓ
P_n	Average TDS concentration of waters on natural land	mg/ℓ
P_s	Average TDS concentration of surface waters	mg/ℓ
P_{sm}	Average TDS concentration of surface water on mined land	mg/ℓ
P_{sn}	Average TDS concentration of surface water on natural land	mg/ℓ
P_t	Average TDS concentration of combined runoff from the total watershed	mg/ℓ
q	Volume of water per unit surface area	L^3/L^2
Q_2	Discharge at Station C2	L^3/T
Q_3	Discharge at Station C3	L^3/T
Q_6	Discharge at Station C6	L^3/T
Q_9	Discharge at Station C9	L^3/T
Q_{10}	Discharge at Station C10	L^3/T
q_{em}	Volume of evapotranspiration on mined land per unit surface area	L^3/L^2
q_{en}	Volume of evapotranspiration on natural land per unit surface area	L^3/L^2
q_{gm}	Volume of subsurface water on mined land per unit surface area	L^3/L^2
q_{gn}	Volume of subsurface water on natural land per unit surface area	L^3/L^2
q_m	Volume of water on mined land per unit surface area	L^3/L^2
q_n	Volume of water on natural land per unit surface area	L^3/L^2
q_p	Volume of precipitation on watershed per unit surface area	L^3/L^2
q_{pm}	Volume of precipitation on mined land per unit surface area	L^3/L^2
q_{pn}	Volume of precipitation on natural land per unit surface area	L^3/L^2
q_{sm}	Volume of overland flow on mined land per unit surface area	L^3/L^2
q_{sn}	Volume of overland flow on natural land per unit surface area	L^3/L^2
Q_t	Total discharge	L^3/T
q_t	Volume of water on total watershed per unit surface area	L^3/L^2
R	Model parameter, ratio of natural land to mined land	
r^2	Coefficient of determination	
S	Stage reading	L
ΔS	Change in storage volume within the watershed	L^3

t	Time	T
TDS	Total dissolved solids	mg/ℓ
V_d	Volume of deep percolation	L^3
V_e	Volume of evapotranspiration	L^3
V_g	Volume of shallow subsurface water	L^3
V_p	Volume of precipitation	L^3
V_s	Volume of overland flow	L^3
V_t	Volume of total runoff	L^3
σ	Standard deviation	

SECTION B

a	Thickness of bed layer	L
a_3	Coefficient in raindrop soil detachment equation	
b_3	Exponent in raindrop soil detachment equation	
C	Sediment concentration by volume	
C_a	Known concentration by volume	
C_w	Concentration of wash load	
C_ξ	Sediment concentration at a distance ξ from bed	
C^p_b	Potential bed-material load concentration	
C^p_w	Potential wash load concentration	
D_b	Amount of detached bed material	L
D_f	Detachment coefficient of runoff	
D_i	Potential rate of soil detachment	L/T
D_p	Maximum depth to which a raindrop can penetrate soil layer	L
d	Depth of flow	L
d_s	Mean size of sediment	L
F_b	Percent of bed-material size in a typical soil sample	
F_w	Percent of wash load size in a typical soil sample	
f	Darcy-Weisbach friction factor	
f_i	Infiltration rate	L/T
f_o	Darcy-Weisbach friction factor without rainfall	
g_b	Bed-material load transport rate	L^3/T
g_c	Sediment transporting capacity	L^3/T
g_s	Total sediment transport rate	L^3/T
g_w	Wash load transport rate	L^3/T

g	Gravitational acceleration	L/T^2
i_r	Rainfall rate	L/T
J_1, J_2	Integrals to evaluate total suspended load	
K_o	Constant representing grain resistance without rainfall for $N_R < 900$	
K_r	Number describing added friction resulting from rainfall	
K_1	Parameter describing grain resistance with rainfall for $N_R < 900$	
L	Length of an overland flow plot	L
N_r	Flow Reynolds number	
q	Water discharge per unit width	L^2/T
q_b	Bed-load transport rate per unit width	L^2/T
q_ℓ	Lateral inflow per unit length of overland flow unit	L^2/T
S_f	Friction slope	
S_o	Bedslope	
t	Time	T
U_*	Shear velocity of flow	L/T
μ_ξ	Point mean velocity at the distance ξ from bed	L/T
V	Mean velocity of water flow	L/T
V_s	Settling velocity of sediment particle	L/T
W	Width of overland flow unit	L
ω	Parameter of sediment suspension	
x	Distance downslope	L
z_m	Equivalent maximum penetrating depth of raindrop impact	L
z	Net depth of loose soil	L
z_b	Depth of loose soil for bed-material load size	L
z_w	Depth of loose soil for wash load size	L
α	Coefficient in d vs. q relation	
β	Exponent in d vs. q relation	
γ	Specific weight of water	F/L^3
γ_s	Specific weight of sediment	F/L^3
ρ	Density of water	M/L^3
Δt	Time increment in computations	T
Δx	Space increment in computations	L
Δz	Mean elevation change	L

Δz^p_b	Potential change in loose soil storage for bed-material size sediment	L
Δz^p_w	Potential change in loose soil storage for wash load size sediment	L
ν	Kinematic viscosity of water	L^2/T
ξ	Depth above the bed	L
τ_o	Boundary shear stress acting on the grain	F/L^2
$(\cdot)^n_j$	Quantity of variable at grid point $x=j\Delta x$ and $t=n\Delta t$	

SECTION C

a	Domain of saturation associated with concave portion of soil-water characteristic	
b	Domain of saturation associated with convex portion of soil-water characteristic	
CR	Relative concentration of ions	
$D(\theta)$	Soil-water diffusivity	L^2/T
g	Acceleration due to gravity	L/T^2
H	Water table elevation or piezometric head	L
h_i	Piezometric head inside disturbed portion of aquifer	L
h_o	Piezometric head outside disturbed portion of aquifer	L
i	Finite difference index	
K_D	Dissociation constant	
K_i	Saturated hydraulic conductivity inside disturbed portion of aquifer	L/T
K_o	Saturated hydraulic conductivity outside disturbed portion of aquifer	L/T
$K(\theta)$	Hydraulic conductivity as function of water content	L/T
K_s	Saturated hydraulic conductivity	L/T
K_{sp}	Solubility product for chemical species	
m	Aquifer thickness	L
m	Shape factor used in Su and Brooks representation of soil-water characteristic	
P_c	Capillary pressure	m/LT^2
P_i	Inflection capillary pressure	m/LT^2
q	Solution flux	L/T
Q	Discharge	L^3/T
R	Radius of disturbed portion	L
S	Sink term used to simulate evapotranspiration	

S	Storage coefficient	
S_{ya}	Apparent specific yield	
W	Width of zone of modified water quality	L
θ	Volumetric water content	L^3/L^3
θ_r	Water content at residual saturation	L^3/L^3
θ_s	Water content at saturation	L^3/L^3
λ	Pore-size distribution index	
ρ	Density of solution	m/L^3
ψ	Stream function	L^2/T
z	Depth	L

ACKNOWLEDGMENT

The field studies reported herein were carried out with the enthusiastic and vigorous cooperation of the Pittsburg and Midway Coal Mining Company, Peabody Coal Company, and Idarado Mining Company. These operators voluntarily contributed man power and equipment to the project on several occasions. Their assistance is greatly appreciated.

The excellent assistance of J. A. Brookman, P. Hammer, S. Brown, and D. Dick, Research Technicians, contributed greatly to the project. Ms. Diane English was responsible for essentially all of the typing and records for this project, and her performance in this capacity was excellent.

Finally, a great deal of expert advice and assistance were provided by Dr. Ruh Ming Li in regard to the sediment transport studies. Dr. Li's help is very much appreciated.

SECTION I

INTRODUCTION

Exploitation of the coal reserves in the United States has accelerated rapidly in recent years in response to dwindling supplies of liquid fossil fuels and the associated high cost of petroleum imports. Emphasis on the surface production of low-sulfur coals, much of which is located in the Western United States, has greatly increased. In the period from 1965 to 1973, production of coal by surface mining increased 302 percent in a region that includes Arizona, Colorado, Montana, North Dakota, New Mexico, and Wyoming (Skelly and Loy, 1975). According to Grim and Hill (1974) a total of 1.8 million hectares of land had been disturbed by surface mining in the United States as of January 1, 1974. Nearly 10 percent (128,000 ha) of this total was located in the above mentioned states. Caudill (1973) puts the total disturbed land somewhat higher at 2.4 million hectares, and indicates that disturbed land was increasing at the rate of 1880 hectares per week in 1973.

State and federal regulations and statutes require an environmental assessment for essentially all new mining projects and extensions of existing operations. The required environmental assessments range from individual site investigations to large scale, regional analyses. One aspect that must be considered in all of these assessments is the water-quality hydrology of the subject area, yet there is often a significant dearth of the data and methods appropriate for a rational, quantitative, cost-effective assessment. This is particularly true for relatively small projects that do not warrant years of data collection and analysis. Yet, in the aggregate, these same small projects and the decisions made concerning them ultimately determine the regional consequences.

At the outset, the purpose of the project from which this report was derived was to develop and verify a mathematical description of the water-quality hydrology affected by surface mining. This was to be accomplished by modifying and adapting several existing models for use in surface-mining assessment and by collecting the data from plot studies in Colorado and Montana appropriate for comparison with the model. We were also charged with monitoring a surface-mined watershed in Colorado with the intent of establishing, on a watershed scale, the magnitude of the impact of surface mining on the water-quality hydrology. This objective involved the identification of the contribution from the mined portion and from the undisturbed portion of the watershed as well as quantifying the contributions from surface and ground water runoff.

All of the above objectives were substantially accomplished. It became apparent, however, during the course of the research that the practicality of some of the model components would be limited for routine use by the combined constraints of cost, data, and technical know-how requirements. Further, it was realized that in pre-mining applications many of the required input parameters would, necessarily, be rough estimates and many of the advantages of the detailed model, relative to simpler models, would not be realized. Therefore, some of the time and finances of the project were directed toward the development of simpler, but hopefully more practical, methods of assessment.

The scope of the work reported herein is so wide that it seems unlikely that a single reader will be interested in all parts of the study. The text, therefore, has been organized by major components of the work in an attempt to provide sections that can be read with minimum reference to other sections. The first section of the text (Section 4) contains the description and results of the watershed monitoring program conducted in Colorado. A simple model, based on water and dissolved solids budgets, is presented in the last portions of Section 4 along with the model application to the field observations. Section 5 contains a theoretical analysis of the limiting effects on the flow pattern and water quality in an aquifer disrupted by surface mining. A description of the plot studies in Colorado and Montana with some typical results are presented in Section 6. The mathematical model for sediment transport and comparison with the results from the plot study are presented in Section 7. Finally, the models for water flow and quality in the partially saturated and saturated zones of the subsurface are presented in Section 8.

The project included a water-quality monitoring program in the vicinity of a mill tailings disposal area in southwestern Colorado in addition to the surface mining study described above. Because the mill tailings portion of the study is not in context with the bulk of this report, the water quality data and discussion for the mill tailings site are included as an appendix.

SECTION 2

CONCLUSIONS

Analyses for ten trace metals were made at selected locations at the Colorado study site. Only manganese and selenium exceeded the Public Health Service drinking water standards a significant number of times in mine drainage. Occurrences of high manganese concentrations were confined to a single sampling station. We presently have no explanation for the anomalous manganese concentrations at the one station. Trace metal concentrations in the receiving waters below the mine remained below drinking water standards.

The most significant change in water quality attributable to surface mining in the study area was an increase in total dissolved solids. The increase results from the disturbance and consequent exposure to contact by percolating waters of geologic strata that were relatively isolated from contact with water before mining.

The ions making the largest contribution to the dissolved solids content in both mine drainage and the receiving waters are calcium, sodium, magnesium, bicarbonate and sulfate. The composition of mine drainage and receiving waters is very similar.

Of the total common ion concentration in subsurface mine drainage, 60-70 percent is sulfate, 12-13 percent is calcium, 8-9 percent is magnesium, and 6-10 percent is bicarbonate. Sodium, potassium, and chloride, together, contribute 4-5 percent. Almost identical composition was obtained in one-to-one extracts prepared from the spoil material.

Comparisons of average electrical conductivity in mine drainage with that of saturation extracts prepared from spoil samples and drill cuttings suggest that the electrical conductivity in the saturation extracts is approximately equal to that of subsurface drainage. The electrical conductivity of saturation extracts can be used for making a first estimate to the quality of subsurface drainage, therefore. The standard deviation from the average was a large percentage of the average, however, suggesting the need for many samples of the spoil.

An apparently linear correlation between the electrical conductivity of subsurface drainage and the electrical conductivity of one-to-one extracts was developed for the four experimental plots at the Colorado site. This result suggests that the electrical conductivity (EC) of one-to-one extracts can be used to estimate the EC of drainage waters. The correlation is, undoubtedly, different for each type of spoil material and saturation percentage, however, and the EC of saturation extracts prepared from samples with a saturation percentage equal to that anticipated in the field is recommended as the best index to the EC of drainage waters. Correction of the EC of saturation extracts from samples with one saturation percentage to an anticipated EC at another saturation percentage by direct volumetric calculations can lead to significant errors.

Concentration of dissolved solids in subsurface drainage from a bank of mine spoils cannot be expected to decline for many decades. This is true because about one pore volume of water throughput must be achieved before the effects of leaching will become apparent in the concentration of salts in the mine drainage. In arid and semi-arid regions where deep percolation does not exceed a few centimeters per year, at most, a long time period is required before the effects of leaching will become noticeable.

The dissolved solids concentration in overland flow runoff is very small compared to that in subsurface runoff. This was noted in both the experimental plots and at various locations on the study area. Overland flow runoff contacts spoil in a very thin layer immediately at the surface of the spoil and this layer is rapidly leached.

The significance of the immediately preceding two conclusions is that, once the dissolved solids concentration in the subsurface drainage and overland flow is measured or estimated, it can be assumed, for practical purposes, that the concentrations will remain constant for a long time period. Therefore, dissolved solids loading of receiving waters can be estimated by modeling the hydrology or otherwise determining the quantities of overland flow and subsurface runoff and multiplying by the corresponding concentration.

The concentration of dissolved solids in receiving waters depends upon the relative discharges from overland flow on the disturbed land, overland flow on undisturbed land, ground water runoff from disturbed land, and groundwater runoff from undisturbed land, and the concentrations in each of these components. An algebraic model was formulated that accounts, approximately, for the above factors.

The model was applied to the watershed data collected at the Colorado site. The average difference between the calculated and measured concentrations of dissolved solids in watersheds partially disturbed by mining was 8.9 percent. The maximum difference was 21.8 percent.

The algebraic model was used to distinguish the contributions from ground water runoff and overland flow runoff. It was concluded that 94 percent of the total runoff from the mine spoils at the Colorado site is ground water runoff. Because the dissolved solids concentration is greater in the ground water runoff than in the overland flow, 99.7 percent of the total load of dissolved solids contributed by the disturbed ground is accounted for by ground water runoff.

The algebraic model was also used to estimate the effect of disturbing the ground at the Colorado site. During 1975, for example, 5.3 million kilograms of dissolved solids were added to the receiving waters from the portion of the watershed investigated. It is estimated that 2.9 million kilograms or 54 percent was contributed by the disturbed area. The disturbed area represented 17 percent of the total watershed area. The increase in salt load due to the disturbance of the geologic strata is estimated to be 2.4 million kilograms or 45 percent of the total observed salt loading.

The average rate of dissolved solids pickup on the disturbed ground at the Colorado site is estimated to be 286 kilograms per hectare per centimeter of combined overland flow and ground water runoff. According to the earlier conclusion that concentrations seem to remain constant for a long time period, this pickup rate should be a constant, independent of runoff volumes. It was, in fact, observed that the pickup rate varied between 283 and 308 kg/ha-cm during the three years of observation. During the same time period, the maximum observed annual runoff volume was nearly double the minimum observed. Therefore, the total salt load from the mined area for a given year can be estimated by multiplying the rate of pickup by the area and by the volume of total runoff in the year of interest.

The study at the Colorado site indicates that the algebraic model can be used to estimate the influence of surface mining on the dissolved solids content of receiving waters. Three chemical parameters are required; P_{mg}, P_{ms}, and P_n. The concentration of ground water runoff from the mined land, P_{mg}, can be estimated from the electrical conductivity of saturation extracts, or alternatively by application of the chemistry model presented. The concentration in overland flow from the mined land, P_{ms}, can be estimated by determining the concentration of dissolved solids in water passing through well leached samples of the spoil. P_n is the background concentration in combined overland flow and ground water runoff from undisturbed ground and can be estimated from pre-mining quality of the waters to be effected by mining.

Two hydrologic parameters are required: the fraction of total mine drainage that is overland flow runoff, f_{sm}, and the ratio of total drainage on the mined land to that on undisturbed ground, K. Methods by which f_{sm} and K can be estimated by indirect means are under development.

Analytic calculations of the flow patterns in aquifers that have been disrupted by mining suggest that the maximum distance to which the pre-mining flow pattern is permanently modified is independent of the hydraulic conductivity of the disrupted portion and of the undisturbed aquifer. Thus, it is possible to estimate the range of distances within which the pre-mining flow pattern will be modified without knowledge of the hydraulic conductivities. Simple equations are provided for this purpose.

Analytic calculations suggest that the maximum width of the zone in which the downstream water quality will be modified by disrupting the aquifer is twice the maximum dimension of the mined area. The maximum width occurs when the hydraulic conductivity of the disrupted portion is very large relative to that in the undisturbed portion. The analytic calculations suggest that the effect on water quality in an aquifer disrupted by mining is minimum when the hydraulic conductivity in the disrupted portion is minimum. In fact, if hydraulic conductivity in the disrupted portion is very small compared to that in the aquifer, there should be no appreciable effect on the water quality in the disrupted aquifer. For other cases, simple equations are provided from which estimates of the effect can be made.

A model for sediment transport in overland flow runoff is presented. Large differences between measured and calculated instantaneous rates of erosion existed; especially for the bed material discharge rates. The calculated total sediment production for each runoff event agreed satisfactorily with measured values, even when total sediment yield was separated into bed load and wash load components.

The erodibility factor in the Universal Soil Loss Equation was calculated from the experimental results. The calculated erodability factor for the Colorado site indicates a relatively low potential for erosion.

Model components for subsurface flow in the partially saturated zone, soil-water chemistry and transport of dissolved species are presented. These three components operate as a unit and are capable of predicting both the quantity and quality of deep percolating waters in mine spoils. Excellent agreement between the calculated and measured concentrations of dissolved solids was obtained. Excellent agreement between measured and calculated infiltration was also obtained. It was found that when the condition to be simulated is that of a water table near the surface, the calculated drainage rate is highly sensitive to the soil properties used to compute the diffusivity coefficient. When the water table is well below the surface (a likely condition in most mine spoil applications) a lower boundary condition of a unit gradient can be applied and the sensitivity of the calculated drainage rate to the diffusivity coefficient is circumvented. Thus, the partially saturated flow model is not recommended for use when the water is near the surface (say, within 2-3 meters) unless the hydraulic properties of the spoil are very accurately known.

A numerical model simulating either confined or unconfined flow in aquifers disrupted by mining is presented. Coupled with the model for flow in the saturated zone is a transport component in which it is assumed that dispersion is negligible and the dissolved species are conservative. The model will handle constant head, constant gradient, and impervious boundary conditions. The aquifer can also be nonhomogeneous with respect to hydraulic conductivity. Input of contaminants to the saturated flow region can be calculated from the output of the unsaturated flow chemistry model.

The flow, chemistry, and transport models presented provide a highly flexible library of tools for analyzing water quality and hydrology in surface mined regions. The major disadvantages are the large input data requirements, computer requirements, and the high degree of proficiency required of the user.

SECTION 3

RECOMMENDATIONS

The study reported herein was conducted on one specific site. The degree to which many of the results can be extrapolated to other sites has not been established and use of specific results in other situations should be done with caution. For example, it is recommended that the observation of a one-to-one correspondence between electrical conductivity of saturation extracts and subsurface drainage be used with caution at other sites. The correlation is not expected to hold in spoils with a significantly higher content of sodium salts than observed in this study. Other investigators have found the dissolved solids content of subsurface waters to be substantially greater than in saturation extracts.

It is recommended that consideration be given to grading of spoils located in high precipitation areas in a manner which tends to minimize the concentration of overland flow in closed depressions and potholes. Ponding of water in such depressions contributed to the unusually large subsurface runoff observed in this study. This recommendation is not inconsistent with the use of surface manipulation techniques which promote infiltration of precipitation in the immediate vicinity of where it falls. Rather, the concern is with closed depressions of a larger scale in which substantial runoff and ponding can occur.

It is further suggested that grading, topsoiling, and revegetation be accomplished to maximize consumptive use of water on the spoils. Maximizing the consumptive use of water will tend to minimize deep percolation and, therefore, salt transport to receiving waters.

SECTION 4

WATERSHED STUDIES

The material in this section constitutes a case history of the water-quality hydrology of a surface mined watershed. To the author's knowledge it is the first published study of its kind for a mine located in the western United States, and therefore, the study is presented in considerable detail. Water and dissolved solids budget equations were used to ascertain the contribution of the disturbed ground to the observed dissolved-solids load in the receiving waters. The contributions to the total increase of dissolved solids resulting from overland flow runoff and groundwater runoff are also estimated.

PHYSICAL PROFILE

Physiography and Geology

The Edna Mine is located on the southeast edge of the Twentymile Park structural basin, about 24 kilometers southwest of Steamboat Springs, Colorado (Figure 1). The topography varies from gently dipping slopes on the eastern flanks of the numerous synclines in the area to steep slopes in the western flanks. The area is drained by tributaries of Trout Creek which in turn flows into the Yampa River near Milner, Colorado. Elevations above mean sea level on the Edna Mine range from 2134 m to 2530 m. The Little Trout Creek watershed, just south of the mine, reaches elevations up to 2775 m and the main Trout Creek watershed ranges from 1980 m to over 3350 m.

As described by Campbell (1923), Twentymile Park consists of a large structural basin surrounded by ridges of considerable height. The Edna Mine is located on the east limb of the Argo Syncline which forms a subordinate basin to Twentymile Park. The Argo Syncline is typical of other synclines in the area being asymmetric with dips on the west limb much steeper than

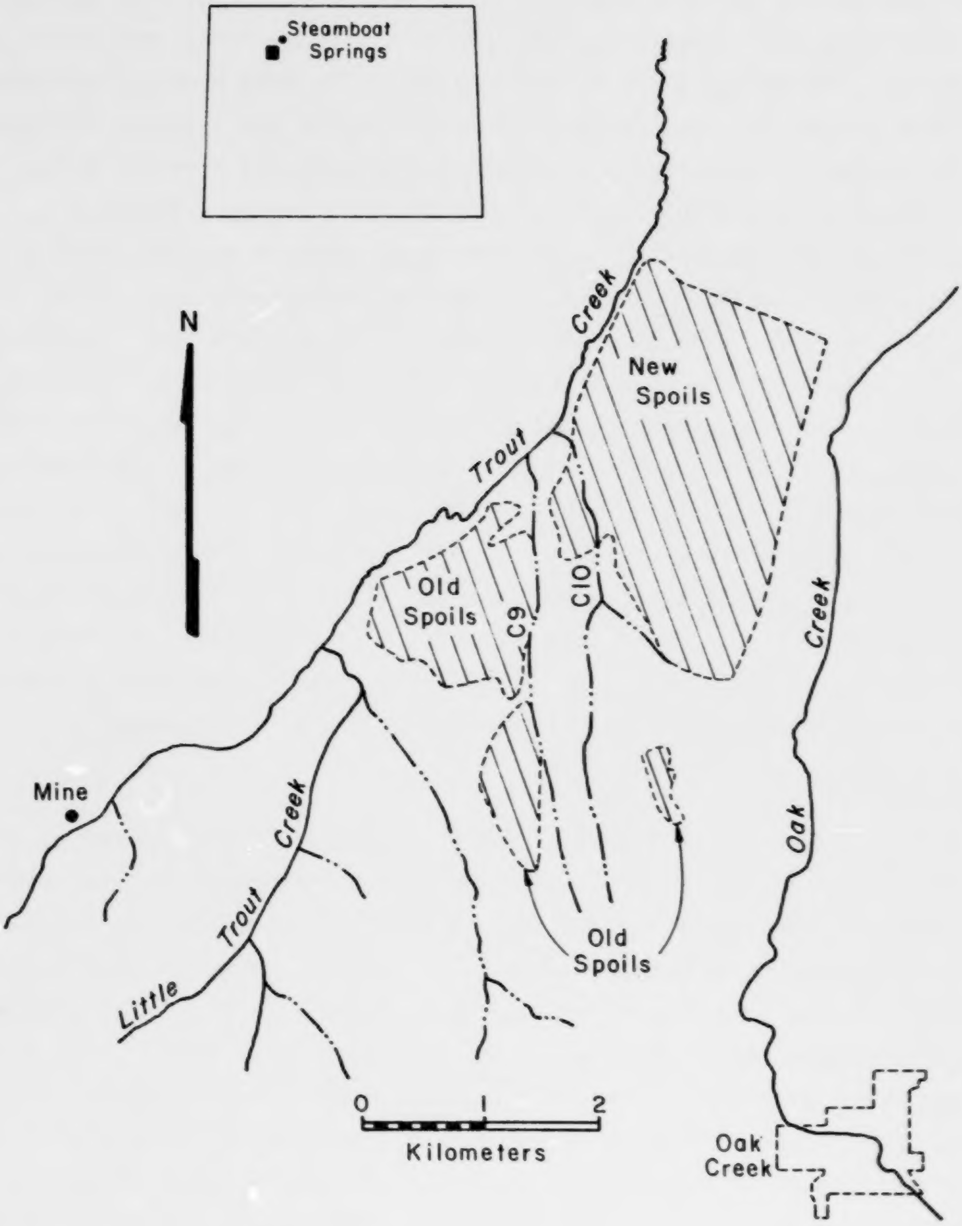
Steamboat
Springs
N
Trout
Creek
New
Spoils
Old
Spoils
C9
C10
Mine
Little
Trout
Creek
Old
Spoils
Oak
Creek
0
1
2
Kilometers
Oak
Creek

Figure 1. Location of the Edna Mine.

those on the east limb. Most rock strata on the Edna Mine are dipping at about ten degrees to the west towards Trout Creek.

Figure 2 is a geologic map and Figure 3 (from Plate 18, USGS Bulletin 1027-D) is a general stratigraphic column of the Upper Cretaceous rocks in the region. The Mancos Shale is not exposed on the Edna Mine but conformably underlies the younger Mesa Verde Group consisting of the Iles and Williams Fork formations. Present mining operations extract coal from the Wadge seam which is part of the Middle Coal group of the Williams Fors formation. In some parts of northwestern Colorado, the Lewis shale conformably overlies the Williams Fork formation. However, at the Edna Mine it has been eroded away along with the Twentymile sandstone member of the Williams Fork formation.

Bass et al. (1955) describe the Williams Fork formation as consisting of interbedded sandstone, sandy shale, and coal beds of marine brackish water and fresh water origin. Of the three bituminous coal beds in the Middle Coal group the Wadge is described as the most uniformly good in quality and workable thickness. Older surface mining operations during the 1940's extracted coal from the Lennox seam in the southern portion of the Edna Mine, but present operations are concentrated on the Wadge seam. The thickness of the Wadge ranges from about 1.5 m to 2.0 m over the mine. The Lennox seam is found 4.5 to 6.0 m above the Wadge and ranges from 0.3 to 1.0 m in thickness.

Mining Operations

Coal is extracted at the Edna Mine by a method of mining known as area or continuous surface mining. This method of mining is common in areas where the topography is fairly flat and the coal is found at relatively shallow depths. Area mining consists of digging a series of parallel cuts to expose and remove the coal. At the Edna Mine overburden is loosened with explosives and removed using a 26.8 cubic meter drag line. The exposed coal is then loaded in trucks and hauled out of the pit eventually to be transported by railroad. Cuts are made parallel to the strike of the slope and after one cut is completed the overburden removed in the next successive cut is deposited in the open trench of the previous cut. The resulting parallel spoil ridges are then graded to conform with the original slope configuration, approximately.

Mining operations are currently located in the northern section of the mine near the top of the ridge between Oak Creek and Trout Creek. The Wadge

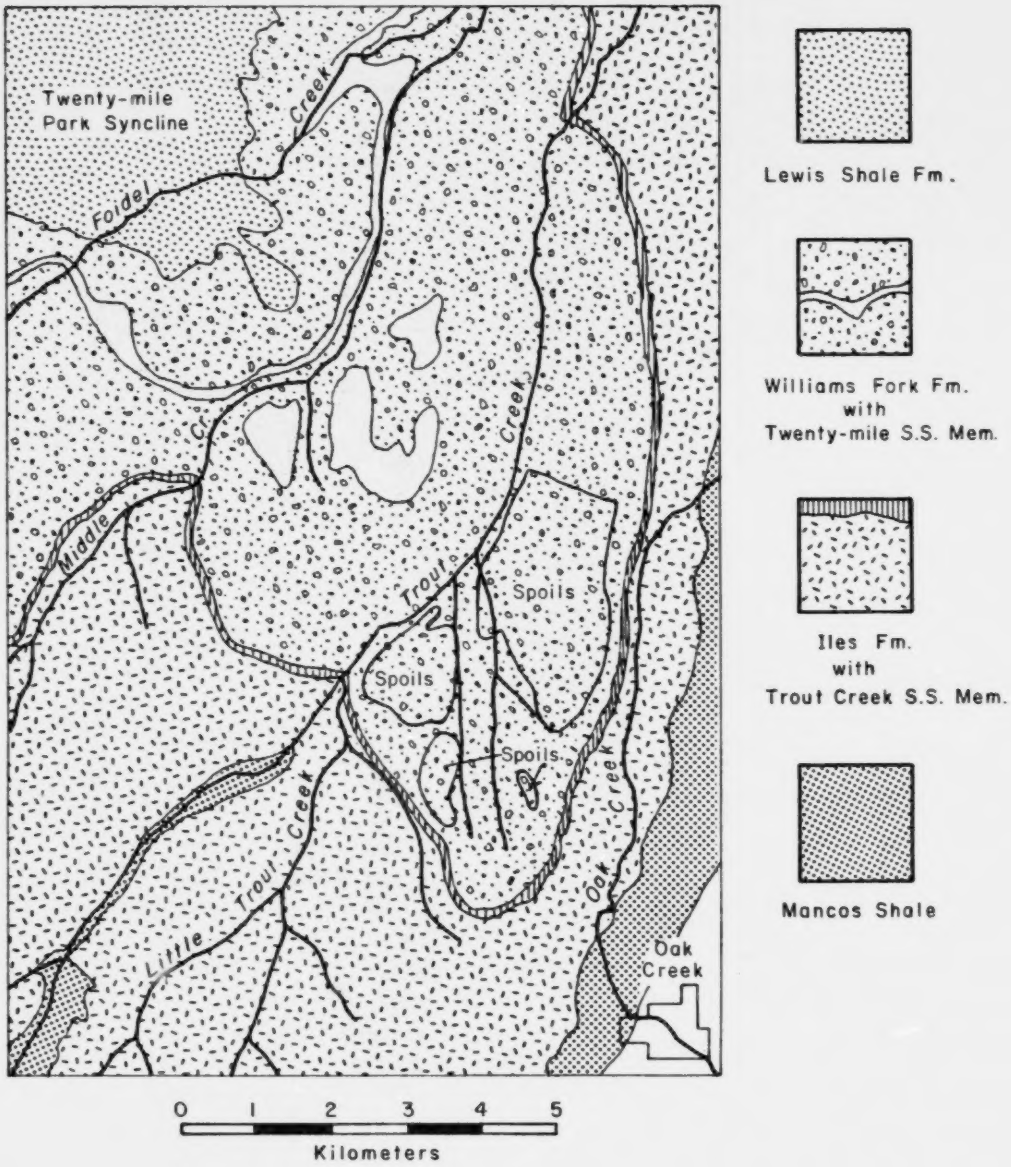
Twenty-mile Park Syncline
Foidel
Creek
Middle
Cr.
Trout
Creek
Spoils
Spoils
Spoils
Little
Trout
Creek
Oak
Creek
Oak Creek
Lewis Shale Fm.
Williams Fork Fm. with Twenty-mile S.S. Mem.
Iles Fm. with Trout Creek S.S. Mem.
Mancos Shale
0
1
2
3
4
5
Kilometers

Figure 2. Geologic map of the Edan Mine and surrounding area.

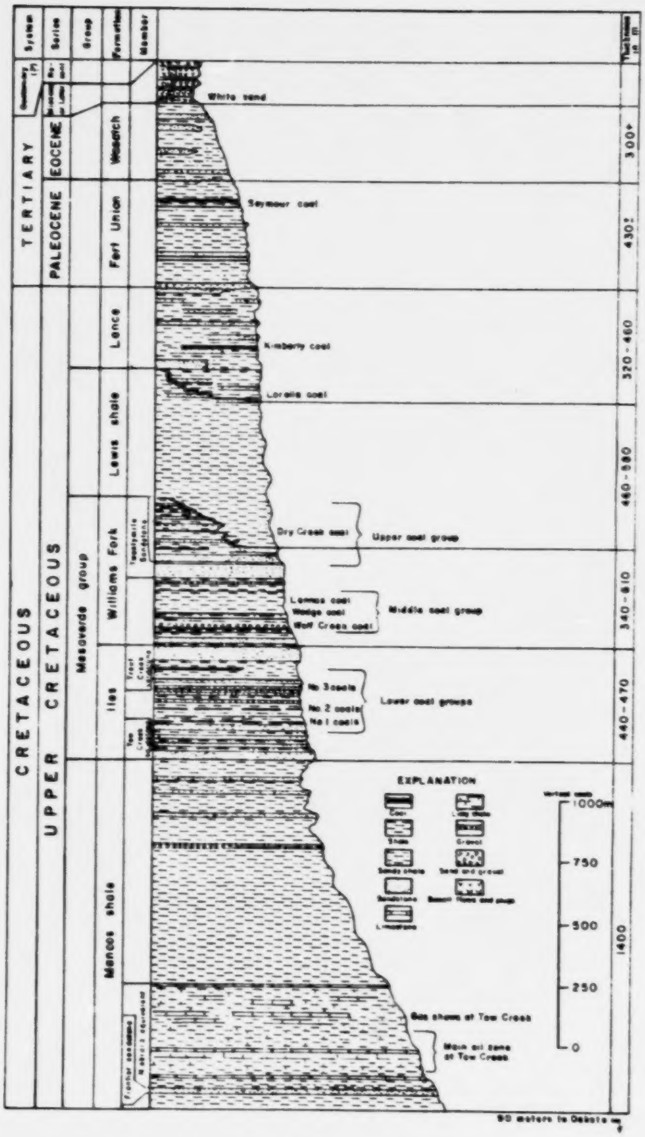
System
Series
Group
Formation
Member
Thickness in m
TERTIARY
EOCENE
PALEOCENE
CRETACEOUS
UPPER CRETACEOUS
Wasatch
Fort Union
Lance
Lewis shale
Williams Fork
Mesaverde group
Iles
Mancos shale
White sand
Seymour coal
Kimberly coal
Loralla coal
Dry Creek coal
Upper coal group
Lennox coal
Wedge coal
Wolf Creek coal
Middle coal group
No 3 coals
No 2 coals
No 1 coals
Lower coal groups
Gas shows at Tow Creek
Main oil zone
at Tow Creek
EXPLANATION
Coal
Shale
Sandy shale
Sandstone
Limestone
Gravel
Sand and gravel
Vertical scale
1000m
750
500
250
0
300+
430±
320-460
460-580
340-610
440-470
1400
90 meters to Dakota

Figure 3. Stratigraphic column of exposed strata found in parts of northwestern Colorado.

seam is found at 15 to 22 m below the ground surface in this area. The highwall and trench at the location of present operations are free from any water seepage indicating no water table existing at this depth and location.

Spoil piles in the older section of the mine south of current operations are not graded. Mining in this section was somewhat sporadic with pits opened and spoils piled to the sides. A map furnished by the Pittsburg and Midway Company which currently operates the Edna Mine indicates that the Wadge was mined only in some areas with the Lennox seam most extensively mined.

Climate

No climatic record is available for the Edna Mine or the immediate vicinity so estimates of precipitation and potential evaporation are taken from U. S. Geological Survey maps (Irons et al., 1965). Mean annual precipitation is estimated to be 51 cm with about one-half of this amount occurring as snow. The temperature measured at Steamboat Springs (elevation 2063 m) located 24 km northeast of the Edna Mine ranges from an average -9°C in January to 17°C in July with the mean annual temperature equal to 4.1°C. These temperatures are probably slightly lower than those at the Edna Mine due to Steamboat Springs closer proximity to high mountains. Snow melt on the mine occurs during April and May and in the upper reaches of Trout Creek during late May and June.

Vegetation and Soils

Natural vegetation on the Edna Mine consists of scrubbrush and grasses at the lower elevations with aspen groves at higher elevations. Older spoils in the southern area of the mine have been revegetated probably both naturally and by man and now support grasses and alfalfa. Portions of the newer spoils in the northern area of the mine have also been revegetated recently with grass and clover. The Little Trout Creek watershed is covered with coniferous and aspen forests over much of its area.

No detailed classification of soils was made; however, some soil samples were taken at various locations for chemical analysis. Soils on the mine with the exception of alluvial flood plain deposits along Trout Creek are residual being derived from the rocks of the Williams Fork formation. Soil over most of the natural land is thin and poorly developed with bedrock found in most places at depths of one meter or less. The soil is light brown to tan and contains a very clayey layer immediately above bedrock. Soil in areas with aspen groves is dark brown to black and may be up to five meters deep. The clay layer is again found near bedrock at locations sampled in the aspen groves.

The spoils have virtually no soil profile but instead are made up of weathered rock debris ranging from boulders more than a meter in diameter down to clay size particles. The spoil material exists down to the maximum depth of excavation and is underlain by undisturbed strata.

Hydrology

Trout Creek, flowing northward along the base at the spoil piles, is the major surface drainage. The Trout Creek watershed above and including the Edna Mine is approximately 110 km^2 in area. The mean annual discharge of Trout Creek measured just downstream of the mine is estimated at $2.8 x 10^7 m^3/yr$ (McWhorter et al., 1975) or an equivalent of about 26 cm of water per year over the entire watershed. Trout Creek has eroded a shallow canyon in parts of its reach along the west side of the mine as evidenced by vertical outcrops of Williams Fork rock. Within these confines Trout Creek meanders across an alluvial aquifer of unknown depth.

The Edna Mine is divided into individual watersheds which contribute to discharge monitoring stations C3, C5, C9, and C10 as shown in Figure 4. The watershed contributing to station C13 is also considered but is not shown in Figure 4. The watershed boundaries are determined on the basis of surface water divides from topographic maps. These boundaries should also approximate the ground water divides on the Edna Mine. Table 1 indicates the mined and undisturbed land areas of each watershed. Inflow refers to the entire watershed area contributing water to Trout Creek between stations C2 and C6.

The surface water divides on undisturbed land are easily found by topographic highs between streams. However, on land disturbed by mining such divides are difficult to define and, in fact, may no longer exist. The spoil piles, both graded and ungraded, have very poor surface drainage patterns. This causes rainfall and snow melt in some areas to pond in depressions and infiltrate into the spoils with little or no overland flow. Northern portions of the mine probably had very little surface drainage even before mining. Present stream channels on the natural land north of the spoils carry water

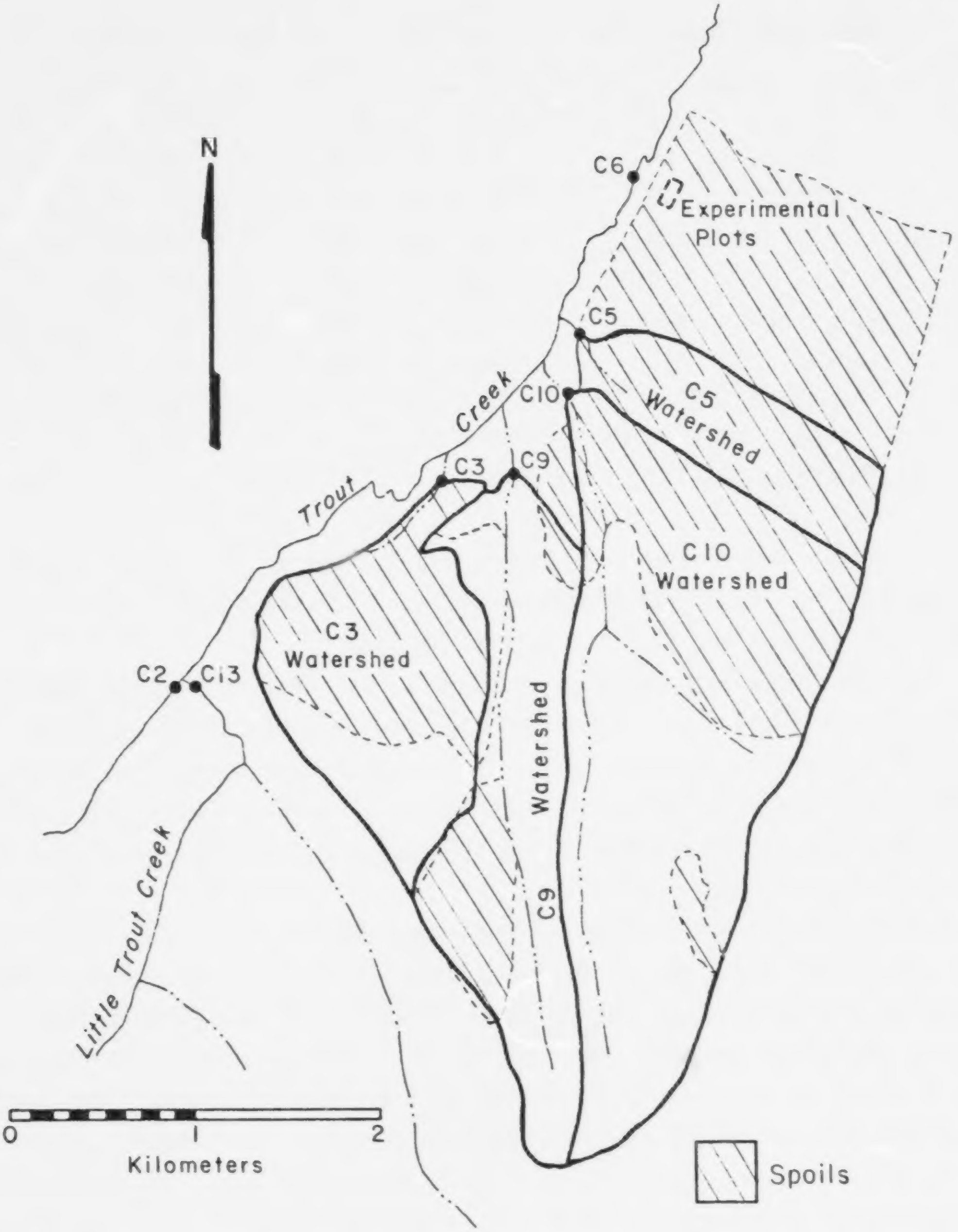
N
C6
Experimental Plots
C5
C10
C5 Watershed
Trout Creek
C3
C9
C10 Watershed
C3 Watershed
C2
C13
C9 Watershed
Little Trout Creek
0
1
2
Kilometers
Spoils

Figure 4. Individual watersheds on the Edna Mine and discharge monitoring stations.

TABLE 1. WATERSHED AREAS

Watershed	Area mined (ha)	Area unmined (ha)	Total (ha)	Fraction mined
C3	116	55	171	0.68
C5	94	0	94	1.00
C9	72	132	204	0.35
C10	188	242	431	0.44
C13	0	2110	2110	0.00
Edna Mine*	689	503	1192	0.58
Inflow†	614	3042	3556	0.17

*Includes area north of Station C6.

†Includes total area between stations C2 and C6.

only during periods of very high runoff due to rain or snow melt. Streams in the southern section of the mine exhibit better drainage patterns in their undisturbed reaches and flow for most of the year.

Because of low precipitation and poor surface drainage on the spoils, much of the rainfall and snow melt on the Edna Mine is lost by evapotranspiration or infiltrates into the ground. On natural land precolating water encounters relatively impermeable rock strata at shallow depths. The water then flows down dip to reappear in the stream channels on the mine site or to seep directly into Trout Creek.

Surface mining has significantly changed the natural surface and subsurface hydrologic conditions of the mined land. Figure 5 is a schematic east-west cross-section through the northern region of the mine near station C6 showing conditions existing after mining. As water percolates into the spoils it encounters no rock strata at shallow depths but continues to flow vertically until reaching a water table or rock strata forming the lower boundary of the spoils. Thus, the depth to which water percolates has been altered by mining from several meters or less to over fifteen meters. This significantly increases the potential for water to dissolve salts as it passes through the spoils.

As water flows down the dip of the rock strata beneath the spoils it encounters a highwall of undisturbed rock which parallels much of the east

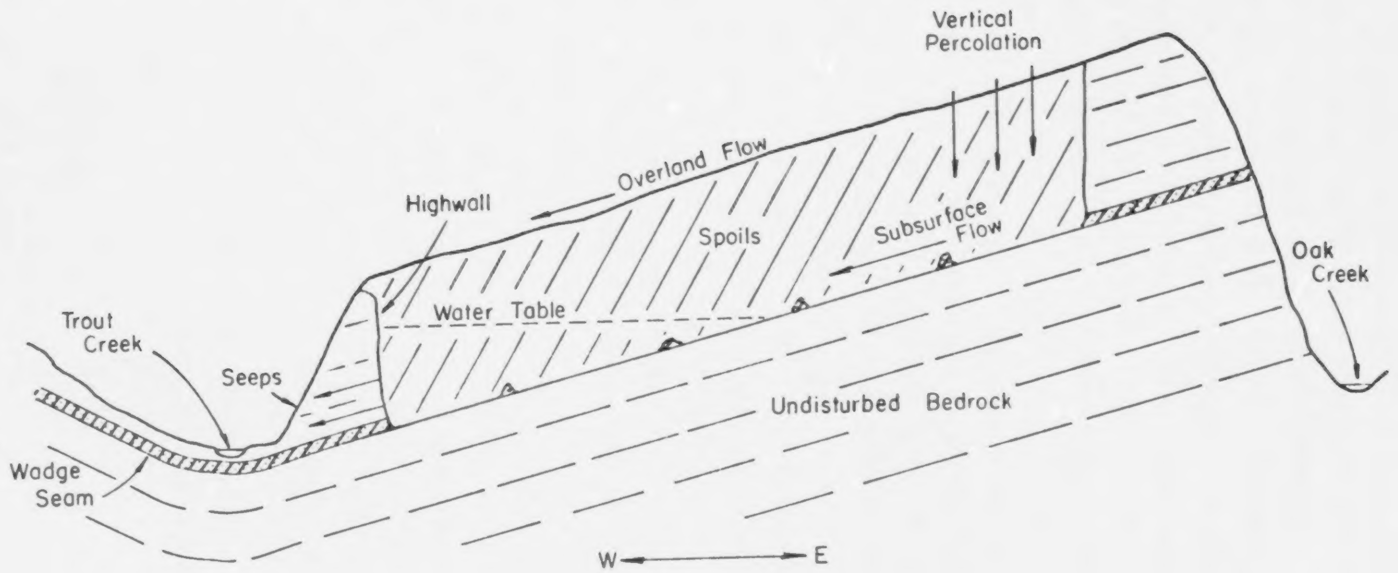
Vertical
Percolation
Overland Flow
Highwall
Spoils
Subsurface
Flow
Oak
Creek
Water Table
Trout
Creek
Seeps
Undisturbed Bedrock
Wadge
Seam
W
E

Figure 5. Schematic east-west cross-section near station C6.

side of Trout Creek. This highwall is visible in the C3 watershed because a trench was left between it and the spoil piles. Water can be seen flowing from the base of the spoils and into this trench which forms a small pond behind station C3. It is assumed that most of the subsurface water from the C5, C9, and C10 watersheds reappears in the stream before flowing from the mine area. There is probably some subsurface water flowing out of these watersheds in the alluvial aquifers occurring below the stream channels. The volume of this underflow is probably small because of the shallow depth to bedrock and the narrow width of the stream valleys. The exact quantity of underflow is not known.

The spoil banks north of the C5 watershed apparently have no natural break in the highwall which is well hidden by the overlying spoils. Numerous subsurface seeps appear in the spring at the base of the spoils along Trout Creek. These are the result of water flowing over the buried highwall or through it along fractures or permeable layers. It is probable that an aquifer forms behind the highwall which supplies water to seeps until mid-summer.

No data is available concerning deep ground water aquifers in the region. The rocks of the Williams Fork and Iles Formations seldom exhibit good aquifer characteristics. Groundwater is most commonly associated with coal beds due to their highly fractured nature (Bureau of Land Management, 1975). For the purpose of this study the base of the spoils is assumed to be the maximum depth reached by percolating water.

Several small drainages enter Trout Creek from the west side between station C2 and station C6. However, their contribution to total inflow is small. Several irrigated fields located on the west side of Trout Creek adjacent to the mine contribute some return flow to Trout Creek. Thick vegetation along several exposed outcrops indicates some ground water seepage. The amount of water entering into Trout Creek from the west side was not monitored but, because of the small land area involved, its contribution to the inflow and salt load should also be small.

METHOD AND PROCEDURES

Water Quality Monitoring

Thirteen water quality monitoring stations were established on and near the Edna Mine with six stations located on Trout Creek, one on Little Trout Creek, five on the Edna Mine watersheds, and one on a natural watershed north of the mine. Figure 6 indicates the location and designation of these stations. Table 2 summarizes the location, installation date, and type of data obtained at each monitoring station.

TABLE 2. DESCRIPTION OF WATER QUALITY AND DISCHARGE MONITORING STATIONS

Station Number	Type Quality	Type Discharge	Date Started	Description
C1	X		Oct, 1973	On Trout Creek above all mining activity
C2	X	X	Oct, 1973	On Trout Creek above Edna Mine
C3	X	X	Oct, 1973	On mine drainage in older spoils
C4	X		Oct, 1973	On Trout Creek adjacent to spoils
C5	X	X	Oct, 1973	On mine drainage in newer spoils
C6	X	X	Oct, 1973	On Trout Creek near northern limit of spoils
C7	X		Oct, 1973	On ground water seep from spoils
C8	X		Oct, 1973	On Trout Creek at northern limit of spoils
C9	X	X	Mar, 1975	On mine drainage in both newer and older spoils
C10	X	X	Mar, 1975	On mine drainage in newer spoils
C11	X		Mar, 1975	On Trout Creek approximately 0.8 km from northern extent of spoils
C12	X		Mar, 1975	On ephemeral stream north of Edna Mine
C13	X	X	Jul, 1975	On Little Trout Creek above Edna Mine

Station C1 is located on Trout Creek upstream of all mining activity. Station C2 is about 2.5 kilometers downstream from Station C1 and is also downstream from one small underground coal mining operation. Other stations along Trout Creek include C4, C6, C8, and C11 with the first three located adjacent to the spoil piles and the latter located downstream from all mining activity. Little Trout Creek was sampled at Station C13 located near its confluence with Trout Creek.

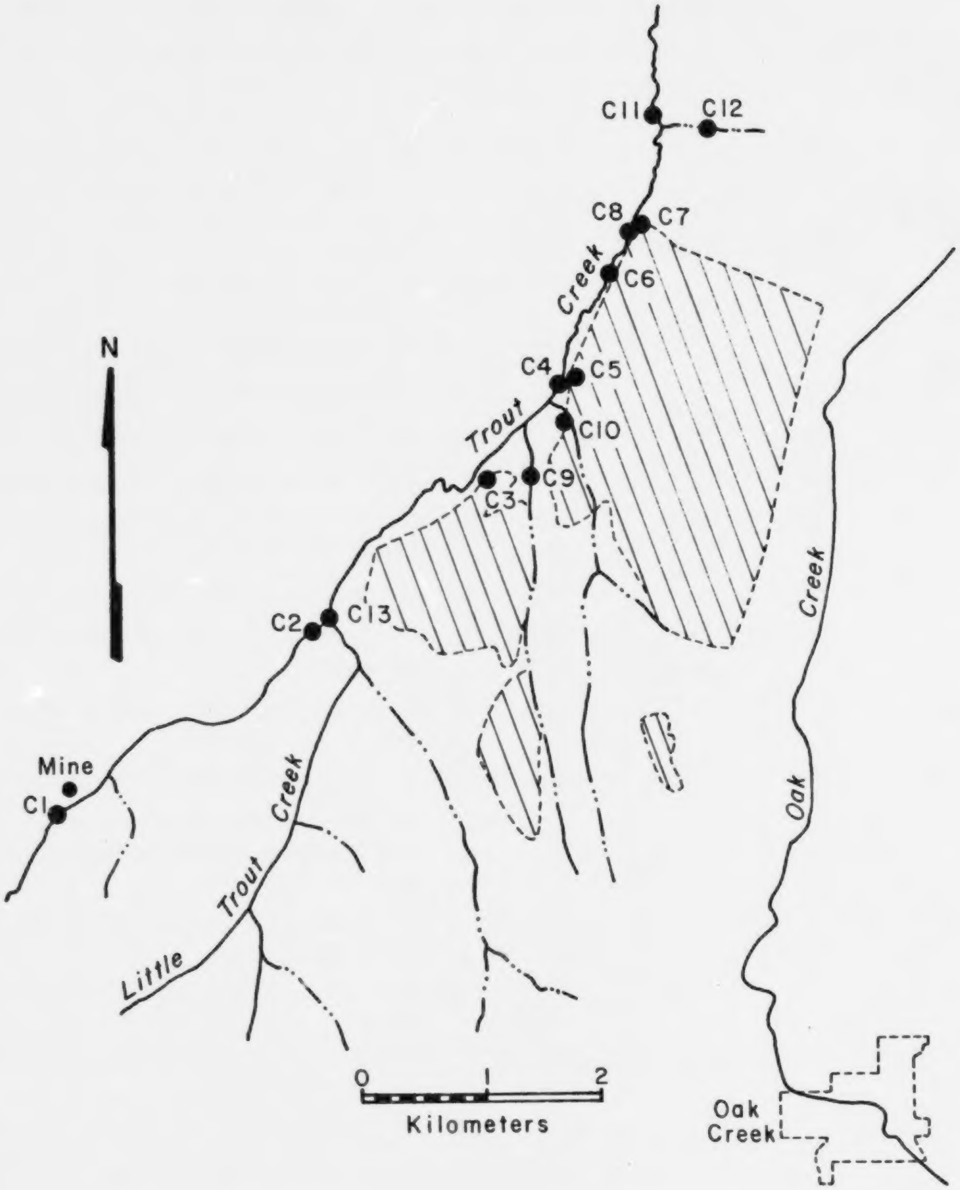
N
C11
C12
C8
C7
C6
Creek
C4
C5
Trout
C10
C3
C9
C2
C13
Mine
C1
Little
Trout
Creek
Creek
Oak
0
1
2
Kilometers
Oak
Creek

Figure 6. Location of water quality monitoring stations.

Stations sampling water flowing from mine watersheds into Trout Creek include C3, C5, C7, C9, and C10. Station C3 sampled water flowing northward along the highwall trench in the older spoils where water can be seen seeping from the base of the spoil piles. Stations C9 and C10 are located on natural streams originating in the upper unmined portions of watersheds which are disturbed by mining in their lower reaches. Water flowing from the base of the spoils in a deep unfilled cut was sampled at Station C5. Station C7 is located at a large subsurface water seep at the base of the spoil piles along Trout Creek. It has no associated surface drainage although there is some indication that a small natural drainage existed before mining. Station C12 is located on a small drainage on natural ground north of the spoils. It flows only during periods of very high runoff resulting in only a few water samples being collected.

Water samples were taken on a monthly basis at all stations with additional samples taken as often as daily at stations C2, C3, C5, C6, C9, C10, and C13 from April through August of 1975 and April through May of 1976. A complete chemical analysis was performed on the monthly samples at most stations and all monthly samples were tested for pH, specific conductance, and total dissolved solids. The more frequent samples taken during the spring and summer were tested only for specific conductance.

During April and May of 1976 additional water quality samples were taken at the supplementary locations shown in Figure 7. These samples were tested for specific conductance and were not taken on a regular basis.

Discharge Monitoring

Discharge monitoring stations were established at several of the water quality stations to determine the total runoff and salt load of the surface drainage. Discharge was measured at stations C2 and C6 on Trout Creek by using a current meter to determine the velocity distribution in a stream cross-section. The corresponding water level was read from a staff gage installed near the measured cross-section. By taking flow measurements of several different water levels, a stage-discharge relationship was found by fitting readings to an equation of the form

$$Q = aS^b$$

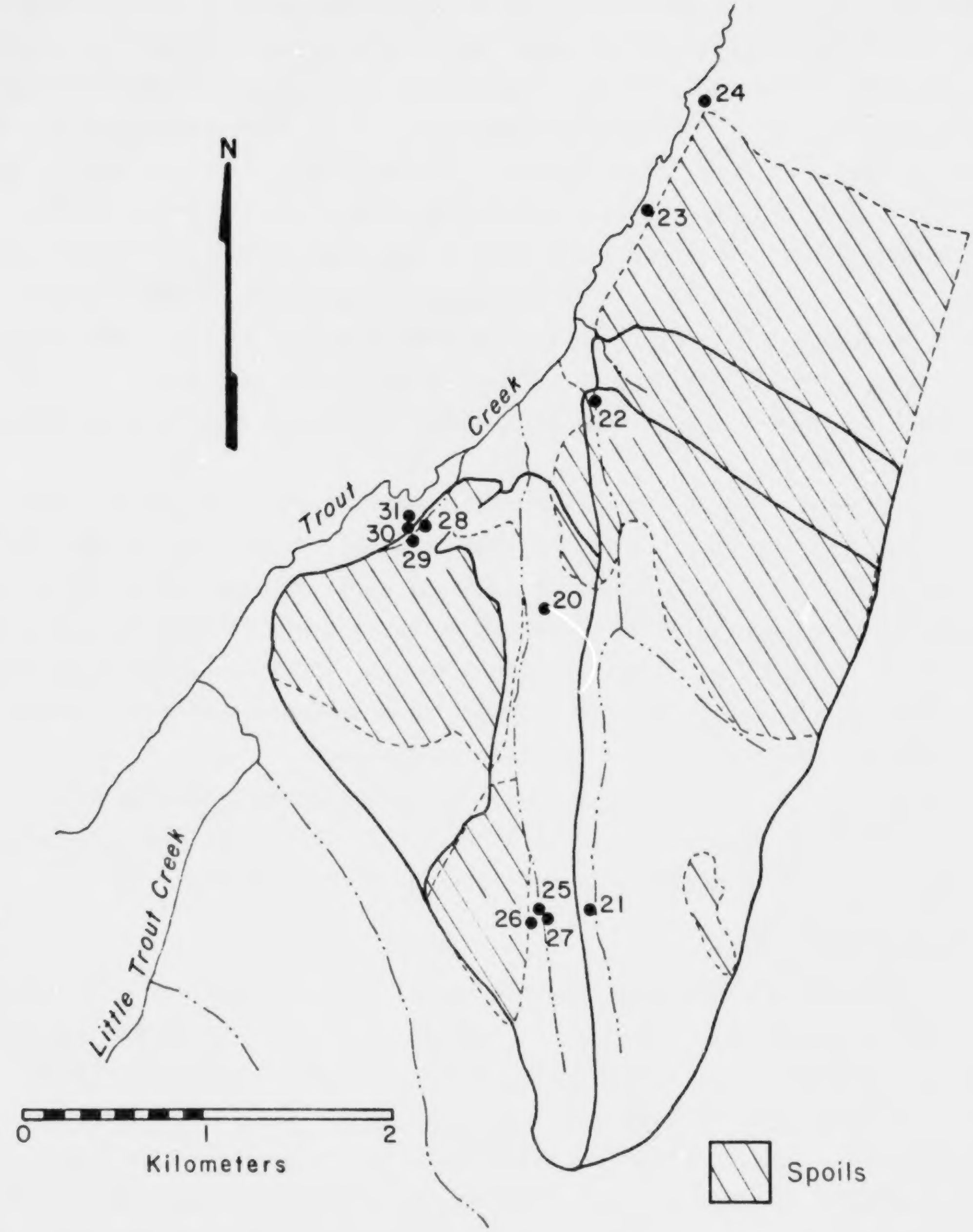
N
24
23
22
Trout Creek
31
28
30
29
20
Little Trout Creek
25
21
26
27
0
1
2
Kilometers
Spoils

Figure 7. Supplementary water sample locations.

where Q is the discharge, S is the staff gage reading, and a and b are regression coefficients. It was found that significant erosion and deposition occurred in Trout Creek from one year to the next resulting in a change in the channel cross-section. The stage-discharge relationships were adjusted as new stream gaging data became available. Figures 8 and 9 are the rating curves for stations C2 and C6, respectively. They demonstrate the variation in the stage-discharge relationship over a period of three years. In addition to a staff gage, station C2 was equipped with a continuous water level recorder on April 21, 1975.

Stations C3, C9, and C10 were equipped with 20.3 cm by 91.4 cm cutthroat flumes and staff gages. Stevens Recorders were also installed on the flumes at these locations for continuous discharge monitoring. Ice in the stilling wells during the early spring prevented reliable records until temperatures warmed up in early April. Recorder charts were changed weekly and were constantly checked for accuracy with staff gage readings.

Stations C5 and C13 were equipped with flumes but not recorders. A 7.6 cm by 91.4 cm cutthroat flume and staff gage was installed at station C5. However, the capacity of the flume was exceeded in April of 1975 so a larger 30.5 cm by 91.4 cm cutthroat flume was installed before the spring of 1976. A 0.46 cm by 2.74 cm Parshall flume and staff gage was installed during July 1975 at station C13. Flow in Little Trout Creek exceeded the capacity of the flume for about a week during late May 1976.

Soil and Spoil Sampling

Samples of native soil and spoils taken at the Edna Mine are used to chemically characterize the surface and subsurface geologic material. In 1973 spoil samples were taken at eight locations on the mine (McWhorter et al. 1975). Three locations at the extreme north end of the spoils, three locations east of station C4, and two locations south of station C3 were sampled every 15 cm to a depth of 120 cm. A number of samples were taken at four locations along the active highwall by collecting drill cuttings at three meter intervals from ground surface to the coal seam. These samples were later composited. Native soil was sampled to a depth of one meter at one location during the same year.

In May 1976 samples were collected with a hand auger at locations shown

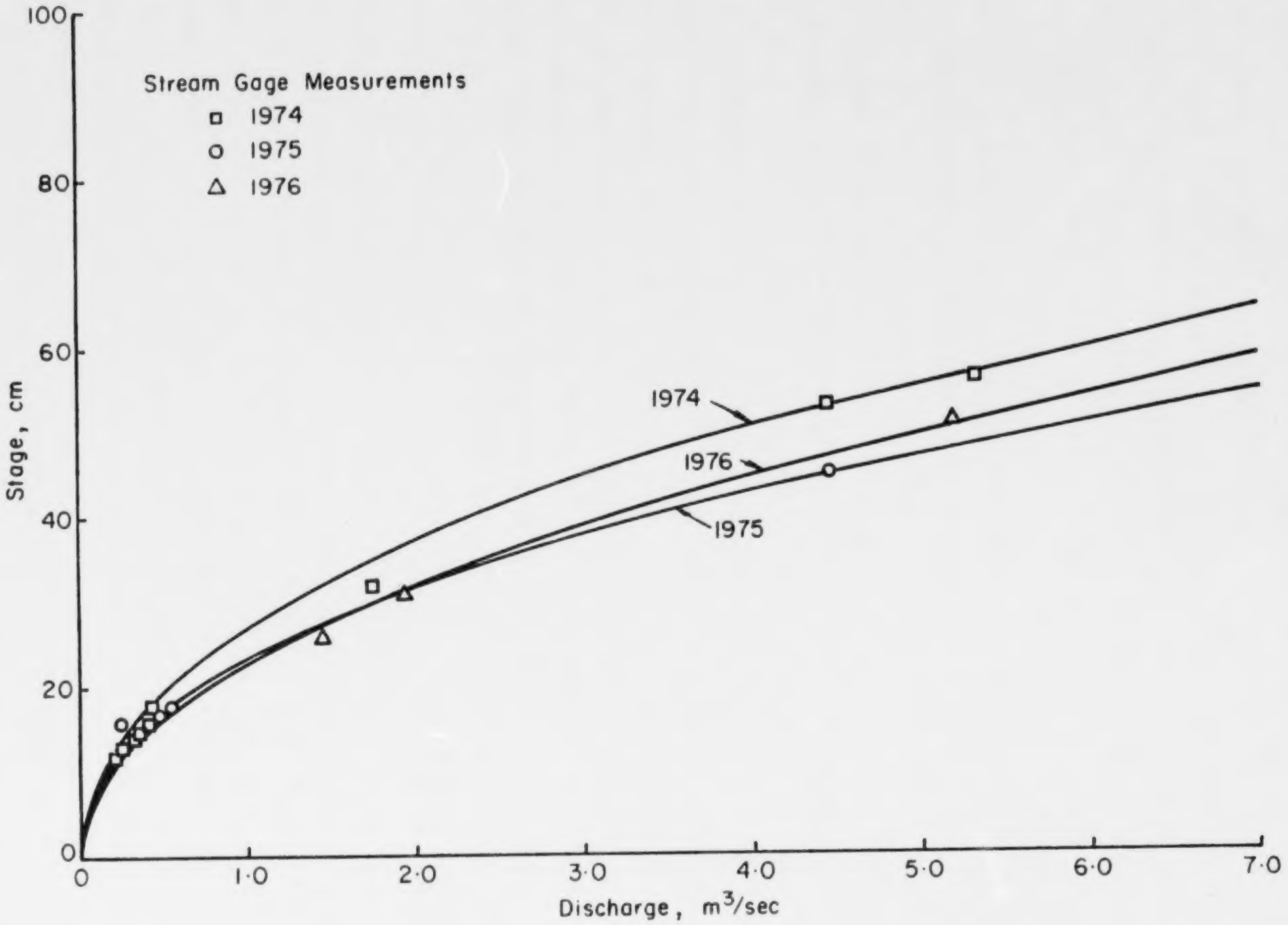

Figure 8. Stage-discharge rating curves for Trout Creek at Station C2.

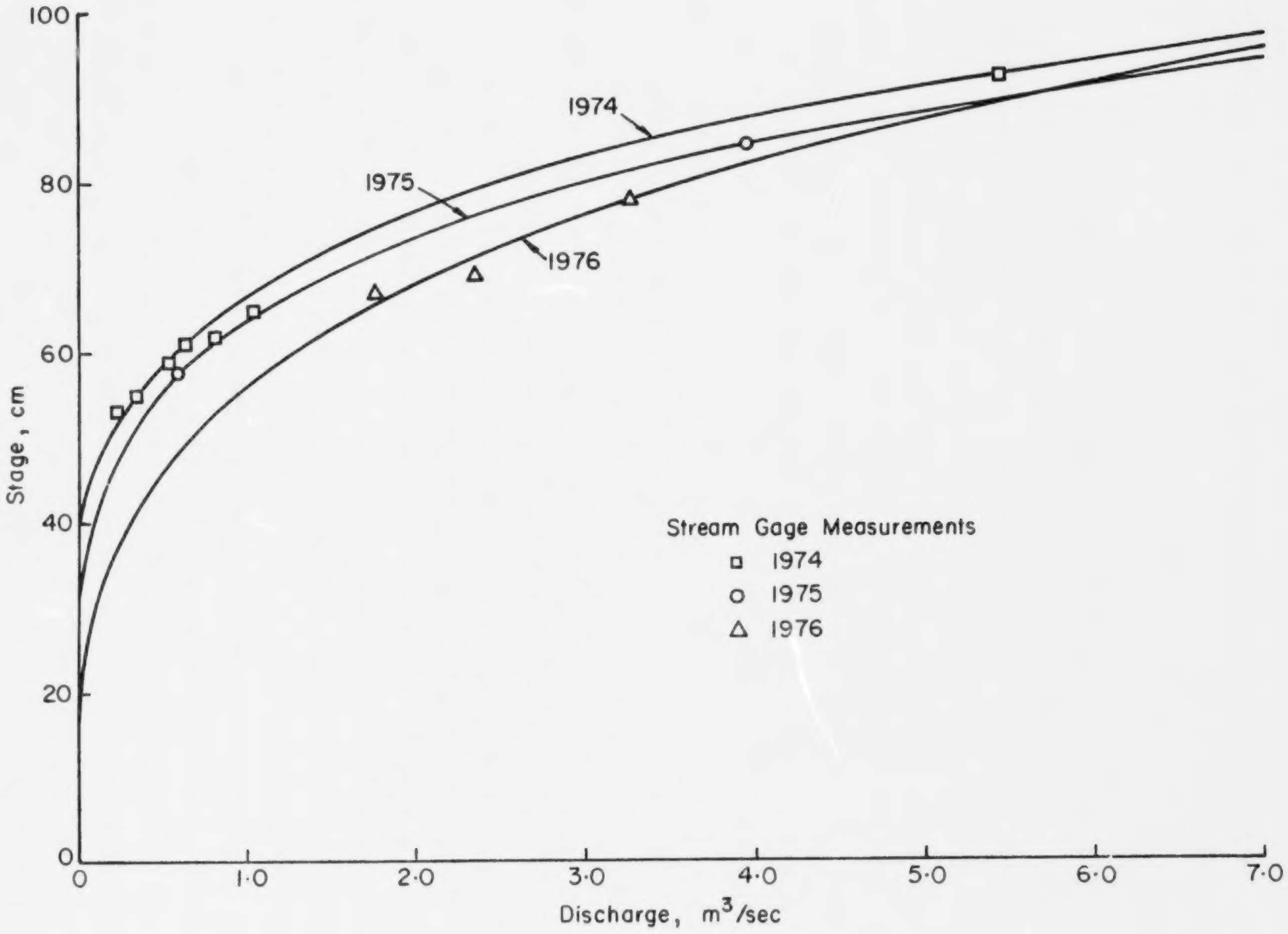

Figure 9. Stage-discharge rating curves for Trout Creek at Station C6.

in Figure 10. These locations include ones in the old spoils, the new spoils, and natural ground. They are coded as SS100 to SS109 with the depth of the sample also indicated. One sample was taken at the surface at all locations. However, in some cases it was impossible to take deep samples because rock was encountered.

Water Analysis

Monthly water samples taken from October 1973 to May 1976 were analyzed for acidity, alkalinity, total hardness, pH, specific conductance, suspended solids, total dissolved solids, and total solids along with concentrations of aluminum, calcium, chloride, copper, dissolved iron, undissolved iron, total iron, potassium, magnesium, manganese, sodium, lead, sulfate, and zinc. Several spot checks for arsenic, cadmium, chromium, mercury, and selenium were also made. The monthly samples were collected and analyzed in accordance with the standard Environmental Protection Agency "Methods for Chemical Analysis of Water and Wastes" (U. S. Department of the Interior, 1970).

Water samples not subjected to chemical analysis were tested for electrical conductivity using a portable soil moisture bridge apparatus. Electrical conductance or specific conductivity is a measure of the ability of a substance to conduct electric current which in turn can be related to the concentration of total dissolved solids. The American Society for Testing and Materials (1966) has defined electrical conductivity as "the reciprocal of the resistance in ohms measured between opposite faces of a centimeter cube of an aqueous solution at a specific temperature." The units shall be "micromhos per centimeter at T°C" where temperature is usually reported at 25°C. Pure liquid water has a very low conductance, only a few hundredths of a micromho per centimeter at 25°C.

Since electrical conductance varies with temperature, it is important to measure the temperature along with the resistance. In dilute solutions for most ions an increase of 1°C increases the electrical conductance by about 2 percent (Hem, 1970). Factors used to adjust electrical conductivity were obtained from Figure 11 which is based on a 0.01 molar potassium chloride solution (American Public Health Association et al., 1971). After electrical conductivity is adjusted to 25°C, it can be converted to the concentration of total dissolved solids by using a relationship developed later in this section.

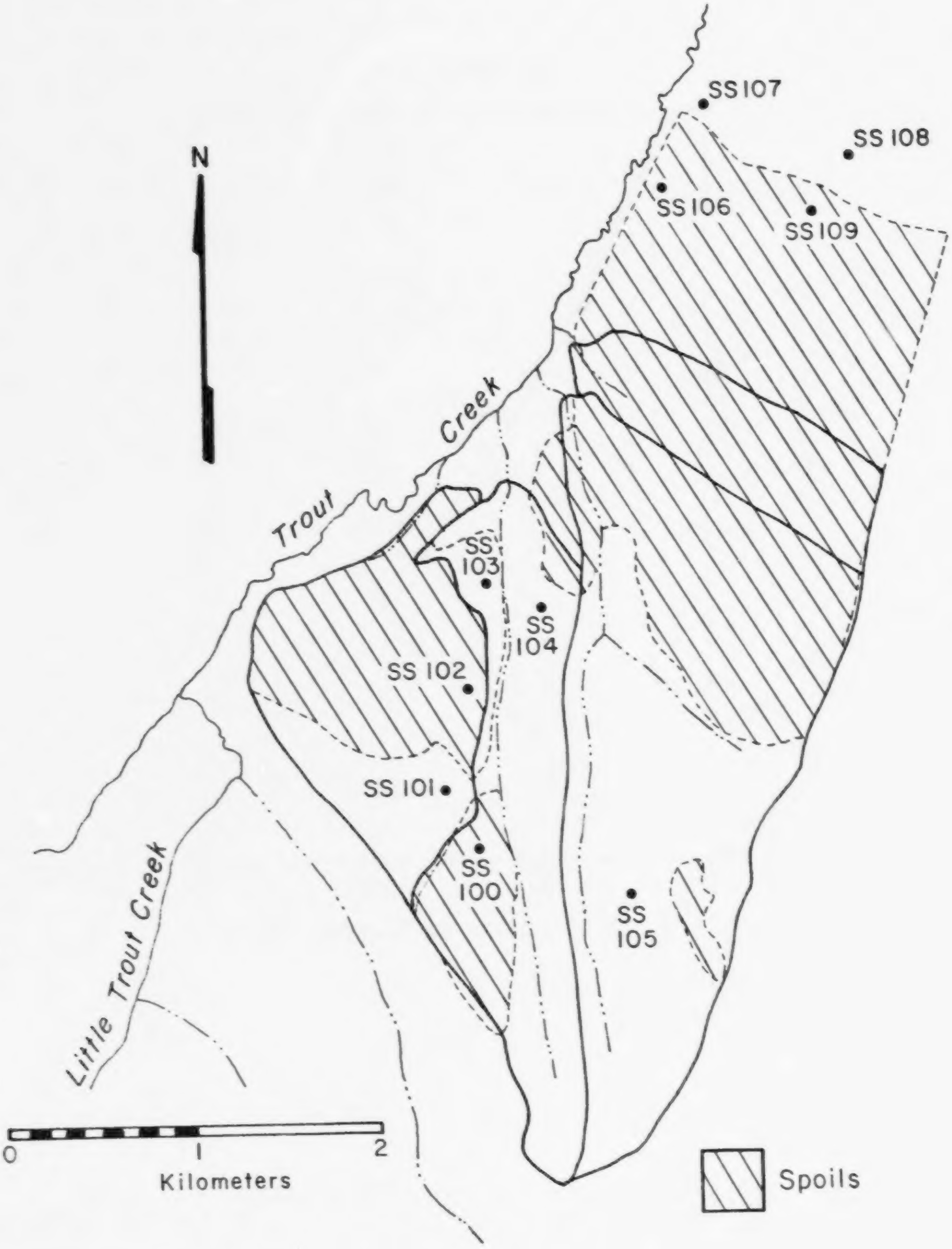
N
Trout Creek
Little Trout Creek
SS 107
SS 108
SS 106
SS 109
SS 103
SS 104
SS 102
SS 101
SS 100
SS 105
0
1
2
Kilometers
Spoils

Figure 10. Location of soil and spoil samples taken in May, 1976.

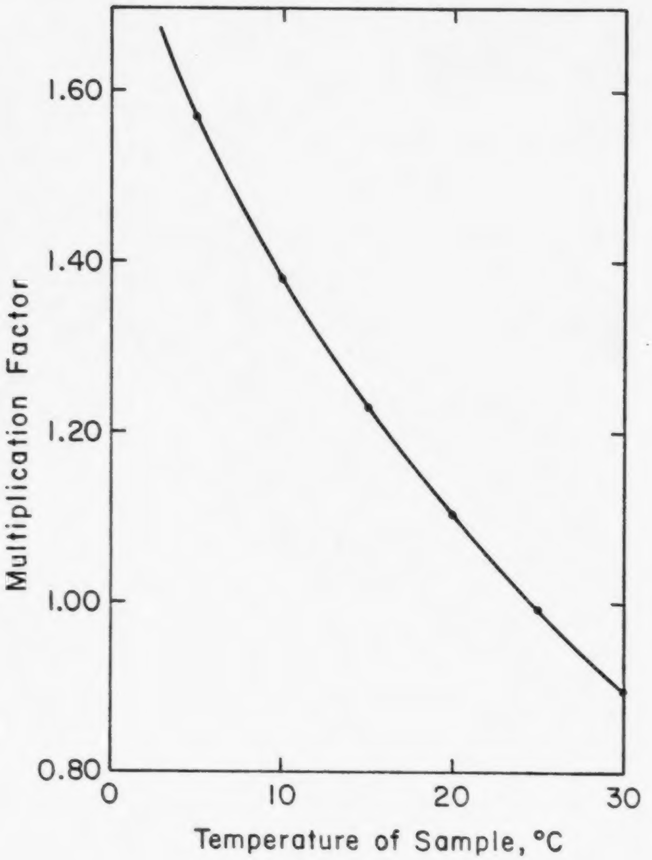

Figure 11. Factors for adjusting specific conductance of water to equivalent values at 25°C (based on a 0.01 M KCl solution).

Soil and Spoil Analysis

The most important factor determining the composition of water is the concentration and type of solutes available in the soil and rock strata. As water percolates into the ground, several processes can change the type and amount of dissolved solids.

Ion exchange is a reversible process by which cations and anions are exchanged between solid and liquid phases and between solid phases if in close enough contact. This process does not change the total concentration in milliequivalents per liter of the solution but it does change the ionic composition. Solid components in the soil or spoils are also capable of adsorbing or releasing (desorption) solutes from or to the solution. This process can increase or decrease the total concentration of solutes in percolating water and is probably the major process causing water in the Edna Mine spoils to increase in total dissolved solids concentration.

Salts found in the soil or the spoils may be readily soluble in water and thus quickly leached or only sparingly soluble and thus only slowly leached by water. Studies indicate that shale in western Colorado will contain $CaSO_4$ as a slightly soluble salt and $MgSO_4$ and $NaSO_4$ as soluble salts (Schmehl and McCaslin, 1969).

The saturated paste method (Richards, 1954) was used to analyze the chemical constituents of the soil and spoil samples from the Edna Mine. It is assumed that this method would best indicate the potential amounts of readily soluble ions available to percolating water. Other factors which have an influence on the pollution potential of spoils such as weathering, microbial activity, acid formation, evapotranspiration, and non-equilibrium reactions are not characterized by saturated paste analysis.

Saturated paste tests were conducted by procedures described by Hergert (1971). The sample is dried and crushed until it will pass through a 2 mm screen. It is then saturated with distilled water, thoroughly mixed and left to stand for 16 hours. The resulting water extract is analyzed for the various chemical constituents desired. For the spoil samples taken in 1973, determinations were made for pH, specific conductance, calcium, magnesium, sodium, carbonate, bicarbonate, chloride, sulfate, and nitrate. The samples taken in May 1976 were tested only for specific conductivity.

Leaching Analysis

Two soil samples from depths of 70 cm and 100 cm were taken at the experimental plots and combined to yield a 558.8 g sample used for leaching tests. The sample was placed in a column 6.85 cm in diameter containing glass beads at the bottom to retain the sample. The purpose of the test was to determine leaching and weathering characteristics of the spoils.

The spoil sample was initially sifted into the column to provide an even distribution. De-ionized water was added to the sample and maintained at a height of about 5 cm above the top of the sample. Water samples were taken for every 100 ml increment of leaching volume and tested for pH and specific conductivity. These water samples were then combined at 500 ml increments for further chemical analysis.

The test was conducted such that after an initial leaching volume was added, the sample was drained and air forced through the column for sixty hours. After addition of a second volume of water, the sample was drained and aerated for five days. A third leaching volume was passed through the column after which the sample was removed, dried, crushed, and finally returned to the column for a fourth volume of leaching water.

WATER QUALITY AND ITS RELATIONSHIP TO SPOIL CHARACTERISTICS

The discharge and water quality data collected at the Edna Mine allow a detailed analysis of the water quality to be made. Observed water quality is examined in terms of the climate, hydrologic system, and physical-chemical characteristics of the geologic material present. The total quantity of salts discharged in the streams from the mine watersheds is computed along with the net inflow of salts in the reach of Trout Creek bordering the western edge of the mine.

Chemical Characteristics of Mine Drainage and Receiving Waters

Detailed chemical analyses were performed on monthly water samples taken at the water quality monitoring stations. From these analyses the average ion concentrations in Table 3 and the maximum ion concentrations in Table 4 were determined. The recommended drinking water standards of the U. S. Public Health Service (1962) are listed in each table for comparison.

TABLE 3. AVERAGE ION CONCENTRATION OF MONTHLY WATER SAMPLES TAKEN OCTOBER 1973 TO NOVEMBER 1975

	pH	Hardness total $CaCO_3$ mg/ℓ	Specific Cond. µmohs/cm	Total Dissolved Solids mg/ℓ	Al mg/ℓ	Ca mg/ℓ	Cl mg/ℓ	Cu mg/ℓ	Fe diss. mg/ℓ	K mg/ℓ	Mg mg/ℓ	Mn mg/ℓ	Na mg/ℓ	Pb mg/ℓ	SO_4 mg/ℓ	Zn mg/ℓ
U.S. Drinking Water Standards	-	-	-	500	-	-	250	1.0	0.30	-	-	0.05	-	0.05	250	5.0
Station C1 Trout Creek	7.8	117	175	128	<0.7	37	<1.0	<1.0	<0.07	1.4	9.7	<0.02	3.3	<0.10	19	<0.014
Station C2 Trout Creek	7.8	112	180	119	<0.7	33	<1.0	<1.0	<0.06	1.2	9.2	<0.02	3.3	<0.10	17	<0.016
Station C3 Mine Drainage	7.7	1502	2294	2194	<0.7	392	3.5	<1.0	<0.09	4.0	139	0.20	19.6	<0.10	1075	<0.039
Station C4 Trout Creek	7.9	231	336	261	<0.7	72	1.2	<1.0	<0.06	1.9	21.3	<0.02	5.7	<0.10	90	<0.011
Station C5 Mine Drainage	7.8	2577	3299	3228	<0.7	353	4.5	<1.0	<0.05	17.4	249	<0.02	111	<0.10	1997	<0.015
Station C6 Trout Creek	7.8	235	367	271	<0.7	74	1.2	<1.0	<0.07	2.1	21.1	<0.03	7.7	<0.10	80	<0.012
Station C7 Ground Water	7.5	2039	4416	3838	<0.7	314	8.1	<1.0	<0.07	12.8	173	<0.03	553	<0.10	784	<0.012
Station C8 Trout Creek	7.8	217	413	292	<0.7	70	1.3	<1.0	<0.07	2.3	20.9	<0.03	9.1	<0.10	115	<0.015

TABLE 4. MAXIMUM ION CONCENTRATIONS OF MONTHLY WATER SAMPLES TAKEN OCTOBER 1973 TO NOVEMBER 1975

	pH high/low	Hardness total $CaCO_3$ mg/ℓ	Specific Cond. µmohs/cm	Total Dissolved Solids mg/ℓ	Al mg/ℓ	Ca mg/ℓ	Cl mg/ℓ	Cu mg/ℓ	Fe diss. mg/ℓ	K mg/ℓ	Mg mg/ℓ	Mn mg/ℓ	Na mg/ℓ	Pb mg/ℓ	SO_4 mg/ℓ	Zn mg/ℓ
U.S. Drinking Water Standards	-	-	-	500	-	-	250	1.0	0.30	-	-	0.05	-	0.05	250	5.0
Station C1 Trout Creek	8.5/7.2	240	249	170	<0.7	51	1.7	<1.0	<0.10	3.6	13	<0.05	4.2	<0.16	130	0.043
Station C2 Trout Creek	8.3/7.0	270	261	170	<0.7	54	2.0	<1.0	0.13	3.6	13	<0.05	4.2	<0.20	82	0.057
Station C3 Mine Drainage	8.4/6.0	3700	2900	2530	<0.7	480	6.0	<1.0	0.29	13.0	190	0.42	29	<0.20	1700	0.11
Station C4 Trout Creek	8.5/7.4	470	853	690	<0.7	210	2.0	<1.0	0.10	5.6	52	0.05	14	<0.16	230	0.017
Station C5 Mine Drainage	8.4/6.4	5500	4220	4160	<0.7	440	10.0	<1.0	<0.10	31	320	<0.05	250	<0.16	2500	0.038
Station C6 Trout Creek	8.6/6.9	550	840	590	<0.7	190	2.0	<1.0	0.10	9.8	47	<0.05	13	<0.16	208	0.025
Station C7 Ground Water	8.3/6.0	3800	5360	4870	<0.7	470	10.0	<1.0	0.14	25.2	250	0.26	1099	0.20	2010	0.020
Station C8 Trout Creek	8.5/6.75	540	1150	820	<0.7	210	2.2	<1.0	0.15	18	63	0.06	18	<0.20	480	0.024

The quality of water from the mine watersheds (C3 and C5) is generally low due to high concentrations of total dissolved solids. Although not listed in Table 3, the average dissolved solids concentrations at stations C9 and C10 exceed the 500 mg/l standard by two to four times. Water from a subsurface seep at station C7 displayed the lowest quality with an average dissolved solids concentration of 3838 mg/l and a maximum of 4870 mg/l. This particular station was consistently anomalous with respect to the other 12 stations, however.

The average water quality of Trout Creek is within the standards. However, there is considerable degradation in quality as Trout Creek flows north adjacent to the mine. The water flowing through station C2 is low in total dissolved solids averaging 119 mg/l. The one underground coal mine between stations C1 and C2 seems to have no effect on water quality which actually improves slightly from station C1 to C2. The dissolved solids concentration in Trout Creek is increased at stations C4 and C6 and averages 292 mg/l at station C8. A greater variation in the quality of Trout Creek is found when maximum dissolved solids concentrations are examined. The maximum found at station C2 is 170 mg/l and the maximum at station C8 is 820 mg/l.

Most average concentrations of individual ions are below drinking water standards. High average sulfate concentrations are found in water from the mine watersheds and the average manganese concentration at station C3 exceeds the standard by four times. A summary of the trace element data on mine drainage is presented in Table 5. The number of observations and number of times standards were exceeded pertain to water samples from stations C3, C5, and C7. These three stations monitor mine drainage with C3 and C5 located on streams and C7 located on a groundwater seep at the base of the spoils along Trout Creek.

The high sulfate and manganese concentrations in mine drainage may be fairly typical of Colorado. Wentz (1974) noted in examining water samples from throughout Colorado that, of thirty sites samples, sulfate exceeded the 250 mg/l standard 53.3 percent of the time. He also noted that dissolved manganese is naturally high in Colorado streams. The reason for the high manganese concentrations at station C3 is not presently known. It is possible that natural concentrations are higher in the older spoils on the C3 watershed or that a significant time delay is involved before manganese is

TABLE 5. HEAVY METALS STANDARDS* AND NUMBER OF TIMES EXCEEDED AT STATIONS C3, C5, AND C7

	Standard	Number Observations	Number Exceeded
Arsenic (As)	0.01 mg/l	19	0
Cadmium (Cd)	0.01 mg/l	22	1
Chromium (Cr)	0.05 mg/l	18	0
Copper (Cu)	1.0 mg/l	82	0
Iron (Fe diss)	0.3 mg/l	83	2
Mercury (Hg)	0.002 mg/l	24	0
Manganese (Mn)	0.05 mg/l	67	30
Lead (Pb)	0.05 mg/l	15	0
Selenium (Se)	0.01 mg/l	18	10
Zinc (Zn)	5.0 mg/l	71	0

released by weathering processes.

The ionic composition of water can be examined graphically by plotting the major cation and anion concentrations in milliequivalents per liter. Concentrations in milliequivalents per liter are found by multiplying milligrams per liter by the reciprocal of the combining weight of the ion. The ionic composition of water at stations C2, C3, C5, and C8 is plotted in this manner in Figures 12, 13, and 14 for January, May, and September, 1975 respectively. These particular months were chosen to illustrate the chemical composition during two low flow periods in January and September, and a high flow period from spring runoff in May. Cations are plotted on the left half of each bar and anions on the right half. If all ions are correctly determined, the total milliequivalents per liter of the cations will equal that of the anions.

The concentration and composition of water at station C2 varies only slightly over the three months considered. However, the ion concentrations at station C8 increase significantly in May primarily due to calcium, magnesium, and sulfate ions. These ions can result from the solution of hydrous sulfates such as gypsum ($CaSO_4 \cdot 2H_2O$) and epsomite ($MgSO_4 \cdot 7H_2O$) which are probably found in the rocks of the Willimas Fork Formation. The Colorado School of Mines Research Institute (1976) is conducting a study of the

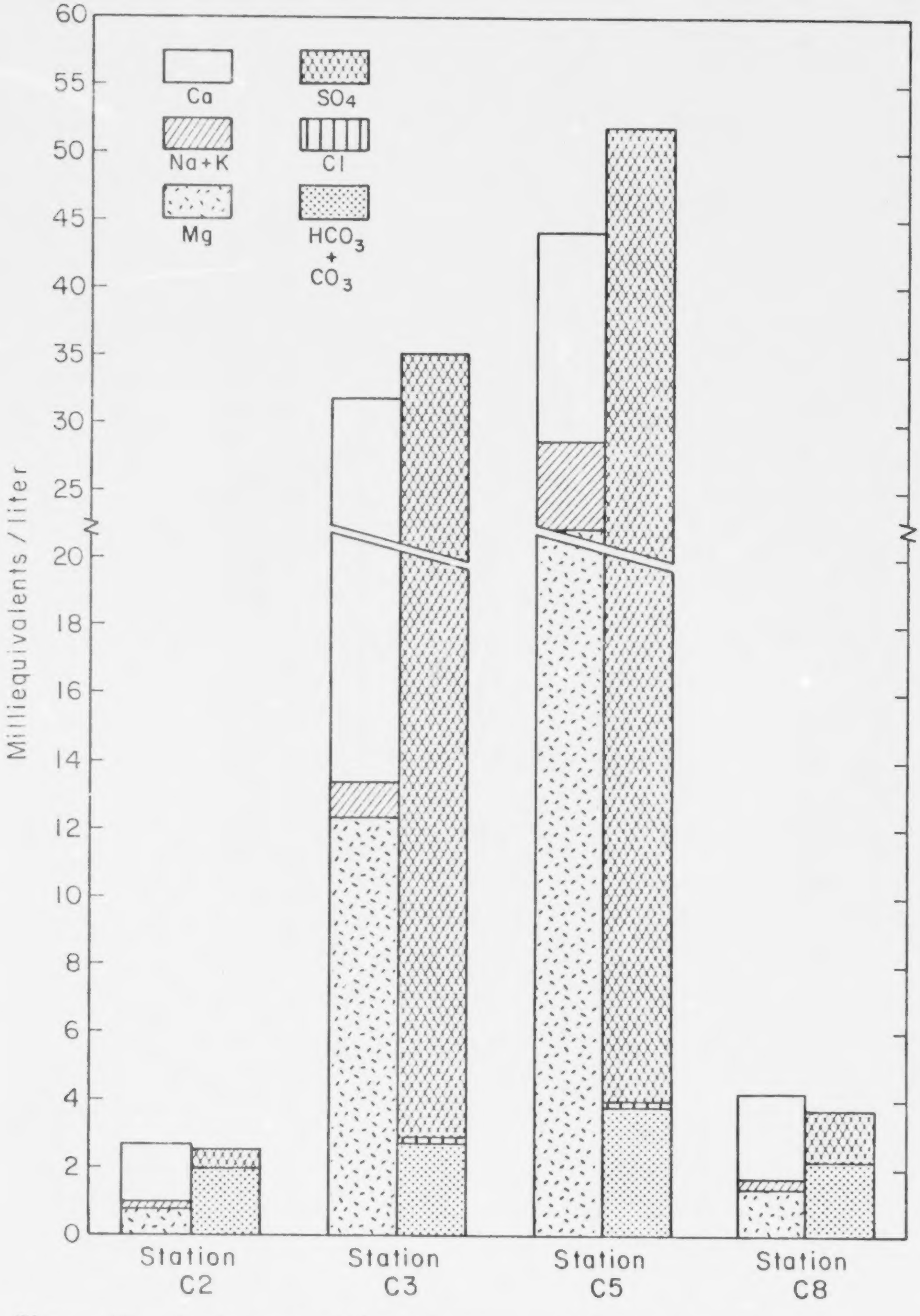

Figure 12. Ionic composition of water in January, 1975.

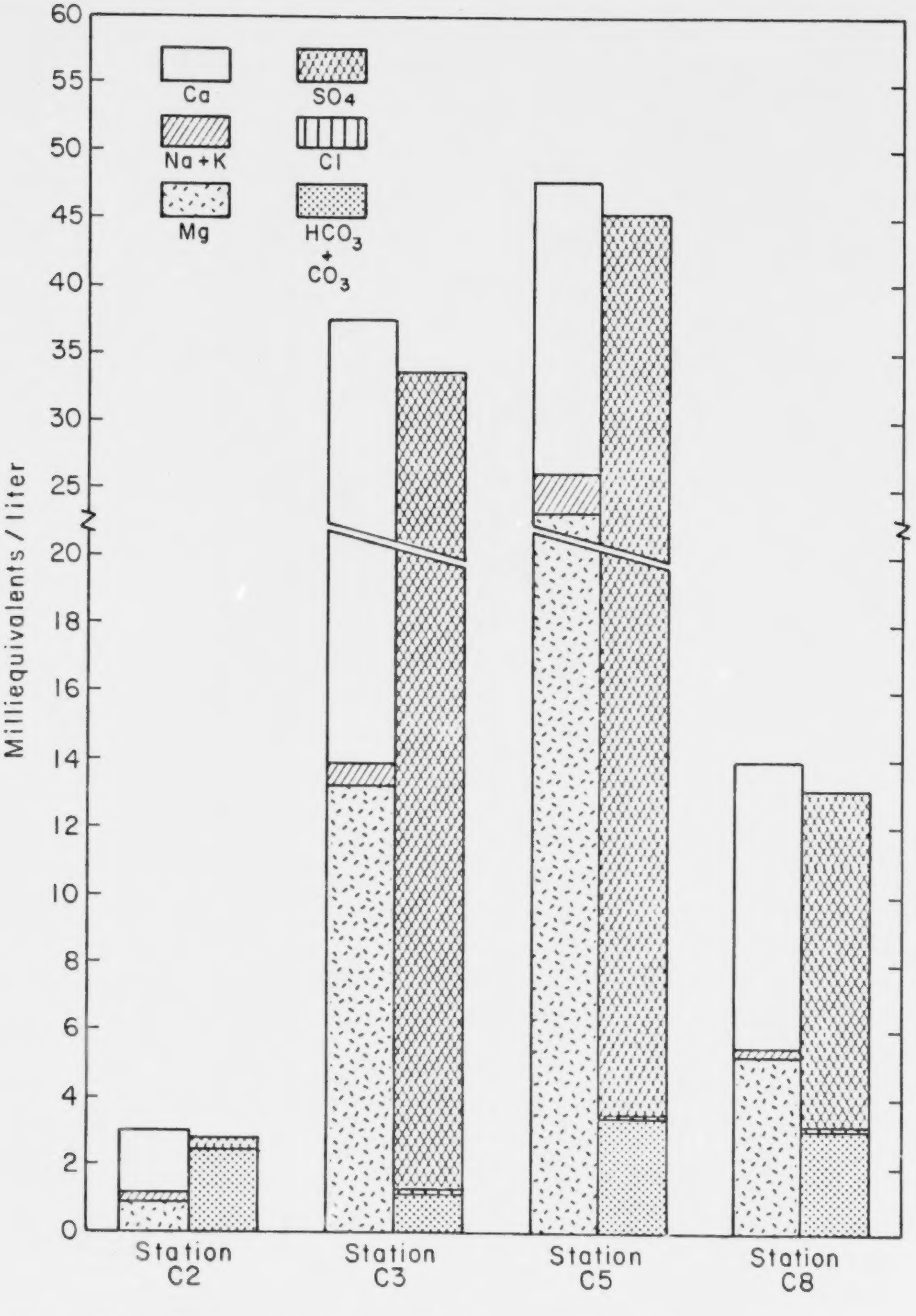

Figure 13. Ionic composition of water in May, 1975.

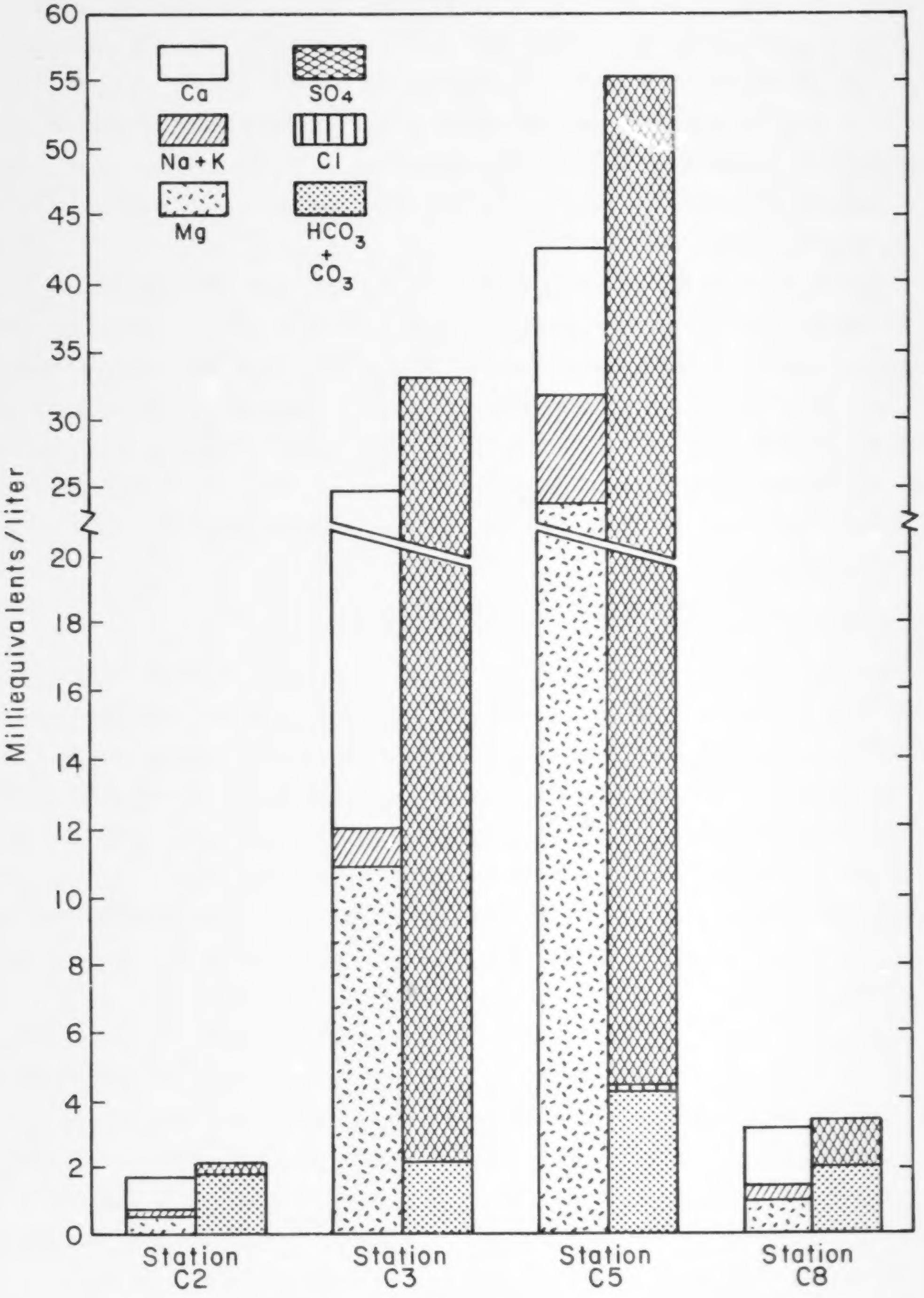

Figure 14. Ionic composition of water in September, 1975.

mineralogy of overburden and spoils as related to the ground water quality and will provide more detailed information on the sources of the various constituents. The composition of water at stations C3 and C5 remains relatively constant over the three months considered with the greatest proportion of dissolved solids coming from calcium and magnesium sulfates. Ions other than those shown in Figures 12, 13, and 14 are not considered due to their relatively small concentrations.

Average ion concentrations in Table 3 for the same four stations considered above are plotted on a logarithmic scale in Figure 15. Note that amounts of sodium, potassium, and manganese are greater in water from the C5 watershed than that from the C3 watershed. This is expected because of the lower solubility of calcium sulfate, compared to magnesium and potassium salts as previously mentioned. The magnesium and potassium are thus leached to a greater extent from the older C3 spoils while calcium remains about the same in both old and new spoils.

Relationship Between Chemistry of Water and Spoils

The chemical composition and the dissolved solids in water which has passed through a spoil bank is a reflection of the chemical composition of the spoils. Numerous methods exist by which the chemical-mineralogical composition of the disturbed material can be characterized. There is a need, however, to relate the quality of waters contacting the spoil with the results of whatever chemical tests are used to characterize the spoil. In this study, the chemical composition and dissolved solids content in saturation and one-to-one extracts (Richards, 1954) were used to characterize the spoil and overburden.

Table 6 contains a comparison of the electrical conductivity (EC) of saturation extracts prepared from spoil and overburden with the EC of water samples in a set of subsurface drains and in the C5 mine drainage. A description of the subsurface drains constructed in the spoil is contained in Section 6 of this report. The waters in the C5 drainage were selected for comparison because essentially all of the contributing watershed has been disturbed by mining and the discharge is dominated by ground water runoff.

The results in Table 6 suggest that the EC (and therefore the dissolved solids) of ground-water runoff can be estimated by determining the EC of

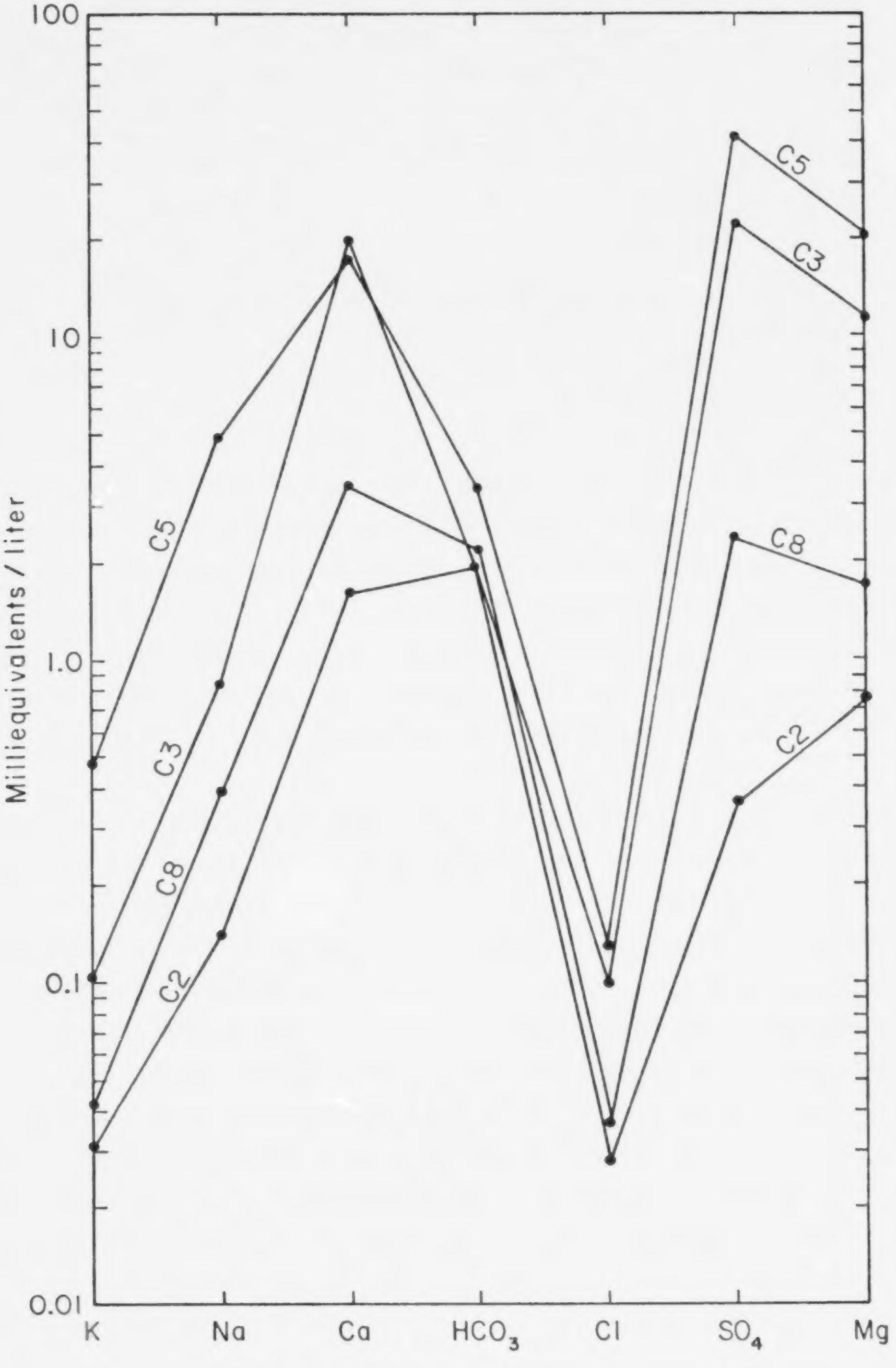

Figure 15. Average concentrations of major ions in water from stations shown.

TABLE 6. COMPARISON OF ELECTRICAL CONDUCTIVITY OF SPOIL, OVERBURDEN, AND SUBSURFACE WATER

	Spoil	Drill Cuttings	Drains	C5
Average EC - μmhos/cm @ 25°C	3100	3000	3400	3400
Number of Samples	14	5*	58	31†
Standard Deviation	930	430	720	430

*Samples were prepared by compositing, by depth interval, samples from four locations along an active highwall.

†Regular monthly samples from October 1973 to June 1976 from C5 mine drainage.

saturation extracts prepared from drill cuttings or samples of the spoil. Care must be taken that the saturation percentage of the samples from which the extracts are prepared is the same as for the spoil material in the field. In the case where drill cuttings are being used to estimate the water quality of spoils to be produced in the future, one must estimate the anticipated saturation percentage of the spoil material. In any case, the standard deviations in Table 6 suggest that a significant range of results should be expected.

While it is expected that the EC of saturation extracts should provide the best index to the EC of ground-water runoff, one-to-one extracts are often prepared. In this study, 1:1 extracts were prepared from 54 samples of the spoil overlying the subsurface drains. The average EC of these extracts was 2200 μmhos/cm, or 65 percent of the average EC of the water in the drains. The average saturation percentage of the samples was 0.474. Based on a calculation where it is assumed that the EC is inversely proportional to the volume of water in the sample for a constant weight of spoil material, one would expect the EC of subsurface drainage to be about twice that of the 1:1 extracts. Instead, the observed EC of the drainage water was only 1.55 times the EC of the 1:1 extracts. This observation is in agreement with data provided by Wadleigh et al. (1951) who showed that the ratio of the EC in a 1:1 extract to that in a saturation extract were always larger than predicted by volumetric dilution calculations; especially when the exchange complex was largely occupied by calcium, and sulfate was present (Richards, 1954). These observations point up that the EC of 1:1 extracts is a less reliable index to the EC of ground-water runoff than is the saturation extract.

Overland flow runoff was collected from plot surfaces above the subsurface drains (see Section 6). The electrical conductivities of 34 samples of overland runoff were averaged to obtain an EC = 360 μmhos/cm at 25°C. These data indicate that the dissolved solids concentration in overland flow runoff is only about 10 percent of that in ground-water runoff. Small dissolved solids concentration in overland flow is explained by the fact that overland flow contacts spoil only in a very thin layer immediately at the surface. The readily soluble materials are quickly leached from this thin layer and subsequent runoff is relatively free of dissolved solids. Similar results are reported by Ponce and Hawkins (1976) from experiments on undisturbed saline soils.

Further insight into the relationship between the quality of mine drainage and the chemical characteristics of the spoil material can be gained by examining and comparing the compositions of ground-water runoff and extracts prepared from the disturbed material. Table 7 shows such a comparison for the dominant constituents. The data in Table 7 were prepared by averaging the concentrations (in mg/l) of each constituent, summing the concentrations of all ions considered and computing the percent of the total that is contributed by each ion. There is an excellent correspondence in the composition among all four sources of the samples indicating that either saturation of 1:1 extracts provide a reliable estimate of the common ion composition in drainage waters from the spoil material.

TABLE 7. COMPARISON OF COMMON ION CONTENTS IN EXTRACTS AND MINE DRAINAGE

	Percent of Total						
	Ca	Mg	Na	K	HCO_3	Cl	SO_4
Saturation Extract - Spoil	3.3	18.8	3.5	2.4	15.4	1.3	55.2
1:1 Extract - Spoil	14.3	8.3	2.3	-	5.3	0.4	69.4
Subsurface Drains	12.6	8.9	3.1	0.8	10.0	0.1	64.4
C5 Mine Drainage	12.1	8.5	3.8	0.6	6.7	0.2	68.2

Chemical Quality and the Water Cycle

The chemical quality of water changes as it moves through the hydrologic system. Figure 16 traces the possible paths available to water movement on a surface mine with conditions similar to those found at the Edna Mine. Impurities present in the atmosphere constitute the first potential source of dissolved solids in water. Precipitation can dissolve these impurities and carry them to the land surface. Overland flow can then dissolve solids from soil and dust particles as it flows to the streams. Both precipitation and overland flow usually have water of better chemical quality than that found in streams.

A substantial portion of precipitation occurring both as rain and snow can infiltrate vertically into the ground and then flow laterally down the dip of the rock strata as groundwater in the saturated zone. This subsurface water can either reappear in streams or leave the watershed as underflow not reappearing as surface runoff. Subsurface water can also flow vertically to deep ground water aquifers if no impermeable boundary exists. Subsurface water possesses a high potential for acquiring dissolved solids from soil and rock strata and thus its quality is generally reduced relative to that of the average in the stream.

At the Edna Mine about one-half of the precipitation occurs as snow fall which, as it melts, reaches the streams by overland and subsurface flow. It is assumed that underflow, that portion of shallow subsurface water not flowing through the discharge monitoring stations, and deep percolation to underlying aquifers are not important on the Edna Mine because of physical conditions previously discussed. The total stream flow reflects a combination of high quality overland flow and lower quality subsurface flow. During heavy spring runoff natural stream flow should exhibit lower dissolved solids concentrations due to large volumes of high quality overland flow. Trout Creek, as observed at station C2, displays this type of behavior as seen in the 1975 discharge and water quality hydrograph in Figure 17. Trout Creek, as observed at station C6, varies from the behavior at station C2 as evidenced by the high dissolved solids concentrations during April and May as shown in Figure 18.

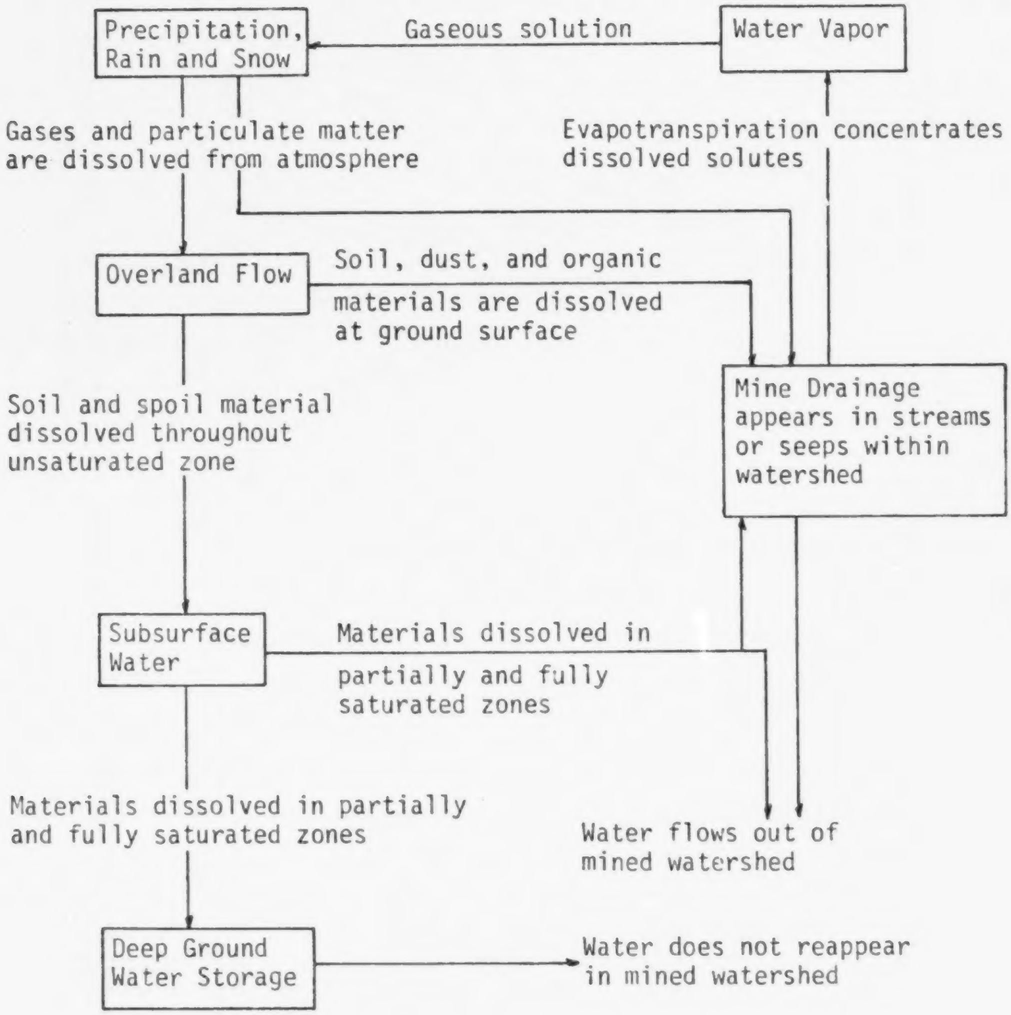
Precipitation, Rain and Snow
Gaseous solution
Water Vapor
Gases and particulate matter are dissolved from atmosphere
Evapotranspiration concentrates dissolved solutes
Overland Flow
Soil, dust, and organic materials are dissolved at ground surface
Mine Drainage appears in streams or seeps within watershed
Soil and spoil material dissolved throughout unsaturated zone
Subsurface Water
Materials dissolved in partially and fully saturated zones
Materials dissolved in partially and fully saturated zones
Water flows out of mined watershed
Deep Ground Water Storage
Water does not reappear in mined watershed

Figure 16. Sources of dissolved solids in the hydrologic system of a mined watershed.

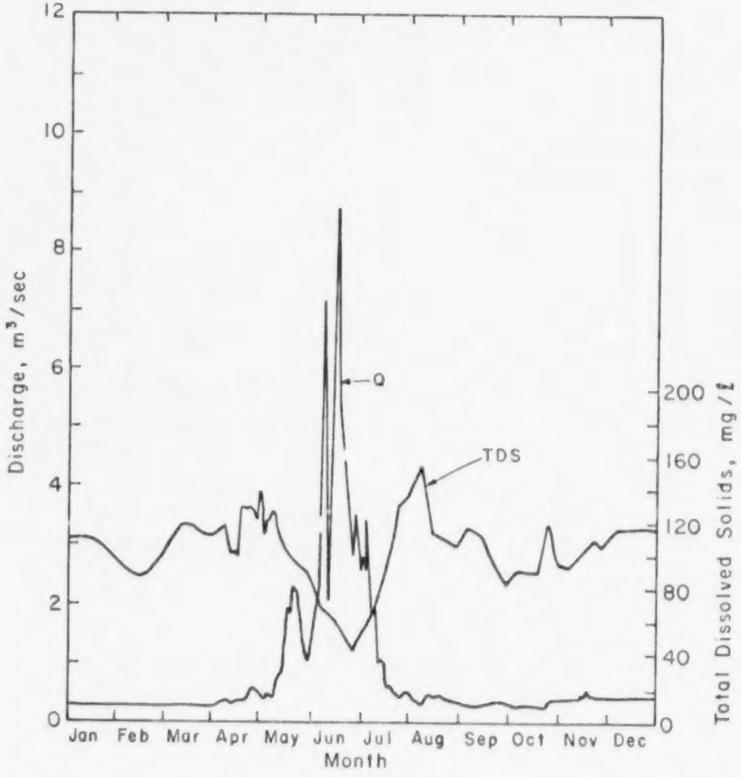

Figure 17. Discharge and water quality hydrograph for station C2, 1975.

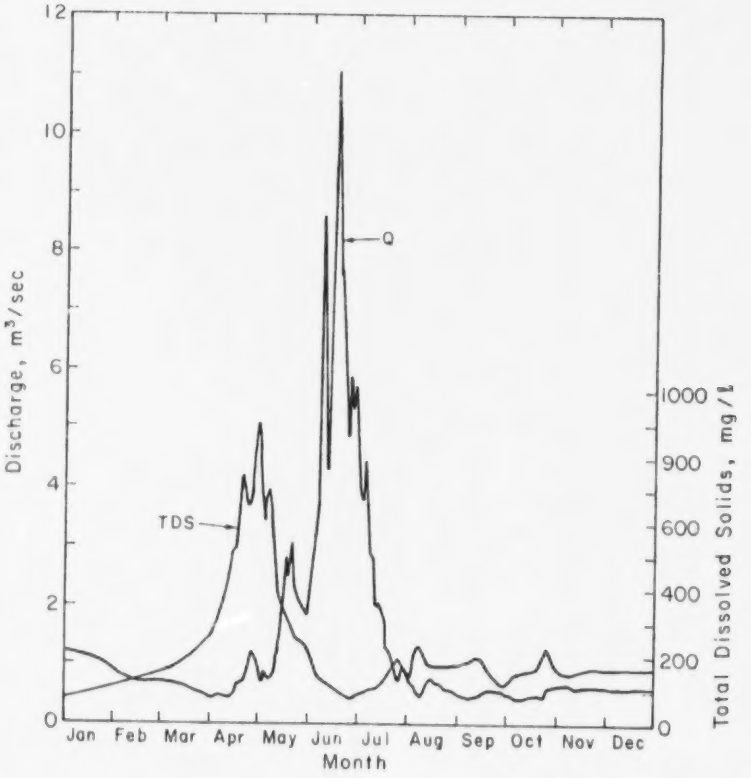

Figure 18. Discharge and water quality hydrograph for station C6, 1975.

The 1975 discharge and water quality hydrographs of the streams flowing from the mine watersheds (Figures 19, 20, and 21) show a rise in dissolved solids during spring runoff rather than the expected decline. This indicates very little overland flow and large quantities of subsurface flow of reduced quality. The peaks of the dissolved solids hydrographs from the mine watersheds correspond approximately with the peak observed on the station C6 dissolved solids hydrograph. No such peak is found at station C2 indicating that the peak is caused by an inflow of dissolved solids between station C2 and station C6. Each component contributing to runoff and its influence on water quality is examined in more detail in the following paragraphs.

Rain and snow dissolve impurities occurring as gasses and particulate matter in the atmosphere. These impurities result primarily from fully or partially burned residues and gases discharged into the atmosphere by man's activities. The greatest potential for atmospheric impurities is found near urban and industrial areas with other areas having only small amounts of atmospheric impurities. Precipitation is generally low in dissolved solids. Feth et al. (1964) report conductivities of melted snow in the western U. S. ranging from 2 to 42 micromhos per centimeter. Archer (1968) reports an average dissolved solids concentration of 35 mg/l in the Erie-Niagra Basin, but this area includes industrial and urban areas.

Very little potential for atmospheric pollution currently exists in the region of the Edna Mine with no large industrial or urban areas in close proximity. Although no samples of precipitation were analyzed, it is reasonable to assume the concentration negligible when compared with other components of stream flow.

Overland flow is that part of rainfall or snowmelt which neither seeps into the ground nor evaporates but flows over the land surface until reaching a stream channel. Overland flow contains the dissolved solids of the precipitation plus any additional solutes picked up from the ground surface. The additional gainin dissolved solids is usually small because of rapid leaching of the top layer of surface material. This surface layer of soil or spoils is exposed to sufficient volumes of water to reduce the quantity of solutes to an amount substantially lower than the layer of soil or spoils immediately beneath the surface. The leached zone is probably very thin, one centimeter or less in thickness. This is sufficient, however, to protect overland flow

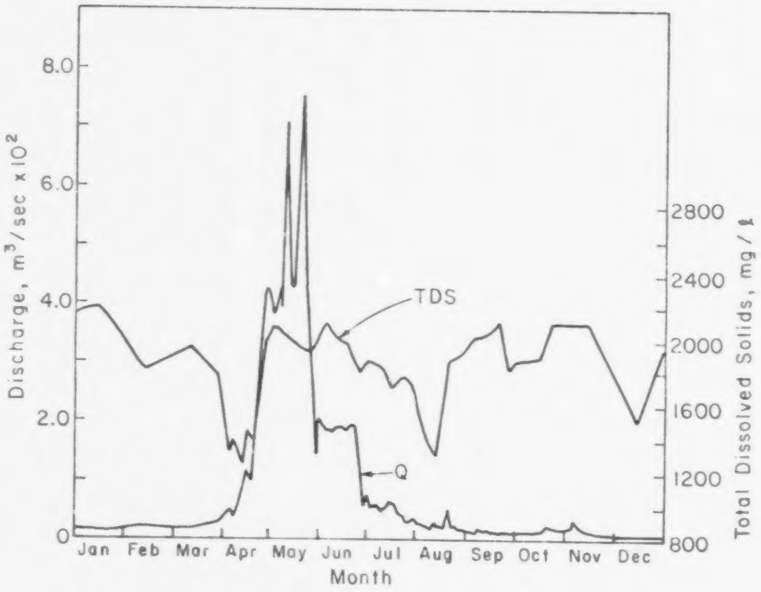

Figure 19. Discharge and water quality hydrograph for station C3, 1975.

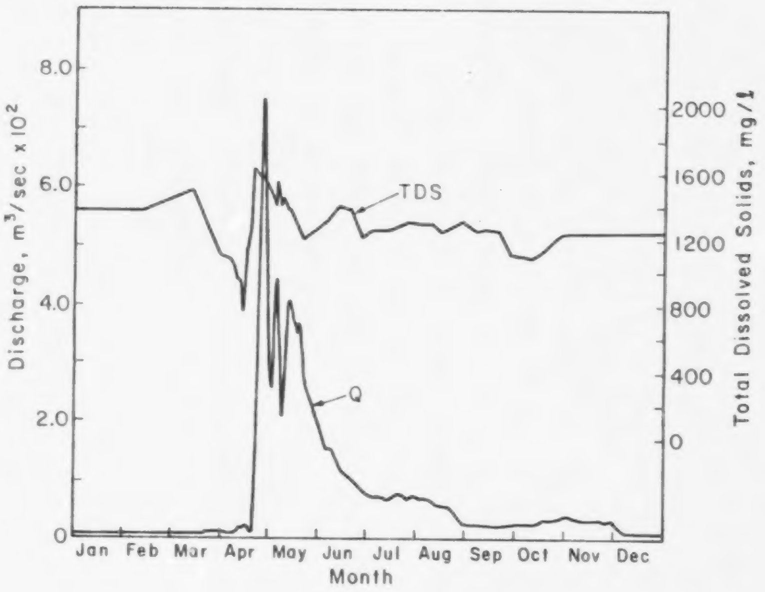

Figure 20. Discharge and water quality hydrograph for station C9, 1975.

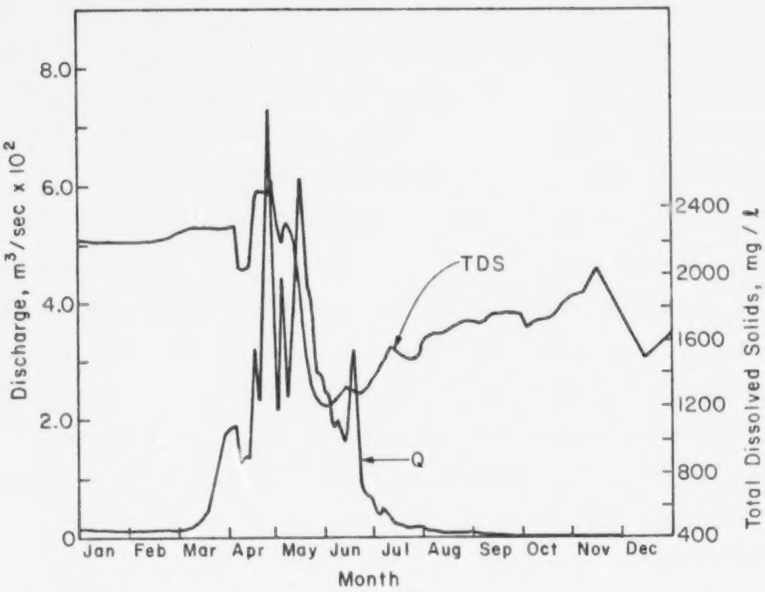

Figure 21. Discharge and water quality hydrograph for station C10, 1975.

from exposure to high concentrations of solutes in the underlying soils or spoils. Due to low precipitation, high potential evapotranspiration, and poor surface drainage, the overland flow component of stream flow is small on the Edna Mine. This observation is substantiated subsequently in this report by the results of model application.

Water samples obtained from surface runoff from the experimental plots averaged about 246 mg/l total dissolved solids with a standard deviation of σ = 58 mg/l. These samples are probably not an accurate indication of the concentration of overland flow over the entire mine site because the individual plots were often disturbed by roughening, raking, etc.. Supplementary surface water samples (see Figure 7) taken during the spring runoff averaged 149 mg/l (σ = 21 mg/l) on natural land and 158 mg/l (σ = 47 mg/l) on mined land indicating very little difference between concentrations of overland flow from mined and natural land. The surface layer on the spoils is apparently leached to a level approximately equal to that of the surface layer on undisturbed ground. A value of 150 mg/l is considered to be the average concentration of overland flow over the entire Edna Mine.

Subsurface flow contributes the largest proportion of water to the total stream flow at the Edna Mine and, therefore, is the major component influencing the concentration of dissolved solids in mine drainage. Spoil piles with their freshly exposed rock material have a large potential for releasing solutes into percolating water. The rock forming the spoils contains minerals which have not been exposed to significant volumes of leaching water before mining took place. Within the spoil piles these minerals can now be dissolved by percolating water and carried away. Natural soil has been depleted of salts by continual leaching through time.

Natural portions of the watersheds studied probably have few, if any, ground water aquifers with the possible exception of small alluvial stream channel aquifers. As water percolates into the ground it encounters bedrock forming an impermeable boundary and then flows down dip eventually to reappear in a stream channel. The concentration of subsurface water in the undisturbed areas is estimated from nineteen water samples taken during the base flow period from July 7 to November 7, 1975 at station C13 to be 462 mg/l (σ = 18 mg/l).

With the destruction of the natural rock strata in the mined areas, water is able to percolate to much greater depths in the spoils before encountering an impermeable boundary or water table. The spoils provide an abundance of soluble salts which are dissolved by leaching waters and carried out of the watershed. Tests conducted at the experimental plots indicate little or no reduction in the salt concentration of leaching water over two years of experiments. Leaching tests discussed later indicate that weathering probably replaces salts as fast as they are leached under conditions existing at the Edna Mine.

It is believed that most of the subsurface water in the spoils reappears as stream flow within the mine watersheds because of the highwall forming the western boundary of the spoils. Subsurface water in the area north of the C5 watershed reappears in numerous seeps along the base of the spoils next to Trout Creek (see Figure 5). Ground-water seeps beneath the spoils were also apparent in the C3 watershed.

The concentration of subsurface water in the spoils varies somewhat with the location and probably the depth. Dissolved solids average 3980 mg/l (σ = 439 mg/l) in 22 water samples taken at station C7 (Figure 6 and Table 2) and 4 samples taken at supplementary station #23 (Figure 7) average 4200 mg/l. An average subsurface water concentration of 3030 mg/l (σ = 540 mg/l) is found from 57 water samples collected from the subsurface drains on the experimental plots. This value is assumed to be representative of the average concentration of subsurface water for all mined portions even though several locations have higher concentrations (up to 4700 mg/l) and several have lower concentrations (down to 2000 mg/l). The C3 watershed displayed consistently lower concentrations of dissolved soilds than did the other watersheds on the mine. This may be due to significant leaching of salts in the older C3 spoils or the fact that the area was mined irregularly leaving areas of natural ground which cannot be differentiated from the mined area.

Effects of Leaching

Leaching tests conducted on a composite spoil sample from the experimental plots indicate large quantities of solids available to leaching waters. Results of the leaching test described previously are plotted in Figure 22. The initial concentration of total dissolved solids before leaching was 1178 mg/l and this concentration was reduced to 207 mg/l upon the addition of 4260 ml of water. This corresponds to 1.35 meters of water passing through the sample column. After sixty hours of aeration, the concentration rose to 318 mg/l and this was subsequently reduced to 35 mg/l with an additional leaching volume of 3600 ml (1.14 m). The sample was then dried and crushed and an initial concentration of 371 mg/l was subsequently reduced to 53 mg/l. The total quantity of water applied throughout the entire test was 12,000 ml (3.79 m).

Previous leaching tests conducted on Edna Mine spoils (McWhorter et al., 1975) indicate that a volume of water equal to about 6.8 times the bulk volume of the sample is needed to reduce the electrical conductivity of the leachate to 5 percent of the original saturated paste conductivity of the sample. Thus, 6.8 cubic meters of water must pass through 1 cubic meter of spoil material to achieve a 95 percent reduction in conductivity. This reduction results in an estimated 2.4 kg/m^3 of salts removed from the spoils. If the spoils are 20 meters in thickness, then 136 m^3 of water per square meter of spoil surface is needed to achieve a 95 percent reduction yielding 48 kg of salts per square meter of spoil area. This estimated salt yield does not include any salts being replaced by the weathering process. If 20 cm of water infiltrates into the spoils annually it would take 680 years to reduce

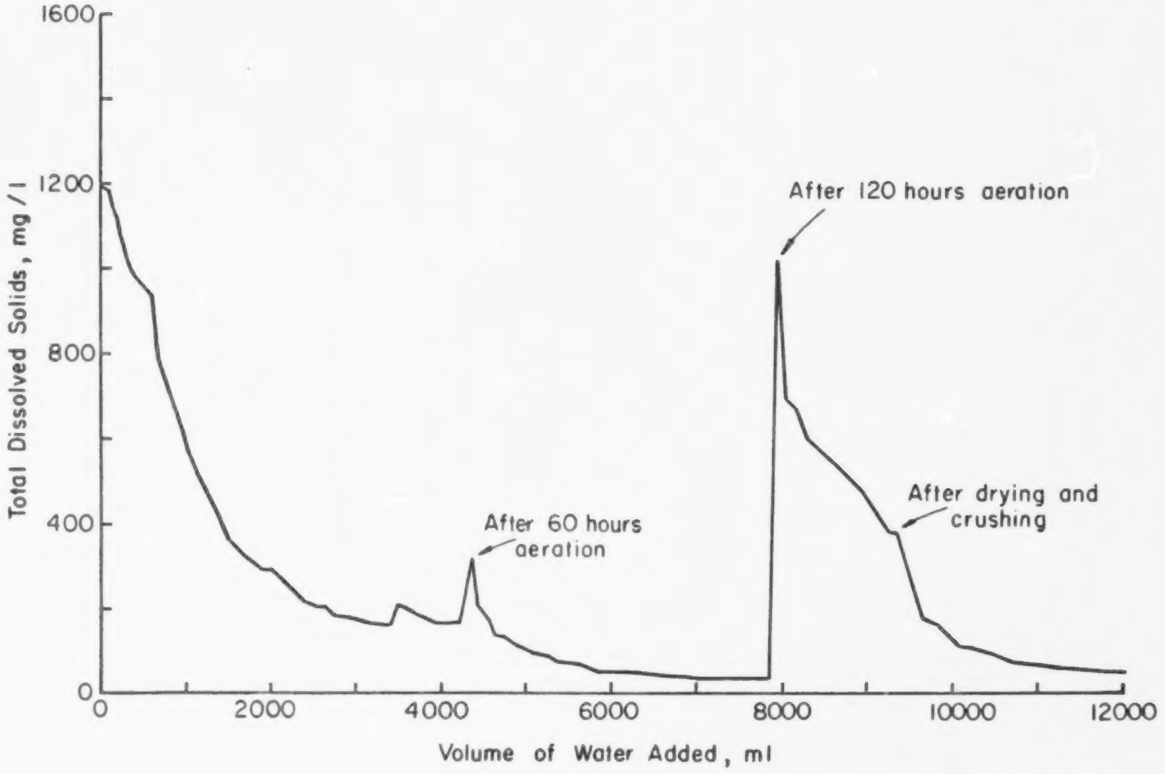

Figure 22. Results of leaching test with aeration of sample to produce weathering.

conductivities by 95 percent if weathering is not considered, and longer if weathering is considered.

Both laboratory tests and theoretical considerations indicate that a volume of water equal to about one pore volume must be passed through the spoil before an appreciable reduction in the dissolved solids concentration of the leachate is realized. A volume of water per unit area equal to about 0.2-0.5 times the total depth of the spoil bank must pass through the spoils before the effects of leaching can be expected to be significant, therefore. In arid and semi-arid regions, it is anticipated that the dissolved solids concentration in ground water runoff will not decrease for many decades after mining, except in cases where the spoil bank is thin.

Observed Discharge and Salt Load

It was mentioned previously that the total dissolved solids (TDS) concentration was not measured directly on all samples, but the electrical conductivity (EC) was determined in each case. To obtain the TDS concentration from the EC required that the relationship between these two variables be developed. The correlation between TDS and EC developed from more than 100 data points is shown in Figure 23. A regression analysis of these data yields

$$\text{TDS} = 0.367(\text{EC})^{1.107} \qquad (1)$$

where the EC is expressed in micro-mhos/cm at 25°C and the TDS concentration is in milli-grams per liter. The coefficient of determination for the above relationship is $r^2 = 0.989$.

Discharge volumes of Trout Creek and three streams flowing from the Edna Mine were determined from staff gage readings and continuous water level recorders. Water levels on the staff gages and recorders placed on the flumes are converted to discharges by using the appropriate equation for free flow conditions in cutthroat flumes developed by Skogerboe et al. (1973). Water levels of Stations C2 and C6 are converted to discharges by using the stage-discharge relationships presented previously (Figures 8 and 9).

The recorder charts were reduced by determining the two hour average stages, converting these stages to discharges, and finally averaging the two hour discharges to obtain the average daily discharge. In some instances the recorder data are not usable for several days due to clock stoppage or debris

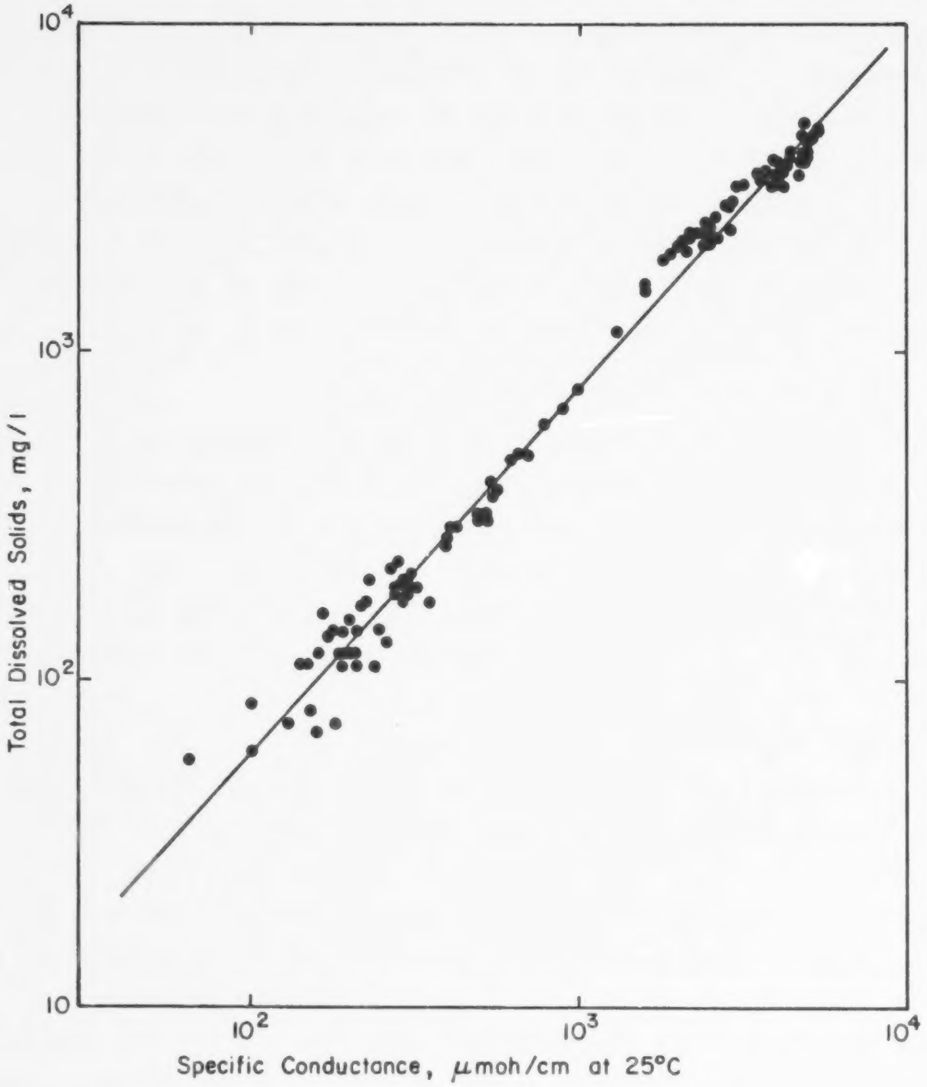

Figure 23. Plot of specific conductance versus total dissolved solids for water at the Edna Mine with line of best fit.

clogging the flumes and stilling wells. The staff gage readings are used to fill in any gaps in the data.

Discharge data are not given for Stations C5 and C13 for several reasons. At Station C5 the capacity of the original flume was often exceeded in the spring and little usable data were obtained. Only several months of data were obtained from the larger flume installed in 1976. Discharge data at Station C13 are not considered important for this study because no portion of the C13 watershed is mined.

Because a continuous record of stage at Station C6 was not obtained, a method for converting the instantaneous stage, taken about every two days, to an average daily discharge was required. Most staff gage readings at Station C6 were taken during a period in which the stage at C2 was at a fairly constant minimum value for three to five hours. The change in channel storage can, therefore, be considered equal to zero at that particular time and does not need to be considered in a routing calculation. Because the change in channel storage is negligible at the time of interest,

$$I(t) = Q_6(t) - Q_2(t) \tag{2}$$

where $I(t)$ is the inflow at time t and $Q_6(t)$ and $Q_2(t)$ are the discharges at Stations C6 and C2 at time t. The mean discharge at Station C2 for the two hour period preceeding the measurement at Station C6 is used. Thus, t actually represents this time period. The combined discharge at Stations C3, C9, and C10 is assumed to be directly proportional to the total inflow.

$$I(t) = K[Q_{10}(t) + Q_9(t) + Q_3(t)] \quad , \tag{3}$$

where $Q_{10}(t)$, $Q_9(t)$, and $Q_3(t)$ refer to the discharge at Stations C10, C9, and C3 at time t. K is a proportionality constant assumed to be invariant during the day such that the mean inflow is proportional to the sum of the mean daily discharges at Stations C10, C9, and C3.

$$I_M = K(Q_{10M} + Q_{9M} + Q_{3M}) \quad . \tag{4}$$

The subscript M refers to the mean values. The mean daily discharge at Station C6 can now be found by adding the mean daily inflow to the mean daily discharge at Station C2.

$$Q_{6M} = Q_{2M} + I_M \quad . \tag{5}$$

The constant K is determined from the instantaneous discharge at C2 and C6 at the time the C6 stage was measured.

During much of the year, excluding the period of spring snowmelt, the inflow remains relatively constant for the entire day. This allows the mean daily discharge at Station C6 to be estimated by the equation

$$Q_{6M} = \frac{Q_6(t) \cdot Q_{2M}}{Q_2(t)} \quad . \tag{6}$$

Equation 6 will yield the same result as using equations 2 through 5 if inflow is constant over the entire day.

Monthly discharge volumes are tabulated along with monthly salt loads and average monthly total dissolved solids concentrations in Table 8. Water volumes are given in units of hectare-meters or hectare-centimeters which can be converted to cubic meters by the factors 1 ha-m = $10^4 m^3$ and 1 ha-cm = $10^2 m^3$. The determination of the salt loads and average dissolved solids concentrations is discussed subsequently.

Discharge volumes in Table 8 are divided by the area of the watershed contributing to stream flow to give total runoff in terms of centimeters per year over the entire watershed area as shown in Table 9. The combined surface and subsurface runoff in 1975 from the three mine watersheds ranges from 14.4 cm on C3 to only 5.3 cm on C10. This indicates varying amounts of water lost by evapotranspiration or flow not measured at the discharge stations. Errors in delineating the watershed areas will also change the calculated runoff values in Table 9. This is especially true on the C10 watershed where surface divides have been destroyed by mining. There is also some uncertainty in determining the groundwater divides which can lead to an error in the calculated values of runoff.

The varying runoff quantities indicated in Table 9 may reflect underflow of water from the mine watersheds that is not measured at the monitoring stations. The highwall and trench on the C3 watershed probably catch most of the subsurface runoff. The highwall is not exposed over most of the C9 and C10 watersheds and thus its effectiveness as a barrier to subsurface flow is not known. During the spring of 1975 and 1976, substantial quantities of water

TABLE 8. MONTHLY DISCHARGE VOLUMES, SALT LOADS, AND AVERAGE DISSOLVED SOLIDS CONCENTRATIONS

		Station C6			Station C2			Inflow			Station C3			Station C9			Station C10		
Month	Year	Q_w (ha-m)	Q_{ds} (kgx10^{-3})	P_a (mg/ℓ)	Q_w (ha-m)	Q_{ds} (kgx10^{-3})	P_a (mg/ℓ)	Q_w (ha-m)	Q_{ds} (kgx10^{-3})	P_a (mg/ℓ)	Q_w (ha-cm)	Q_{ds} (kgx10^{-3})	P_a (mg/ℓ)	Q_w (ha-cm)	Q_{ds} (kgx10^{-3})	P_a (mg/ℓ)	Q_w (ha-cm)	Q_{ds} (kgx10^{-3})	P_a (mg/ℓ)
Nov	1973	-	139	181	77	80	104	-	59	-	66.1	15	2269	-	-	-	-	-	-
Dec	1973	-	313	243	129	155	120	-	158	-	60.5	13	2149	-	-	-	-	-	-
Jan	1974	-	182	188	97	116	120	-	66	-	68.3	14	2050	-	-	-	-	-	-
Feb	1974	-	182	303	60	83	138	-	99	-	56.6	10	1767	-	-	-	-	-	-
Mar	1974	-	372	517	72	114	158	-	258	-	75.8	13	1715	-	-	-	-	-	-
Apr	1974	-	411	587	70	90	129	-	321	-	316.0	49	1551	-	-	-	-	-	-
May	1974	-	4650	391	1189	1618	136	-	3032	-	2790.0	577	2068	-	-	-	-	-	-
Jun	1974	-	2650	192	1380	1200	87	-	1450	-	285.0	58	2035	-	-	-	-	-	-
Jul	1974	193	288	149	152	185	122	41	103	251	136.0	26	1912	-	-	-	-	-	-
Aug	1974	167	341	204	121	160	132	46	181	393	68.3	14	2050	-	-	-	-	-	-
Sep	1974	-	204	346	59	86	146	-	118	-	51.3	12	2339	-	-	-	-	-	-
Oct	1974	91	250	275	57	83	146	34	167	491	45.5	11	2418	-	-	-	-	-	-
Nov	1974	95	384	404	81	140	173	14	244	-	58.6	14	2389	-	-	-	-	-	-
Dec	1974	-	241	219	110	179	163	-	62	-	30.3	7	2310	-	-	-	-	-	-
Total	1974	-	10155	-	3448	4054	118	-	6101	-	3981.7	805	2022	-	-	-	-	-	-
Jan	1975	137	273	199	76	83	109	61	190	311	44.4	6.4	1441	49.4	3.1	628	14.8	2.7	1824
Feb	1975	128	160	125	71	62	87	57	98	172	49.4	7.9	1599	49.4	3.1	628	14.8	2.7	1824
Mar	1975	137	259	189	76	91	120	61	168	275	49.4	10.0	2024	30.9	4.3	1392	49.4	11.0	2227
Apr	1975	205	1184	578	118	137	116	86	1047	1217	355.5	57.4	1615	398.7	62.6	1570	589.9	145.2	2461
May	1975	590	2061	349	480	481	100	110	1580	1436	1185.1	233.5	1970	796.2	104.3	1310	974.0	176.1	1808
Jun	1975	1632	1858	112	1435	876	61	248	1012	408	448.1	86.5	1930	307.4	38.5	1252	451.8	57.2	1266
Jul	1975	635	689	109	518	367	71	117	322	275	128.4	23.2	1807	190.1	24.9	1310	80.2	12.5	1559
Aug	1975	193	345	179	126	148	117	67	197	294	50.6	9.9	1957	135.8	18.5	1362	29.6	5.9	1993
Sep	1975	153	249	163	86	89	103	67	160	239	29.6	5.9	1993	50.6	5.6	1107	18.5	3.2	1730
Oct	1975	161	282	175	86	84	98	75	198	264	37.0	7.3	1973	70.4	8.0	1136	16.0	2.8	1750
Nov	1975	138	298	216	126	128	102	12	170	1417	44.4	9.3	2095	70.4	6.4	909	14.8	2.7	1824
Dec	1975	153	265	173	98	118	120	55	147	267	44.4	9.3	2095	70.4	6.4	909	14.8	2.7	1824
Total	1975	4312	7953	184	3296	2664	81	1016	5289	521	2466.3	466.6	1892	2219.7	285.7	1287	2268.6	424.7	1872
Jan	1976	159	240	151	91	86	95	68	154	226	45.5	9.6	2110	3.0	0.4	1333	45.5	9.8	2154
Feb	1976	144	217	151	82	77	94	61	140	230	45.5	8.6	1890	3.0	0.4	1333	45.5	9.5	2088
Mar	1976	224	307	137	114	118	104	110	189	172	52.1	8.0	1536	3.0	0.4	1333	102.3	24.0	2346
Apr	1976	376	1493	397	167	173	104	209	1320	632	449.5	69.8	1553	390.9	46.0	1177	364.7	69.3	1900
May	1976	752	1113	148	552	374	68	201	739	368	277.5	43.6	1571	397.7	48.0	1207	212.7	30.7	1443
Total	1976	1655	3370	204	1006	828	82	649	2542	392	870.1	139.6	1604	797.6	95.2	1194	770.7	143.3	1859

TABLE 9. TOTAL YEARLY RUNOFF (CENTIMETERS)

Year	Station C2	Inflow	Station C3	Station C9	Station C10
1974	46.5	-	23.3	-	-
1975	44.5	27.8	14.4	10.9	5.3
1976*	13.6	17.8	5.1	3.9	1.8

*January through May stream flow.

were observed flowing from the base of the spoils and entering the C10 stream below the monitoring station. This water was sampled at the supplementary Station #22 and averaged about 2700 mg/l (σ = 187 mg/l). In the spring of 1976, some water from the C10 stream was diverted along a road ditch to the C9 stream due to a partially clogged culvert beneath the road. This occurred in the upper reaches of the watershed above most of the disturbed land. It is not known whether the culvert was also partially clogged in 1975 causing a similar loss of water from the C10 watershed during that year. These two water losses from the stream measured at Station C10 may explain the low runoff volumes calculated for the C10 watershed.

Total runoff of combined surface and subsurface flow over the inflow watershed between Stations C2 and C6 is about 60 percent of the total runoff on the watershed above Station C2 on a per unit area basis. Precipitation in the upper Trout Creek watershed ranges from 75 to 100 cm per year. Thus, the total runoff per unit area above Station C2 is expected to be greater than the total runoff per unit area of the watershed between Station C2 and C6 which receives only about 50 cm of precipitation per year.

The total quantity of salts discharged from the watersheds on the Edna Mine and the net increase of salts in Trout Creek from Station C2 to Station C6 are calculated from the stream flow and water quality data. Daily discharge and dissolved solids concentrations are multiplied to obtain daily salt loads which are summed to yield the monthly salt loads shown in Table 8. The average monthly total dissolved solids concentrations shown in Table 8 are found by dividing the monthly salt load by the volume of discharge. The 1974 data is from a previous study but is included here for completeness (McWhorter et al., 1975).

In 1974, 4,054,000 kg of dissolved solids passed through Station C2 and 10,155,000 kg passed through Station C6 for a net inflow of 6,101,000 kg of salts. Of this total 80 percent came in April, May, and June. The totals for 1975 were lower reflecting less runoff with 2,664,000 kg passing through Station C2 and 7,953,000 kg passing through Station C6 for a net inflow of 5,290,000 kg. Of this total 70 percent came in April, May, and June. Partial totals for 1976 show 828,000 kg passing Station C2 and 3,370,000 kg passing Station C6 for a net inflow of 2,542,000 kg by the end of May.

A more graphic representation of the water quality difference between Station C2 and Station C6 is seen by plotting average monthly dissolved solids concentrations (discharge weighted) from Table 8 in Figure 24. The concentrations at Station C2 do not vary widely during the year with the highest concentrations occurring during periods of lowest stream flow. The best water quality is found in May and June due to the dilution effect of high quality snowmelt in the upper reaches of Trout Creek.

Concentrations at Station C6 reflect a large inflow of dissolved solids during April and May between Stations C2 and C6. This inflow probably continues into June. However, the increased discharge in Trout Creek results in a lower total concentration at Station C6. The high concentrations observed at Station C6 correspond to the period of snowmelt at the elevation of the Edna Mine. As explained earlier, most of the snowmelt runoff percolates into the ground and increases in concentration before flowing into Trout Creek. Natural subsurface water concentrations (462 mg/l) are sufficiently high to increase the concentration of Trout Creek at Station C6. Therefore, the total increase in the concentration at Trout Creek is not entirely attributable to surface mining.

Dissolved solids concentrations can be normalized by dividing the total salts by the total discharge volume to give an average dissolved solids concentration which can be considered as a salt pickup rate. This rate indicates the quantity of salts dissolved per unit area per unit of runoff. Monthly dissolved solids concentrations expressed in kilograms per hectare per centimeter of runoff are plotted as the solid line in Figure 25. Estimates of these values were also made by averaging total dissolved solids concentrations from water samples without using the discharge volume as a weighting factor. The close agreement between the measured and estimated values indicates that

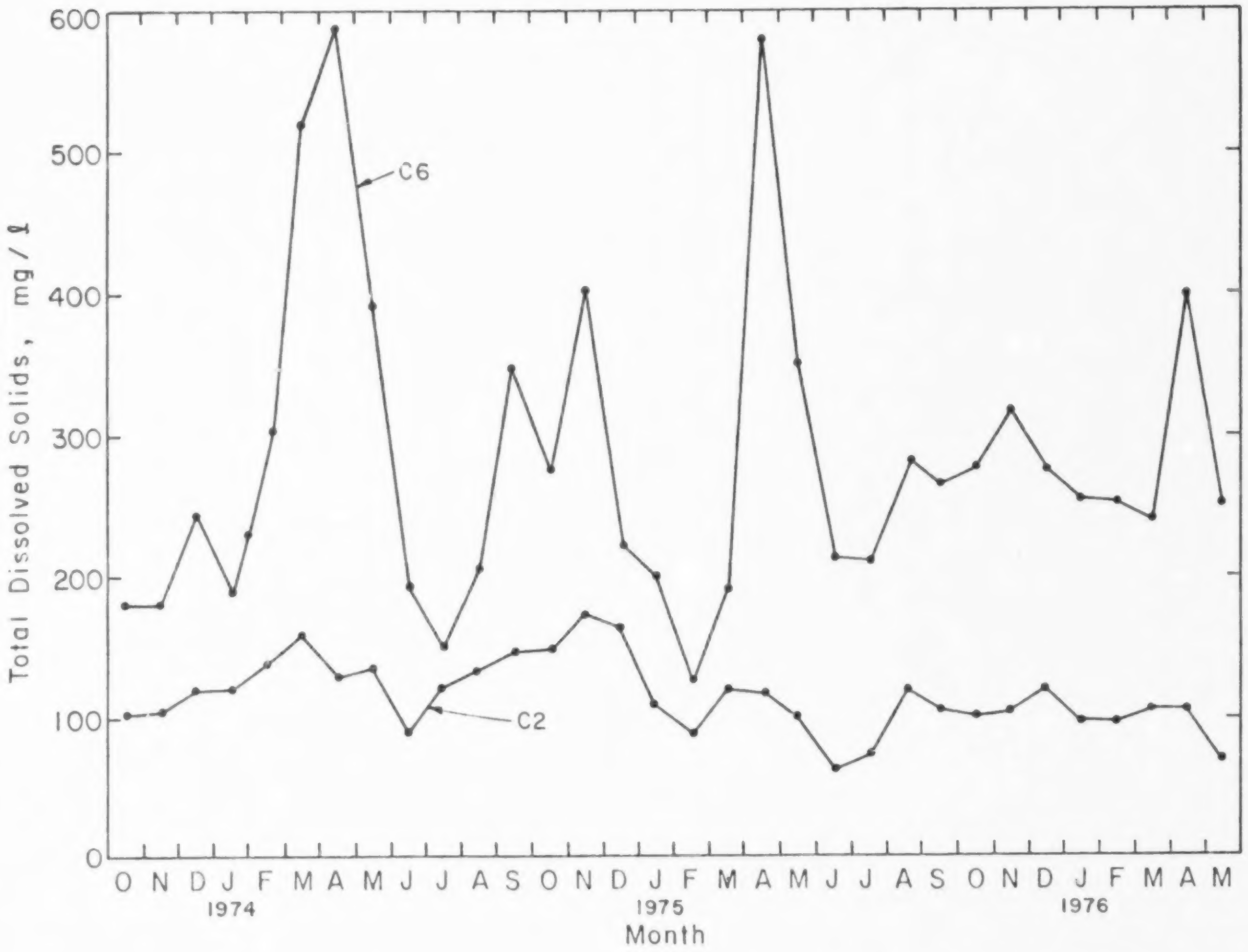

Figure 24. Average monthly dissolved solids concentrations for stations C2 and C6 on Trout Creek (discharge weighted).

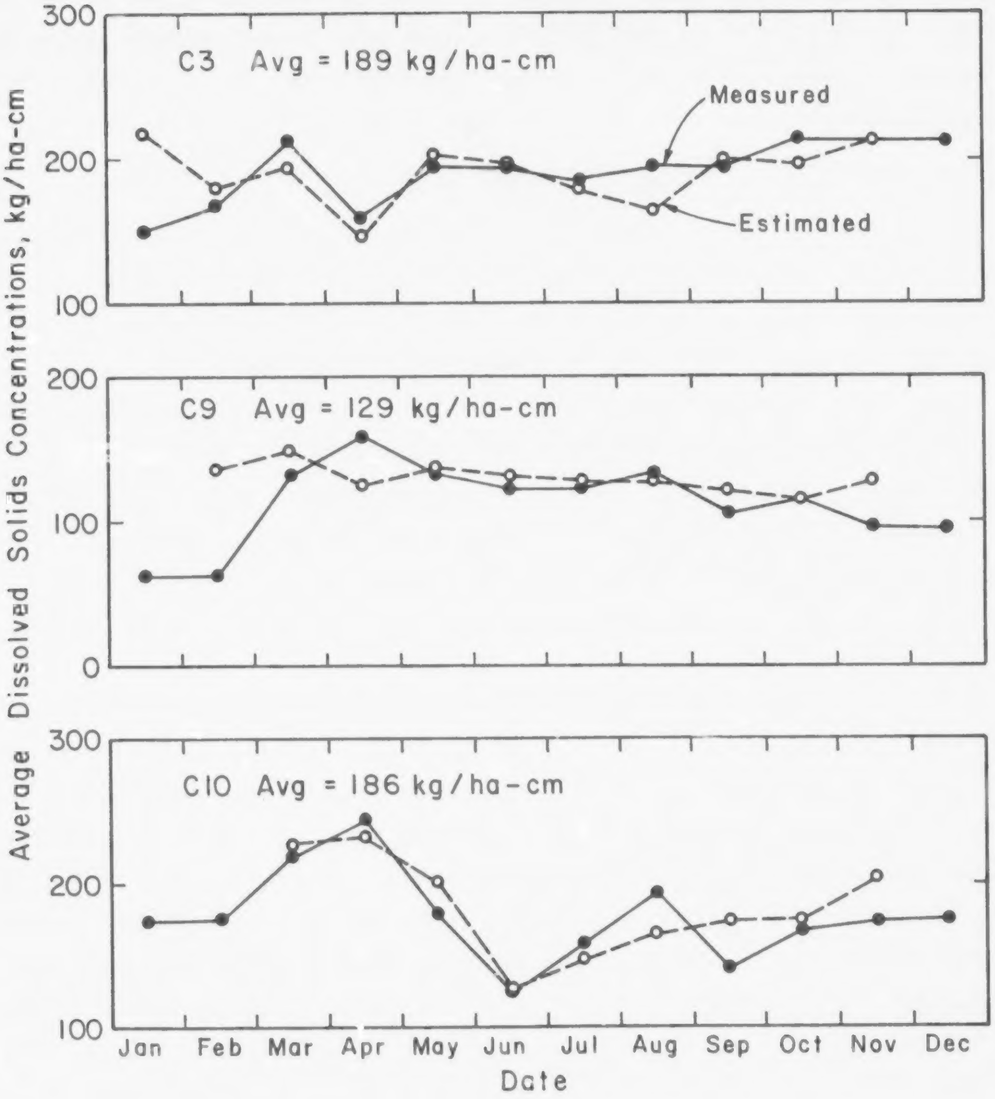

Figure 25. Comparison of actual (discharge weighted) and estimated average monthly dissolved solids concentrations.

discharge monitoring may not be necessary to determine fairly accurate average dissolved solids concentrations on a monthly or yearly basis when total dissolved concentrations remain fairly constant. Average dissolved solids concentrations at Station C5 were determined in this manner because of the lack of discharge data. In general, average concentrations should be weighted with discharge, if possible.

ANALYSIS OF FACTORS CONTRIBUTING TO SALT LOAD

In this sub-section a simple model is developed which predicts the degradation of water quality due to high concentrations of dissolved solids in mine drainage. The model is derived with respect to conditions found at the Edna Mine and is tested using the data presented in this report. The model is developed from a combination of water and mass balances written for the mine watersheds. Several investigators have used a similar approach to predict the ground water component of storm runoff and construct a base flow hydrograph.

Pinder and Jones (1969) use a mixing model to predict ground water runoff on three small watersheds in Nova Scotia. They use the equation

$$C_{tr} = (Q_{dr}C_{dr} + Q_{gw}C_{gw})/Q_{tr}$$

where C is the total dissolved solids concentration and Q is the instantaneous discharge. The subscripts tr, dr, and gw refer to total, direct (overland flow), and ground water runoff respectively. Satisfactory results are achieved when the base flow calculated from the mixing model was compared to that calculated from water levels in observation wells. The concentration of ground water was determined from water samples taken during low flow and the concentration of direct runoff was determined from water samples taken in small streams and rills during periods of very high runoff. Visocky (1969) uses the same approach to predict base flow in the Panther Creek Basin in Illinois and also finds the results satisfactory.

Water Balance

The water balance for a watershed can be expressed in terms of the volumes in each budget component during a specified time interval, Δt. For example,

$$V_p - V_e - V_s - V_g - V_d = \Delta S \quad , \qquad (7)$$

where V_p = volume of precipitation in Δt,
V_e = volume of evapotranspiration in Δt,
V_s = volume of overland flow in Δt,
V_g = volume of interflow and ground water in Δt,
V_d = volume of ground water in Δt that percolates to deep aquifers not contributing to stream flow within the boundaries of the watershed,
ΔS = change in storage volume in the watershed in Δt.

It is assumed that over a long period of time, say one year, the change in storage approaches zero. This occurs if the hydrologic system is in a state of dynamic equilibrium where total inflow equals total outflow. This must be considered as an engineering approximation since the watersheds being considered are in the process of being disturbed by mining and the inputs to the system certainly vary from year to year.

At the Edna Mine V_d is assumed to equal zero due to geologic and hydrologic conditions previously discussed. In many areas conditions are such that significant volumes of water are lost by percolation to deep aquifers in which case V_d must be considered. This component is easily incorporated into the model if the volume of water lost can be estimated.

With ΔS and V_d equal to zero, equation 7 can be rearranged so that

$$V_p - V_e = V_s + V_g = V_t \quad , \qquad (8)$$

where V_t is the total volume of drainage from the watershed in Δt.

Let A_m be the area disturbed by mining, A_n be the area undisturbed, and A_t be the total area of the watershed. The subscripts t, m, and n will refer to total, mined, and natural respectively throughout this report. Equation 8 can be written as

$$V_t = q_t A_t = q_m A_m + q_n A_n = (q_{pm} - q_{em})A_m + (q_{pn} - q_{en})A_n \qquad (9)$$

where the subscripts p and e refer to precipitation and evapotranspiration and q represents the volume of water per unit surface area of watershed.

Letting $F_m = A_m/A_t$ and $(1-F_m) = A_n/A_t$ and rearranging equation 9 gives

$$q_t = q_m F_m + q_n(1-F_m) = (q_{pm} - q_{em})F_m + (q_{pn} - q_{en})(1-F_m) \qquad (10)$$

where F_m represents the fraction of the total watershed that is disturbed by mining.

Considering the precipitation to be uniformly distributed over the watershed, then $Q_{pm} = q_{pn} = q_p$ and equation 10 can be divided by q_p and written as

$$q_t/q_p = [1 - (q_{em}/q_p)]F_m + [1 - (q_{en}/q_p)](1-F_m) \quad . \tag{11}$$

Now, let

$$f_{em} = q_{em}/q_p \quad , \quad f_{en} = q_{en}/q_p \quad , \tag{12}$$

where f_{em} and f_{en} are the fraction of precipitation lost through evapotranspiration from the mined and natural land respectively. Combining equations 11 and 12 yields

$$q_t/q_p = (1-f_{em})F_m + (1-f_m)(1-F_m) \quad . \tag{13}$$

Equation 13 states that the unit volume of combined surface and subsurface runoff as a fraction of the precipitation is a function of the fraction of precipitation lost by evapotranspiration on undisturbed and mined land and the fraction of land disturbed by mining. The two factors f_{en} and f_{em} may not be equal due to variations in vegetation, overland flow, infiltration, etc..

Dissolved Solids Balance

In formulating a mass balance it is assumed that the quantity of soluble solids available to water remains relatively constant in each component contributing to runoff. This should be an acceptable approximation for time periods of, say, several decades for reasons presented previously.

With this assumption the mass balance can be expressed as

$$V_t P_t = V_m P_m + V_n P_n \quad , \tag{14}$$

where P_t, P_m, and P_n equal the average TDS concentrations in time Δt, in drainage volumes from the entire watershed, the mined portion of the watershed, and the natural portion of the watershed, respectively. Expressed in terms of volumes per unit area, equation 14 becomes

$$A_t q_t P_t = A_m q_m P_m + A_n q_n P_n \quad , \tag{15}$$

or

$$P_t = \frac{q_m}{q_t} F_m P_m + \frac{q_n}{q_t} (1-F_m) P_n \quad . \qquad (16)$$

Since $q_m = q_p - q_{em}$ and $q_n = q_p - q_{en}$, equation 16 can be written as

$$P_t = \left(\frac{q_p - q_{em}}{q_t} \right) F_m P_m + \left(\frac{q_n - q_{en}}{q_t} \right) (1-F_m) P_n \quad . \qquad (17)$$

Multiplying by q_p/q_p and using equation 12 yields

$$P_t = \frac{q_p}{q_t} (1-f_{em}) F_m P_n + \frac{q_p}{q_t} (1-f_{en})(1-F_m) P_n \quad . \qquad (18)$$

Combination of Water and Dissolved Solids Budgets

Equation 13 can be substituted into equation 18 to give

$$P_t = \frac{(1-f_{em}) F_m P_m + (1-f_{en})(1-F_m) P_n}{(1-f_{em}) F_m + (1-f_{en})(1-F_m)} \quad . \qquad (19)$$

which can be rearranged to yield

$$P_t = \frac{P_m}{1 + \left(\frac{1-f_{en}}{1-f_{em}}\right)\left(\frac{1-F_m}{F_m}\right)} + \frac{P_n}{1 + \left(\frac{1-f_{em}}{1-f_{en}}\right)\left(\frac{F_m}{1-F_m}\right)} \quad . \qquad (20)$$

Two watershed parameters, K and R, are defined as

$$K = (1-f_{en})/(1-F_{em}) \qquad (21)$$

and

$$R = (1-F_m)/F_m \quad . \qquad (22)$$

From these definitions it is seen that K is the ratio of combined surface and subsurface runoff from the natural portion of the watershed to that of the mined portion. This means that any factors which influence the evapotranspiration on the two portions of the watershed will also influence K. For example, if runoff is greater on the mined land due to lack of vegetation, then K is less than unity. If evapotranspiration is the same on both mined and unmined portions, then K equals unity. By definition R is the ratio of the area of the natural land to the area of land disturbed by mining. Thus, R is zero for a completely mined watershed, unity for a fifty percent mined area, and infinity for a watershed with no disturbance from mining.

Substituting K and R into equation 20 yields

$$P_t = \frac{P_m}{1+KR} + \frac{P_n}{1 + \frac{1}{KR}} \tag{23}$$

or

$$P_t = \frac{KP_nR + P_m}{1+KR} \quad . \tag{24}$$

Equation 24 predicts the concentration of the total runoff from a watershed provided the parameters K and R are known and the average concentrations of flow components from the mined and natural portions of the watershed can be determined.

The concentrations of the surface water and subsurface water from mined and unmined portions of a watershed are not equal, usually. The total amount of dissolved solids from each portion can be written as a sum of surface and subsurface components such that

$$q_mP_m = q_{sm}P_{sm} + q_{gm}P_{gm} \tag{25}$$

and

$$q_nP_n = q_{sn}P_{sn} + q_{gn}P_{gn} \quad , \tag{26}$$

where the subscripts s and g refer to surface and subsurface respectively. Dividing equation 25 by q_m and equation 26 by q_n and defining

$$f_{sm} = q_{sm}/q_m \quad , \quad f_{sn} = q_{sn}/q_n \quad , \tag{27}$$

allows equations 25 and 26 to be written as

$$P_m = f_{sm}P_{sm} + (1-f_{sm})P_{gm} \tag{28}$$

and

$$P_n = f_{sn}P_{sn} + (1-f_{sn})P_{gn} \quad . \tag{29}$$

The parameter f_{sm} is the fraction of total drainage from the mined land that is overland flow and f_{sn} is the fraction of total drainage from the natural land that occurs as overland flow. Using equations 28 and 29, equation 24 can be written in an expanded form yielding

$$P_t = \frac{KR[f_{sn}P_{sn} + (1-f_{sn})P_{gn}] + f_{sm}P_{sm} + (1-f_{sm})P_{gm}}{1 + KR} \quad . \qquad (30)$$

The preceding derivation assumes that there is no chemical interaction, once in the stream, between solutes in the surface and subsurface water so that the average concentration of total runoff, P_m and P_n, can be written as a sum of the two components. The model also assumes that the volume of each component is directly related to the fraction of land mined. For instance, the model does not allow for significant volumes of groundwater from the natural land to flow underground to the mined land. Adjustments in the model to include this interaction between water from mined and natural land before it appears as streamflow may be possible but are not considered here.

An additional term must be added to the water quality model if a significant amount of water percolates to deep aquifers and, therefore, does not reappear within the boundaries of the watershed being considered. Addition of a term for deep ground water changes the water balance, equation 13, to

$$q_t/q_p = (1-f_{em} - f_{dm})F_m + (1-f_{en} - f_{dn})(1-F_m) \qquad (31)$$

and the mass balance, equation 18, becomes

$$P_t = \frac{q_p}{q_t}(1-f_{em} - f_{dm})F_m + \frac{q_p}{q_t}(1-f_{en} - f_{dn})(1-F_m)P_n \qquad (32)$$

where f_{dm} and f_{dn} are the fraction of percipitation lost by deep ground water percolation on the mined and natural land respectively.

A combination of water and mass balances again yields equation 24. However, K is now defined to include the deep ground water component and is called K'.

$$P_t = \frac{K'P_nR + P_m}{1+K'R} \qquad (33)$$

where

$$K' = \frac{1-f_{en} - f_{dn}}{1-f_{em} - f_{dm}} \quad . \qquad (34)$$

The parameters R, P_n, and P_m remain as previously defined.

Application of Budget Model

The water quality model represented by equation 30 predicts that the average concentration of runoff from a mine watershed will depend upon precipitation, evapotranspiration from natural and mined land, the fraction of the watershed mined, and average concentrations of surface and subsurface water from the natural and mined portions. If these parameters, except for the fraction of the watershed mined, do not vary from one watershed to another, then a plot of R versus the average concentration of runoff, P_t, for all watersheds on the mine will form a relationship that can be approximated by the budget equation derived above.

Before proceeding, it is convenient to summarize here all of the data and equations pertinent to the discussion in this subsection. The applicable equations are 23, 28, and 29.

$$P_t = \frac{KP_nR + P_m}{1+KR} \quad , \qquad (23)$$

$$P_m = f_{sm}P_{sm} + (1-f_{sm})P_{gm} \quad , \qquad (28)$$

$$P_n = f_{sn}P_{sn} + (1-f_{sn})P_{gn} \quad . \qquad (29)$$

Other pertinent data are contained in Table 10. The procedures by which these data were obtained have been discussed previously in this report.

A least squares regression was used to determine the fit of equation 28 to the data in Table 10. Since there are three unknowns (K, P_n, and P_m) in equation 23, the technique was one of trial and error. All of the paired values (P_t,R) in Table 10 were used except those for the inflow watershed (total watershed contributing between C2 and C6). The parameters determined from the regression analysis are K=1.04, P_m=286 kg/ha-cm, and P_n=44 kg/ha-cm. Putting these values of P_m and P_n in equations 28 and 29 along with the values of P_{sm}, P_{gm}, P_{sn}, and P_{gn} from Table 10 yields $f_{sn}=f_{sm}=0.06$.

A value of K=1.04 implies that the total runoff from the disturbed area is practically the same as from the undisturbed area. The fact that $f_{sm}=0.06$ means that only 6 percent of the total runoff occurs as overland flow. Small overland flow relative to ground water runoff results from highly permeable spoils, a spoil topography that does not contain well developed drainage

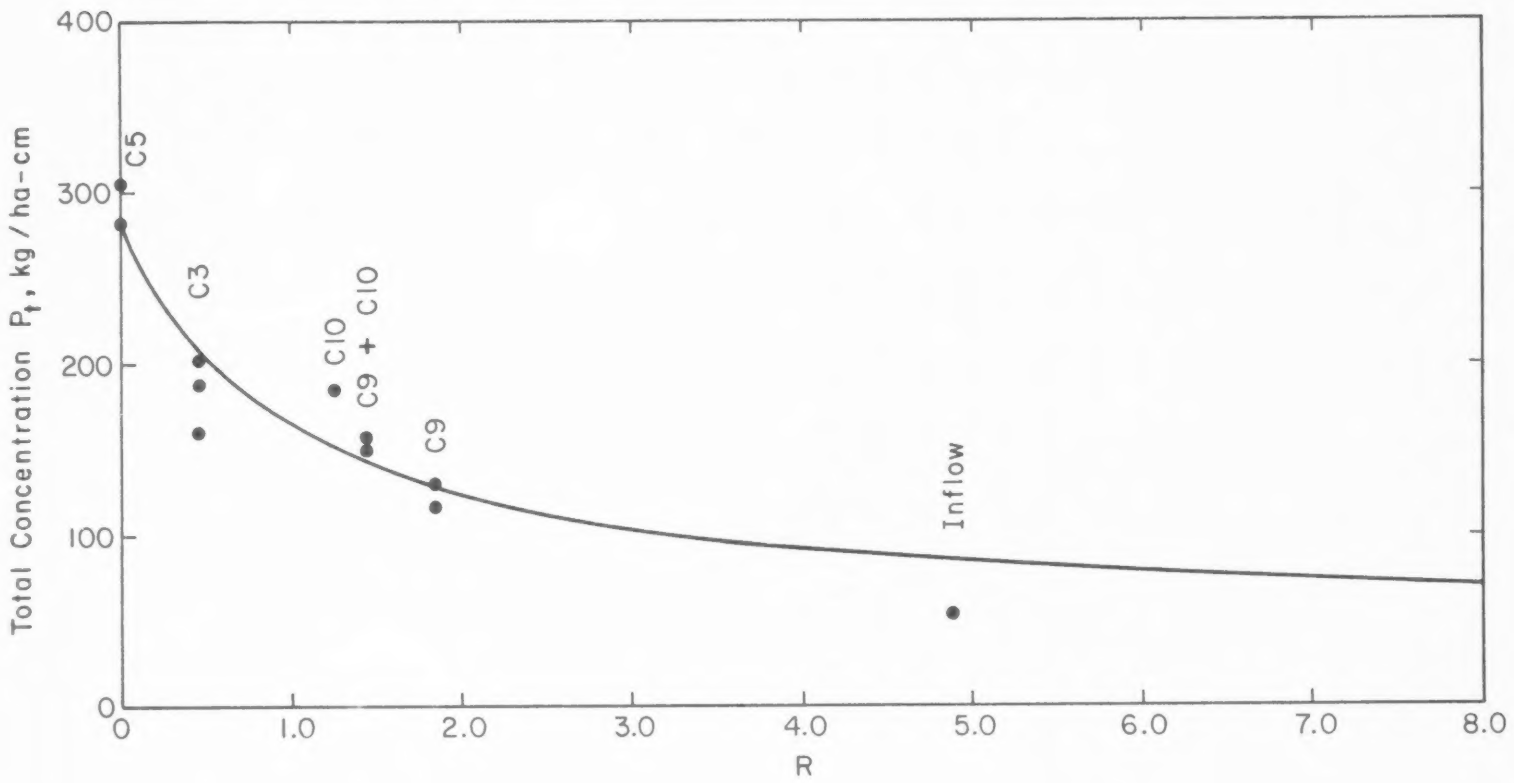

Figure 26. Plot of R versus P_t with best fit curve found for $K = 1.04$, $f_s = 0.06$.

TABLE 10. SUMMARY OF DATA USED IN APPLICATION OF MODEL TO STUDY AREA

Watershed	Year	F_m	R	P_t	P_{gm}	P_{gn}	P_{sm}	P_{sn}
					(kg/ha-cm)			
C3	1974	0.68	0.47	203	303	46	15	15
C5	1974	1.00	0.00	283	303	46	15	15
C3	1975	0.68	0.47	189	303	46	15	15
C5	1975	1.00	0.00	283	303	46	15	15
C9	1975	0.35	1.86	129	303	46	15	15
C10	1975	0.44	1.27	186	303	46	15	15
C9+C10	1975	0.41	1.44	158	303	46	15	15
Inflow	1975	0.17	4.88	52	303	46	15	15
C3	1976	0.68	0.47	161	303	46	15	15
C5	1976	1.00	0.00	308	303	46	15	15
C9	1976	0.35	1.86	119	303	46	15	15
C10	1976	0.44	1.27	185	303	46	15	15
C9+C10	1976	0.41	1.44	152	303	46	15	15
Inflow	1976	0.71	4.88	39	303	46	15	15

patterns, and the relatively low rate at which water from snowmelt becomes available for runoff.

The degree to which equation 23, with the parameters determined from the regression analysis, agrees with the field observations is shown in Table 11. The indicated agreement is believed to be good considering the complexity of the physical-chemical processes involved and the simplicity of the model.

The values of P_t and R measured for the entire inflow watershed were not included in the above analysis because the watershed is made up largely of areas not affected by mining and because it is sufficiently large to cause doubt that the parameters in the model are the same as on the C3, C5, C9, and C10 watersheds. It is, nevertheless, instructive to assume that model applies to the inflow watershed as well. Also, since the indicated value of K is near unity, K is set equal to 1.0. In this case, equation 23 becomes

$$P_t = (P_m - P_n)F_m + P_n \quad , \qquad (35)$$

TABLE 11. COMPARISON OF MEASURED AND CALCULATED CONCENTRATIONS OF DISSOLVED SOLIDS IN WATERSHED DRAINAGE

Station	Year	Observed P_t kg/ha-cm	Calculated P_t kg/ha-cm	Error %
C3	1974	203	206	+ 1.5
C5	1974	283	286	+ 1.0
C3	1975	189	206	+ 8.0
C5	1975	283	286	+ 1.0
C9	1975	129	126	- 2.3
C10	1975	186	148	-20.4
C9+C10	1975	158	141	-10.8
C3	1976	161	206	+21.8
C5	1976	308	286	- 7.1
C9	1976	119	126	+ 5.6
C10	1976	185	148	-20.0
C9+C10	1976	152	141	- 7.2
			Average =	+ 8.9

indicating a linear relationship between P_t and the fraction F_m of the watershed that is disturbed. Equations 28 and 29 are unchanged.

Figure 27 shows a linear regression fit of equation 35 to the data in Table 10. Note that in data for the inflow watershed has been included in this analysis. The regression coefficients yield P_m=292 and P_n=29. Also, from equations 28 and 29, f_{sm}=0.04, implying that only 4 percent of the total runoff from the disturbed ground is overland flow, and f_{sn}=0.55 which indicates that 55 percent of the runoff from the natural area is overland flow. The undisturbed C13 watershed constitutes a large fraction of the inflow watershed and is significantly steeper than the C3, C5, C9, and C10 watersheds. It is reasonable to assume that overland flow from the C13 watershed would, indeed, comprise a larger percentage of the total runoff than on the other watersheds in the study area. However, the C13 watershed rises to much greater elevations than the other watersheds in the study, and definitely receives more precipitation. This fact violates the assumption of uniform precipitation over the area to which the model is applied and the indicated

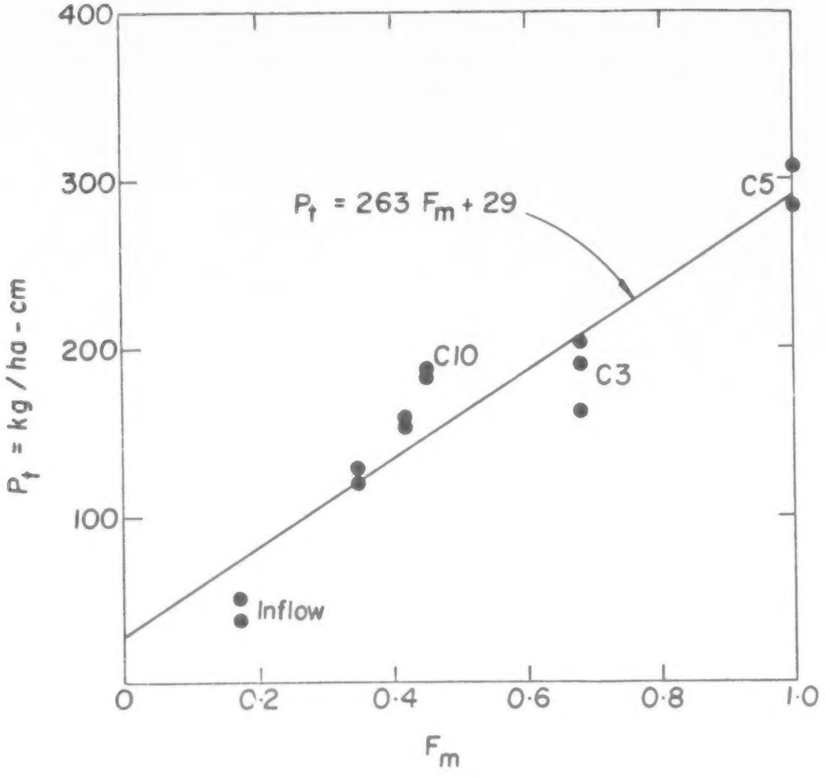

Figure 27. Linear regression line.

f_{sn} is probably too large for the C3, C5, C9, and C10 watersheds.

Influence of Disturbed Ground on Observed Salt Pickup

Ideally, the influence of mining should be determined by comparing the water quality hydrology before and after mining. This was not possible, of course, in this study and the effect of the mined land had to be estimated from the post-mining data. This is accomplished by using the model parameters estimated above.

In Table 12, the effect of the disturbed ground on the measured salt pickup between Stations C2 and C6 is summarized. The calculations are based on the assumption that the model parameters determined from the data on the C3, C5, C9, and C10 watersheds apply to the inflow watershed. Note that 54 percent of the total salt pickup was contributed by the disturbed ground which

TABLE 12. EFFECT OF MINING ON SALT PICKUP BETWEEN C2 AND C6 IN 1975

	Area		Total salt pickup	Contribution from area now occupied by spoils					
				Total		Overland Flow		Groundwater	
State (1)	Disturbed ha (2)	Natural ha (3)	ha (4)	kg (5)	% of (4) (6)	kg (7)	% of (5) (8)	kg (9)	%of(5) (10)
Without Mining	0	3656	2,924,000	491,000	17	9000	2	482,000	98
With Mining	614	3042	5,289,000	2,856,000	54	9000	0.3	2,847,000	99.7
Increase	-	-	2,365,000	2,365,000	100	0	-	2,365,000	100

comprises 17 percent of the total contributing area. Also, it is estimated the more than 99 percent of the total salt pickup from the disturbed area results from dissolved solids in the ground water runoff.

According to the theory developed herein, the above percentages are constants and do not change with the amount of precipitation. Thus, the contribution from the mined area, in terms of percent, will be the same from year to year. This is only approximately true in reality, of course, because the assumptions underlying the development of the model do not correspond, in all respects, to the actual phenomena. The values of salt pickup, on the other hand, depend directly upon the precipitation and will, therefore, vary from year to year. The fact that this simple model is independent of input volumes means that one can generate runoff volumes by any appropriate method and, after this is accomplished, calculate the salt pickup on a year to year basis. In other words, it is possible to model the hydrology without regard for water quality considerations and then, subsequently, compute the salt pickup rates based on the estimated runoff volumes. In fact, it is for this reason that the concentrations in the model have been expressed in units of kg/ha-cm. All that is required to obtain salt pickup is to multiply by the area in hectares and the runoff in cm.

The above data strongly suggest that spoil management practices that promote overland flow runoff relative to ground water runoff will improve the resulting water quality. Other considerations, such as maximizing soil moisture for plant growth and soil erosion control are not necessarily compatible with a practice of promoting surface runoff, however. Maximizing the evapotranspiration on the disturbed ground will also increase the quality of total runoff by reducing the volume of ground water runoff. In the study area, however, it is probable that infiltration from snowmelt in the spring exceeds the water holding capacity of the root zone (at least for shallow rooted species) and deep percolation will occur even under well vegetated spoils. In other areas that receive less precipitation or where water becomes available for infiltration more uniformly in time, vegetation should be an effective agent for the reduction of deep percolation and, therefore, the improvement of water quality.

The effect upon the water quality of increasing consumptive use of water by revegetation or of increasing overland flow at the expense of ground water runoff can be estimated with the simple model under discussion. For example, several curves of P_t vs. R are shown in Figure 28 with different values of the water use factor K and the runoff factor $f_s=f_{sm}$. The concentrations of surface and subsurface water found in the study area are used to calculate these curves. It is apparent that increasing the fraction of overland flow while holding K constant decreases the concentration in the total runoff. The concentration also decreases if K is increased while holding f_s constant.

As a more concrete example of how the model can be used to evaluate management practices, the effect of increasing the fraction of overland flow on the disturbed area from 0.06 to 0.4 on the Edna Mine is calculated and the results presented in Table 13. The water use factor K is held constant and equal to unity. This calculation indicates that the increase in the overland flow component of runoff at the expense of ground water runoff on the disturbed area will decrease the concentration of mine drainage by 34 percent and decrease the concentration and total salt pickup on the inflow watershed by 20 percent.

TABLE 13. EFFECT OF INCREASING OVERLAND FLOW FROM 6 TO 40 PERCENT ON THE DISTURBED GROUND AT THE EDNA MINE

	Area		Concentrations		Total salt pickup
	Disturbed (ha)	Natural (ha)	P_m (kg/ha-cm)	P_t	(kg)
Present, $f_{sm}=0.06$	614	3042	286	85	5,289,000
Modified, $f_{sm}=0.4$	614	3042	188	68	4,231,000
% Reduction	-	-	34	20	20

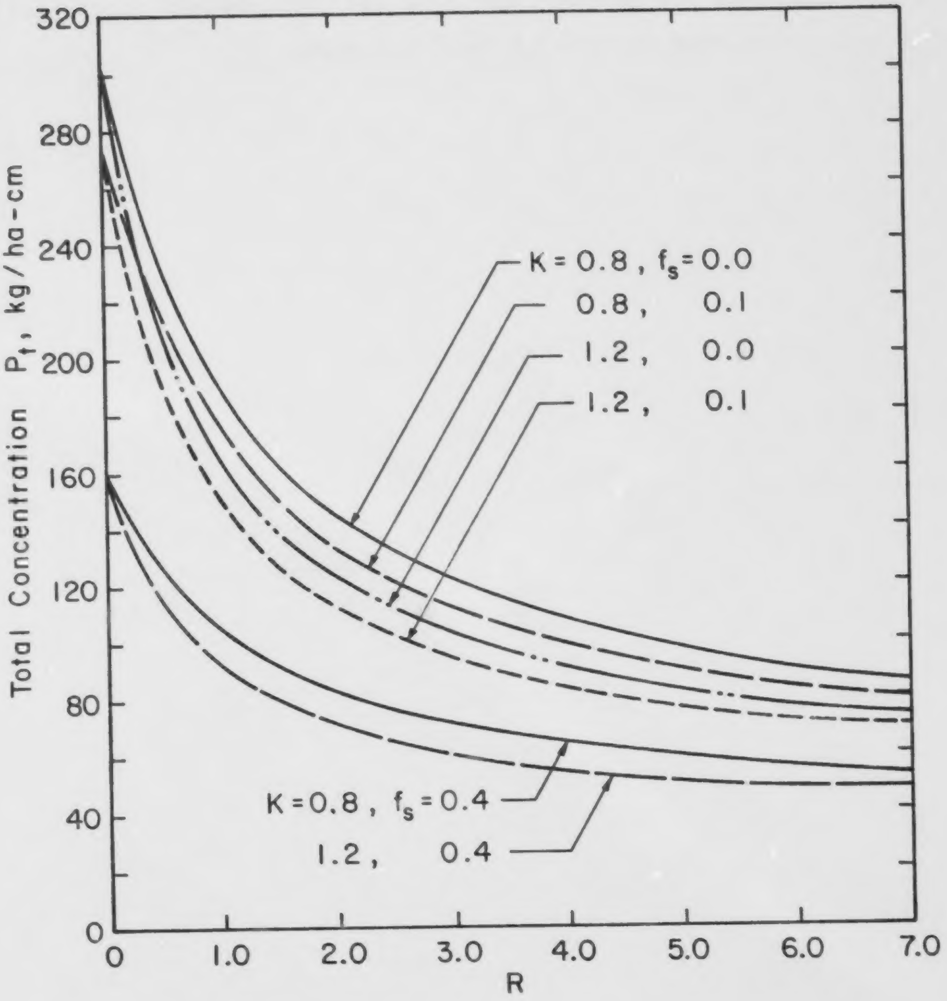

Figure 28. Plot of R versus P_t for various values of K and f_s.

A similar calculation can be made for an increased consumptive use of water on the mined area. However, the data (K=1.04) indicates that the average consumptive use of water on the disturbed ground is already practically equal to that on the natural watershed at the present time. It is not likely that the consumptive use on the mined area can be increased appreciably above that of the undisturbed portion by practical means.

SECTION 5

SOME LIMITING EFFECTS OF AQUIFER DISRUPTION

The mine described in Section 4 is, for all practical purposes, a dry mine. No significant aquifer was disrupted in the process of coal extraction from the Wadge seam. In some areas of the western states, aquifers exist above the coal seam and sometimes the coal seam itself is an aquifer. In a subsequent section of this report, a numerical model is presented that is capable of predicting the effect of aquifer disruption upon the flow in the aquifer as a function of time and mined area geometry. However, some interesting and important limiting effects of aquifer disruption can be derived analytically for a simple geometry. For example, it is found that the maximum distance to which the long term steady flow pattern is modified by disrupting an aquifer and replacing it with spoil material is independent of both the permeability in the aquifer and in the disrupted portion. This is important because it permits one to calculate the maximum effect of the disruption without knowledge of permeability values. Thus, the results of this section should be useful in preliminary planning and feasibility analyses.

STEADY FLOW PATTERNS IN DISRUPTED AQUIFERS

The actual flow pattern in a disrupted aquifer is quite complex, undoubtedly, and must depend upon the original flow pattern, time, the geometry of the disrupted area, the location of the disrupted area with respect to aquifer boundaries, and the distributions of hydraulic conductivity (permeability) in the disturbed and undisturbed portions of the aquifer. Prediction of the post-mining flow pattern, in all its complexity, is a difficult task requiring a great deal of data that is, often, not available. A first approximation to the post-mining pattern of flow in a disrupted aquifer can be derived by assuming that:

1) the aquifer is very large in areal extent,

2) the flow in the aquifer is uniform and one-dimensional at large distances from the mined area,

3) the hydraulic conductivity K_i of the spoil material in the disturbed portion of the aquifer is a constant,

4) the hydraulic conductivity K_o of the undisturbed aquifer is a constant,

5) the geometry of the disturbed portion of the aquifer is that of a cylinder with the axis normal to the plane of the flow, and

6) the flow is two-dimensional and steady.

In plan view, the portion of the aquifer that has been removed by mining and replaced with spoil material is a circle (Figure 29) under the above assumptions. Also shown in Figure 29 is the uniform flow in the x-direction as well as the polar coordinate (r,θ) system.

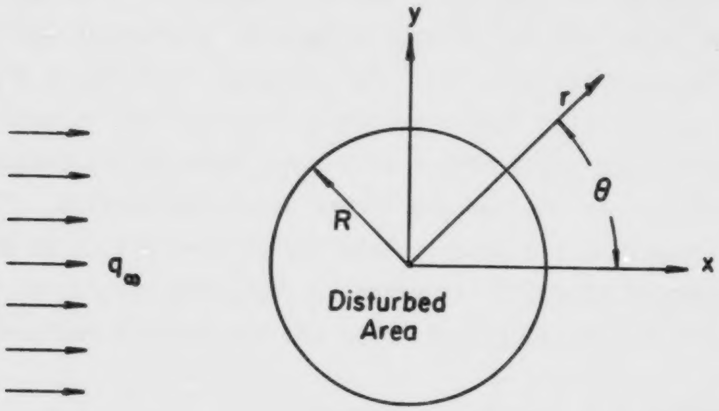

Figure 29. The coordinate system and geometry used to calculate the pattern of flow in a disturbed aquifer.

Let $h_i(r,\theta)$ be the piezometric head inside the disturbed region and $h_o(r,\theta)$ be the head outside the disturbed region. The differential equation for which solutions describe the flow pattern is the Laplace equation in both regions with h_i as the dependent variable inside the disturbed region and h_o the dependent variable outside the disturbed region. The condition of continuity requires that the component of volume flux normal to the boundary between the regions be the same for region i and region o at the boundary. Furthermore, there can be no discontinuity in piezometric head on the boundary.

Mathematically,

$$K_i \frac{\partial h_i}{\partial r} = K_o \frac{\partial h_o}{\partial r} \quad \text{on} \quad r=R \tag{36}$$

and

$$h_i = h_o \quad \text{on} \quad r=R \tag{37}$$

where R is the radius of the disturbed portion.

The solution when K_i is zero is well known, being a classical problem in hydrodynamics. The solution when K_i is not zero is written

$$h_i = Ax \tag{38}$$

$$h_o = \frac{q_\infty}{K_o} + \frac{Bx}{r^2} \tag{39}$$

which satisfy the Laplace equation and the boundary conditions at infinity. It remains to determine the constants A and B so that equations 36 and 37 are satisfied. This is accomplished by putting equations 38 and 39 into conditions 36 and 37, yielding two equations in the unknowns A and B. Solving the equations simultaneously for A and B yields the desired results:

$$h_o = \frac{q_\infty}{K_o} x \{1 + (\frac{K_o-K_i}{K_o+K_i})(\frac{R^2}{x^2+y^2})\} \tag{40}$$

$$h_i = \frac{2q_\infty}{K_o+K_i} x \quad . \tag{41}$$

Equations 40 and 41 can be used to compute equipotential lines inside and outside the disturbed region if desired. The flow pattern is more readily visualized, however, by deriving the stream functions from which streamlines are computed. The relationship between the stream function ψ and the piezometric head h are

$$\frac{\partial\psi}{\partial x} = q_y = - K \frac{\partial h}{\partial y} \tag{42}$$

and

$$\frac{\partial\psi}{\partial y} = -q_x = K \frac{\partial h}{\partial x} \quad . \tag{43}$$

Applying equations 42 and 43 with equations 40 and 41 yields the following equations for the stream functions outside and inside the disturbed area, respectively.

$$\psi_o = q_\infty\, y\{1 - (\frac{K_o-K_i}{K_o+K_i})(\frac{R^2}{x^2+y^2})\} \qquad (44)$$

$$\psi_i = (\frac{2q\ K_o}{K_o+K_i})\, y \quad . \qquad (45)$$

Examples of flow patterns predicted by the stream functions are shown in figuges 30a and 30b for $K_i/K_o = 0.5$ and $K_i/K_o = 5$. It is evident that there is a tendency for the streamlines to converge toward the mined area if the hydraulic conductivity in the disturbed area is greater than outside the disrupted portion. Flow tends to be diverted around the mined area if K_i is less than K_o.

The practical limits of the area within which the aquifer disruption modifies the flow pattern appreciably can be computed from equation 44. This is accomplished by noting that all of the effects of the mined area on the flow are represented by the second term in braces in equation 44. Therefore, the effect of the aquifer disruption on the flow pattern is negligible when

$$\left|\frac{K_o-K_i}{K_o+K_i}\right| \frac{R^2}{x^2+y^2} = C << 1 \quad , \qquad (46)$$

where C is a positive constant. From equation 46, the perimeter of the area within which the flow pattern is significantly modified forms a circle of radius r given by

$$r = \frac{R}{\sqrt{C}} \left(\left|\frac{K_o-K_i}{K_o+K_i}\right| \right)^{\frac{1}{2}} \quad . \qquad (47)$$

The value of the constant C is determined by the user's judgement as to what constitutes a negligible effect. For example, suppose $K_i = 2K_o$ and the effect of the disruption on the flow pattern can be considered negligible if the effect is 5 percent or less. Then $C = 0.05$ and $r = 2.6R$ from equation 47. This computation means that outside of a circle of radius 2.6R the flow pattern is not significantly different from the pre-mining pattern.

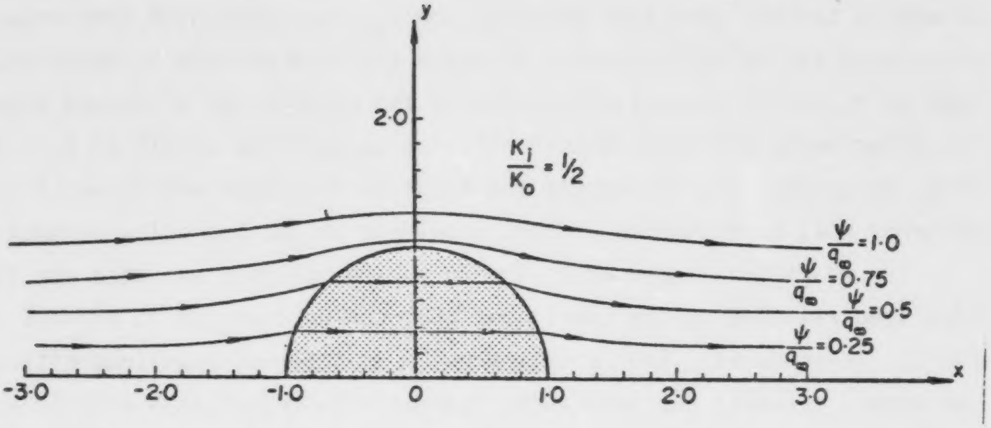
y
2·0
$\frac{K_i}{K_o} = 1/2$
$\frac{\psi}{q_\infty} = 1{\cdot}0$
$\frac{\psi}{q_\infty} = 0{\cdot}75$
$\frac{\psi}{q_\infty} = 0{\cdot}5$
$\frac{\psi}{q_\infty} = 0{\cdot}25$
x
-3·0
-2·0
-1·0
0
1·0
2·0
3·0

Figure 30a. Flow pattern in a disrupted aquifer, $K_i/K_o = 0.5$.

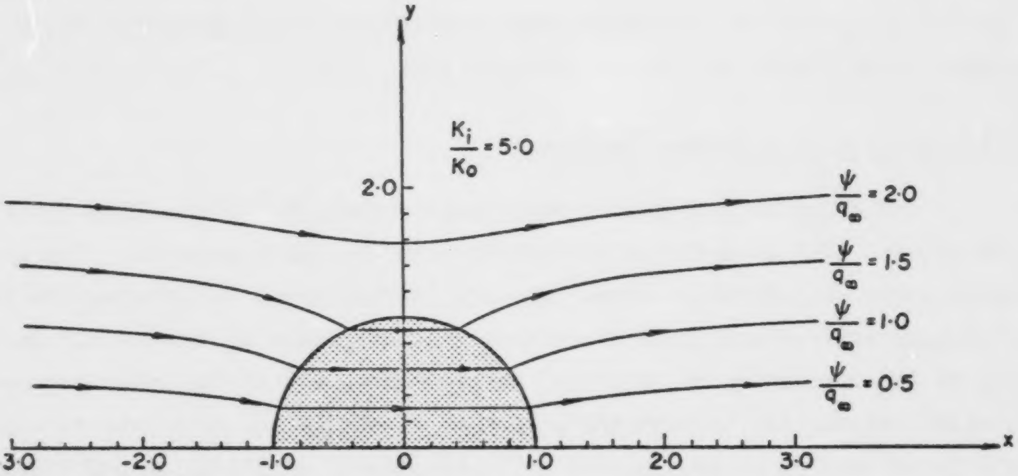
y
$\frac{K_i}{K_o} = 5{\cdot}0$
2·0
$\frac{\psi}{q_\infty} = 2{\cdot}0$
$\frac{\psi}{q_\infty} = 1{\cdot}5$
$\frac{\psi}{q_\infty} = 1{\cdot}0$
$\frac{\psi}{q_\infty} = 0{\cdot}5$
x
-3·0
-2·0
-1·0
0
1·0
2·0
3·0

Figure 30b. Flow pattern in a disrupted aquifer, $K_i/K_o = 5$.

It is important to note that r in equation 47 approaches a maximum

$$r_{max} = R/\sqrt{C} \tag{48}$$

when either K_i approaches zero or K_i approaches infinity. Since K_i will always be between zero and infinity, the r_{max} as calculated from equation 48 represents the maximum distance to which the flow pattern is modified, regardless of hydraulic conductivities inside and outside the disturbed area. On the other hand, the flow pattern will not be modified at all if $K_i = K_o$. Thus, it is possible to compute the range of distances within which the flow patterns will be disturbed without knowledge of the hydraulic conductivities.

The conditions under which the foregoing analysis was made are highly idealized relative to the conditions that can be expected to prevail in the field. Nevertheless, the results provide an order-of-magnitude estimate of the extent to which the long-term, post-mining flow pattern will be modified. When used with caution and good judgement, the results should be useful in preliminary planning, screening, and evaluation. For example, one criticism that can be raised immediately is that rarely, if ever, is the plan view geometry of a mine that of a circle. However, if one uses one-half the maximum dimension of the disturbed area, regardless of its geometry, for R the resulting estimates will be on the safe side.

WATER QUALITY IN DISRUPTED AQUIFERS

The quality of groundwater which passes through the disrupted portion of the aquifer will be modified by contact with the spoil material. The groundwater under consideration here, however, is that which is contained in the disrupted aquifer and is distinct from that discussed in Section 4. According to the preceeding mathematical developments, all of the water between the streamlines passing through the points (0,R) and (0,-R) must pass through the disrupted portion of the aquifer. If the effects of diffusion and dispersion are negligible, the water of modified quality will remain between these two streamlines, downstream of the disruption. The values of the stream function ψ_o/q_∞ for x = 0 and y = ±R are

$$\psi_o/q_\infty = \pm R \{1 - \frac{K_o-K_i}{K_o+K_i}\} \tag{49}$$

and the equations of the streamlines between which the water of modified quality is constrained are

$$y \{1 - (\frac{K_o-K_i}{K_o+K_i})(\frac{R^2}{x^2+y^2})\} = \pm R \{1 - (\frac{K_o-K_i}{K_o+K_i})\} \qquad (50)$$

The streamlines represented by equation 50 are the practical boundaries between which water of modified quality will be constrained. The width W of the zone of modified water quality far downstream of the disrupted portion is

$$W = \frac{4RK_i}{K_o+K_i} \qquad (51)$$

obtained by letting x become large in equation 50. Clearly, if $K_i = K_o$, the width of the affected zone is equal to the diameter of the disrupted portion; if K_i is less than K_o, the downstream width of the effect zone is less than the diameter of the mined area. The maximum W is obtained when the hydraulic conductivity K_i is very large relative to the hydraulic conductivity K_o outside the disrupted region:

$$W_{max} = 4R \quad . \qquad (52)$$

It is apparent that the maximum width of the zone of modified water quality is independent of the hydraulic properties of the aquifers, just as is the case for the zone of modified flow pattern.

The rate of movement of inorganic dissolved solids into the aquifer downstream of the disturbed area is the product of the discharge Q_a through the mined portion and the concentration P_a of dissolved solids. The data and discussion in Section 4 of this report suggest that P_a can be estimated from the TDS concentration in saturation extracts prepared from drill cuttings of the overburden or from the spoils themselves if available. The discharge Q_a through the disrupted portion of the aquifer is calculated from Darcy's law and equation 41 or by calculating the difference between the values of the streamlines given in equation 50. Multiplying Q_a by P_a yields

$$Q_a P_a = \frac{4q_\infty mK_i}{K_o+K_i} P_a \qquad (53)$$

where m is the aquifer thickness. Before mining, the rate of movement of dissolved solids through the same area is $Q_oP_o = 2Rq_\infty mP_o$. Therefore, the ratio of post-mining discharge of dissolved solids to the pre-mining value is

$$\frac{Q_aP_a}{Q_oP_o} = \left(\frac{2K_i}{K_o+K_i} \right) \frac{P_a}{P_o} \quad . \tag{54}$$

Supposing for the moment that water that passes through the disrupted portion picks up additional dissolved solids (i.e., $P_a > P_o$), equation 54 predicts that maximum degradation of downstream receiving waters will occur when K_i is very large relative to K_o. In the limit,

$$\left(\frac{Q_aP_a}{Q_oP_o} \right)_{max} = 2 \frac{P_a}{P_o} \quad , \tag{55}$$

a result that is, again, independent of the hydraulic properties of the aquifers. Equation 55 actually implies that the maximum discharge Q_a through the disrupted region is twice that which flowed through the same region prior to disturbance. Equations 51 and 54 both suggest that the effect of aquifer disruption on water quality is minimum when K_i is minimum. In fact, if K_i is very small relative to K_o, the disturbed portion will have no appreciable effect on the water quality in the disrupted aquifer.

SECTION 6

EXPERIMENTAL STUDIES

Several experimental investigations were conducted as an integral part of the project. The primary purposes of the experiments were to obtain data for comparison with the mathematical models to be described in subsequent sections of this report and to obtain various functions and parameters required in the models. Results from the experiments are presented where they are used in conjunction with the model studies rather than in this section.

MATERIALS AND METHODS

Experiments were carried out in the field in Colorado and Montana on volumetric lysimeters filled with mine spoils. These facilities were equipped so that subsurface drainage, surface runoff, and soil-moisture storage could be monitored.

Lysimeter Construction

The field test plots consist of volumetric lysimeters with a water application system. The original proposal called for the construction of four such facilities at the Edna Mine. The project expansion on July 1, 1975, called for two lysimeters to be constructed at the Montana site. The four lysimeters in Colorado were completed in the fall of 1974, and those in Montana in September 1975. Two parallel depressions in the mine spoils were located which roughly suited the plot requirements. Two D-9 bulldozers, provided by the Pittsburg and Midway Company, were used to fill and shape these depressions to fit the plot dimensions more closely. The final excavations formed an H-shaped depression, 3-4 meters deep with nearly vertical sides. Two plots were constructed on each leg of the H. The transverse excavation connecting the legs of the H is being used for the subsurface drain outlet facilities for all the plots. The general layout of the plots, drain lines, and instrument houses are shown in Figure 31.

The plots were surveyed and staked and then leveled and smoothed by hand. The base dimensions of the plots are 4.0 m by 9.2 m. The next step was to spread a vinyl membrane over the base of the plots. The membrane was provided by the manufacturer in one continuous piece, 260 feet long and 38 feet wide. It was only necessary to cut the curtain into 4 desired lengths. The membrane is a 10 mil poly-vinyl-chloride material which is quite resistant to puncture and ripping.

After the membrane was spread on the base of the plots, a layer of gravel, approximately 6-8 inches thick was spread by hand. Elevations of the corners of the plots were measured and recorded. A trench was made by hand in the gravel down the center of the plot, and 4-inch perforated plastic pipe was placed on a grade. The drain was then covered with gravel to form a filter to minimize the intrusion of fill material into the perforations. A hole was cut in the vinyl membrane at the lower end of the plot to provide an exit for the drain pipe. The membrane was sealed around the pipe using a taped, silicon-cemented joint. Non-perforated plastic pipe was connected to the perforated pipe. The end of the pipe was built into the collection box where samples of the drainage water from each plot could easily be obtained.

To facilitate the filling of the plots, 4 foot by 8 foot sheets of 3/4-inch plywood were set upright around the outside edge of the plot and the vinyl membrane was stretched over the plywood such that the membrane was on the plot interior. The plywood will be used later to construct collection boxes for the surface runoff.

A D-6 bulldozer and a front-end loader and their operators were provided by the Pittsburg and Midway Coal Mining Company for the purpose of filling the plots with the spoil material. As the fill material was placed in the plot, spoil was also placed outside against the plywood sheets. Up to 30 cm of fill was placed on both sides of the membrane and plywood forms, then the plywood was raised by hand. The filling operation required that one end of the plot remain open to provide access for the loader, so the plots were filled at one end before any filling was begun at the other end. The plywood sheets were set up at the unfilled end of the plot, and the plots were then filled completely. The plywood sheets were removed entirely as the desired depth of fill was obtained, both inside and outside the membrane.

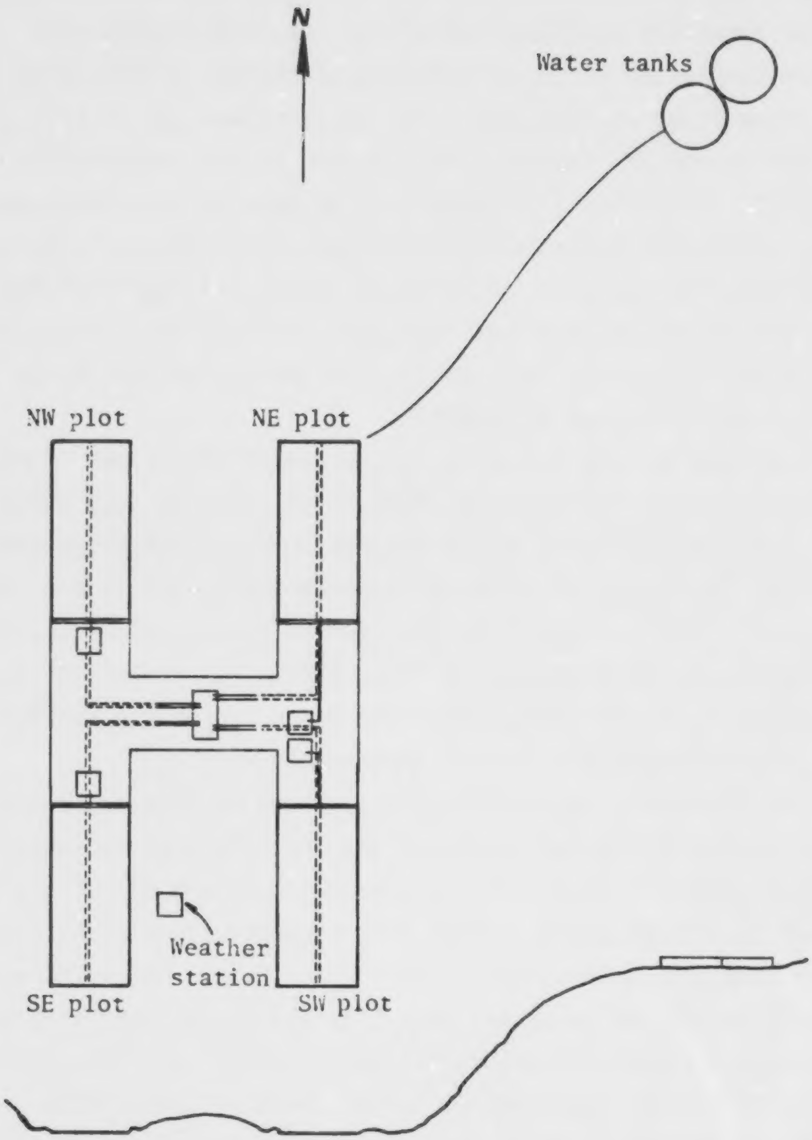
N
Water tanks
NW plot
NE plot
Weather station
SE plot
SW plot

Figure 31. Field plot layout at the Colorado site.

The spoil material contained numerous large rocks, and care was taken in placing the material so that these rocks did not pierce the membrane. Holes which were cut by rocks were patched with vinyl membrane and PVC cement. Figure 32 shows the configuration of the completed lysimeters.

Upon completion of the backfilling operation, a small berm was built around three sides of each plot. On the downslope end of each plot, a galvanized steel trough was placed. The function of the trough was to collect surface runoff. The collection trough can be seen in the photograph in Figure 33.

The volumetric lysimeters constructed at the Montana site are significantly different from those at the Colorado site. A large front-end loader was used to excavate a large trench some 10 m wide and 20 m long. The trench was about 3 m deep at the deepest point. The spoil removed from the trench was stockpiled for later use as backfill.

A concrete pad was poured in the bottom of the trench. The pad was 9 m long, 6 m wide and approximately 15 cm thick. The pad was poured on a slight grade. The vertical walls of the lysimeter were constructed with light-weight block. The first lift of block was leveled and sealed to the pad with mortar in the usual manner. Mortar was not used in subsequent lifts, however. A surface plaster, impregnated with fiber glass, was trowelled onto both sides of the block which had simply been stacked on top of one another to form the wall. This technique provides an impermeable wall.

A perimeter wall was constructed to a height of about 2.8 m. A wall down the center of the pad separated the facility into two bins, 8.8 m long, 2.8 m wide and 2.8 m deep. During construction one end of the facility was left open to provide access. Four-inch diameter plastic drain pipe was placed on grade down the center line of each of the bins. The perforated pipe was completely surrounded by gravel (see Figure 34). A layer of gravel about 6 inches thick was spread over the entire bottom of each bin. The drain pipe was extended through the block wall, and the hole sealed with mortar and a flexible, impermeable cement. Outside the lysimeters the drain pipes were extended to a convenient outlet. The entire facility was now ready for backfilling. Surface-runoff collectors were installed at the downslope end after backfilling was complete.

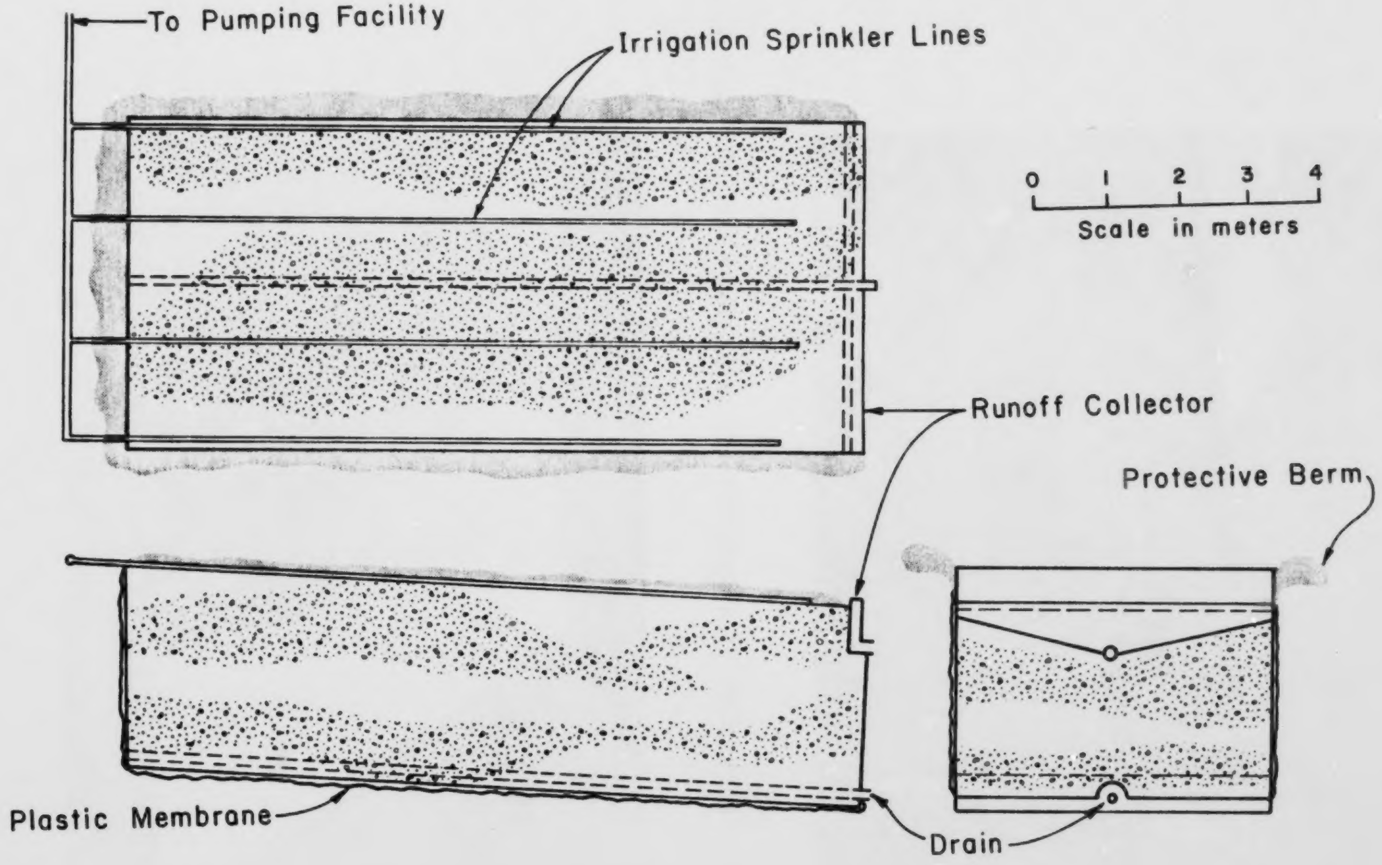
To Pumping Facility
Irrigation Sprinkler Lines
0
1
2
3
4
Scale in meters
Runoff Collector
Protective Berm
Plastic Membrane
Drain

Figure 32. Diagram of experimental test plot.

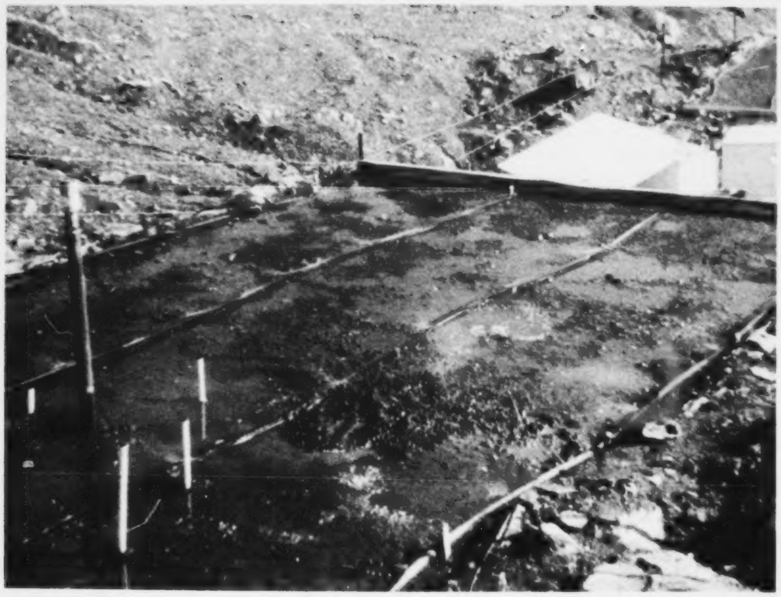

Figure 33. Photograph of a lysimeter installation at the Colorado site.

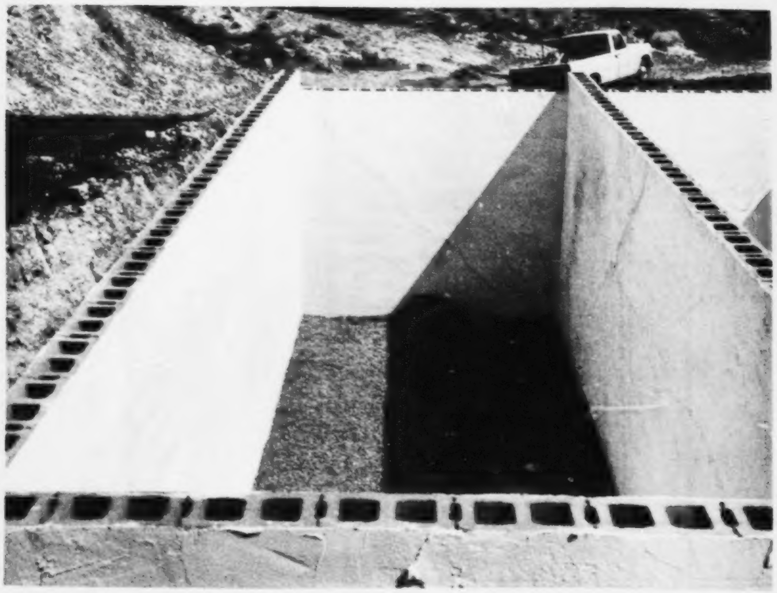

Figure 34. Photograph of lysimeter before backfilling - Montana site.

Instrumentation

Surface runoff was transported from the collector troughs to bins where volumetric measurements were made by monitoring the depth in a container. These data provided cumulative runoff as a function of time. Subsurface discharge from the drains was measured in the same manner during the first part of the study. Subsequently, totalizing water meters (CORAD) were installed on the drains. These meters also provided the cumulative discharge as a function of time but could be used to obtain rates by measuring the cumulative discharge over a small time interval. The water meters could not be used for measuring surface runoff because of sediment in the water.

Tensiometer cups were installed at several depths in each lysimeter facility. This was accomplished by cementing the ceramic tensiometer cups to lengths of C-PVC tubing and placing in a hole that had been augered to the desired depth. The annular space between the tubing and the hole well was backfilled. Installation of the tensiometers was accomplished soon after backfilling was complete. Settlement of the spoil material in the facilities during the subsequent winter and spring provided contact between the spoil and the ceramic cup.

One set of tensiometers, numbered from 4 to 5 terminating at depth intervals of about 30 cm, were placed in each of the four plots in the Colorado site. In the Montana facilities, two sets were placed in each plot. At both sites, the tensiometers were located on the perimeter of a circle one meter or so in diameter. Nylon tubing was used to connect the tensiometers to a reservoir of mercury. Suction was indicated by the rise of mercury in the nylon tube above the free surface elevation of the mercury reservoir. The soil-moisture suction at the tensiometer was calculated by correcting the indicated suction for the difference in elevation between the mercury reservoir and the tensiometer cup.

Near the center of each circle of tensiometers a neutron access tube was installed by augering a hole that terminated just above the gravel blanket at the bottom of the lysimeter. Troxler soil-moisture neutron probes were used to monitor soil-moisture status. As with the tensiometers, the access tubes were installed shortly following the completion of backfilling, and the spoil material had the opportunity to settle around the tubes through the winter and spring before any data was collected.

For use at the Colorado site, the soil moisture probe was calibrated in the laboratory. To meet the recommended minimum volume required for the calibration of the probe, a 1.2 m by 1.2 m by 1.2 m box was constructed of 3/4-inch plywood. The interior of the box was painted with a waterproof paint and all joints were sealed with rubber cement. As an added precaution against leakage, the box was lined with a sheet of plastic similar to that used in the lysimeter construction.

A 5.1 cm steel pipe was used as the neutron probe access tube. The pipe was held upright in the center of the box while the box was filled with spoil taken from the Colorado site. The spoil had been oven-dried to establish the initial soil moisture content equal to zero throughout the box. Initial probe readings were taken at 6-inch depth increments in the dry spoil.

After estimating the porosity of the spoil material in the box to be 0.40, a volume of water equal to 10 percent of the pore volume was applied to the spoil surface using a watering can. The box was then covered with a sheet of plastic in order to minimize evaporation losses. Neutron probe readings were taken daily until the readings for each depth did not vary by more than about 2 percent from day-to-day. Another premeasured volume of water was then added and the procedure was repeated. The second water application was again equal to 1 percent of the pore volume and subsequent applications were 5 percent until a saturation value of 40 percent porosity was reached. The period between applications was generally between one and two weeks.

For each average content, the final neutron probe measurements were plotted against depth providing an approximation of the moisture content distribution within the box. The area under the curve represented the volume of water applied if evaporation losses were negligible. The neutron probe measurements were converted to saturation percentages using a graphical analysis technique for each 6-inch depth segment. Since the manufacturer's calibration of the neutron probe indicated that a linear relationship existed between moisture content and the probe results, it was assumed that a linear relationship could be derived for the mine spoil. A linear regression analysis was used to derive the equation for soil moisture content using the neutron probe data. The results are shown in Figure 35. Because the neutron probe which had been calibrated for field use malfunctioned periodically, the relationship

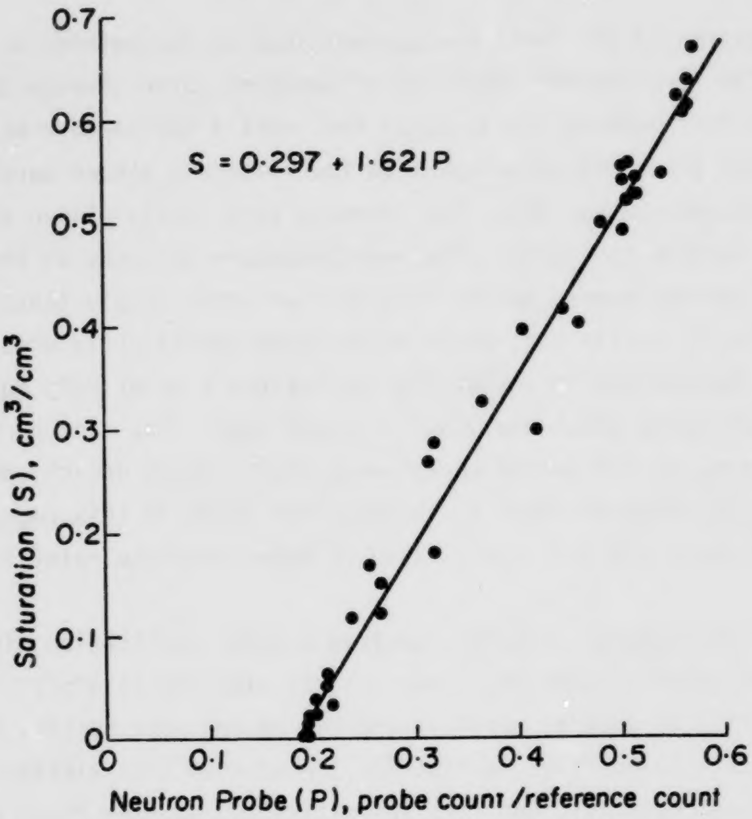

Figure 35. Calibration curve for the neutron-moisture-meter.

between measurements with the calibrated probe and with the second probe was determined. The second probe was used on a standby basis.

A weather station was set up at the Colorado site. Included in the station were a Class A evaporation pan, a hygro-thermagraph, solar radiation meter, rain gauge, and a totalizing anemometer.

Water Application

Water application to the plots was accomplished by two methods at the Colorado site. The first method consisted of applying water through Greenlawn shrubbery nozzles that produce a flat spray that wets a fanshaped area. The nozzles were spaced about one meter apart in four laterals placed parallel to the plot slope (Figures 32 and 33). The laterals were simply placed on the plot surface and secured to stakes. The same procedure was used at the Montana site. Water was pumped to the nozzles from water supply tanks. The maximum application intensity that could be achieved was slightly greater than 11 cm per hour. The minimum intensity that maintained a relatively good distribution of water on the plots was about 3 cm per hour. The main purpose of the above application system was to apply water with a small detachment capacity for use with the sediment model to be described later in this report. Note that, in no sense, did this application of water simulate rainfall precipitation.

A portion of the sediment studies required a water application with a greater detachment capacity that would more nearly simulate rainfall. Criterion for simulation of natural rainfall include an adequate spatial distribution of rainfall intensities, a distribution of drop size similar to the drop sizes of natural rainfall, and fall velocities approaching those of natural rainfall. Though conventional rainfall simulators designed for field conditions can usually provide excellent spatial distribution for given rainfall intensities, criterion for approximating terminal velocities and drop size distribution are rarely if ever met. According to Laws and Parsons (1943), mean drop sizes for natural rainfall with intensities of 0.254, 50.8, and 101.6 millimeters per hour are 1, 2, and 3 millimeters. For these drop sizes, a respective fall distance of about 2.50, 9.14, and 12.19 meters is required to obtain terminal velocity of 3.85, 6.58, and 8.08 meters per second, respectively. Because of physical limitations in obtaining sufficient fall distance, no attempt was made to simulate fall velocities of natural rainfall in the given study. However, consideration was given to a design which would provide an adequate spatial distribution of rainfall.

To investigate the effect of simulated rain droplet impact as a detaching agent in mine spoil erosion, a portable sprinkler system consisting of seven, 3-meter high risers was designed to simulate rainfall over the test plots. A schematic diagram of each sprinkler riser is given in Figure 36. Each riser consists of a Hayes Measurflow Series No. 2305 flow regulator and a Rainjet sprinkler head Model No. 75C.

Figure 37 illustrates the grid pattern of sprinkler risers for simulation of rainfall on a test plot. Operation of four sprinklers, as indicated in the figure, provided an intensity of 36.5 millimeters per hour. With three additional sprinkler risers, a higher intensity of 57.4 millimeters per hour was obtained. The two application intensities were calibrated by placing containers on the plot surface and measuring accumulative volumes for a specified time period. Data from the calibration indicate a coefficient of variation equal to 0.074 for the spatial distribution of rainfall at the lower intensity and a value of 0.035 for the higher intensity. A limited available water supply for experimental purposes allowed for a simulated rainfall period of about 50 and 65 minutes for high and low intensities, respectively.

Sediment Production Experiments

For convenience, the sediment experiments are divided into two categories; those conducted with shrubbery sprinkler application system (overland flow) and those conducted with the Rainjet sprinkler heads on the risers (simulated rainfall).

Overland Flow Tests

Three types of experiments with this sprinkler system included runs at a low and high intensity on a smooth surface, and experiments performed at a high intensity on a roughened or gouged plot surface. The smooth plot surface consisted of a finely raked, plane surface, with the largest material exposed being about gravel size. For a roughened surface, a pickblade was run over the plot at a depth of approximately 7 cm, in directions transverse to the slope. A gouged surface configuration consisted of pock marks approximately

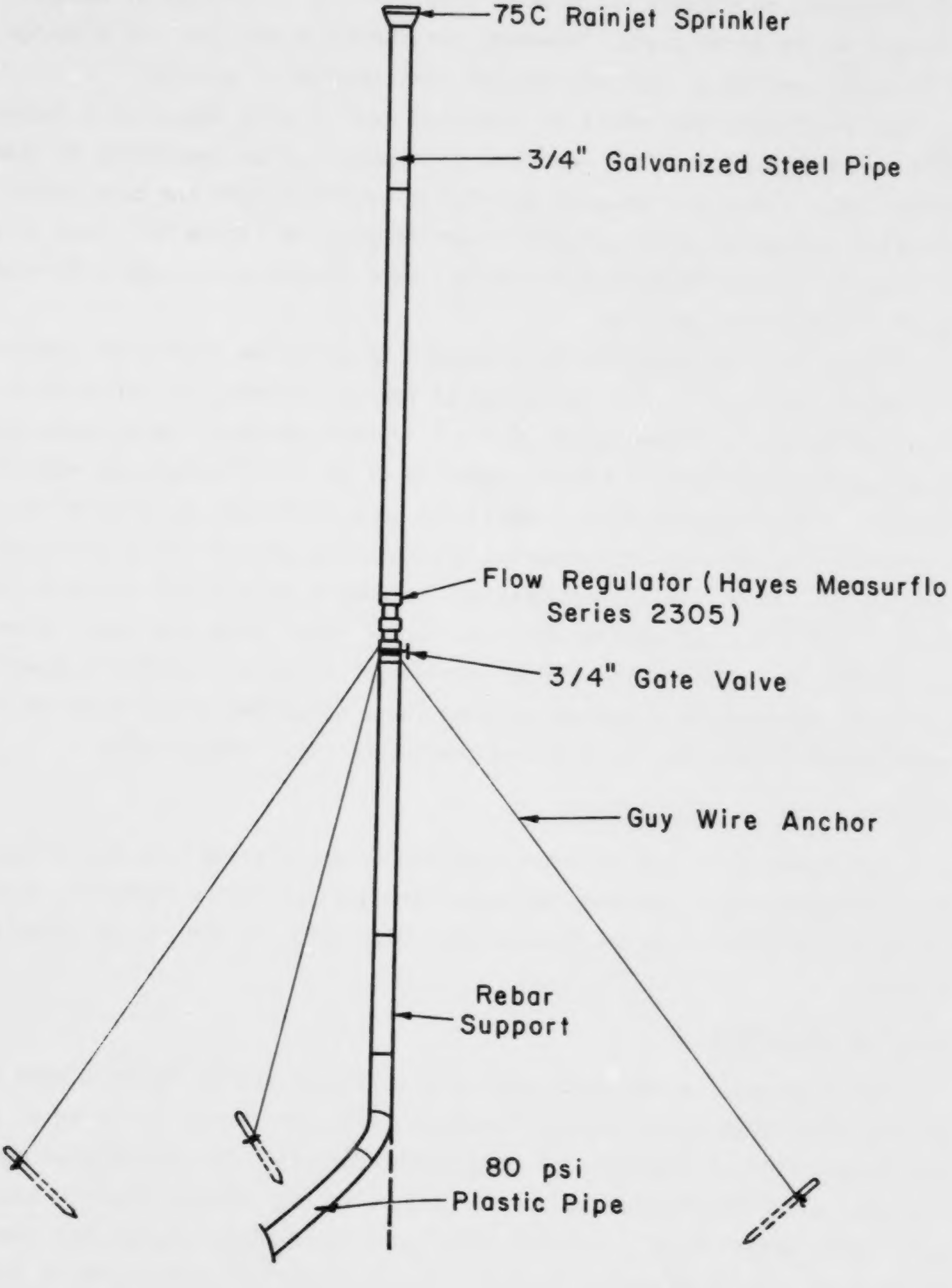

75C Rainjet Sprinkler
3/4" Galvanized Steel Pipe
Flow Regulator (Hayes Measurflo Series 2305)
3/4" Gate Valve
Guy Wire Anchor
Rebar Support
80 psi Plastic Pipe

Figure 36. Rainfall sprinkler riser design.

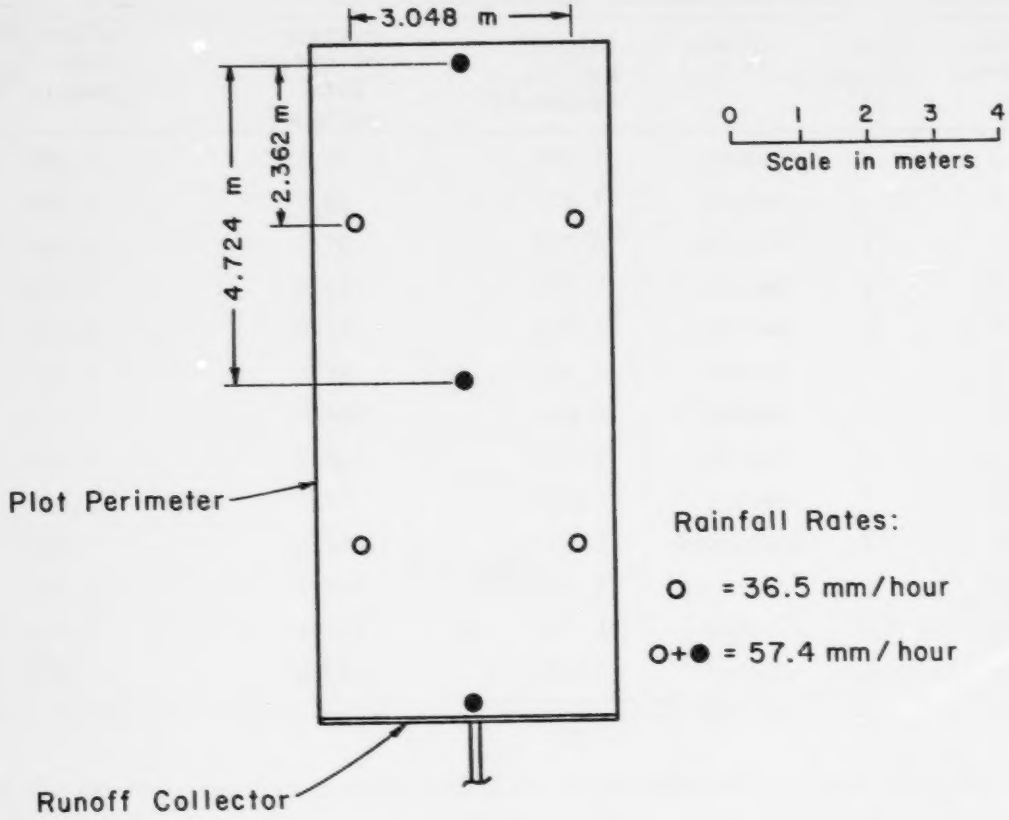
3.048 m
2.362 m
4.724 m
0 1 2 3 4
Scale in meters
Plot Perimeter
Rainfall Rates:
○ = 36.5 mm/hour
○+● = 57.4 mm/hour
Runoff Collector

Figure 37. Sprinkler design layout for test plots.

13 cm in diameter and 13 cm deep, staggered across the plot at about 30 cm intervals.

For the experimental treatments mentioned above, plot surfaces consisted of fresh, dry spoil material. In Table 14, a summary of these simulated snowmelt runoff experiments conducted at the Colorado field site during 1975 is given. Different application intensities as indicated in the table were the result of difficulties in regulation of water applied during experimentation.

For each imposed application intensity and surface configuration, runoff hydrographs were prepared from volumetric measurements made during experimentation. An example of the data collected is shown in Figure 38. Similar data were collected for runs 3, 5, and 6 through 13 and are included in the appendix.

TABLE 14. SUMMARY OF OVERLAND FLOW RUNOFF EXPERIMENTS CONDUCTED DURING 1975

Run Number	Plot Slope (%)	Surface Condition	Volume Applied (meters^3)	Average Application Rate (mm/hour)	Volume of Runoff (meters^3)
1	1	Smooth	1.948	38.1	0.066
2	1	Smooth	1.427	39.9	0.000
3	3	Smooth	4.738	37.7	0.089
4	5	Smooth	5.105	35.6	0.012
5	7	Smooth	3.217	39.9	0.223
6	1	Smooth	5.336	86.6	1.903
7	3	Smooth	5.686	104.9	1.758
8	5	Smooth	5.696	102.7	1.519
9	7	Smooth	5.857	97.2	2.631
10	3	Roughened	5.667	88.3	2.407
11	1	Roughened	5.777	105.3	1.707
12	7	Gouged	5.769	114.4	1.119
13	5	Gouged	5.908	110.5	0.483

Average application intensities of 37.7 and 39.9 mm per hour for runs 3 and 5, respectively resulted in very low steady-state runoff rates of 1.5 and 3.4 mm per hour, respectively. Runs 6 through 9 performed on a smooth plot surface at application intensities ranging from 86.6 to 104.9 mm per hour resulted in similar outflow runoff rates. Roughened plot surfaces for runs 10 and 11 appeared to have no effect on runoff rates, as compared to runs 6 and 7 on the 1 and 3 percent bed slopes, respectively. However, gouged surface configurations in runs 12 and 13 resulted in marked increases in infiltration rates. Assuming similar application intensities for runs 9 and 12 made on the 7 percent slope, the gouged surface manipulation reduced outflow surface runoff rates by nearly one-half. This surface treatment was even more effective on the 5 percent slope, where steady state runoff rates were reduced by almost two-thirds.

To evaluate the sediment runoff characteristics of the spoil materials on the test plots, sediment samples were collected in conjunction with the measurement of surface runoff during field experimentation. Sediment samples

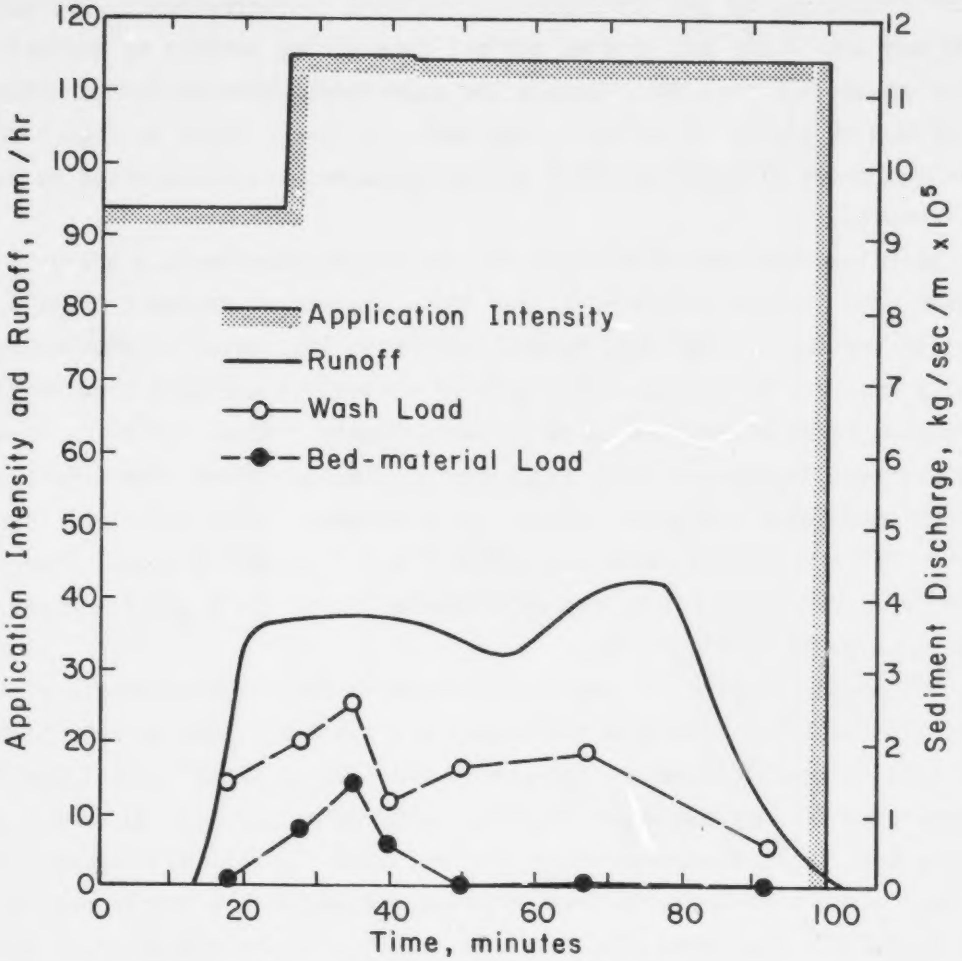

Figure 38. Runoff and sediment discharge for run 6.

were collected in the runoff facilities beginning with the initiation of surface runoff and continued until runoff had ceased. The total sediment load was divided into bed-material load and wash load components, with the former portion consisting of particles greater than 0.062 mm in diameter, and the latter comprising the remainder. Samples were wet sieved for splitting at the sand-silt division point. Both the coarse and fine grained portions of the samples were oven dryed in evaporating dishes and subsequently weighed to determine sediment concentrations.

Erosion rates for the experiments were computed by multiplying surface runoff discharges by the corresponding sediment concentrations. Bed-material loads and wash loads are plotted against time during periods of surface runoff as shown in Figure 38. Because the experiments were performed without the effect of simulated rainfall, sediment discharges shown in Figure 38 represent rates of spoil material erosion detached and transported by overland flow runoff.

Wash load sediment discharges for the given experiments are highly dependent upon surface runoff rates and loose amounts of sediment readily available for transport. The data suggest that wash load rates of erosion are usually greatest during the first several minutes of overland flow runoff. Decreasing rates of erosion through time indicate gradual depletion of wash load sediment discharges among experiments. Time-dependent logarithmic plots of wash loads were prepared. Figure 39 illustrates these wash load rates of erosion for experiments performed on the 1 and 3 percent slopes. Time-dependent wash load erosion rates from experimentation on the 5 and 7 percent bed slopes are given in Figure 40.

As shown in Figure 39, rates of erosion through time on smooth plot surfaces for the 1 and 3 percent bed slopes are similar. Here average measured wash load sediment discharges for runs 6 and 7 are 1.47×10^{-5} and 1.08×10^{-5} kilograms per second per meter of plot width, respectively. In runs 8 and 9 (Figure 40), similar average rates are indicated, though the transport rates for each run are markedly different during the respective runoff periods. In runs 10 and 11, roughened plot surfaces resulted in the transport of greater quantities of wash load sediment, especially during the first 30 minutes of runoff. Average wash load sediment discharges for these experiments are 3.00×10^{-5} and 3.46×10^{-5} kilograms per second per meter, respectively, and are about two and one-half times greater than the average measured wash load discharges reported in runs 6 and 7. This occurrence likely reflects the additional amounts of sediment transported as a result of plot roughening immediately before experimentation. Data from run 13 suggest that the gouged plot surface was effective in reducing both surface runoff rates and the erosion rate of wash load sediment. Here the average measured sediment discharge is 1.63×10^{-5} kilograms per second per meter, about one-fifth the wash load rate of erosion reported in run 8. A similar experiment performed on the 7 percent

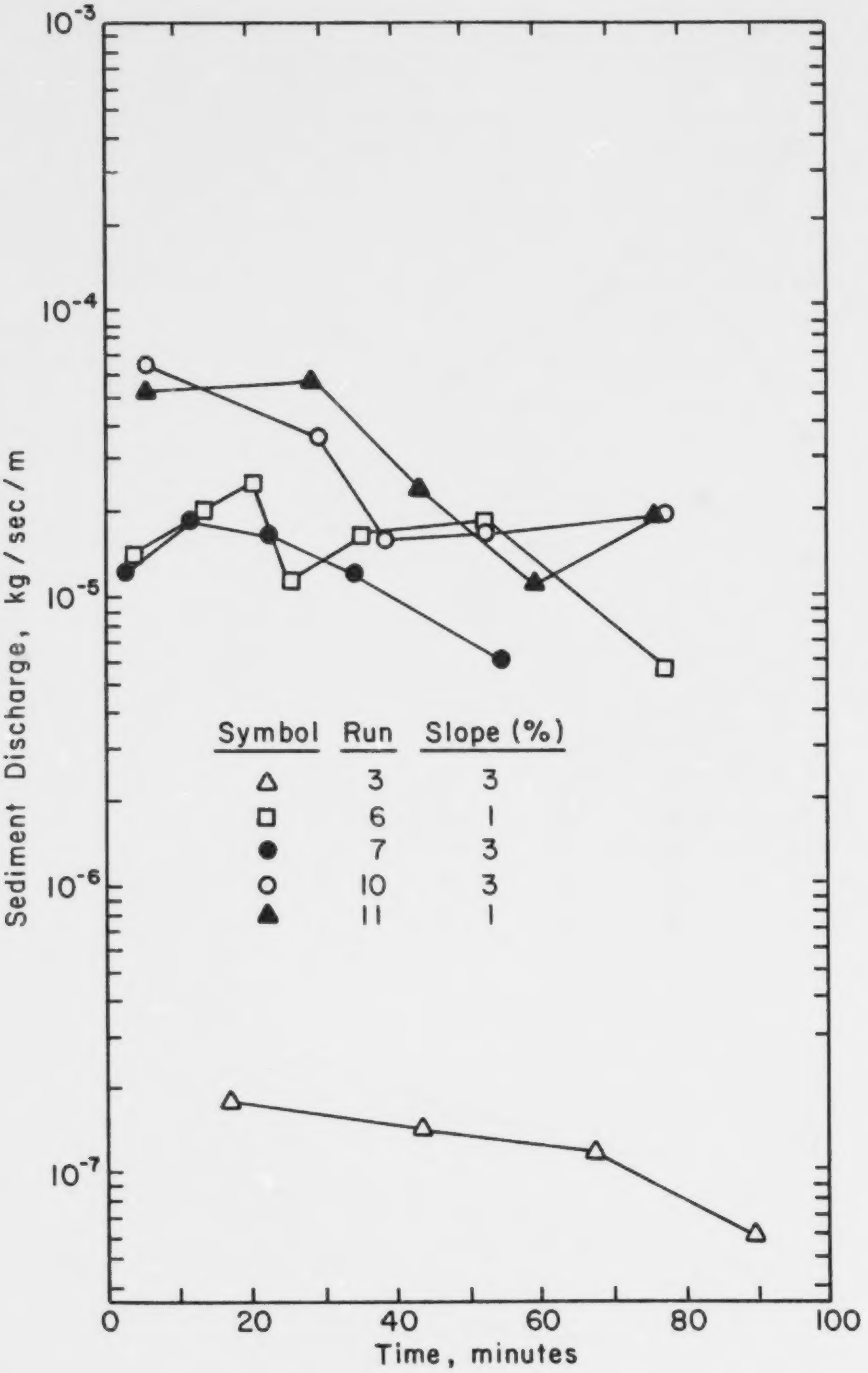

Figure 39. Time-dependent wash load erosion rate for experiments on 1 and 3 percent bed slopes.

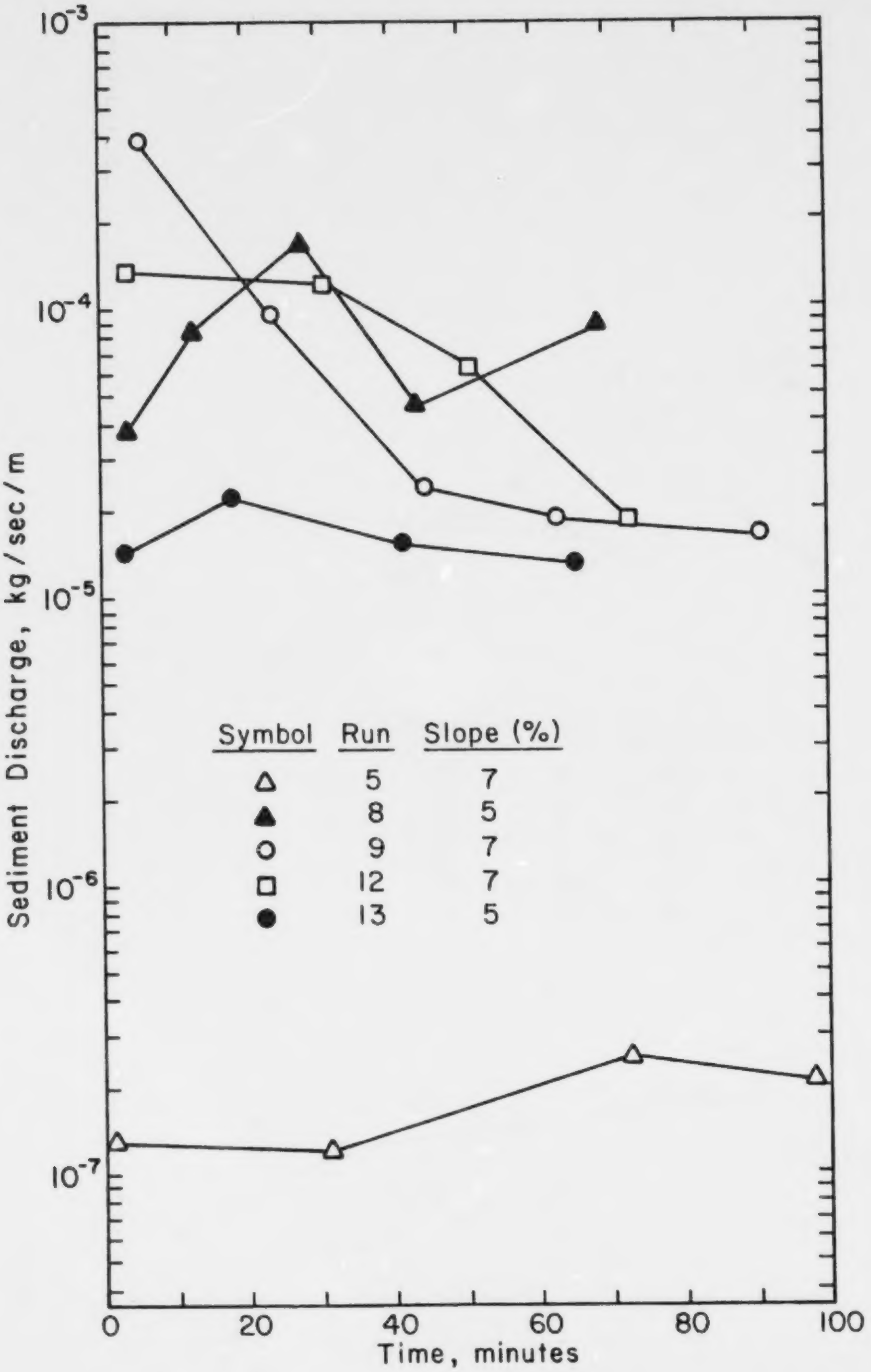

Figure 40. Time-dependent wash load erosion rate for experiments on 5 and 7 percent bed slopes.

slope resulted in a reduction of overland flow runoff by nearly one-half, with little change in the average measured wash load discharge. This was an unexpected result, as a smaller overland flow runoff rate should have a smaller potential for detachment and transport of wash load sediment.

Bed-material load sediment discharges reflect varied responses for given application intensities, infiltration rates and plot surface conditions. Steady rates of erosion are indicated in runs 8 through 11 and 13. Sudden changes with time in bed-material sediment discharges are noted in runs 6, 7, and 12. Because the transport of bed-material sediment is highly dependent upon processes of aggradation and degradation occurring on the eroding plot surface, abrupt changes in bed-material load are the result of rapid upslope adjustments in the bed. In that efforts to monitor adjustments in the eroding bed surface were not undertaken in the current study, no attempt was made to explain reported changes of bed-material discharge during experimentation.

In Table 15 a summary of sediment discharge data collected in 1975 from overland flow experiments is presented. These data represent rates of erosion detached and transported by surface runoff. Very small sediment discharges for runs 3 and 5 are apparent in comparison to the remainder of the experiments. A significant increase in average measured wash load discharges in runs 8 and 9 as compared to 6 and 7 is suggestive of a critical steepness, below which there is little appreciable detaching capacity for overland flow runoff. Considerable differences in average measured bed-material sediment discharges among experiments indicates varying degrees of upslope bed stability.

Simulated Rainfall Tests

A total of six experiments was performed with the rainfall simulator which included experiments on the 1 and 7 percent bed slopes at the Edna Mine field site. These tests included runs at the lower and higher intensity on the two respective slopes, which were smoothed to a plane surface with fresh, dry spoil material. With surface adjustments made on the 7 percent bed slope, experiments with concave and convex slopes were performed at the higher intensity. Table 16 summarizes the hydrologic and plot surface information pertaining to the 1976 experimental runs. Unlike other test runs performed under simulated rainfall, run 15 consisted of a rainfall application of 37.5

TABLE 15. SUMMARY OF SEDIMENT DISCHARGE DATA COLLECTED FROM OVERLAND FLOW RUNOFF EXPERIMENTS

Run No.	Average Application Rate (mm/hr)	Average Infiltration Rate (mm/hr)	Bed Slope (%)	Average Measured Sediment Discharge kg/sec/m x 10^{+5} Wash Load	Bed-Material Load	Total Load
3	37.7	36.4	3	0.0122	0.000	0.0122
5	39.9	36.7	7	0.0183	0.000	0.0183
6	86.6	50.7	1	1.47	0.255	1.72
7	104.9	73.9	3	1.08	1.10	2.18
8	102.7	73.6	5	8.72	2.69	11.4
9	97.2	56.0	7	8.75	0.724	9.47
10	88.3	51.9	3	3.00	2.80	5.80
11	105.3	71.7	1	3.46	0.350	3.81
12	114.4	90.7	7	8.80	4.41	13.3
13	110.5	100.6	5	1.63	0.250	1.88

TABLE 16. SUMMARY OF SIMULATED RAINFALL EXPERIMENTS CONDUCTED DURING 1976

Run Number	Plot Slope (%)	Surface Shape	Volume Applied (meters^3)	Average Application Rate (mm/hr)	Volume of Runoff (meters^3)
14	7	Uniform	1.907	57.4	1.024
15	7	Uniform	1.394 0.494	36.5 57.4	0.801 0.464
16	7	Convex	1.766	57.4	0.821
17	7	Concave	1.624	57.4	0.879
18	1	Uniform	1.805	57.4	0.868
19	1	Uniform	1.441	36.5	1.018

mm per hour for 62 minutes, followed by an application at the higher intensity for 14 minutes. Figure 41, a sketch, illustrates plot surfaces for uniform, convex, and concave shapes in runs 14, 16, and 17, respectively.

Water and sediment discharge hydrographs for the test runs with simulated rainfall were prepared in the same manner as described for pervious experiments. Figures 42 through 47 illustrate surface runoff hydrographs and sediment discharge relations characteristic to each experiment. For constant rainfall application rates, hydrograph shapes are similar to those reported in the overland flow experiments conducted during 1975.

Greater rates of infiltration due to surface preparation for run 16 resulted in slightly lower surface runoff rates in comparison to those reported in run 14. Surface manipulation for preparation of run 17 resulted in an even more pronounced effect, in that a steady-state equilibrium runoff rate was not attained during the period of rainfall application.

Efforts to more adequately quantify rates of erosion for wash load and bed-material load size sediments during field experimentation in 1976 included a more rigorous sampling frequency. Under the detachment by simulated rainfall, data from nearly all the 1976 experiments indicate substantially greater rates of erosion for both wash load and bed-material load, as compared to the 1975 overland flow runoff data.

As shown in Figures 43 through 45 and 47, wash load sediment discharges are highly dependent upon rates of surface runoff. The data indicate that for these test runs, detachment by rainfall droplets provides sufficient wash load sediment available for transport during the period of overland flow runoff. Rising and falling hydrograph limbs clearly illustrate periods when the erosion rate of wash load sediment is limited by the transporting capacity of the flow. In run 18, the wash load rate of erosion decayed in an exponential fashion after reaching an initial peak of 28.0×10^{-5} kilograms per second per meter of plot width. For this experiment, the availability of wash load sediment for transport is limiting.

Data collected in runs 14, 16, and 17 indicated few discernible differences in wash load sediment yields for experiments performed on uniform, convex, and concave surface shapes. An interesting observation for these runs, however, is the difference in time-dependent wash load rates of erosion. Gradually decreasing erosion rates were observed in run 14 (uniform slope)

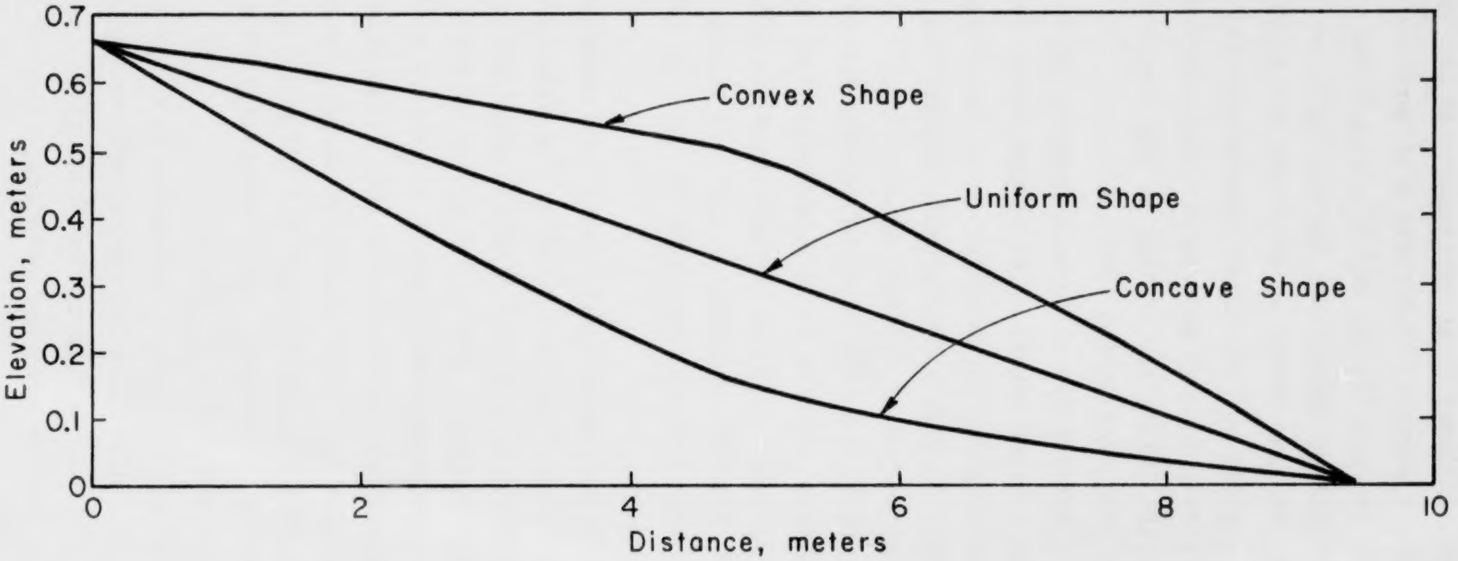

Figure 41. Definition sketch for concave, uniform, and convex shapes on the 7 percent bed slope.

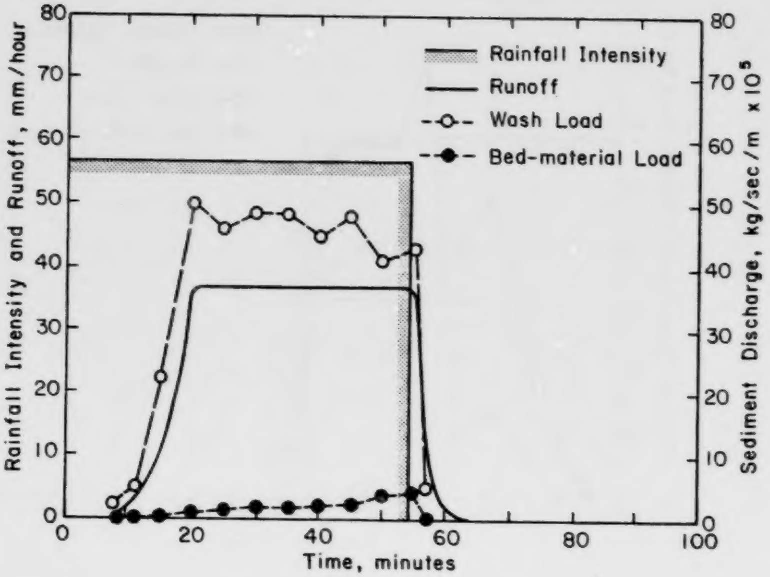

Figure 42. Runoff and sediment discharge for run 14.

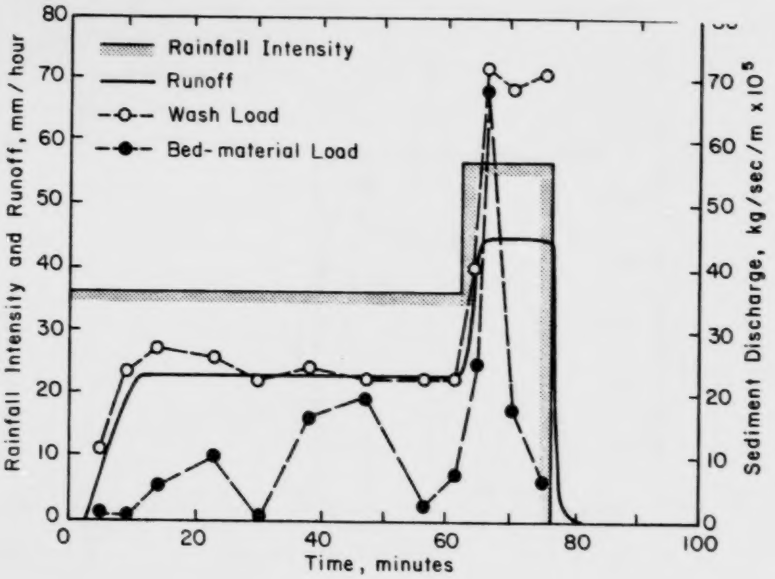

Figure 43. Runoff and sediment discharge for run 15.

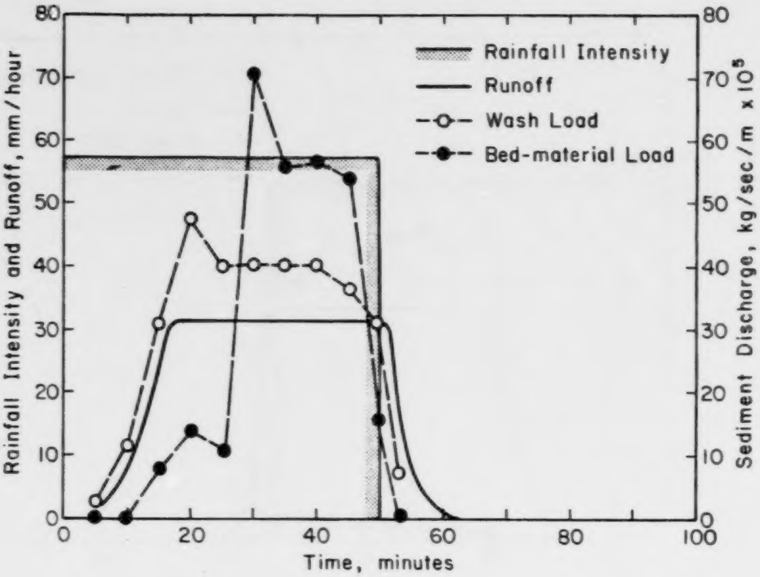

Figure 44. Runoff and sedimend discharge for run 16.

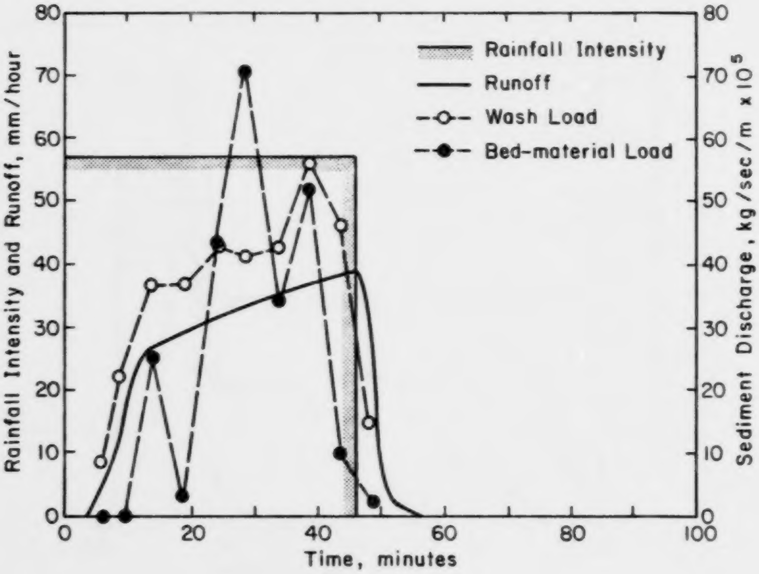

Figure 45. Runoff and sediment discharge for run 17.

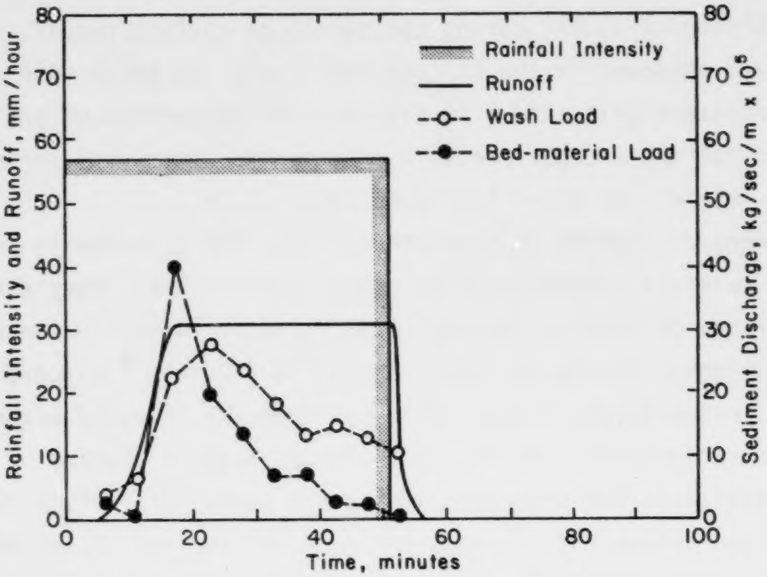

Figure 46. Runoff and sediment discharge for run 18.

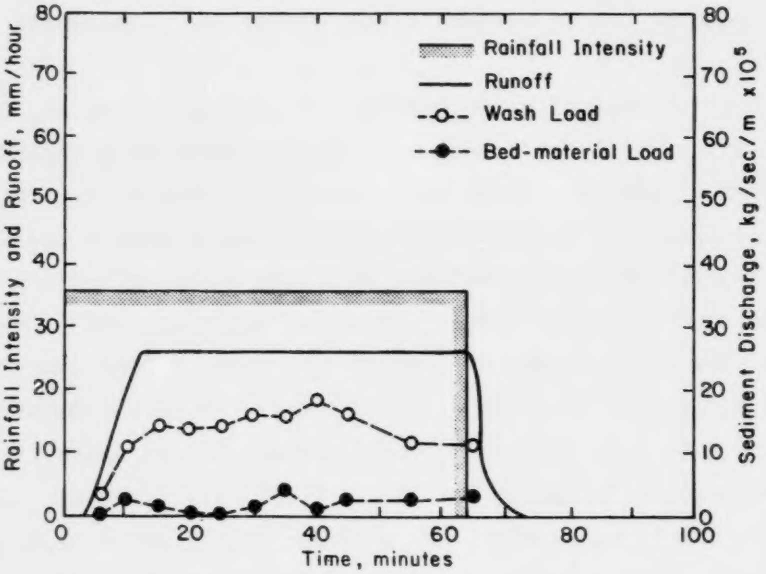

Figure 47. Runoff and sediment discharge for run 19.

and run 16 (convex slope) during the period of surface runoff. The opposite behavior was observed in run 17 (concave slope), in which wash load rates of erosion increased with time. An illustrative comparison of the wash load rates of erosion for these experiments in addition to other runs performed under simulated rainfall is given in Figure 48.

Sediment discharges of bed-material load for experiments performed under simulated rainfall reflect a broad range in responses. Very steady bed-material load rates of erosion are indicated for runs 14 and 19, in which average measured sediment discharges are 1.82×10^{-5} and 2.3×10^{-5} kilograms per second per meter, respectively. Data collected from run 18 would suggest that the time-dependent erosion rate for bed-material load is limited by the supply of sediment available for transport during the period of surface runoff. Bed-material load sediment discharges for runs 15, 16, and 17 reflect very abrupt changes in erosion rates from one sediment sampling interval to the next. During run 17, for example, the sediment discharge varies from 3.75 to 71.2 $\times 10^{-5}$ kilograms per second per meter over a time interval of only 10 minutes. As previously stated, these rapid changes in erosion rates for bed-material load size sediment likely reflect sudden and abrupt adjustments in the eroding bed surface.

Bed-material load rates of erosion for runs on convex and concave surface shapes reflect markedly different sediment responses than reported in run 14 (uniform slope). For slopes of equal average steepness, the total amount of bed-material load size sediment transported from a concave bed slope is typically much smaller in comparison with that from either a uniform or a convex shape. Tests on irregular slopes (Young and Mutchler, 1969; Onstad et al., 1967) have shown that sediment losses from a slope depend upon the steepness of a short segment of that slope lying directly above the point of measurement. However, the data from the given investigation did not support this conclusion. Average measured bed-material load of 24.4×10^{-5} kilograms per second per meter in run 17 is nearly the same as the sediment discharge of 26.0×10^{-5} kilograms per second per meter reported in run 16. These bed-material load sediment discharges from runs on irregular shaped bedslopes are about 14 times greater than the sediment discharge reported in run 14. It was concluded that the surface manipulation to provide experimental conditions for erodible concave and convex surfaces substantially increased the availability of loose

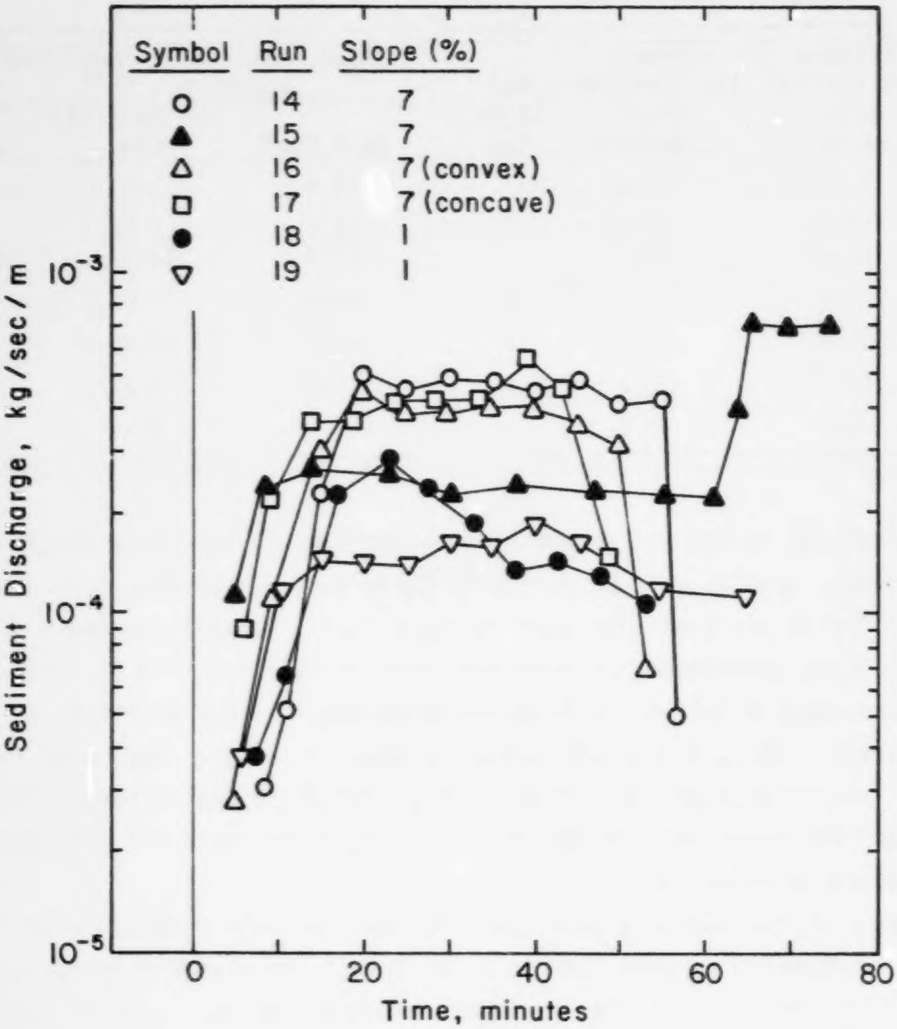

Figure 48. Time-dependent wash load erosion rate for experiments with simulated rainfall on 1 and 7 percent bed slopes.

bed-material load size sediment for transport.

A summary of sediment data collected from experiments run under simulated rainfall is presented in Table 17. Though direct comparisons of experiments performed with and without simulated rainfall cannot be made, the effect of rainfall as a detaching agent for upland erosion of the spoil material is apparent.

TABLE 17. SUMMARY OF SEDIMENT DISCHARGE DATA COLLECTED FROM SIMULATED RAINFALL EXPERIMENTS

Run No.	Average Application Rate (mm/hr)	Average Infiltration Rate (mm/hr)	Bed Slope (%)	Average Measured Sediment Discharge kg/sec/m x 10^{+5} Wash Load	Bed-Material Load	Total Load
14	57.4	31.8	7	36.8	1.83	38.7
15	36.5	14.5	7	22.6	7.02	29.6
	57.4	19.7		70.0	30.5	100.5
16	57.4	36.2	7	29.8	26.0	55.8
17	57.4	32.3	7	35.1	24.4	59.5
18	57.4	32.7	1	15.5	9.60	25.1
19	36.5	12.6	1	13.2	2.36	15.5

In addition to the collection of sediment samples for analysis of sediment concentration, samples were periodically taken during the 1976 field experimentation for analysis of size distribution. Spoil material sediment size distribution was determined by sieve analysis for the fraction of total sediment coarser than 0.062 mm. Following the procedure given by the U. S. Geological Survey (1969), a selected number of pipette analyses were made for material finer than 0.062 mm. Plots of the size distribution versus "percent finer than" for composite samples of wash load and bed-material load sediments are presented in Figure 49.

Results of the size analyses indicate that the mean particle size for sediment transported as wash load is 0.00878 mm, with standard deviation of 0.00686. For bed-material load sediment, the mean particle size in transport is 1.342 mm, with deviations from the mean equal to 0.971.

WATER QUALITY AND QUANTITY

Experiments in 1976 were performed primarily for use in the sediment studies, and the 1975 experiments (referred to as overland flow test above) were used in both sediment and water-quality hydrology studies. The run numbers referred to in this subsection correspond to those discussed above. In this subsection, the emphasis is on the subsurface water movement and upon inorganic water quality. The overland flow hydrographs were included with the sediment

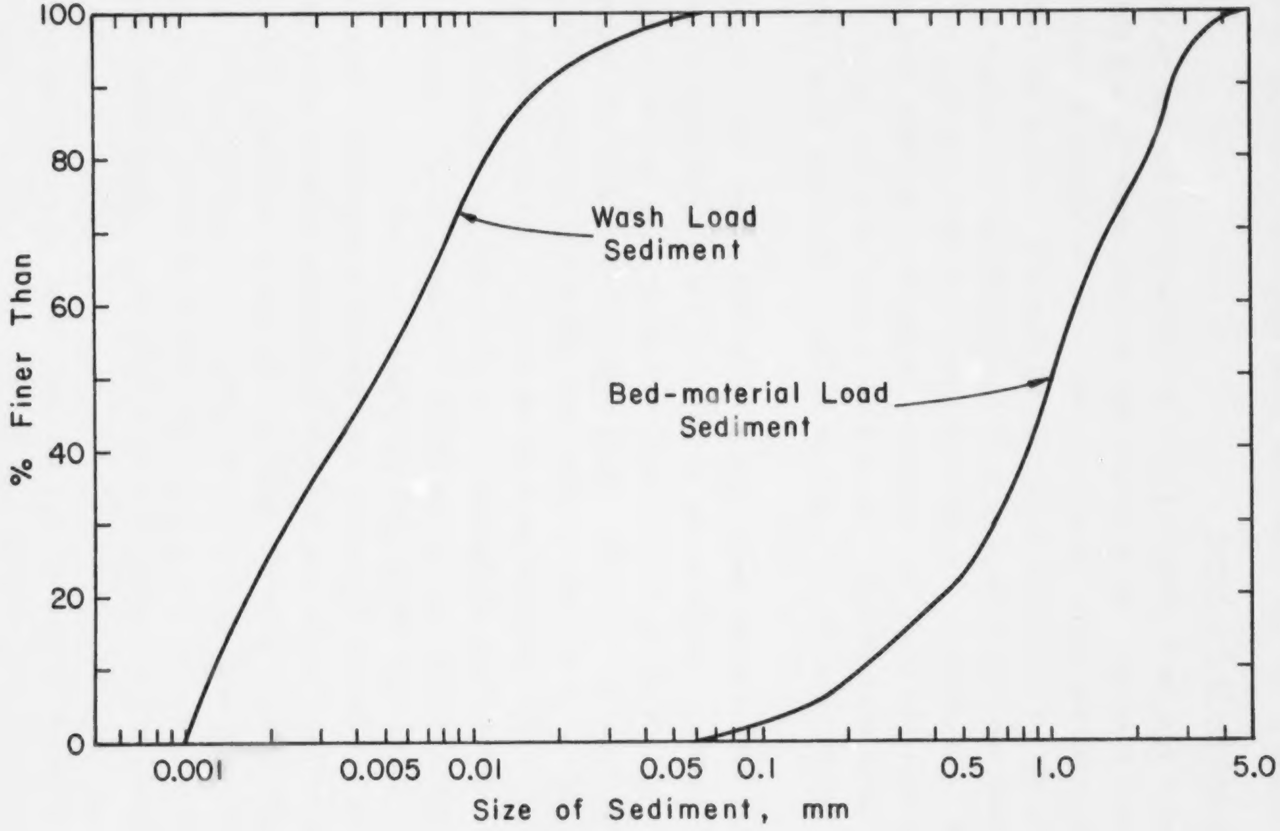

Figure 49. Size distribution for composite samples of wash load and bed-material load sediments.

data and will not be repeated here. Also, the application rates, total volumes applied and volume of surface runoff had previously been presented in Table 14.

Water Balance and Drain Discharge

The first 5 runs were conducted with no knowledge of the way in which the lysimeters would respond. The procedure was to apply water through the sprinkler system at about the lowest practical rate until subsurface drainage was observed. The sprinkler system would then be shut off. During the experiment the total volume and flow rate of both surface runoff and subsurface drainage were measured. Measurements for subsurface drainage were continued for several days. The initial and final soil moisture content distributions were obtained from neutron probe measurements. Water samples were collected for electrical conductivity and pH measurements and then put away for future laboratory analysis.

The second set of experiments, two runs on each of the four lysimeters, consisted of applying a given volume of water at the highest practical application rate. Neutron probe readings and tensiometer data were collected before, during and after each run. These data, together with the measured volumes in Table 14, permit water budget computations to be made. The results are shown in Table 18. Evaporation from the plots is the only component of the water balance that was not measured. If there were no experimental errors in all other measurements, the column headed "residual depth" would be the depth of water evaporated during each experiment. Evaporation from the plots should not, theoretically, be greater than the pan evaporation. Thus, by comparing the residual depth with the pan evaporation for each experiment, the experiments with a small error in water balance can be selected. These experiments are indicated with an asterisk in Table 18. Experiments 3, 7, and 10 were performed on the plot with a 3 percent surface slope for which a leak in the lysimeter wall was detected. The water balance for these three experiments was expected to show large errors.

Figures 50 and 51 illustrate how the cumulative volume drained and drain discharge varied with time for run 2 on the plot with a one percent surface slope. These data are typical of those measured during the other experimental runs. Further discussion of these data is presented when the moisture flow model is discussed later in this report.

TABLE 18. WATER BALANCE FOR EXPERIMENTAL PLOTS - COLORADO SITE

Exper. No.	Depth Applied (cm)	Depth Runoff (cm)	Depth Drainage (cm)	Depth of Storage (cm)	Residual Depth (cm)	Measured Pan Evap. (cm)
1*	5.27	0.18	1.34	2.05	1.70	2.13
2*	4.36	0.00	1.71	2.12	0.53	4.05
3	11.94	0.22	0.92	5.85	4.95	0.94
4	13.46	0.03	3.02	5.96	4.45	2.70
5*	8.69	0.71	1.68	5.36	0.94	1.65
6*	15.89	5.15	5.41	2,80	2.53	9.05
7	14.33	4.43	0.12	6.16	3.62	0.98
8	14.45	3.83	1.90	2.66	6.06	0.56
9*	16.18	7.05	3.38	3.92	1.83	1.03
10	14.85	6.07	0.63	4.40	3.75	0.61
11*	15.80	4.65	5.88	5.00	0.27	1.30
12*	15.65	3.00	7.20	4.39	1.06	0.60
13*	17.25	1.22	8.12	6.99	0.92	-

TABLE 19. SPOIL CHEMISTRY AS MEASURED IN 1:1 EXTRACTS - PLOT WITH 1% SLOPE
COLORADO SITE

Layer No.	pH	EC micromhos per cm	Ca	Mg	Na	HCO_3	Cl	SO_4	NO_3	NH_4	CEC $\frac{meqv}{100gm}$
			meqv/l								
1	7.8	3400	18.5	15.2	3.6	1.6	<0.2	30.0	0.4	0.1	17.8
2	7.6	3200	17.8	14.8	3.9	1.8	<0.2	27.5	0.5	0.1	16.5
3	7.8	3200	18.6	15.5	3.9	2.0	<0.2	26.0	0.7	0.1	16.9
4	7.8	3300	15.1	14.0	5.4	1.6	<0.2	26.0	0.2	0.1	18.8
5	7.7	3100	17.2	14.4	4.0	1.8	<0.2	28.5	0.4	0.2	18.6
6	7.7	2300	13.7	11.8	2.2	1.8	<0.2	23.0	0.7	0.2	16.5
7	7.8	2300	14.2	12.1	0.8	1.7	<0.2	22.0	0.5	0.2	15.7

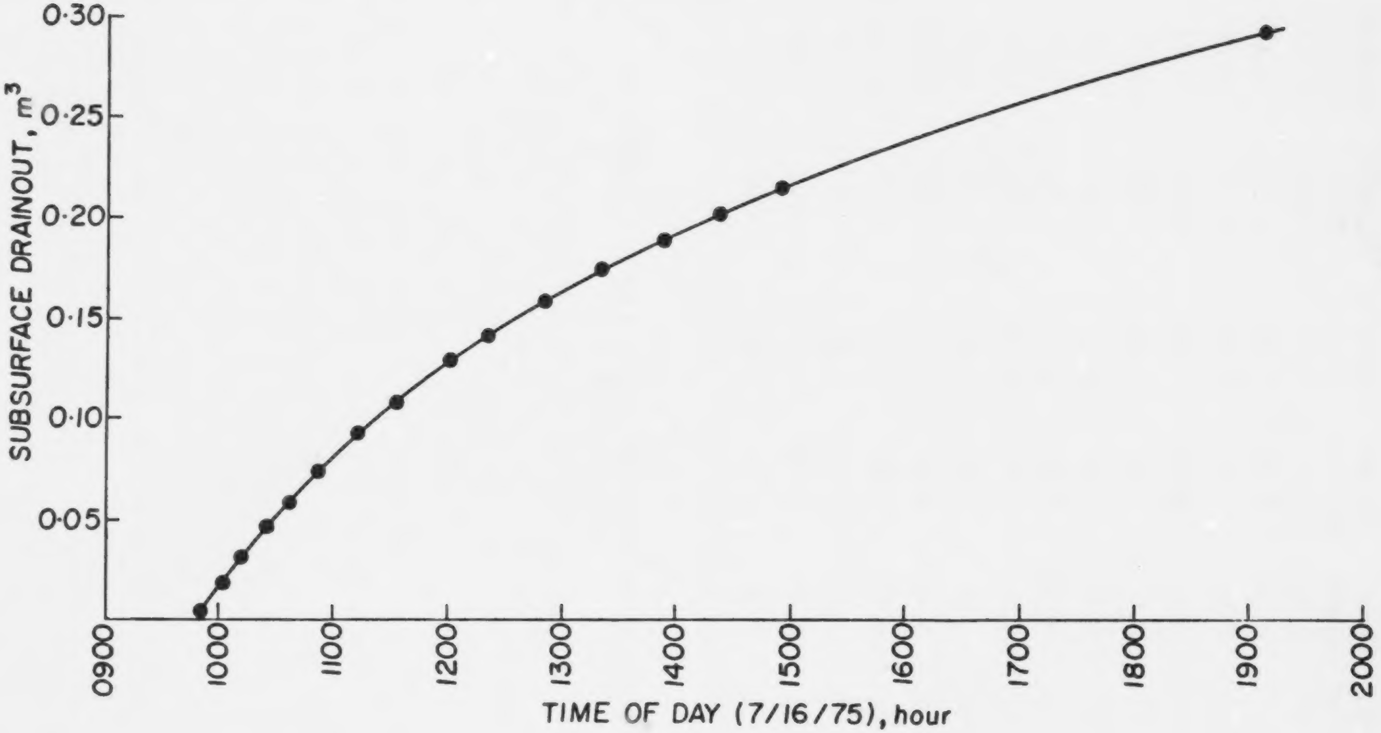

Figure 50. Cumulative drainout for Run 2.

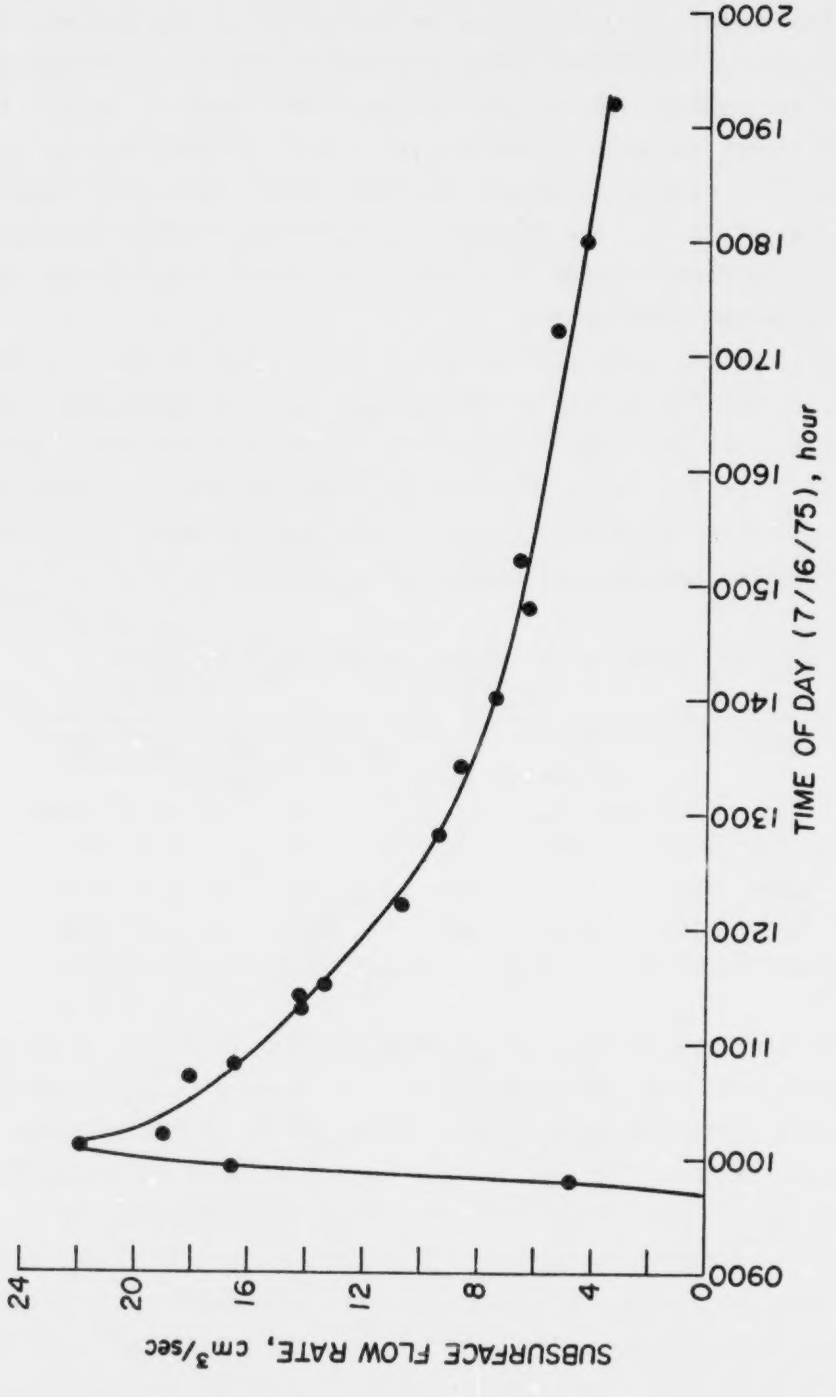

Figure 51. Drain discharge for Run 2.

Water Quality and Spoil Chemistry

During the process of backfilling the lysimeters at the Colorado site, the spoil was sampled as various lifts were added. One-to-one extracts were prepared from the samples and the chemical characteristics of the spoil was determined by layers for each lysimeter plot. Table 19 contains the data by layers for the plot with a one percent surface slope. Each layer constitutes a depth interval of 25 cm. The data for the remaining plots is included in the appendix. The data in Table 19 is that required as input to the chemistry model to be described subsequently.

The quality of the water applied to the plot with a 1% slope is given in Table 20. Note that the quality of the applied water is quite good. The corresponding quality of surface runoff from the 1% plot for runs 6 and 11 is illustrated in Table 21. It is important to note that the quality of surface runoff does not differ greatly from that of the applied water. The reasons for this observation have been discussed in Section 4.

TABLE 20. QUALITY OF APPLIED WATER - PLOT 1% SLOPE COLORADO SITE

Run No.	Date	Time	EC micromhos per cm	TDS mg/l	Na	Ca	Mg	HCO_3	SO_4
					meqv/l				
2	7/16	0900	200	130	0.1	1.0	0.7	1.5	0.7
6	8/16	0935	300	200	0.2	1.7	1.2	2.3	1.0
11	8/19	0945	300	200	0.2	1.6	1.0	2.4	0.9

The quality of subsurface drainage from the plot with a 1% slope is shown in Table 22. The depth of spoil in this plot averaged 180 cm. A total of four experimental runs were made on this plot. The EC of the drainage water varied somewhat with time and from run to run as indicated in the table. A similar variation was observed in the other plots and the variation is apparently random. Notice that the average EC values by run differ very little from one another and indicate a nearly constant concentration of dissolved solids in the drainage water. The somewhat lower EC values for run 1 are probably due to some short circuiting of applied water to the drain blanket

TABLE 21. QUALITY OF SURFACE RUNOFF FROM PLOT WITH 1% SLOPE
COLORADO SITE

Run No.	Date	Time	EC micromhos per cm	TDS mg/l	Na	Ca	Mg	HCO_3	SO_4
					meqv/l				
6	8/6	0957	300	200	0.3	2.1	1.3	2.3	1.4
		1017	300	200	0.3	1.9	1.2	2.8	1.4
		1102	300	200	0.3	1.9	1.3	2.6	1.2
			300	200	0.3	2.0	1.3	2.6	1.4
11	8/19	0954	300	200	0.2	1.6	1.1	2.4	1.2
		1235	300	200	0.2	1.8	1.2	2.6	1.2
			300	200	0.2	1.7	1.2	2.5	1.2

through several cracks that had developed. This problem was corrected before subsequent runs were made.

Figure 52 shows the correlation between the EC in the 1:1 extracts and the EC of the subsurface drainage from the corresponding plots at the Colorado site. To obtain the data points in Figure 52, all EC data from each plot was

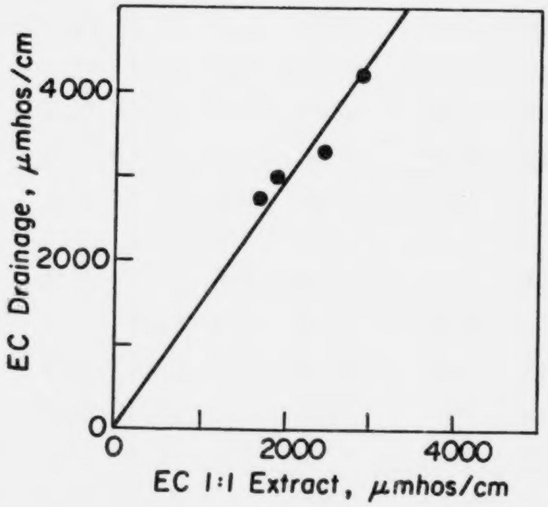

Figure 52. Correlation of EC of drainage with EC of spoils.

TABLE 22. QUALITY OF SUBSURFACE DRAINAGE FROM PLOT WITH 1% SLOPE COLORADO SITE

Run No.	Date	Time	EC micromhos per cm	TDS mg/l	Na	Ca	Mg	HCO_3	SO_4
					meqv/l				
1	7/10	1017	2900	2500	4.6	17.2	19.9	4.1	38.7
		1212	3200	2800	5.2	20.5	23.7	4.6	45.7
		1350	3300	2900	5.4	21.0	26.7	4.6	51.6
		1910	3600	3200	5.1	21.0	27.1	4.8	55.5
	7/13	0900	4600	4200	8.6	22.8	33.1	5.6	64.8
			3500	3100	5.8	20.5	26.1	4.7	51.3
2	7/16	0948	3900	3500	6.5	22.1	28.6	6.5	55.5
		1000	4200	3800	5.9	27.5	34.0	5.9	58.4
		1320	3400	3000	4.7	19.9	22.9	5.6	45.3
		1520	3400	3000	4.1	12.2	24.7	4.8	42.8
	7/17	0855	4600	4200	7.8	26.6	36.6	6.4	60.9
	7/18	0740	4600	4200	8.3	26.4	38.6	6.7	62.5
		0940	4600	4200	8.5	27.4	36.8	6.6	62.4
			4100	3700	6.5	23.2	31.7	6.1	55.4
6	8/6	1100	4900	4500	10.6	25.4	40.0	6.9	65.1
		1133	3800	3400	6.7	21.1	27.9	5.4	48.2
		1215	4100	3700	6.2	22.2	27.9	5.6	46.9
		1325	4100	3700	8.1	23.2	31.0	6.6	54.7
		1515	4500	4100	10.1	23.8	34.4	7.0	62.4
	8/7	0815	4900	4500	11.2	24.6	39.2	7.9	65.6
			4400	4000	8.8	23.4	33.4	6.6	57.2
11	8/19	0950	3600	3200	5.2	18.4	27.0	7.3	45.6
		1125	3900	3500	4.5	20.7	27.5	6.1	49.5
		1230	4200	3800	5.4	22.1	32.3	6.9	54.7
		1445	4600	4200	7.8	23.1	34.8	7.3	58.6
		1855	4600	4200	7.0	23.4	35.6	8.0	60.8
	8/20	0750	4600	4200	8.1	23.4	37.7	8.1	59.4
			4200	3800	6.3	21.8	32.5	7.3	54.8

averaged and the EC data of the subsurface drainage from all runs on each plot were averaged to obtain the corresponding EC of the drainage water. The correlation indicates that the EC of 1:1 extracts can be useful for estimating the EC of subsurface drainage. However, use of 1:1 extracts requires that a correlation similar to that shown in Figure 52 be developed for each spoil material. As mentioned previously in Section 4, the EC of saturation extracts should provide a direct indication of EC of drainage waters and, therefore, requires less experimental work. A reduction in the scatter of the data can be achieved by assuring that the saturation percentage of the samples is the same as that in the field.

Experiments similar to those described above were conducted at the Montana site. Table 23 contains the chemical characteristics of the spoil in the two lysimeters as determined from saturation extracts. Samples were obtained with a split-tube sampler at three locations in each plot after backfilling was complete. The data for each depth interval for the three locations were averaged and entered into Table 23. The spoil in the lysimeters at the Montana site is very homogeneous with respect to chemistry.

TABLE 23. SPOIL CHEMISTRY AS MEASURED IN SATURATION EXTRACTS - MONTANA SITE

Depth (cm)	pH	EC micromhos per cm	Ca	Mg	Na	HCO_3	Cl	SO_4	NO_3	NH_4	CEC meqv/100gm
			meqv/l								
					NORTH PLOT						
0-30	7.7	4100	27.6	30.1	4.4	2.4	0.7	52.8	2.7	0.4	9.7
60-90	7.7	4100	27.2	30.1	4.0	2.2	0.6	52.4	2.4	0.4	9.5
120-150	7.6	4100	26.8	32.4	4.0	2.7	0.8	53.4	3.2	0.3	10.0
180-210	7.6	4100	27.0	29.4	3.7	2.4	0.4	51.4	2.3	0.2	10.4
					SOUTH PLOT						
0-30	7.7	3900	26.7	27.3	5.1	2.4	2.5	49.1	2.1	0.4	9.0
60-90	7.5	4100	26.9	29.2	4.7	2.7	1.7	52.3	1.8	0.4	9.6
120-150	7.6	4100	26.0	31.3	4.6	2.9	1.7	53.0	2.7	0.4	8.2
180-210	7.6	4300	26.8	30.4	5.3	2.4	4.8	49.0	2.0	0.4	9.0

Tables 24, 25 and 26 illustrate the quality of applied water, surface runoff, and subsurface drainage, respectively, at the Montana site.

TABLE 24. QUALITY OF APPLIED WATER - MONTANA SITE

Run No.	Plot	Date	Time	EC micromhos per cm	TDS mg/l	Na	Ca	Mg	HCO_3	SO_4
						meqv/l				
1	North	5/27	1018	940	790	0.7	5.5	-	-	10.2
2	South	7/13	1310	1100	720	0.5	5.5	6.4	0.1	6.7
3	North	7/14	1045	-	673	0.4	5.5	5.8	0.1	9.4
4	North	8/10	1740	1200	950	0.5	10.0	8.2	0.3	12.7
5	North	8/31	1545	-	1200	1.0	6.0	10.7	0.6	16.0

TABLE 25. QUALITY OF SURFACE RUNOFF - MONTANA SITE

Run No.	Plot	Date	Time	EC micromhos per cm	TDS mg/l	Na	Ca	Mg	HCO_3	SO_4
						meqv/l				
2	South	7.13	1444	1300	1040	0.6	8.5	7.8	0.6	14.6
			1454	1100	806	0.5	6.5	6.4	0.2	10.8
			1535	1080	750	0.5	6.0	6.7	0.3	10.0
3	North	7/14	1147	1350	866	0.5	7.0	7.3	0.5	12.5
			1314	1050	725	0.5	6.0	6.2	0.4	9.4
4	North	8/10	1117	-	1200	0.6	7.0	9.0	0.4	14.8
			1730	-	1200	0.8	6.0	10.0	0.5	16.7

The spoil material placed in the lysimeters at the Montana site contained very little moisture at the time of placement. Thus a great deal of water was required to wet the material before subsurface drainage could be expected. Nevertheless, the subsurface drains began to produce some water within a few hours after water was applied. This drainage was, undoubtedly, water that short circuited the spoil through cracks and/or piping. Tensiometer and moisture probe data clearly indicated that the spoils had not been wet up near the bottom until late in run 5. Thus, the quality of subsurface drainage indicated in Table 26, probably, does not reflect the quality of percolate in the spoil

TABLE 26. QUALITY OF SUBSURFACE DRAINAGE - MONTANA SITE

Run No.	Plot	Date	Time	EC micromhos per cm	TDS mg/l	Na	Ca	Mg	HCO_3	SO_4
						meqv/l				
1	North	5/27	1100	2300	1910	7.4	7.0	10.7	-	22.5
			1107	2600	2100	8.3	8.0	9.1	-	26.2
2	South	7/13	1500	2050	1450	2.4	8.0	12.4	2.1	16.5
			1520	2000	1637	2.7	9.0	14.0	1.6	19.6
			1535	1080	750	0.5	6.0	6.7	0.3	10.0
3	North	7/14	1123	2250	1714	0.9	12.0	13.2	0.6	22.9
5	North	8/28	1545	2560	1600	1.0	8.0	12.4	0.4	20.8
		9/2	-	1920	1400	1.1	6.0	9.9	0.7	17.7
				1610	1400	1.9	5.5	10.7	0.5	17.3
		9/8	-	1710	-	-	-	-	-	-
		9/9	-	1390	-	-	-	-	-	-
		9/10	-	1610	-	-	-	-	-	-
		9/11	-	1670	-	-	-	-	-	-
		9/12	-	1670	-	-	-	-	-	-
		9/14	-	1720	-	-	-	-	-	-
		9/15	-	1720	-	-	-	-	-	-

material. It is evident that the EC of the drainage water remained well below that expected from the saturation extracts. The spoil material placed in the Montana lysimeters exhibited an extremely low hydraulic conductivity relative to that at the Colorado site and a great deal of time was required to wet up the material. The water supply was a small pond and was entirely depleted during run 5 and it is believed that valid water quality data for subsurface drainage were not obtained.

HYDRAULIC PROPERTIES OF THE SPOIL

The moisture flow model used in this study requires that the hydraulic properties of the spoil be known. The properties include the functional relationships between hydraulic conductivity and volumetric moisture content and between soil-moisture suction (capillary-pressure head) and volumetric moisture content. There are available methods by which these data can be obtained in the field but laboratory methods were selected for use in the present study. One of the most important parameters is the hydraulic conductivity at the maximum moisture content obtainable and this parameter was measured in the field.

Moisture Retention

The experimental apparatus used to measure the relationship between soil-moisture tension and water content is illustrated in Figure 53. Oven dried spoil was placed in the spoil container at a known bulk density and porosity and then vacuum saturated. The top of the cup containing the sample is a removable section equipped with a porous plastic membrane (PORVIC) that is pressed into contact with the sample. When a suction is applied to the membrane by the leveling bottles, water is withdrawn from the sample through the membrane and into the glass tube as indicated by the cross-hatching in Figure 53. Following an incremental increase in suction, accomplished by adjusting the leveling bottles, the air-water interface advances until the suction in the spoil sample is equal to that indicated by the difference in elevation of the leveling bottles. The cap of the sample container is removed and the change in moisture content is determined by weighing the sample. The equilibration of the suction in the spoil with that imposed on the membrane is made more rapid by allowing evaporation from the spoil to occur. The spoil in the container was exposed to the atmosphere through a fine wire mesh that constitutes part of the lateral surface of the container; thus permitting evaporation to occur.

The experiment was initiated with a saturated sample at a very low suction and proceeded to successively larger suctions. The data are, therefore, those obtained on a desaturation or drying cycle. In the field, moisture content changes during both wetting and drying and it is well known that the relationships between suction and moisture content are not the same for both processes. The moisture-flow model accomodates only one function, however, and the function during the drying process was used throughout.

The desaturation data for the spoils from the Colorado site are shown in Figure 53. The data represent averages from three determinations at bulk densities that cover the range that existed in the lysimeter installations.

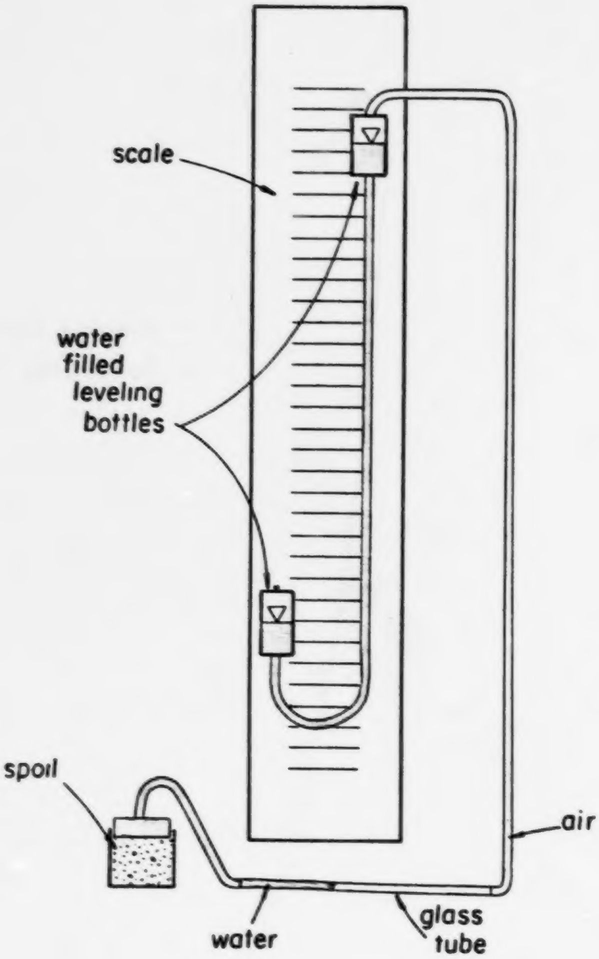
scale
water filled leveling bottles
spoil
air
water
glass tube

Figure 53. Apparatus for measuring the relationship between soil moisture content and suction.

The solid curve in Figure 54 was calculated by fitting the Su-Brooks (1975) parametric equation to the data. The Su-Brooks equation is

$$\frac{p_c}{\rho g} = \frac{p_i}{\rho g} \left[\frac{S-S_r}{a} \right]^{-m} \left[\frac{1-S}{b} \right]^{bm/a} \qquad (56)$$

where

$p_c/\rho g$ = capillary pressure (suction) head,

$p_i/\rho g$ = capillary pressure head at inflection point,

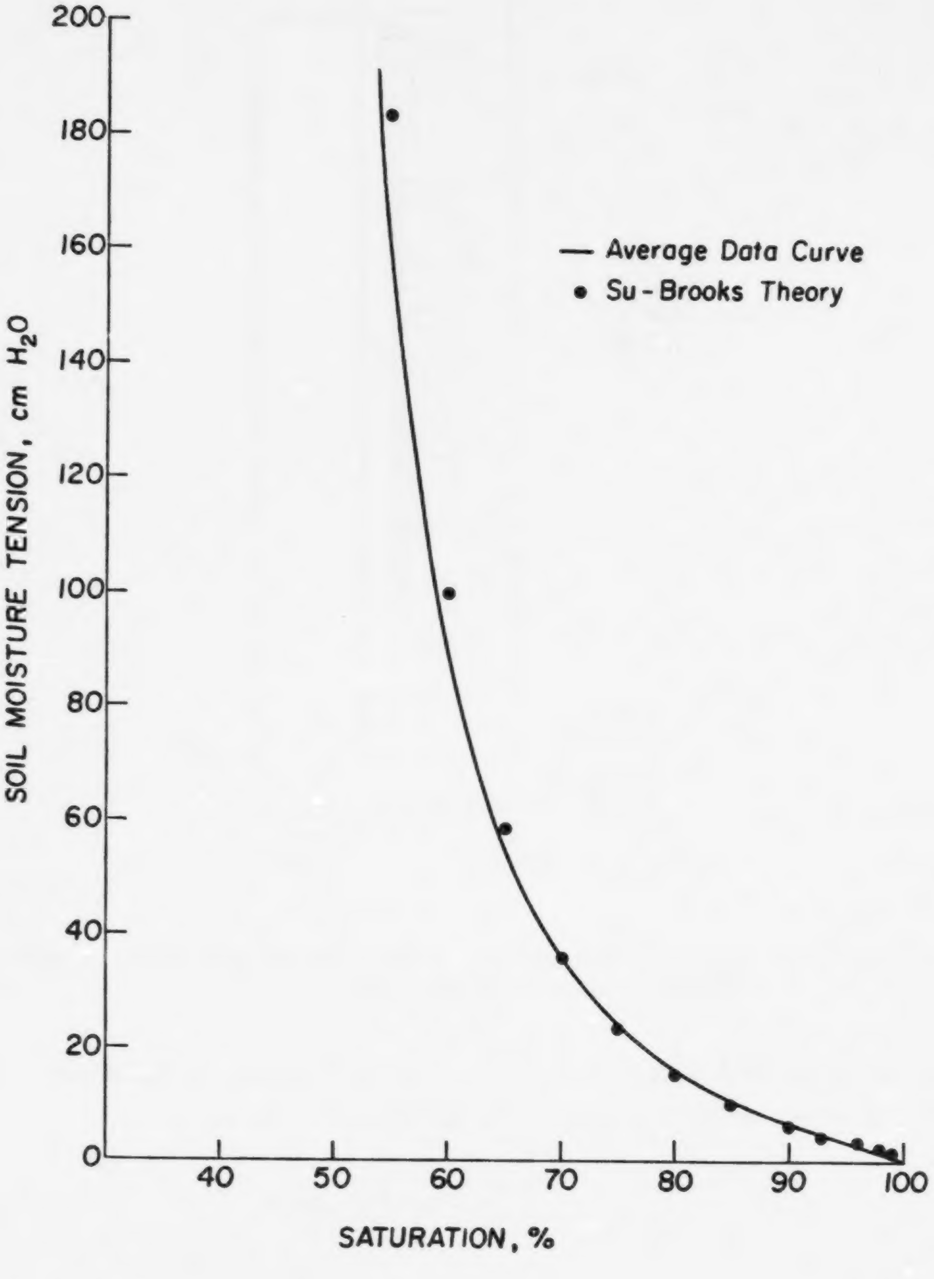

Figure 54. Desaturation curve for spoil from the Colorado site.

S = saturation,

S_r = residual saturation,

m = shape factor of the curve,

a = domain of saturation associated with concave portion of curve,

b = domain of saturation associated with convex portion of curve.

The parameters for equation 56 determined from the desaturation data are $a = 0.647$, $b = 0.072$, $m = 3.34$, $S_r = 0.223$, and $p_i/\rho g = 5.0$ cm of water.

Hydraulic Conductivity

The Brooks-Corey parametric equation for hydraulic conductivity as a function of saturation was used (Brooks and Corey, 1964). This equation is

$$K = K_s\left[\frac{S-S_r}{1-S_r}\right]^{\frac{2+3\lambda}{\lambda}} \tag{57}$$

where

K = hydraulic conductivity at S,

K_s = hydraulic conductivity at $S = 1.0$,

λ = pore-size distribution index,

and other symbols are as previously defined. From the theoretical relationship between m in equation 56 and λ in equation 57 (Ayars, 1976), the parameter λ was determined to be 0.285. Therefore, all that was required to complete the relationship between hydraulic conductivity and saturation is K_s. The relationships indicated in equations 56 and 57 can be converted to the volumetric water content form by noting that $\theta = \phi S$, where ϕ is porosity and θ is volumetric water content.

Values for K_s were obtained by both laboratory and field determinations. In the laboratory, a constant head permeameter (Figure 55) was used to measure K_s for several bulk densities. Dry spoil was placed in the permeameter and allowed to wet by upward flow. Thus, the measured K_s reflects the reduction in hydraulic conductivity attributable to entrapped air. The measured K_s values ranged from 52 cm/day at the largest bulk density to 1700 cm/day for the smallest bulk density. Values were also obtained by determining the infiltration rate during periods of constant surface runoff and assuming this value

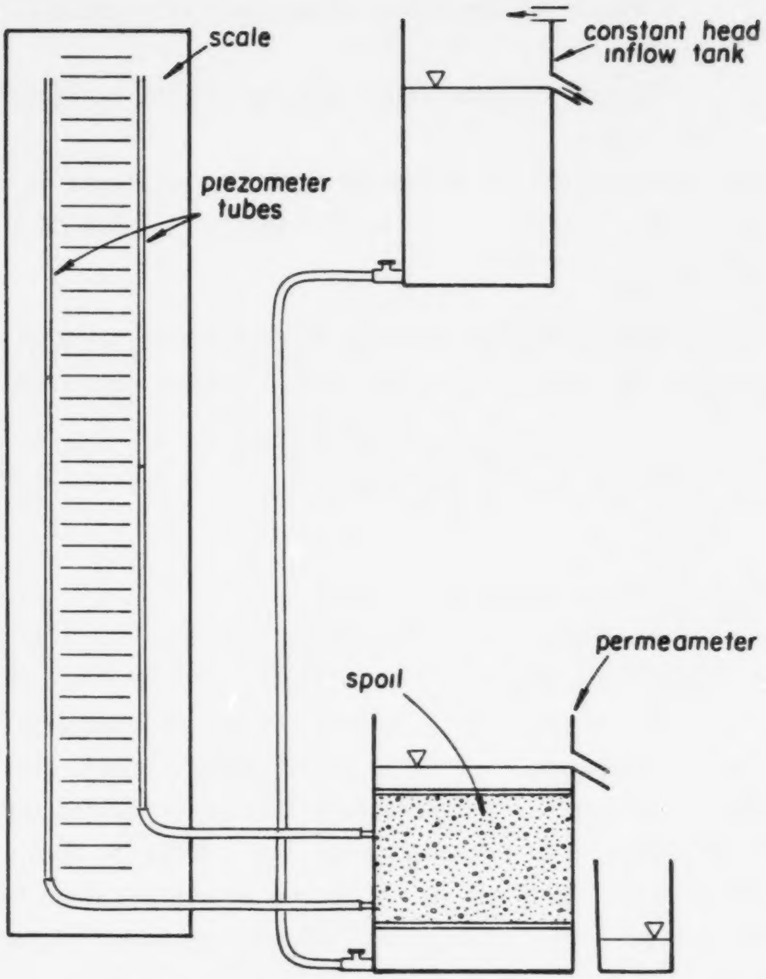
scale
constant head inflow tank
piezometer tubes
permeameter
spoil

Figure 55. A constant head permeameter.

to be equal to K_s. There are indications, however, that the values of K_s determined in this manner were much too large, probably due to the fact that capillary pressure gradients remained significant causing the infiltration rate to be larger than the base intake rate.

SECTION 7

SEDIMENT MODELING

BACKGROUND DESCRIPTION OF SOIL EROSION PROCESSES

The process of soil erosion in upland areas is the result of detachment and transport of soil particles downslope through the action of raindrop splash and surface runoff. More than 30 years ago, W. D. Ellison (1946) recognized the importance of rainfall and runoff as erosive agents and emphasized the need of studying them separately. Interactions of soil and watershed characteristics and energy sources complicate the soil erosion process. Only in recent years have intensified efforts been undertaken to examine the mechanics of detachment, transport and deposition of soil debris during storm events.

Factors Influencing Soil Detachment

Detachment of soil particles or aggregates from a soil matrix is the initial phase of soil erosion. The energy required for soil detachment may be supplied by raindrop splash, runoff, the gravitational effect, and seepage forces (Onstad and Moldenhauer, 1975). Whether or not a soil particle is displaced also depends upon its position relative to surrounding particles.

As reported by Mutchler and Young (1972), raindrop splash is the primary agent in soil detachment that causes soil transport from overland flow areas to micro-channels. Studies by Moldenhauer and Koswara (1968) indicate that for a constant rainfall intensity, the detachment of soil particles by raindrop impact is a time-dependent function. They report that particle detachment increases rapidly at the beginning of rainfall, reaches a peak, and then decays in an exponential fashion to a steady-state rate.

The concentration of flow in micro-channels as a result of micro-topography or previous erosion is referred to as rill flow. Development of rills by concentrated surface runoff flow is known to be a function of slope length. Meyer et al. (1972) indicate that interrill or sheet erosion due to raindrop impact increases to a nearly constant value at some distance downslope, while rill erosion increases at a nearly linear rate. The cross-sectional shape of rills also determines soil detachment characteristics. For two micro-channels of equal depth, a rill with rectangular cross-sectional shape will have a larger area than a rill with triangular shape.

In addition to the detachment of soil by raindrop splash and surface runoff, physical and hydrological properties may significantly affect soil erodibility characteristics. Grissinger (1972) reports that for cohesive soils, erodibility decreases with increased soil wetting time because cohesive forces have time to develop and strains produced by water sorption are dissipated. To illustrate another example, Onstad and Moldenhauer (1975) point out that soil aggregates are usually more stable when dry, so high rainfall intensities at the beginning of a storm may detach less soil than if they occurred at the end of a storm. Rainfall intensity patterns may also affect overland flow peaks and volumes which in turn alter detachment characteristics. Protection of the soil surface from direct raindrop impact by vegetative cover, ground litter, and stone is still another important factor affecting soil detachment in upland areas.

Factors Influencing Soil Transport

With the detachment of soil particles, erosion occurs as the result of transport by raindrop splash or runoff. Such factors as the amount of rain, slope steepness, microtopography, and soil properties determine the capacity for rainfall to transport soil particles. Ekern (1953) reported that the net downslope movement of detached soil due to raindrop splash is proportional to slope steepness.

The extent and development of rills in upland areas is a significant factor in the transport characteristics of detached soil particles. The capacity of flowing water to transport soil was shown by Laursen (1958) to be approximately proportional to the fifth power of velocity. Studies by Young and Wiersma (1973) and Meyer et al. (1972) indicate that rill flow has a much greater transporting capacity than sheet flow because of its runoff concentration.

In the uppermost reaches of a watershed, raindrop splash is the primary agent for soil detachment and transport at the onset of a rainstorm. Here soil erosion is largely dependent upon rainfall energy and slope gradient if detachment is limiting (Wischmeier, 1973). Soil particles detached by raindrop impact are transported in microthin layers by overland flow and concentrated into rills. In the lower reaches of the watershed, the role of runoff as a detaching and transporting agent becomes increasingly important relative to that of rainfall. At the outlet of the catchment basin, transporting capacity of surface runoff limits the amount of sediment actually carried out of the watershed.

Development of Mathematical Models For Erosion Processes

Spatial and temporal variations in the processes and interactions of agents governing soil detachment and transport complicate the process of soil erosion. Onstad and Moldenhauer (1975) point out the need for transforming a watershed into a framework wherein sediment and hydrologic components can be simulated. Recent interests in predicting sediment yields from watersheds has lead to the formulation of mathematical models which consider both passive watershed factors such as soil type, topography, and vegetative characteristics as well as erosive agents including raindrop splash and runoff energy which vary in time and space. The development of such models has been highly beneficial as a design tool for the control of sediment losses and prevention of erosion damage.

A mathematical model developed by Negev (1967) considered processes of soil splash by raindrop impact, transport by overland flow, rilling and gullying, and channel transport of both coarse and fine sediment. A framework describing the process of soil erosion by rainfall and runoff was presented by Meyer and Wischmeier (1969). Coupling theoretical considerations with laboratory flume data, plot erosion data, and rainfall simulation erosion rates, their approach to erosion simulation emphasized soil detachment and transport by rainfall and runoff. By using the continuity equation for mass transport and a sediment laden - flow detachment interrelationship, Foster and Meyer (1972) developed a mathematical model capable of describing the erosion process at any point in time and at any location in a watershed. Their model considered both sheet and rill erosion source areas of sediment.

In this study the mathematical model adapted for predicting water and sediment routing and yield on mine spoils is one developed by Li (1974).

This numerical scheme requires less calibration than other water and sediment routing models available today. With the lack of available knowledge on the development, frequency, and cross-sectional geometry of rills, Li's model considers sheet erosion to be the main process in overland flow erosion.

WATER ROUTING MODEL FOR OVERLAND FLOW

The model used for predicting water routing on the mine spoil test plots is one developed by Li (1974). The water routing for this particular model is accomplished by a second-order nonlinear scheme developed to numerically solve the kinematic wave equation. The equations of continuity, momentum, and the laws of resistance are used to describe runoff on an overland flow unit for Reynolds number less than 900. Herein, the governing equations as described by Li (1974) in the development of the numerical scheme for overland flow water routing are presented, with application to the present study.

Momentum Equation

The momentum equation for overland flow on a unit width basis may be expressed as

$$S_f = S_o - \frac{\partial d}{\partial x} - \frac{1}{gd}\frac{\partial q}{\partial t} - \frac{1}{gd}\frac{\partial}{\partial x}\left(\frac{q^2}{d}\right)^2 \qquad (58)$$

where S_f is the friction slope, S_o is the bedslope, d is the depth of flow, x is the distance downslope, g is the gravitational acceleration, q is the discharge per unit bed width, and t is the time. By assuming that the gradients due to local and convective accelerations are negligible, and that the water surface slope is nearly equal to the bed slope, the momentum equation may be simplified and written in the form

$$S_f \simeq S_o = f\,\frac{q^2}{8gd^3} \qquad (59)$$

in which f is the Darcy-Weisbach friction factor. Equation 59 may be referred to as the kinematic wave representation for overland flow.

Continuity Equation

The continuity equation for overland flow is

$$\frac{\partial q}{\partial x} + \frac{\partial d}{\partial t} = q_\ell \tag{60}$$

in which q_ℓ is the lateral inflow rate per length of overland flow unit, equal to the mean rainfall excess rate.

Resistance Equations

For surface runoff on rigid boundaries, the Darcy-Weisbach friction factor is dependent upon the depth of flow, the roughness of the boundary, the Reynolds number of the flow, and the rainfall intensity. The Reynolds number N_r may be written

$$N_r = \frac{q}{\nu} \quad . \tag{61}$$

For uniform flow over a soil surface, the downslope component of water weight is balanced by the force due to grain resistance. That is,

$$\gamma d S_o = \frac{1}{8} f \rho V^2 \quad . \tag{62}$$

Here γ is the specific weight of water, ρ is the density of water, and V is the mean velocity of water flow. For overland flow, this grain resistance may be defined as the skin resistance which acts on particles forming the bedslope.

In addition to energy losses due to rigid boundaries, the effect of rainfall on flow resistance is a significant factor in shallow, overland flow depths. The impact of raindrops falling on the flow roughens the water surface and retards the velocity of the overland flow. Shen and Li (1973) have experimentally determined equations for estimating friction factors for flows as functions of boundary roughness, Reynolds number, and the raindrop intensity.

To estimate the grain resistance with and without rainfall for laminar flows (N_r < 900), the equations are

$$f = \frac{K_1}{N_r} = \frac{K_o + K_r i_r^{0.407}}{N_r} \tag{63}$$

and

$$f = \frac{K_o}{N_r} \tag{64}$$

where K_1 is a parameter which varies with rainfall intensity, K_0 is a constant describing the Darcy-Weisbach friction factor without rainfall, i_r is the rainfall intensity in inches per hour, and K_r is a number describing the additional energy losses due to rainfall. Simons et al. (1975) assumed that grain resistance factors are applicable to friction factors for rigid boundaries. Then the grain resistance factor K_0 may be estimated from the friction factor - Reynolds number - relative roughness relation commonly found in fluid mechanics textbooks (for example, Chow, 1959, p. 11).

Unit Discharge and Flow Depth Relation

For overland flow processes, the depth of flow may be expressed as a power function of the unit discharge (Lighthill and Whitham, 1955). That is,

$$d = \alpha q^{\beta} \tag{65}$$

in which α and β are coefficients which depend upon the roughness of the overland flow unit. For Reynolds number less than 900, the value of β is 1/3.

Using the Darcy-Weisbach friction factor, the value of α may be determined by substituting equations 61 and 62 into equation 59 and comparing with equation 65. This results in

$$\alpha = \left[\frac{K_1 \nu}{257.6\ S_0} \right]^{1/3} \quad . \tag{66}$$

Numerical Model

The second-order nonlinear scheme developed by Li to solve the kinematic wave equation numerically may be used to obtain solutions to the cases of time-variant inflows and varying roughness. A linear scheme developed by Li is used to provide first approximations of flow conditions which are then refined by the nonlinear scheme.

Equation 60 may be expressed in finite-difference form as

$$\frac{q_{j+1}^{n+1} - q_j^{n+1}}{\Delta x} + \frac{d_{j+1}^{n+1} - d_{j+1}^{n}}{\Delta t} = \frac{q_{\ell_{j+1}}^{n+1} + q_{\ell_{j+1}}^{n}}{2} \tag{67}$$

in which q_j^n is the quantity q at grid point $x=j\Delta x$, $t=n\Delta t$, and Δx and Δt are space and time increments, respectively. The unknowns in Equation 67 are

q_{j+1}^{n+1} and d_{j+1}^{n+1}.

From Equation 60, finite difference forms may be represented as

$$d_{j+1}^{n+1} = \alpha(q_{j+1}^{n+1})^{\beta} \tag{68}$$

and

$$d_{j+1}^{n} = \alpha(q_{j+1}^{n})^{\beta} \quad . \tag{69}$$

Substituting equations 68 and 69 into equation 67 and rearranging yields

$$\frac{\partial t}{\partial x} q_{j+1}^{n+1} + \alpha(d_{j+1}^{n+1})^{\beta} = \frac{\partial t}{\partial x} q_{j}^{n+1} + \alpha(q_{j+1}^{n})^{\beta} + \frac{\Delta t(q_{\ell_{j+1}}^{n+1} + q_{\ell_{j+1}}^{n})}{2} \tag{70}$$

where the right-hand side of the equation contains known quantities. Li's use of a Taylor Series expansion provides solutions to this nonlinear scheme.

The term $\partial d/\partial t$ in equation 60 may be written as

$$\frac{\partial d}{\partial t} = \frac{\partial d}{\partial q}\frac{\partial q}{\partial t} \quad . \tag{71}$$

In addition,

$$\frac{\partial d}{\partial q} = \alpha\beta q^{\beta-1} \tag{72}$$

from equation 65. Substituting equations 71 and 72 into 60 results in

$$\frac{\partial q}{\partial x} + \alpha\beta q^{\beta-1}\frac{\partial q}{\partial t} = q_{\ell} \quad . \tag{73}$$

Expressing equation 73 in finite-difference form and rearranging,

$$q_{j+1}^{n+1} = \frac{\frac{\Delta t}{\Delta x} q_{j}^{n+1} + \alpha\beta q_{j+1}^{n}\left(\frac{q_{j+1}^{n} + q_{j}^{n+1}}{2}\right)^{\beta-1} + \Delta t\left(\frac{q_{\ell_{j+1}}^{n+1} + q_{\ell_{j+1}}^{n}}{2}\right)}{\frac{\Delta t}{\Delta x} + \alpha\beta\left(\frac{q_{j+1}^{n} + q_{j}^{n+1}}{2}\right)^{\beta-1}} \quad . \tag{74}$$

This equation provides the initial estimate for the nonlinear scheme. For details concerning the stability and convergence of the numerical scheme for water routing, the reader is referred to Li (1974), or Li et al. (1975).

SEDIMENT ROUTING FOR OVERLAND FLOW

Continuity Equation For Sediment

The sediment continuity equation for overland flow may be expressed as

$$\frac{\partial g_s}{\partial x} + \frac{\partial C_s d}{\partial t} + \frac{\partial z}{\partial t} = 0 \tag{75}$$

where

$$C_s = \frac{g_s}{q} \tag{76}$$

and g_s is the sediment transport rate, C_s is the sediment concentration by volume, and z is the net depth of loose soil.

The total sediment load in transport may be divided into a wash load and a bed-material load. For the present study, it is assumed that the wash load consists of those particles with diameter smaller than 0.062 mm, the division point between sand and silt (Simons, 1975)*. Particles greater than 0.062 mm diameter are regarded as bed-material load. For these two sediment categories, the continuity equation can be divided into two parts,

$$\frac{\partial g_b}{\partial x} + \frac{\partial C_b d}{\partial t} + \frac{\partial z_b}{\partial t} = 0 \tag{77}$$

and

$$\frac{\partial g_w}{\partial x} + \frac{\partial C_w d}{\partial t} + \frac{\partial z_w}{\partial t} = 0 \tag{78}$$

where g_b and g_w are, respectively, the bed-material load and the wash load transport rates, C_b and C_w are, respectively, the concentrations of suspended wash load, and z_b and z_w are, respectively, depths of loose soil for the bed-material load size and wash load size. In addition,

$$g_s = g_b + g_w \quad , \tag{79}$$

$$C_b = \frac{g_b}{q} \quad , \tag{80}$$

$$C_w = \frac{g_w}{q} \quad , \tag{81}$$

---

*Simons, D. B., 1975, personal communication, November.

and

$$z = z_b + z_w \quad . \tag{82}$$

Sediment Transport Equations

The sediment transporting capacity of a given flow is determined by a sediment transport equation. Typically, the rate of transport consists of a bed load transport rate and a suspended load transport rate. The former represents the capability of the flow to transport entrained particles close to the bed of the overland flow unit. Such sediment motion occurs as rolling, sliding, or sometimes saltating. Suspended load transport rate describes the capability of the flow to transport sediment particles in suspension for an appreciable length of time.

The bed load discharge for both bed-material and wash load size sediments was fit to the function

$$q_b = \beta_1 \tau^{\beta_2} \tag{83}$$

where q_b is the bed load transport rate, τ is the boundary shear stress, and β_1 and β_2 are constants.

The boundary shear stress is defined as

$$\tau = \gamma d S_o \tag{84}$$

in which d is determined by the kinematic wave approximation described previously.

As reported by Einstein in 1950, the concentration profile for sediment transported in the suspended load is

$$\frac{C_\xi}{C_a} = \left(\frac{d-\xi}{\xi} \frac{a}{d-a} \right)^{\omega} \tag{85}$$

where C_ξ is the sediment concentration at the distance ξ from the bed, C_a is the known concentration at the distance a above the bed, d is the total depth of flow, and ω is a parameter defined as

$$\omega = \frac{V_s}{0.4U_*} \quad . \tag{86}$$

Here V_s is the settling velocity of the sediment particle and U_* is the shear velocity of the flow.

For overland flow conditions, a logarithmic velocity profile is assumed, which takes the form

$$\frac{U_\xi}{U_*} = B + 2.5 \ln\left(\frac{\xi}{n_s} \right) \tag{87}$$

where U_ξ is the point mean velocity at a distance ξ from the bed, U_* is the shear velocity of flow defined as $\sqrt{\tau/\rho}$, B is a constant dependent on roughness, and n_s is the roughness height.

The integral of suspended load above a distance a in the flow may be written as

$$q_s = \int_a^d U_\xi C_\xi d\xi \quad . \tag{88}$$

Substituting in expressions for U_ξ and C_ξ yields

$$q_s = C_a U_* \int_a^d \left[B + 2.5 \ln\left(\frac{\xi}{n_s} \right)\right]\left(\frac{d-\xi}{\xi} \frac{a}{d-a} \right)^\omega d\xi \quad . \tag{89}$$

Letting $r = \xi/d$ and $G = a/d$, then

$$q_s = C_a U_* a \frac{G^{\omega-1}}{(1-G)^\omega} \left\{\left[B + 2.5 \ln\left(\frac{d}{n_s} \right)\right] \int_G^1 \left(\frac{1-r}{r} \right)^\omega dr + 2.5 \int_G^1 \ln r\left(\frac{1-r}{r} \right)^\omega dr \right\} \quad . \tag{90}$$

The concentration near the bed layer C_a as defined by Einstein (1950) is related to the bed load transport rate q_b by the expression

$$q_b = 11.6\ C_a U_* a \tag{91}$$

in which a is now taken as the thickness of the bed layer which is twice the size of the sediment particle.

The average flow velocity V is given by the expression

$$V = \left(\int_0^d \mu_\xi d\xi \right) / \left(\int_0^d d\xi \right) \quad . \tag{92}$$

Then, using equation 87,

$$\frac{V}{U_*} = B + 2.5 \ln\left(\frac{d}{n_s} \right) - 2.5 \quad . \tag{93}$$

The two integrals in equation 87 were defined by Einstein (1950) as

$$J_1 = \int_G^1 \left(\frac{1-r}{r} \right)^{\omega} dr \tag{94}$$

and

$$J_2 = \int_G^1 \left(\frac{1-r}{r} \right)^{\omega} \ln r \, dr \quad . \tag{95}$$

These integrals cannot be integrated in closed form for most values of ω so a numerical scheme is necessary. Li (1974) has developed an efficient method for determining J_1 and J_2 which is used in the current investigation.

Substituting equations 91, 92, 93, and 95 into equation 90 results in the expression

$$q_s = \frac{q_b}{11.6} \frac{G^{\omega-1}}{(1-G)^{\omega}} \left[\left(\frac{V}{U_*} + 2.5 \right) J_1 + 2.5 J_2 \right] \quad . \tag{96}$$

Values of G, V, and U_* are determined by the water routing procedure and q_b is computed from equation 83. By letting

$$\overline{G} = \frac{G^{\omega-1}}{11.6(1-G)^{\omega}} \left[\left(\frac{V}{U_*} + 2.5 \right) J_1 + 2.5 J_2 \right] \tag{97}$$

and by combining the bed load and suspended load discharges, the total rate of sediment transport per unit width may be written

$$g_c = q_b \left[1 + \overline{G} \right] \quad . \tag{98}$$

Equations For Sediment Supply

The supply of sediment for overland flow units depends upon the amounts of soil detached by raindrop impact and overland flow erosion. For sediment modeling on the mine spoil test plots, these two detachment components were considered in the routing process.

The detachment of soil particles from an eroding bed surface due to raindrop impact is known to be related to the rainfall intensity of a particular storm. A number of past studies (Wischmeier and Smith, 1958; Bubezer and Jones, 1971; and Meyer and Wischmeier, 1969) have indicated that soil detachment is proportional to the square of rainfall intensity.

Simons et al. (1975) assumed that raindrop impact has a potential rate of soil detachment equal to

$$D_i = a_3 i_r^{b_3} (1 - z/z_m) \quad , \quad \text{if } z \leq z_m \quad . \tag{99}$$

If $z > z_m$, then

$$D_i = 0 \quad . \tag{100}$$

D_i represents the potential rate of soil detachment in units of depth per unit time, a_3 and b_3 are coefficients dependent upon soil erodibility and z_m is the equivalent maximum penetration depth of raindrop impact on the soil layer. New amounts of loose spoil material available for transport at $t+\Delta t$ may be written as

$$z_b(t+\Delta t) = a_b(t) + F_b D_i \Delta t \tag{101}$$

and

$$z_w(t+\Delta t) = z_w(t) + F_w D_i \Delta t \quad . \tag{102}$$

Here $z_b(t)$ and $z_w(t)$ are, respectively, the amounts of loose bed material load soil and wash load soil available for transport at time t, and F_b and F_w are the respective percentages of bed material load size and wash load size in a typical spoils sample.

By comparing the available amount of loose soil and the sediment transporting capacity of the flow, the amount of soil detachment by overland flow surface runoff can be determined. For sediment routing, Simons et al. (1975) assumed that due to the armoring effect of larger size sediments, wash load size sediment is not detached unless some bed material has been detached by overland flow. The potential change in loose soil storage for bed material load size Δz_b^p is found by substituting the the bed material load transporting capacity g_c given by equation 98 into the bed material load transport rate g_b given by equation 77. Then,

$$z_b^p = \frac{\partial z_b}{\partial t} \Delta t \quad . \tag{103}$$

For the case where $\Delta z_b^p \geq -z_b$, the loose soil storage is enough for transport and no detachment of spoil material is expected. If $\Delta z_b^p < -z_b$, soil is detached, and the amount of detachment is assumed to be

$$D_b = -D_f(\Delta z_b^p + z_b) \tag{104}$$

where D_b is the amount of detached bed material soil, and D_f is a constant depending on soil erodibility.

New amounts of loose soil available for transport at time $t+\Delta t$ are then

$$z_b(t+\Delta t) = z_b(t) + D_b \tag{105}$$

and

$$z_w(t+\Delta t) = z_w(t) + D_b F_w / F_b \quad . \tag{106}$$

Numerical Scheme For Sediment Routing

By coupling the equations governing sediment motion with the water routing procedure described previously, Simons et al. (1975) have developed a numerical scheme for bed material load and wash load sediment routing. In Figure 56, a flow chart of their model is given. The following is a description of their procedure for wash load routing. For either size sediment, the numerical scheme is similar.

The potential change in loose storage for wash load size sediment may be written

$$\Delta z_w^p = (g_{w_j}^{n+1} - C_w^p \, g_{j+1}^{n+1}) \frac{\Delta t}{\Delta x} - C_w^p \, d_{j+1}^{n+1} + C_{w_{j+1}}^n \, d_{j+1}^n \tag{107}$$

in which

$$C_w^p = \frac{g_{c_{j+1}}^{n+1} \text{ (wash load)}}{q_{j+1}^{n+1}} \quad . \tag{108}$$

The wash load availability is greater than the transporting capacity of the flow if $\Delta z_w^p \geq -z_w$. Hence, the wash load transport rate is equal to the transporting capacity or

$$C_{w_{j+1}}^{n+1} = C_w^p \tag{109}$$

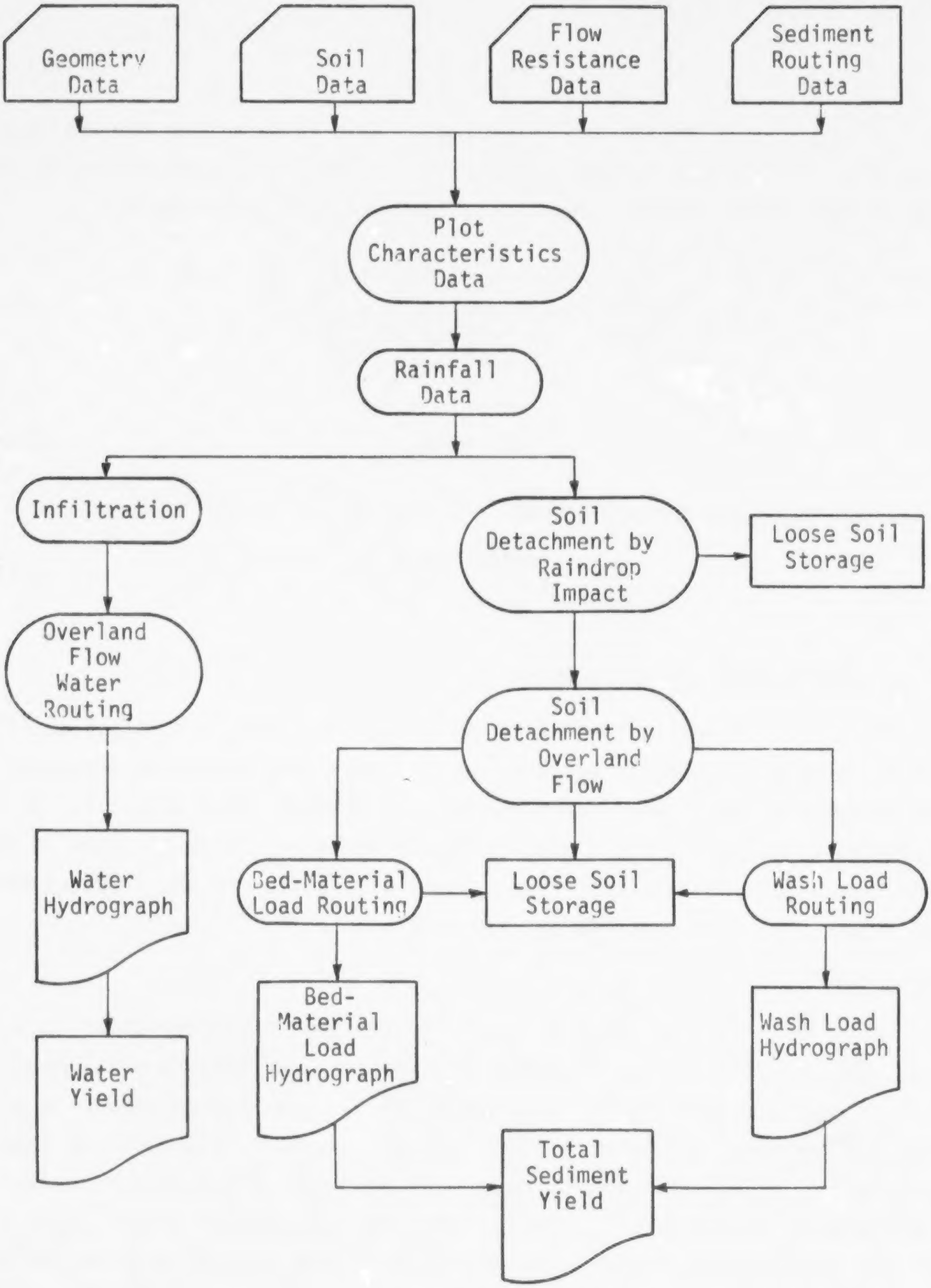
Geometry Data
Soil Data
Flow Resistance Data
Sediment Routing Data
Plot Characteristics Data
Rainfall Data
Infiltration
Soil Detachment by Raindrop Impact
Loose Soil Storage
Overland Flow Water Routing
Soil Detachment by Overland Flow
Water Hydrograph
Bed-Material Load Routing
Loose Soil Storage
Wash Load Routing
Water Yield
Bed-Material Load Hydrograph
Wash Load Hydrograph
Total Sediment Yield

Figure 56. Flow chart for water and sediment routing model.

with the change in z_w equal to

$$\Delta z_w = \Delta z_w^p \quad . \tag{110}$$

If $\Delta z_w^p < -z_w$, the availability of wash load is less than the transporting capacity. For this case, the availability of soil limits the amount of wash load actually transported. Therefore, the wash load concentration is

$$C_{w_{j+1}}^{n+1} = \frac{z_w + C_{w_{j+1}}^n d_{j+1}^n + g_{w_j}^{n+1} \frac{\Delta t}{\Delta x}}{d_{j+1}^{n+1} + q_{j+1}^{n+1} \frac{\Delta t}{\Delta x}} \tag{111}$$

and

$$\Delta z_w = -z_w \quad . \tag{112}$$

Thus, the wash load transport rate is determined by equation 81 and

$$g_{w_{j+1}}^{n+1} = C_{w_{j+1}}^{n+1} q \quad . \tag{113}$$

MODEL VERIFICATION AND APPLICATION

From the mathematical models developed by Li (1974) and Simons et al. (1975), a computer program was adopted for simulating water and sediment hydrographs for experiments performed at the Colorado test site. In the appendix, a listing of the computer program is given. A description of input data, model calibration, test results, and application of the proposed model for predicting surface runoff and sediment production follows.

Input Data

Data input for the proposed model include plot characteristics information, and rainfall or runoff excess information. Included in plot characteristics data are geometry and spoil material data, a flow resistance descriptor, and sediment routing parameters, all of which are assumed to be time-invariant. In Table 27, a listing of the input data required for the water and sediment routing model is given. For the mathematical model, surface runoff and sediment routing are generated from a given rainstorm or runoff event, with the assumption of known rates of infiltration during the event.

TABLE 27. INPUT DATA REQUIRED FOR THE SIMULATION MODEL

Data Type	Definition	Symbol
Plot data	Slope length	L
	Bed slope	S_o
	Mean wash load size	ds_w
	Particle size distribution	$F_{b,w}$
Runoff event data	Rainfall intensity	i_r
	Infiltration rate	f_i
Flow resistance parameters	Constant representing grain resistance without rainfall for $N_r<900$	K_o
	Constant describing additional resistance to flow due to raindrop impact	K_r
Sediment routing parameters	Coefficient in sediment transport equation	β_1
	Exponent in sediment transport equation	β_2
	Detachment coefficient of runoff	D_f
	Coefficient in raindrop soil detachment equation	a_3
	Exponent in raindrop soil detachment equation	b_3
	Maximum depth to which a raindrop can penetrate the soil layer	D_p

TABLE 28. SUMMARY OF EXPERIMENTAL PLOT DIMENSIONS AND PERCENTAGES OF BED-MATERIAL LOAD SIZE SEDIMENT AT THE EDNA MINE FIELD SITE

Plot Slope (%)	Length (meters)	Area (square meters)	Percentage of bed-material load size sediment for plot (%)
1	9.85	36.97	25.3
3	9.94	39.66	31.1
5	9.62	39.63	32.5
7	9.54	36.91	34.2

For the proposed model, the respective percentages of bed-material load size and wash load size sediments in a typical soil sample are required. From the analysis of four surface samples taken from quadrants on each of the test plots, the percentage of bed-material load size in the spoil material was computed. The soil samples were wet sieved for determining the percentage of material coarser than the 0.062 mm diameter size. The results of the analysis are given in Table 28, which indicate similar particle size distributions among the test plots. Also shown in the table are dimensions of the experimental plots.

For routing of a runoff excess event, the parameter K_o used to describe grain resistance without rainfall was taken to be 45, the value given for flow in rough channels (see Chow, 1959, p. 11). In the routing of rainfall excess, a value of 27 was selected for the coefficient K_r used to describe the added friction resulting from rainfall. This is the value reported by Shen and Li (1973) for raindrops with terminal velocities. The parameter D_p, a measure of the maximum depth to which a raindrop can penetrate the soil layer, was assumed to have a value of 0.03 meter.

The sediment transport equation given by equation 98 describes the sediment transporting capacity of a given flow for either bed-material load or wash load sediments. As previously mentioned, the amount of sediment transported in the suspended load is dependent upon the parameter of suspension ω described by equation 86. According to Li (1974), flows with ω greater than 5.5 can transport little or no sediment in suspension. In addition, Li (1974) indicates that for the condition wherein the parameter G (the ratio of twice the size of the mean sediment particle in transport to the average flow depth) is greater than 0.9, no appreciable transport of sediment in suspension will occur. As evidenced by high fall velocities for bed-material load size sediment, shallow flow depths, and small shear velocities for overland flow, the transport of bed-material in suspension was assumed to be negligible. Hence, the equation of sediment transport for bed-material load reduces to

$$g_c = \beta_1 \tau^{\beta_2} \quad . \qquad (114)$$

The constants β_1 and β_2 in equations 114 and 98 describing sediment transport for bed-material and wash load sediments, respectively, require calibration.

In equation 99, the parameters a_3 and b_3 describe the potential soil detachment rate by raindrop impact. As discussed previously, studies have indicated that the detachment of soil by raindrop impact is proportional to the square of rainfall intensity. Hence, a value of b_3 equal to 2.0 was assumed for the given study. Simons et al. (1975) indicate that the value of a_3 is dependent upon soil erodibility and is related to wash load sediment yield. A calibration procedure was used to estimate this parameter. The amount of soil detached by surface runoff is determined by the detachment coefficient D_f. The value of D_f was also determined by calibration.

Model Calibration

The purpose of calibrating a mathematical model is to determine model parameters which correctly simulate system responses. Model parameters are selected in a manner which allows the model to perform as well as possible within constraints imposed by physical conditions and field measurements (Simons and Li, 1976). Optimization is one means by which model parameters can be calibrated. For the proposed mathematical model, parameters were estimated for sediment transport functions (equations 98 and 114) and coefficients describing soil erodibility due to rainfall (equation 99) and runoff (equation 104).

The manner in which the estimation of parameters was made for the simulation model is shown below.

1. Using regression analysis, determine parameters β_1 and β_2, which describe sediment transporting capacity for bed-material and wash load sediments.
2. Set the rainfall detachment coefficient equal to zero. Calibrate the surface runoff detachment coefficient D_f by adjusting its value to make the computed bed-material load equal to the measured bed-material load.
3. With the value of D_f determined in step 2, calibrate a_3 by adjusting its value to make the computed wash load equal to the measured wash load.

To determine the constants β_1 and β_2 for the equations of sediment transport, a procedure suggested by Li was utilized. This method assumes that no change occurs in the bedslope when the flow just reaches equilibrium. From equations 114 and 98, total rates of sediment transport for wash load and bed-material load sediment may be expressed as

$$g_c = \beta_1 \tau^{\beta_2}(1+\overline{G}) \tag{98}$$

and

$$g_c = \beta_1 \tau^{\beta_2} \tag{114}$$

respectively.

Here g_c was measured at the beginning of runoff during experimentation, and τ and $\overline{G}$ were determined in the following manner.

The unit width discharge at the end of a test plot q_p is

$$q_p = q_\ell L \tag{115}$$

when the flow reaches equilibrium.

The depth of flow at the end of a test plot d_p can be found by rearranging the approximate momentum equation (equation 59) for overland flow. This results in

$$d_p = (f \frac{q_p^2}{8gS_o})^{1/3} \quad . \tag{116}$$

In addition, the average flow velocity at the end of a test plot V_p can be determined by

$$V_p = \frac{q_p}{d_p} \quad . \tag{117}$$

By knowing values of d_p and V_p, τ and $\overline{G}$ may be computed from equations 84 and 97, respectively.

From data collected at the beginning of the 1976 field experiments performed under simulated rainfall, a least squares regression was run for the function

$$Y = \alpha_1 X^{\alpha_2} \tag{118}$$

used to describe bed-material load transport (equation 114). Here Y and X are the dependent and independent variables, respectively, and α_1 and α_2 are regression coefficients.

For wash load sediment, a nonlinear regression analysis was run for the function

$$Y = \alpha_1 X^{\alpha_2}(1+Z) \qquad (119)$$

in which Z is an independent variable representing $\overline{G}$ in equation 97.

Results of the regression analyses run for bed-material load and wash load sediments are summarized in Table 29. The magnitude of the exponent α_2 in equation 114 compares favorably with the relation suggested by DuBoys (1879), in which the rate of sediment transport is said to be a function of the shear stress squared. The exponent in equation 98 falls within the range of 1.5 to 1.8, values of the exponent reported by the U. S. Waterways and Experiment Station (1935) for sand mixtures of $0.025 < d < 0.560$ mm.

TABLE 29. SUMMARY OF REGRESSION RESULTS FOR SEDIMENT TRANSPORT EQUATIONS

Sediment Transport Equation	Correlation Coefficient	Estimate Coefficients	
		α_1	α_2
Eq. 114	0.997	0.01714	2.005
Eq. 108	0.978	0.000121	1.601

The collection of sediment runoff data from experiments performed with and without simulated rainfall offered a unique opportunity for calibrating the coefficients describing soil detachment by rainfall and runoff. With the calibrated sediment transport equations, the surface runoff detachment coefficient D_f was estimated from the overland flow runoff data collected during 1975, and the rainfall detachment coefficient a_3 was calibrated from simulated rainfall experiments performed in 1976.

As mentioned previously, it is assumed that the erosion of bed-material is the primary concern for detachment of soil by surface runoff. Surface runoff was the primary sediment detaching agent in overland flow experiments performed during 1975. Hence, the calibration of the runoff detachment coefficient D_f was based upon bed-material sediment data collected during the

1975 runs. In that no bed-material sediment was reported for runs 3 and 5, runoff data from these experiments were not included in the calibration procedure. The estimation of the coefficient D_f was determined by using a simple optimization scheme. The objective function minimized was the sum of squares of logarithmic deviations, defined as

$$F = \sum_{i=1}^{N} [\ln R_i^e - \ln R_i^o]^2 \quad . \tag{120}$$

Here F is the objective function to be minimized, N is the number of observations, R_i^e is the estimated bed-material sediment yield utilizing the mathematical model for the ith experiment, and R_i^o is the measured bed-material sediment yield for the ith experiment. The optimization search was initiated by assuming a particular value of D_f. Computer simulations of runs 6 through 13 were then made, to obtain computed bed-material sediment yields. Using equation 120, a value for the objective function F was determined by comparing measured and simulated bed-material sediment yields. A new value of D_f was assumed, and the procedure to evaluate the objective function was repeated. Through successive searches, a minimum value of F was computed, corresponding to the optimal runoff detachment coefficient D_f. The results of the calibration based upon bed-material sediment data collected during 1975 indicate a value of D_f equal to 0.0031.

The rainfall detachment coefficient a_3 was estimated from experimental data collected during runs 14 through 19. In these simulated rainfall experiments, both rainfall and runoff were sediment detaching agents. The estimation of the coefficient a_3 was made by including runoff as a detaching agent in the numerical computations. As the rainfall detachment coefficient is primarily related to wash load sediment yield, the objective function minimized to determine its value was

$$F = \sum_{i=1}^{N} [\ln R_i^e - \ln R_i^o]^2 \quad . \tag{121}$$

Here R_i^e and R_i^o represent total amounts of simulated and measured wash load sediment for the ith experiment respectively. Following the same format as discussed in estimation of D_f, a trial and error solution was used to calibrate a_3. Based upon the 1976 field data, the estimated value of the rainfall detachment coefficient was 0.000044.

Test Results

The numerical scheme for computing water and sediment routing was based upon a time increment Δt equal to 1 minute and space increment ΔX equal to 0.3048 meter. For simulating overland flow runoff events, a runoff excess was routed with the assumption of a known runoff event. In the simulation of a runoff event resulting from a given rainstorm, a rainfall excess was routed. Data necessary for adequately establishing rates of infiltration during a particular rainfall or overland flow runoff experiment were not readily available. For periods of steady-state runoff during experimental runs, constant rates of infiltration were assumed. The mean rainfall or runoff excess rate was then computed as the difference between the average water application rate and the constant infiltration rate per length of overland flow unit. Without available information to describe changes in soil moisture depletion during the first several minutes of a particular experiment, it was necessary to assume that the beginning time of a simulated rainfall or runoff event corresponded to the initiation of runoff reported in the field measurements. This assumption allowed for the correct simulation of the rising hydrograph limb in the experimental data. With the construction of simulated runoff hydrographs based upon measured runoff data, evaluation of the degree of accuracy between measured and simulated bed-material load and wash load discharges was made.

Comparison of simulated and measured results for bed load discharges was not good. In most cases, the sediment model over-predicted the bed load discharge. Agreement between the calculated and measured wash load discharges for the conditions of simulated rainfall (experiments 14 through 19) was considered good. Figures 57 and 58 show the typical comparisons obtained for the experiments under simulated rainfall. It was concluded that the model is capable of simulating wash load discharge rates to the ±39 percent (average error was much smaller) but larger errors should be expected in calculated bed load discharges.

The largest difference between simulated and measured results are to be expected when discharges are compared. Integration of sediment discharges over time to obtain sediment yields smooths both the simulated and measured

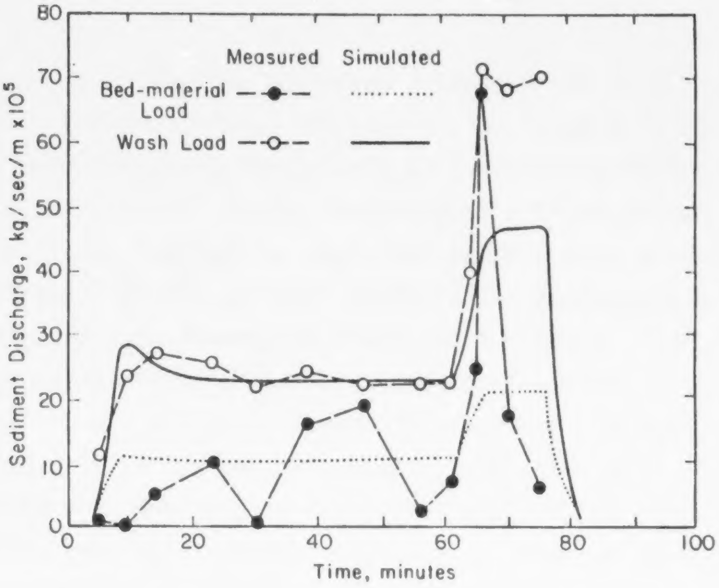

Figure 57. Comparison of simulated and measured sediment discharges for run 15.

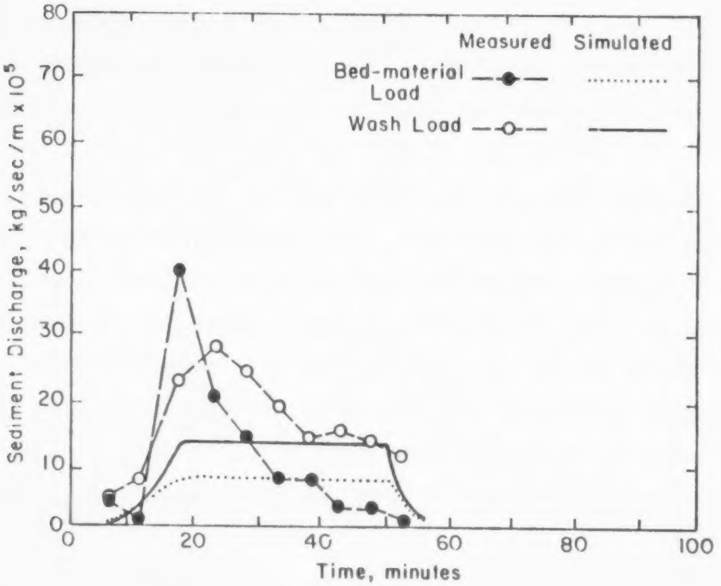

Figure 58. Comparison of simulated and measured sediment discharges for run 18.

results. Figures 59 and 60 show comparisons between the calculated and measured sediment yields, separated into wash load yield and bed load yield, respectively. The two data points that fall well off the line in Figure 59 are both from the plot with a 1% surface slope. It is believed that, for this small slope, processes of aggradation and degradation periodically resulted in a nearly level bedslope; a condition for which the model does not apply. As expected, the agreement between the measured and calculated bed load yield was not as good as for the wash load, although the agreement in Figure 60 is considered satisfactory.

SPOIL ERODIBILITY

One of the useful means for describing the erodibility of a given soil is the K factor in the Universal Soil Loss Equation. Determining the erodibility characteristics of a soil can be a beneficial tool in developing sound conservation practices for agricultural land and areas distrubed by construction and mining activities. Herein the erodibility factor is evaluated for spoil materials on the Edna Mine in the Yampa Coal Field of Routt County, Colorado. Based upon experimental data collected from simulated rainfall events on test plots, the soil erodibility factor was computed from

$$K = A/[R(LS)CP]$$

where

K = soil erodibility factor, in tons per acre per unit of R for a specific soil and standard conditions,
A = measured soil loss in tons per acre,
R = rainfall factor,
LS = topographic factor,
C = cropping-management factor,
P = conservation practice factor.

In that no special management or conservation practices were employed on the test plots during experimentation, the product of C and P in the equation above were assumed to be equal to 1.0. The value of R was computed as the product of the kinetic energy in hundreds of foot-tons per acre, times the maximum 30-minute intensity, in inches per hour. Hence, for a given experimental run on a test plot,

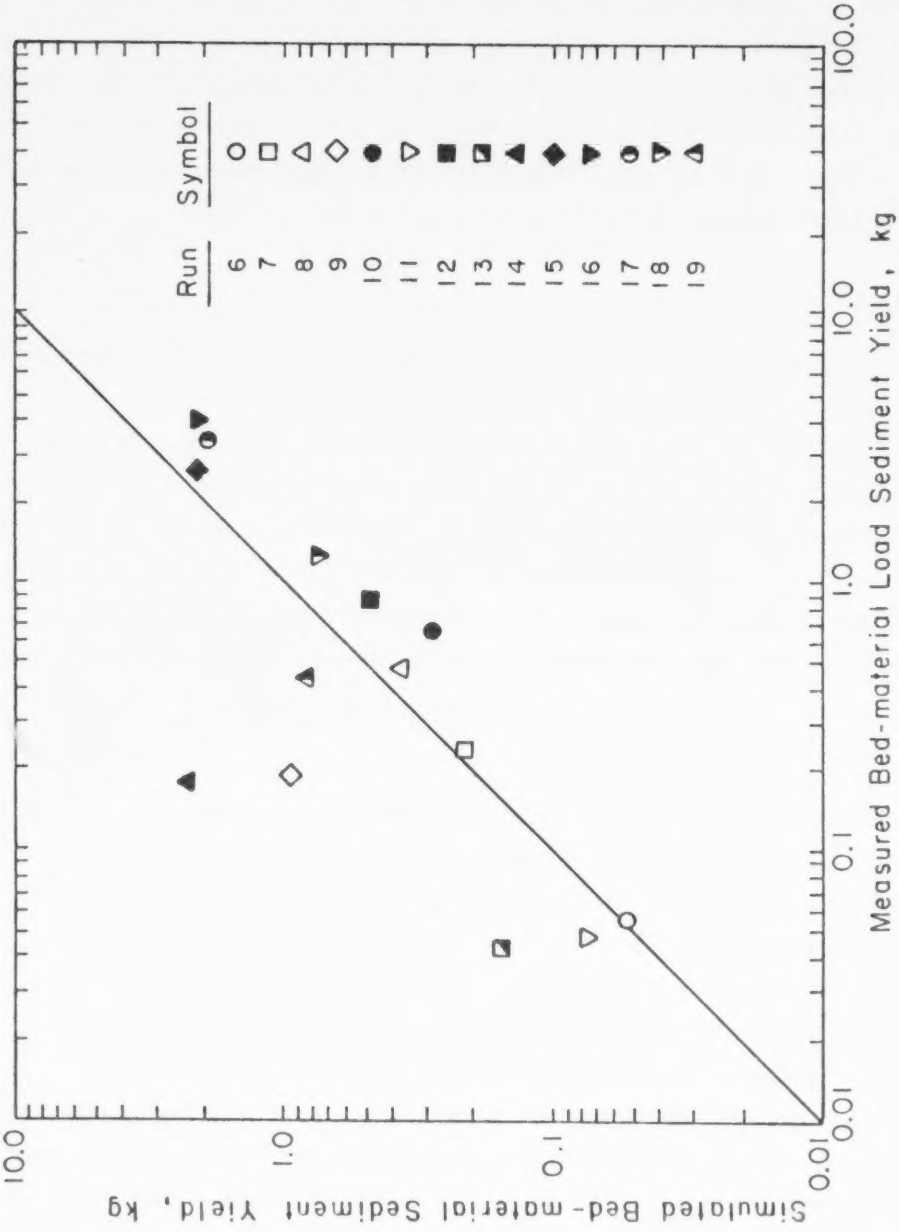

Figure 59. Comparison of measured and simulated bed-material sediment yields.

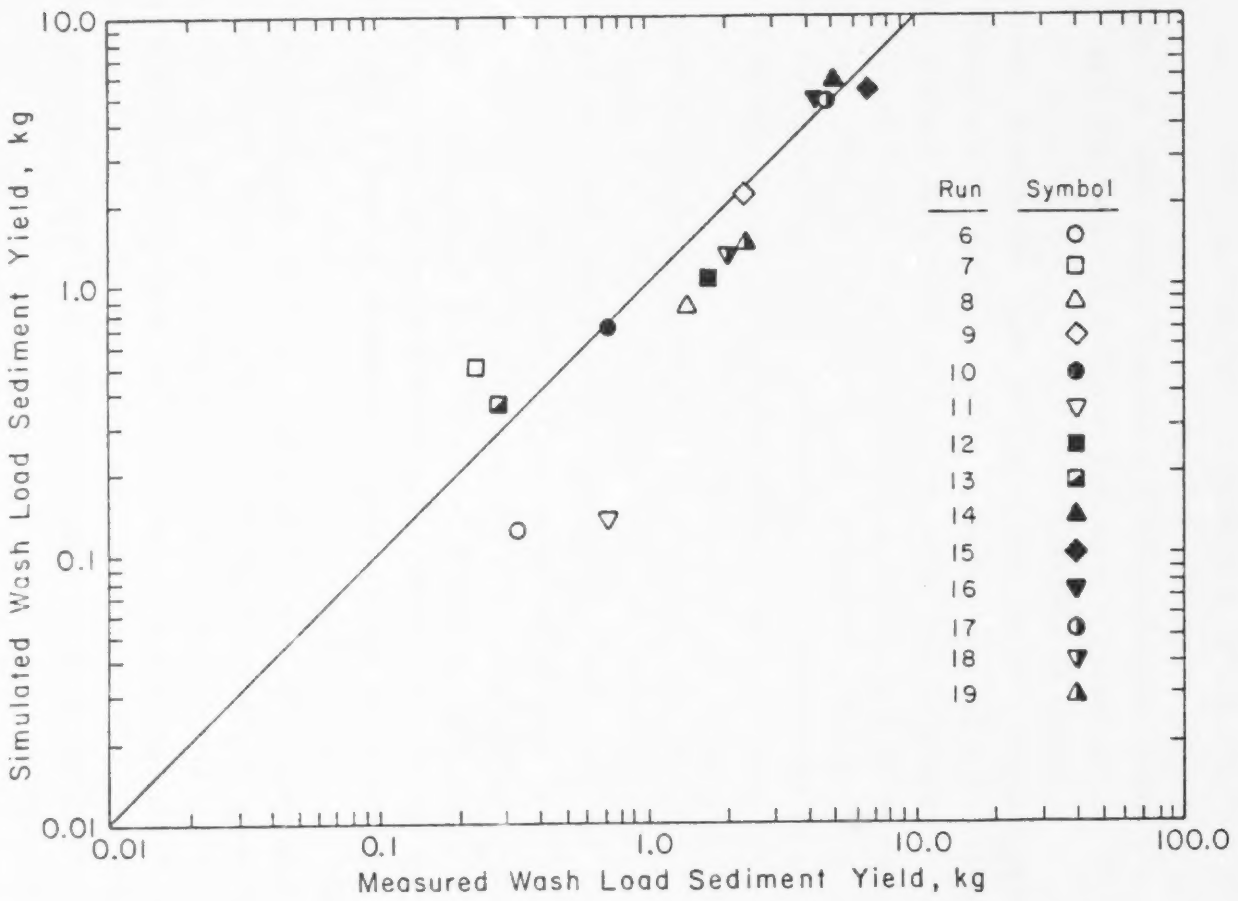

Figure 60. Comparison of measured and simulated wash load sediment yields.

$$R = T[(KE)(0.01)(i)^2][S]$$

in which

T = duration time of a simulated event in hours,

KE = kinetic energy in hundreds of foot-tons per acre,

i = rainfall intensity, in inches per hour,

S = energy associated with a simulated rainfall event as compared to the energy of a natural rainstorm of comparable size, expressed as a percent.

At intensities of 1.44 and 2.26 inches per hour, the rainfall simulator used in the investigation provided about 44 and 39 percent of the kinetic energy associated with natural rainstorms of comparable size, respectively.

The experimental site consisted of test plots with average bed slopes of 1 and 7 percent, and approximately 13 feet wide and 30 feet long. The topographic factor in the equation $K = A[R(LS)CP]$ was based upon these plot dimensions and slope gradients. Values of LS were computed from Wischmeier's slope effect chart (Wischmeier and Smith, 1965).

For six experimental runs performed under simulated rainfall, test plot surfaces consisted of fresh, dry spoil material. In Table 30 a summary of the experimental data collected is presented. The computed erodibility factor for each experiment is shown in the table. Results of the analysis for computing the K factor in the Universal Soil Loss Equation indicate a wide range in values, from 0.08 in run 14 to 0.46 in run 19. By averaging the K values calculated in the six runs, a mean value for describing the erodibility of the spoil material tested was determined. An average value of K equal to 0.20 was computed.

From hundreds of plot years of data collected from agricultural soils east of the Rocky Mountains, values of the erodibility factor range from about 0.03 to 0.7 with an average of approximately 0.30. Data analyzed in the current investigation would suggest that the particular spoil banks at the Edna Mine have a relatively low potential for erosion. The computed K factor of 0.20 determined in this analysis should be used with caution, subject to the following assumptions.

1. The Universal Soil Loss Equation, developed for computing annual soil losses, is valid for specific rainfall events.

TABLE 30. SUMMARY OF EXPERIMENTAL FIELD DATA COLLECTED UNDER SIMULATED RAINFALL AND COMPUTED TERMS IN THE UNIVERSAL SOIL LOSS EQUATION

Run No.	Simulated Rainfall Intensity (inches/hour)	Time of Duration (hour)	Kinetic Energy (hundreds of foot-tons per acre)	Computed Terms in Universal Soil Loss Equation			
				(rainfall factor)	(soil loss factor)	(topographic factor)	(erodibility factor)
14	2.26	0.900	400	18.4	0.706	0.460	0.08
15	1.44	1.033	427	9.14	0.531	0.460	0.13
16	2.26	0.833	400	17.0	1.036	0.460	0.13
17	2.26	0.767	400	15.7	0.960	0.460	0.13
18	2.26	0.850	400	17.4	0.396	0.077	0.30
19	1.44	1.067	427	9.44	0.335	0.077	0.46

2. Data collected under simulated rainfall can be used to describe expected sediment responses from natural rainfall events.
3. The Universal Soil Loss Equation as based upon data collected on agricultural lands in the Eastern United States, can be extended to include soils and rock fragments disturbed by surface mining.
4. The cropping management and the conservation practice factors are assumed to be equal to 1.0.

SECTION 8

WATER QUALITY MODELING

The water quality model used in this study consists of both water flow and chemical calculations. The model is presented in terms of the four major components: flow in the partially saturated zone, flow in the saturated zone, the chemistry, and dissolved solids transport. As stated in the introduction, the model is composed by adapting and modifying components originally developed for other purposes. Much of the original work was accomplished by Dutt et al. (1972), Ayars (1976) and Eckhardt (1976). It is necessary to present a somewhat abbreviated discussion of the model in the interest of keeping this already long report within reasonable bounds. The computer program listings for the model are included as appendices.

FLOW IN THE PARTIALLY SATURATED ZONE

Water which enters the spoil material via infiltration percolates into the subsurface at pressures less than atmospheric pressure. Typically, the spoil will remain less than fully saturated between the surface of the spoil and the water table (except for a small zone immediately above the water table). In this report, the region between the surface and the water table is referred to as the partially saturated zone.

Mathematical Basis

A volumetric-moisture content form of the Richard's (1931) equation forms the starting place for calculating the flow in the partially saturated zone:

$$\frac{\partial\theta}{\partial t} = \frac{\partial}{\partial z}\left[D(\theta)\frac{\partial\theta}{\partial z} - K(\theta)\right] - S \quad , \qquad (122)$$

where θ is the volumetric moisture content, $D(\theta)$ is the diffusivity as a function of θ, K is hydraulic conductivity as a function of θ, z is the vertical space coordinate and S is a sink term that is used to simulate the processes of evaporation and transpiration.

The finite difference form of equation 122 used in the model is

$$\frac{\theta_j^i - \theta_j^{i-1}}{\Delta t} = [D_{j-\frac{1}{2}}^{i-\frac{1}{2}} (\theta_{j+1}^i + \theta_{j+1}^{i-1} - \theta_j^i - \theta_j^{i-1}) - 2\Delta z K_{j+\frac{1}{2}}^{i-1}$$

$$- D_{j-\frac{1}{2}}^{i-\frac{1}{2}} (\theta_j^i + \theta_j^{i-1} - \theta_{j-1}^i - \theta_{j-1}^{i-1}) - 2\Delta z K_{j-\frac{1}{2}}^{i-1}] / 2\Delta z^2 - S_j^i \qquad (123)$$

where the superscript i denotes the time step and the subscript j denotes the depth increment. For example, θ_j^{i+1} denotes the volumetric moisture content at time step i+1 and depth j. The finite-difference approximation is backwards in time, meaning that moisture contents from the previous time step are used to calculate values for the present time.

When the algebraic equation 123 is applied to each grid point in the system and the boundary conditions are introduced, a system of n equations in n unknowns is formed. An implicit solution method (Richtmyer, 1957) is used to solve for the n unknowns.

Boundary and Initial Conditions

Boundary conditions at the ground surface and at any arbitrary depth below the ground surface must be specified. Three conditions at the ground surface can be simulated. These are infiltration, evaporation, and zero flux. Infiltration is simulated by specifying a constant moisture content, equal to the maximum θ obtainable, at the surface. This condition corresponds to the physical condition of infiltration from very shallow ponded water on the surface as occurs during overland flow. Evaporation is simulated by specifying the evaporation rate and setting the sink term in the first grid below the surface equal to the evaporation rate. Thus, evaporation is not computed as the result of an imposed evaporative potential at the surface and the resulting upward flow in response to that potential. Simulating the evaporation by use of the sink term must be estimated by independent means. This is not a great disadvantage, however, because evaporation and transpiration are usually combined into a single quantity and calculated by independent formulas. The user can specify a distribution of uptake from different levels in the root zone by assigning different values for the sink S at different levels.

Two lower boundary conditions are provided for in the model. A constant value of θ at any depth can be specified. If a value of θ equal to the porosity is specified at a particular depth, the condition of a water table at that depth is simulated. This is true because the relationship between soil-moisture suction and θ used in the model requires that the suction be zero when θ is equal to the porosity. The water table is defined as the surface on which the suction is zero. When the water table is a great distance below the ground surface, the model predicts that there is a region, extending from the water table to within about 2-3 m from the surface, that acts only as a transmission zone. In this transmission zone, the moisture content is practically constant and so is the dissolved solids in the soil solution. A great deal of computer time can be saved by not carrying out the computations in this zone, therefore. This is accomplished by specifying a unit gradient at a depth of 2-3 m and calculating the discharge and water quality at that depth. The calculated discharge and water quality are simply used as inputs to the saturated zone below the water table. Use of a unit gardient at a particular depth does not imply either constant flux of soil solution nor constant moisture content.

The initial condition must be specified in terms of a water content distribution with depth of the spoil material. The initial water-content distribution is arbitrary and can be uniform or nonuniform.

Hydraulic Properties

The functional relationships $D(\theta)$ and $K(\theta)$ are required for operation of the model. The diffusivity $D(\theta)$ is defined by

$$D(\theta) = -K(\theta)\,\frac{dP_c/\rho g}{d\theta} \qquad (124)$$

where K is hydraulic conductivity and $P_c/\rho g$ is capillary-pressure head. The functions $K(\theta)$ and $P_c/\rho g(\theta)$ have been discussed previously and are given by equations 56 and 57. Combining equations 56, 57, and 124 yields (Ayars, 1976),

$$D(\theta) = K_s[\frac{1}{\theta_s-\theta_r}]^{\frac{2+3\lambda}{\lambda}} \frac{mP_i}{\rho g} [\frac{1}{a\theta_s}]^{-m}[\frac{1}{b\theta_s}]^{\frac{bm}{a}}$$

$$[(\theta-\theta_r)^{(\frac{2+3\lambda}{\lambda}-m)} (\theta_s-\theta)^{\frac{bm}{a}}][(\frac{\theta-\theta_r}{\theta_s-\theta})\frac{b}{a}+1] \qquad (125)$$

where θ_s is the maximum volumetric water content, θ_r is the residual water content, and other terms are as previously defined.

The value of diffusivity $D_{j+\frac{1}{2}}$ used in the difference equation corresponds to a value at a point midway between adjacent nodes. This average value is computed from

$$D_{j+\frac{1}{2}} = \frac{1}{\theta_{j+1}-\theta_j} \int_{\theta_j}^{\theta_{j+1}} D(\theta)d\theta \qquad (126)$$

in which equation 125 is used.

FLOW IN THE SATURATED ZONE

Flow in either confined or unconfined aquifers is simulated. Provision is made for leaky conditions and hydraulic connection (as saturated flow) between the aquifer (or aquifers) and lakes, streams, or other surface water bodies. The hydrologic and geologic parameters that define an area are incorporated and each parameter can vary in time and space. Variables and parameters considered include recharge by irrigation or precipitation, recharge from surface water bodies, withdrawals by pumps or phreatophytes; and hydro-geologic parameters of hydraulic conductivity, storage coefficient, specific yield, and the distributions of bedrock, ground surface and water table elevations.

Mathematical Basis

The nonlinear partial differential equation for transient, two-dimensional flow in a saturated porous medium can be derived from the mass continuity equation and Darcy's law and may be written as:

$$\frac{\partial}{\partial x}(Kh\frac{\partial H}{\partial x}) + \frac{\partial}{\partial y}(Kh\frac{\partial H}{\partial y}) = S\frac{\partial H}{\partial t} + \frac{Q}{\Delta x\Delta y} \qquad (127)$$

where

K = hydraulic conductivity (L/T),

h = saturated thickness of aquifer or confined aquifer thickness (L),

H = water table elevation or piezometric head, referred to an established datum (L),

S = storage coefficient for confined case or effective porosity for unconfined case (dimensionless),

Q = net groundwater withdrawal (L^3/T),

x,y = space dimensions (L),

t = time dimension (T).

Dividing the region of groundwater flow into a rectangular grid system and using an implicit central finite-difference scheme, the above equation, written for one grid, becomes:

$$A^t H^{t+\Delta t}_{i,j-1} + B^t H^{t+\Delta t}_{i,j+1} + C^t H^{t+\Delta t}_{i-1,j} + D^t H^{t+\Delta t}_{i+1,j} - (A+B+C+D+E)^t H^{t+\Delta t}_{i,j}$$

$$= Q^{t+\Delta t/2}_{i,j} - EH^t_{i,j}$$

where

$$A^t = \frac{2K_{i,j}K_{i,j-1}\Delta y_{i,j}\Delta y_{i,j-1}h^t_{i,j-1/2}}{\Delta y_{i,j}K_{i,j}\Delta x_{i,j-1} + \Delta y_{i,j-1}K_{i,j-1}\Delta x_{i,j}} \qquad (128)$$

$$B^t = \frac{2K_{i,j}K_{i,j+1}\Delta y_{i,j}\Delta y_{i,j+1}h^t_{i,j+1/2}}{\Delta y_{i,j}K_{i,j}\Delta x_{i,j+1} + \Delta y_{i,j+1}K_{i,j+1}\Delta x_{i,j}}$$

$$C^t = \frac{2K_{i,j}K_{i-1,j}\Delta x_{i,j}\Delta x_{i-1,j}h^t_{i-1/2,j}}{\Delta x_{i,j}K_{i,j}\Delta y_{i-1,j} + \Delta x_{i-1,j}K_{i-1,j}\Delta y_{i,j}}$$

$$D^t = \frac{2K_{i,j}K_{i+1,j}\Delta x_{i,j}\Delta x_{i+1,j}h^t_{i+1/2,j}}{\Delta x_{i,j}K_{i,j}\Delta y_{i+1,j} + \Delta x_{i+1,j}K_{i+1,j}\Delta y_{i,j}}$$

$$E = \frac{S_{i,j}\Delta x_{i,j}\Delta y_{i,j}}{\Delta t} .$$

The i,j notation refers to the grid for which a particular equation is written and the superscripts represent the time level of computation. The term ($h^t_{i,j-1/2}$) in the coefficient A^t and its counterpart in the other coefficients is the effective saturated thickness or confined aquifer thickness whichever is smallest, between the grids (i,j-1) and (i,j). $h^t_{i,j-1/2}$ is computed by the following equations.

$$u_{i,j} = \min(G_{i,j}, H_{i,j})$$

$$u_{i,j-1} = \min(G_{i,j-1}, H_{i,j-1})$$

$$h^t_{i,j-1/2} = \max(u^t_{i,j}, u^t_{i,j-1}) - \max(z_{i,j}, z_{i,j-1})$$

where

G = top elevation of confined aquifer or ground surface of an unconfined aquifer analysis, both referred to a datum (L),

z = bedrock elevation, referred to a datum (L).

This equation ensures that the flux out of a dry grid will be zero.

The coefficients A^t, B^t, C^t, D^t are computed at the beginning of each time increment and held constant throughout the time increment. This approximation effectively linearizes the difference equation for the unconfined case and makes solution possible. For the confined case, the equation is already linear and the coefficients A, B, C, and D are, in fact, constants. The coefficient E is held constant for each grid throughout the analysis. The net groundwater withdrawal, Q, which may be positive or negative, is the net volume of water added or withdrawn through the top or bottom of each grid in a given time interval. It is held constant throughout each time step at the average value it has at the center of the increment.

Equation 128 is written for each grid in the entire grid system. The resulting set of equations are then solved simultaneously by the Gauss Elimination scheme.

Boundary and Initial Conditions

The model is capable of simulating any combination of impermeable, constant head, or constant gradient boundary conditions. The first condition is used on boundary segments formed by practically impervious geologic materials. Constant head is used to simulate the condition on boundary segments in contact with surface water bodies and the constant gradient condition is used when there is a constant inflow or outflow from the area of interest.

Values of hydraulic conductivity can be different in every grid of the system. Of particular interest is the simulation of flow in and around a region which has been disturbed by mining. The conditions on the boundary between the disturbed and undisturbed aquifers are those given in Section 5. The geometry of the disturbed area can be any desired shape.

Initial conditions with respect to piezometric head or water-table elevation are arbitrary. Unlike the analytic calculations presented in Section 5, the finite difference model simulates the nonsteady state and can be used to compute such effects as mine dewatering or the transients that occur during and after mining.

INORGANIC CHEMISTRY MODEL

The computations described in this subsection are a summary of the work of Dutt et al. (1972) as described by Ayars (1976). These previous studies form the basis for the chemistry calculations made in the present study. In the original work of Dutt et al. (1972) provision was made for the computation of the nitrogen chemistry. While the nitrogen component of the calculations has been retained in the present version of the model, it was not used in the study.

The chemical reactions to be described below are assumed to occur in the partially saturated zone. This zone was divided into segments or cells for application of the flow model as described previously. The same soil segments are regarded as containers in which the pertinent chemical reactions occur. The basic assumption underlying the chemical computations is that of instantaneous chemical equilibrium. This is justified because the residence time of soil solution in each segment is large relative to the reaction time. The procedure is to calculate the equilibrium concentrations of all species considered for each cell at a particular time, given the moisture content in each segment from the output of the flow model. Once the equilibrium concentrations have been calculated, time is advanced and transport of species from one cell to the next occurs and the moisture content distribution is changed in accordance with the flow model. Equilibrium concentrations of species are again computed, and the process is repeated. The equilibrium reactions considered in the model are described in the following subsections.

Solubility and Precipitation of Gypsum

The equilibrium equation for gypsum is

$$CaSO_4 \times 2H_2O \rightleftarrows Ca + SO_4 + 2H_2O \quad . \tag{129}$$

The equilibrium concentrations for equation 129 in soil-water systems, given either initial concentrations of approximations of the constituent concentrations, are calculated using

$$x^2 + Bx + C = 0 \tag{130}$$

where x equals the change in concentration of Ca and SO_4 to reach equilibrium. The coefficients are given by

$$B = C'_{Ca} + SO_4$$

$$C = C'_{Ca}C'_{SO_4} - K_{SP}/\gamma_2^2$$

where C' is the initial or approximate concentration of the ion indicated by subscripts, K_{SP} is the solubility product equal to 2.4×10^{-5} and γ_2 is the divalent activity coefficient.

Undissociated Calcium and Magnesium Sulfate

Since the chemistry for undissociated Ca and Mg sulfate in solution is similar, the reactions will be considered together. The chemical reactions occurring in water are

$$CaSO_4 \rightleftarrows Ca + SO_4 \tag{131}$$

$$MgSO_4 \rightleftarrows Mg + SO_4 \quad . \tag{132}$$

The equation used to calculate equilibrium concentrations of the above reactions is

$$Ax^2 + Bx + C = 0 \tag{133}$$

where

x = the change in SO_4 and Ca or Mg concentrations to reach equilibrium,

$A = \gamma_2^2$ (divalent activity coefficient),

$$B = (K_D + {}_2^2C'_{\text{Ca or Mg}} + {}_2^2C'_{SO_4}),$$

$$C = {}_2^2C'_{\text{Ca or Mg}}C'_{SO_4} - K_D C'_{CaSO_4 \text{ or } MgSO_4},$$

and K_D is the appropriate dissociation constant. When the system contains gypsum, the undissociated $CaSO_4$ becomes a constant

$$C'_{CaSO_4} = \frac{K_{SP}}{K_D} \quad . \tag{134}$$

Calcium and Magnesium Exchange

The equation used to calculate the Ca-Mg exchange process is

$$Ay^2 + By + C = 0 \tag{135}$$

where

y = change in concentration of Mg and Ca to reach equilibrium.

The constants and coefficients are defined as:

$A = \beta(1 - K_{Mg\text{-}Ca})$,

$B = \beta(N'_{Mg} + K_{Mg\text{-}Ca}N'_{Ca}) + C'_{Ca} - K_{Mg\text{-}Ca}C'_{Mg}$,

$C = C'_{Ca}N'_{Mg} - K_{CaMg}C'_{Mg}N'_{Ca}$,

β = liter of water per gram of soil,

$K_{Mg\text{-}Ca}$ = Ca-Mg exchange constant,

N' = approximation of initial concentration of exchangeable ion indicated by the subscript.

Calcium and Sodium Exchange

The Gapon equation is used to describe the Na-Ca exchange. The equation for the equilibrium conditions is

$$Ax^4 + Bx^3 + Cx^2 + Dx + E = 0 \tag{136}$$

where

x = change in concentration of Ca to reach equilibrium,

$A = -4\,K^2_{Ca\text{-}Na}\beta^2$,

$$B = 4(\gamma_{\frac{1}{2}} + 2K^2_{Ca-Na}N'_{Ca}\beta + K^2_{Ca-Na}C'_{Na}),$$

$$C = 4\gamma_{\frac{1}{2}}(C'_{Ca} + N'_{Na}\beta) - 4K^2_{Ca-Na}\beta N'_{Ca}(\beta N'_{Ca} + 2C'_{Na}) - K^2_{Ca-Na}C'^2_{Na} ,$$

$$D = N'_{Na}\gamma_{\frac{1}{2}}(4C'_{Ca} + N'_{Na}\beta) + 2K^2_{Ca-Na}N'_{Ca}C'_{Na}(2\beta N'_{Ca} + C'_{Na}),$$

$$E = N'^2_{Na}C'_{Ca}\gamma_{\frac{1}{2}} - K^2_{Ca-Na}C'^2_{Na}N'^2_{Ca} ,$$

and

$\gamma_{\frac{1}{2}} = \gamma_1/\gamma_2$ with γ_1 = monovalent activity coefficient.

Dissociation of $CaCO_3$ in Water

The dissociation of $CaCO_3$ is given as

$$CaCO_3 \rightleftarrows Ca + CO_3 \quad . \tag{137}$$

Dutt (1972) states that the CO_3 concentration is a function of CO_2 partial pressure and HCO_2 is usually the predominant form of CO_3 occurring in soil-water systems. The following reaction is considered in the model:

$$H_2CO_3 + CaCO_3 \rightleftarrows Ca + 2HCO_3 \tag{138}$$

with

$$KK = \frac{a_{Ca}a^2_{HCO_3}}{a_{H_2CO_3}} \tag{139}$$

or

$$KK = \frac{K_{SP}K_1}{K_2} \quad , \tag{140}$$

where

a = activity coefficient of subscripted ion,

K_1, K_2 = first and second acid dissociation constants for H_2CO_3,

K_{SP} = thermodynamic solubility product.

If an equilibrium system is at constant CO_2 pressure and the activity of the uncharged species is unity, equation 139 becomes

$$\frac{K'}{\gamma_1^2\gamma_2} = \frac{KKC_{H_2CO_3}}{\gamma_1^2\gamma_2} = C'_{Ca}C^2_{HCO_3} \tag{141}$$

with

γ_1 = monovalent activity coefficient,
γ_2 = divalent activity coefficient,
C = equilibrium concentration of subscripted species.

The equation describing the dissociation of $CaCO_3$ was developed by substituting the stoichiometric relations

$$C_{Ca} = C'_{Ca} + Z \qquad (142)$$

$$C_{HCO_3} = C'_{HCO_3} + 2Z \qquad (143)$$

into equation 139, where C'_x are concentrations of species before equilibria existed or approximate concentrations of indicated species, and Z is the change (in moles) to reach equilibrium. The resulting equations are

$$AZ^3 + BZ^2 + CZ + E = 0.0 \qquad (144)$$

where

$A = 4.0,$
$B = 4.0(C'_{NCO_3} + C'_{Ca}),$
$C = C'_{HCO_3} + 4.0C'_{Ca}C_{HCO_3},$
$E = C'^{2}_{HCO_3}C'_{Ca} - K'/\gamma_1^{2}\gamma_2.$

Dutt et al. (1972) investigated the change in $CaCO_3$ solubility with changes in soil moisture and included this representation in the model. Through laboratory determination of Ca, CO_3 and HCO_3 concentration in extracts at three moisture levels (saturation, 100 and 500 percent) from 6 calcareous soils a functional relationship was derived to describe the solubility. The derived relationship was then assumed to hold at field moisture levels and is used in the model.

Effect of Sulfate and Undissociated $CaSO_4$ and $MgSO_4$ on Exchange Processes

Dutt et al. (1972) included the effects of ionic sulfate and undissociated $CaSO_4$ and $MgSO_4$ on the exchangeable Na, Ca and Mg in the system. The total $CaSO_4$, Ca and Mg in solution is

$$C_{SO_4T} = C_{SO_4} + C_{CaSO_4} + C_{MgSO_4} \quad , \tag{145}$$

$$C_{CaT} = C_{Ca} + C_{CaSO_4} \quad , \tag{146}$$

$$C_{MgT} = C_{Mg} + C_{MgSO_4} \quad . \tag{147}$$

The thermodynamic equilibrium constants for equilibrium between the undissociated species in solution and the appropriate ions are

$$K_{CaSO_4} = \frac{a_{Ca}a_{SO_4}}{a_{CaSO_4}} \tag{148}$$

$$K_{MgSO_4} = \frac{a_{Mg}a_{SO_4}}{a_{MgSO_4}} \quad . \tag{149}$$

Combining equations 146, 147, 148 and 149, the concentrations of $CaSO_4$ and $MgSO_4$ can be calculated. When these expressions are entered into equation 145 (assuming the divalent activity coefficients of $MgSO_4$ and $CaSO_4$ equal), the equation necessary to calculate the concentration of Ca and Mg is derived. The equation is

$$Ax^3 + Bx^2 + Cx + D = 0 \tag{150}$$

where

$$x = C_{SO_4}$$

$$A = \gamma_2^2 = (\gamma_{Ca}\gamma_{SO_4}) = (\gamma_{Mg}\gamma_{SO_4})$$

$$B = \gamma_2[(K_{CaSO_4} + K_{MgSO_4}) + \gamma_2(C_{MgT} + C_{CaT} - C_{SO_4T})]$$

$$C = K_{CaSO_4}K_{MgSO_4} + \gamma_2[C_{MgT}K_{CaSO_4} + C_{CaT}K_{MgSO_4} - C_{SO_4}(K_{CaSO_4} + K_{MgSO_4})]$$

$$D = -C_{SO_4T}K_{MgSO_4}K_{CaSO_4} \quad .$$

The Ca-Mg exchange is given by

$$\frac{a_{Ca}}{a_{Mg}} = K_1 \frac{N_{Ca}}{N_{Mg}} \tag{151}$$

where N is the concentration of the subscripted exchangeable ion.

The Gapon equation,

$$\frac{a_{Na}}{a_{Ca}} = K_2 \frac{N_{Na}}{N_{Ca}} \tag{152}$$

is used for the Na-Ca exchange. The total concentration of exchangeable ions (N_T) then is

$$N_T = N_{Na} + N_{Ca} + N_{Mg} \quad . \tag{153}$$

Using equations 151, 152, and 153, the equation for exchange of calcium is

$$N_{Ca} = \frac{N_T a_{Ca}{}^{\frac{1}{2}} K_2}{a_{Na}} + \frac{K_1 a_{Mg}}{a_{Ca}} + 1 \quad . \tag{154}$$

Once the activity coefficients, ionic concentrations in an equilibrium extract for Ca, Mg, Na and the total exchangeable bases are known, the exchangeable Ca can be calculated and in turn the exchangeable Na from equation 152 and the exchangeable Mg from equation 153. In practice the exchange capacity is assumed to equal N_T.

Exchangeable NH_4 is computed using

$$\frac{C_{NH_4}}{C_{Na}} = K_o \frac{N_{NH_4}}{N_{Na}} \tag{154}$$

with K_o assumed equal to 0.22.

CHEMICAL TRANSPORT CALCULATIONS

The spatial distribution of the concentrations of dissolved species in the soil solution or ground water depends upon the flow of the solution as well as the chemical reactions that occur. The transport of species from point to point is often described by the hydrodynamic dispersion equation which includes the transport mechanisms of molecular diffusion, mechanical dispersion and convection. Diffusion and dispersion are neglected and all transport is assumed to occur as the result of convection.

Transport in the Partially Saturated Zone

The mixing cell concept is used to calculate dissolved solids transport in the partially saturated zone. The dissolved species are assumed to move with the soil solution and to remain at their equilibrium concentrations throughout the cell. When time is advanced, species are moved in and out of each cell. The model calculates the mass of each species transferred and the net gain or loss to each segment is included when the equilibrium concentrations are computed. Constituents in infiltrating water are treated as inputs to the first segment below the surface.

Transport in the Saturated Zone

It is assumed that no chemical reactions occur in the saturated zone. Thus, all ions that are input to the ground water from the partially saturated zone are, henceforth, treated as being conservative.

On a large scale basis such as encountered in groundwater aquifers, the contribution of dispersion and diffusion to the transport of ions should be small compared to convective transport and consequently is neglected in this analysis. The transport equation at a particular instant in time is, therefore,

$$\frac{\partial CR}{\partial t} = - \frac{\partial}{\partial x} (v_x CR) - \frac{\partial}{\partial y} (v_y CR) \qquad (156)$$

where

CR = relative concentration of ions,
v_x = velocity in the X-direction,
v_y = velocity in the Y-direction.

In different form, using the explicit scheme, this becomes:

$$CR_{i,j}^{t+\Delta t} = CR_{i,j}^{t} \, \Delta t[1 - \frac{B^t(H_{i,j+1}-H_{i,j})^{t+\Delta t}}{V_{i,j}} - \frac{D^t(H_{i+1,j}-H_{i,j})^{t+\Delta t}}{V_{i,j}}]$$

$$+ \frac{\Delta t A^t(H_{i,j}-H_{i,j-1})^{t+\Delta t} CR_{i,j-1}}{V_{i,j}} + \frac{\Delta t C^t(H_{i,j}-H_{i-1,j})^{t+\Delta t} CR_{i-1,j}}{V_{i,j}}$$

where $V_{i,j}$ is the volume of water stored in grid i,j and is

$$V_{i,j} = \Delta x_{i,j} \Delta y_{i,j} S_{i,j} (H_{i,j} - z_{i,j})$$

for the confined case, and

$$V_{i,j} = \Delta x_{i,j} \Delta y_{i,j} [S_{i,j} (G_{i,j} - z_{i,j}) + SC_{i,j} (H_{i,j} - G_{i,j})]$$

for the unconfined case.

In the above equations $SC_{i,j}$ is the storage coefficient for the confined case. The values of heads at the new time $t+\Delta t$ for each grid are computed first. These values are used in equation 155 and, hence, one obtains an explicit solution for relative concentrations in each grid. The solution for relative concentrations lags the solution for heads by approximately $\frac{1}{2}\Delta t$.

SECTION 9

RESULTS OF WATER QUALITY MODELING

Some components of the model described in Section 8 were tested with data collected on the experimental sites. Due to the lack of data, it was not possible to test the flow patterns and concentration distribution predicted by the model components specifically designed for ground water conditions. An example computation of the flow and concentration distributions in a ground water aquifer disturbed by mining is provided.

FLOW IN THE PARTIALLY SATURATED ZONE

A test of the model component that calculates flow in the partially saturated zone is presented using experimental data from the plot with a 1 percent surface slope at the Colorado site. Four experimental runs (runs 1, 2, 6 and 11) were performed on this plot and form the most comprehensive set of experimental data that is available.

Summary of Input Data

The average depth of spoil in the plot was 183 cm and this interval was divided into 9 equal increments of 20.3 cm each. These increments form the grid required for the flow computations and also the cells in which the chemical reactions take place. An additional grid (or cell) was added at the bottom of the profile in which a water table, at constant elevation, was simulated. The ten grid intervals provide 10 nodes at which the initial volumetric moisture content was specified. The initial distribution is that measured on July 5, 1975 and is presented in Table 31. Also shown in Table 31 are the volumes of water applied and the time intervals over which the applications were made. Rainfall occurrences that exceeded 5 mm were included as applications, but the time interval over which they occurred are not known.

No vegetation was permitted to grow during the experimental period and transpiration was set to zero, therefore. Evaporation was included in the

TABLE 31. INITIAL MOISTURE DISTRIBUTION AND WATER APPLICATION SCHEDULE

Node	Depth cm	θ	Date	Volume Applied-cm	Application Interval-min	Source
1	0.0	0.240	7/6	0.55	-	rainfall
2	20.3	0.274	7/8	0.55	-	rainfall
3	40.6	0.338	7/10	5.08	83	irrigation
4	60.9	0.340	7/13	0.48	-	rainfall
5	81.2	0.339	7/16	4.36	58	irrigation
6	101.5	0.341	8/6	9.28	100	irrigation
7	121.5	0.355	8/12	0.90	-	rainfall
8	142.1	0.377	8/14	0.48	-	rainfall
9	162.4	0.405	8/19	10.97	89	irrigation
10	182.7	0.441	8/21	1.35	-	rainfall

simulation by permitting water to be withdrawn at node 2 through the sink term. Cumulative evaporation was assumed to vary directly with the square root of time, so the sink term in Equation 122 is

$$S = \text{constant}\ t^{-1/2}$$

from which average evaporation rates were computed for each time increment. The constant was obtained by assuming the residuals in Table 18 in Section 5 are values of cumulative evaporation in the period over which the water balance computation was made.

The functional relationship given by Equation 125 was used for $D(\theta)$ in the simulation. The values of the parameters are $\theta_s = 0.441$, θ_r 0.223, $a = 0.647$, $b = 0.072$, $m = 3.34$, $P_i/\rho g = 5.0$ cm, and $\lambda = 0.285$. Values of K_s used are $K_s = 79$ cm/d from July 5 to July 31, $K_s = 157$ cm/d from August 1 to August 19, and $K_s = 171$ cm/d from August 19 to the end of the simulation run.

Analysis of Results

The development of the model for flow in the partially saturated zone assumed that the spoil material is homogeneous with respect to flow properties. The backfilled experimental plots were not homogeneous, however. During the backfilling operation, each lift was compacted by the front-end loader used to transport the spoil into the facility. This compaction existed to approximately one-half the depth of the spoil in the lysimeter. The top half was placed by simply dumping over the side walls and drifting the material by hand. The result is a loose zone in the upper 80-90 cm and a compacted layer below. The hydraulic properties of the upper zone are quite different from that below, therefore.

Infiltration of applied water into the spoil is governed by the hydraulic properties of the upper zone. The capability of the model to predict infiltration was tested using the best estimates of the hydraulic properties in the upper zone, therefore. These properties were presented in the previous subsection. A summary comparison of the measured and calculated results are shown in Table 32. The close agreement between the measured and calculated infiltration volumes and the corresponding times of infiltration suggest that the flow model accurately simulates the infiltration phenomenon. It should be noted that the simulation run was made for the time period from July 5, 1975 to August 29, 1975 as one continuous calculation. No updating of information was made during the run, other than increasing K_s in accordance with the measured values. This means, for example, that infiltration for the various events was calculated using the predicted moisture content profiles and not measured ones.

TABLE 32. COMPARISON OF FLOW MODEL WITH EXPERIMENTAL DATA

Run No.	Cumulative Infiltration		Time of Infiltration		Cumulative Drainage and Δ Storage	
	Measured cm	Calculated cm	Measured min	Calculated min	Measured cm	Calculated cm
1	5.09	5.02	83	-	3.36	3.63
2	4.36	4.30	58	-	3.83	3.43
6	10.66	10.66	100	88	7.88	10.04
11	10.97	10.97	89	82	9.75	10.75

The cumulative drainage plus the change in storage, indicated in the two right-hand columns of Table 32, were determined at corresponding times. For example, the moisture content distribution was measured just before a water application and then again several days following the application and the change in storage and cumulative drainage were computed for that time interval.

For the same time interval, the corresponding results were determined from the model and compared with the measured results as shown. Again, it should be noted that, in the model, no updating of information was made. Satisfactory agreement between the measured and calculated data in the two right-hand columns is apparent.

Comparison of measured and calculated subsurface drainage did not indicate such satisfactory agreement. The effect of the great deal of compaction on the hydraulic properties in the lower zone of the spoils was not known, and it is this zone which has the greatest effect on the drainage rate. Our best estimate of K_s for the lower zone was 10 cm/d. Also, the compacted zone can be expected to exhibit a moisture retention curve that is shifted upward relative to that for the loose zone. It was not possible to independently estimate the magnitude of the shift, however, and the parameters for the loose zone were used for the compacted zone. The volumes of subsurface drainage are shown in Figure 61.

Reasons for the disparity between the measured and predicted results were investigated. The lower boundary condition used in the simulation run was that of a water table at a depth of 183 cm. The existance of the gravel drain blanket and the fact that the drain tube discharged into the atmosphere caused the pressure head in the water at the 183 cm depth to become slightly less than atmospheric when the spoils were draining. The maximum possible suction that could be developed on the interface between the gravel and the spoil is about 7-10 cm of water, based on the thickness of the drain blanket. Thus, the boundary condition used in the simulation and that which existed in the experimental facility were very nearly the same.

The volume flux of soil solution across the water table is the rate of subsurface drainage. At the water table the spoil is at maximum water content and the equation for the volume flux is (from Darcy's law in water content form),

$$q = D_s \frac{\partial \theta}{\partial z} - K_s$$

where D_s is the diffusivity at $\theta = \theta_s$ and K_s is the hydraulic conductivity at θ_s. The coordinate z is measured positive downward so $\partial\theta/\partial z$ is a positive number. The diffusivity is also positive by definition. Therefore, the drainage rate is determined by the indicated difference. When the flow is zero (i.e., a

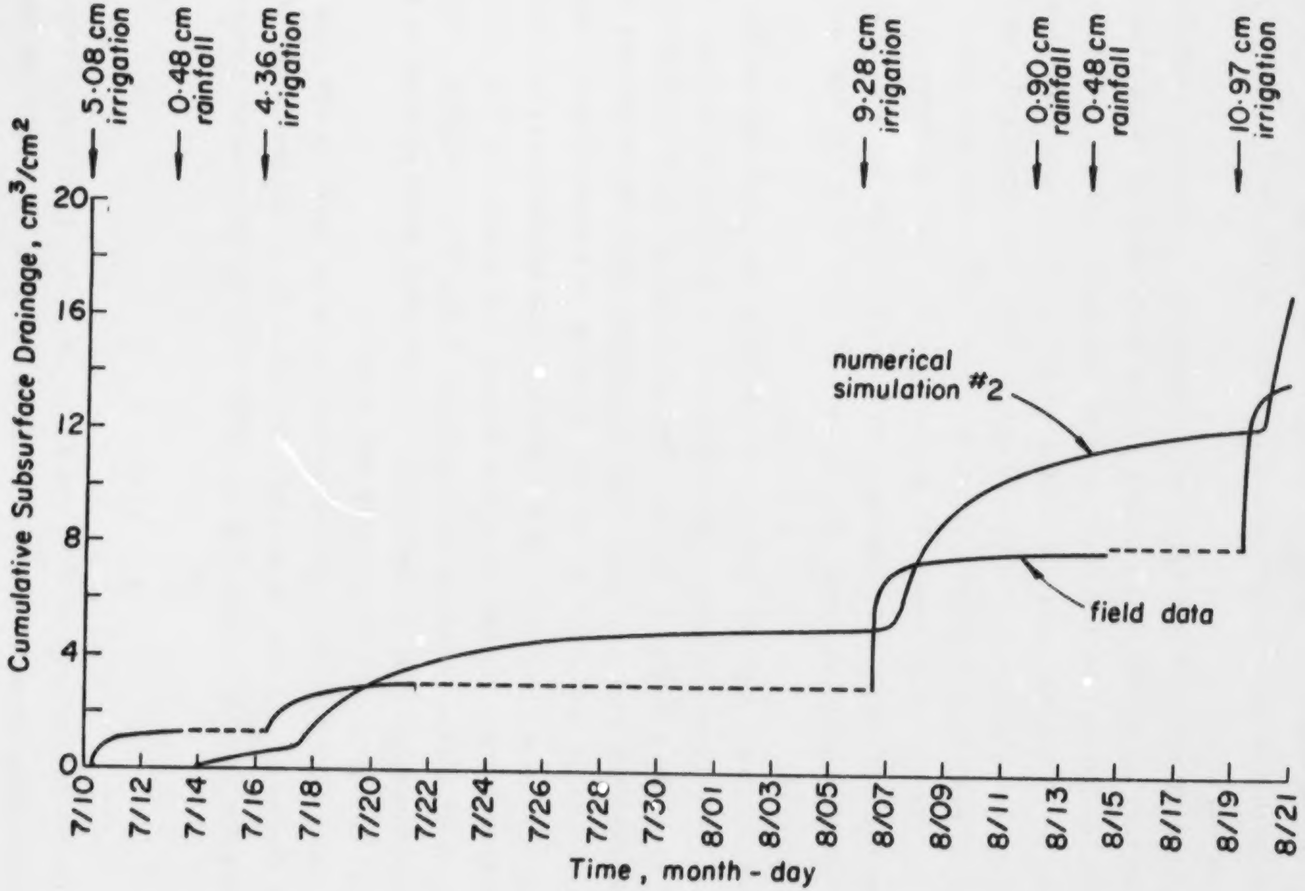

Figure 61. Volumes of subsurface drainage.

static case) the two terms on the right are equal in magnitude and their difference is zero. In all cases, the rate of drainage must be less than K_s. Measured drainage rates indicate that the average difference between the terms on the right of the above equation was much less than 1 cm/d; the point being that the difference is a very small number relative to the magnitude of D_s which is much larger than K_s. Recall that D_s is a function that must be determined from experimental data. Furthermore, it is required that the derivative $(dP_c/\rho g)/d$ be calculated from the experimentally determined relationship between capillary-pressure head and volumetric water content. This relationship in the vicinty of $\theta \simeq \theta_s$ becomes very steep so that the derivative is large causing D_s to be large. Even a very small error in the determination of the slope (say, ±5 percent) can cause D_s to be incorrect to the same order as the difference between the terms on the right of the flux equation. Therefore, even small errors in D_s can cause a very large percentage error in the computed drainage rate, particularly when the rate is small. Simulation runs with the flow model verified the sensitivity of the drainage rate to the value of D_s. It is believed that the sensitivity of the model to D_s is the major reason for the relatively poor agreement achieved between the measured and simulated subsurface drainage rates. Undoubtedly, better agreement could have been achieved by adjusting the hydraulic parameters (i.e., calibrating the model). It seems, however, presenting the results in which the hydraulic parameters were determined independently provides the reader with a more objective view of the accuracy that can be expected in applications because the parameters cannot, normally, be determined by historic matching. It is emphasized that the agreement indicated is not a reflection of the theoretical correctness of the model but, rather, a reflection of the difficulty in obtaining sufficiently accurate input data. Because D_s is difficult to establish accurately, a serious limitation is imposed upon the usefulness of the model for computing flow across a water table. However, in most applications to flow in spoil banks, the water table is at least several meters below the surface. In this case, drainage is controlled by flow through a transmission zone well above the water table and a boundary condition of a unit gradient (i.e., $\partial\theta/\partial z = 0$) at, say, 3 meters depth can be used. This boundary condition predicts that the drainage rate is equal to $K(\theta)$ which changes with time as θ at the boundary changes with time. From a computational standpoint, an advantage is gained because the drainage rate becomes less sensitive to the accuracy of the soil properties that must be specified. Ayars (1976) found satisfactory agreement between measured and computed drainage rates in a situation where a unit gradient was the appropriate boundary condition.

PREDICTED CHEMISTRY OF DRAINAGE WATERS

The input data required for the inorganic chemistry component of the model are the concentrations of calcium, magnesium, sodium, chloride, bicarbonate, and sulfate in 1:1 extracts prepared from spoil taken from each segment of the profile. These data have been presented previously in Table 19 of Section 6. Also required are the concentrations of the same species in the applied water as shown in Table 20 of Section 6. In addition to the above data, the cation-exchange capacity (CEC), the quantity of gypsum (meq/100 g), and the percent calcium carbonate are required for each segment. The partial pressure of carbon dioxide in the spoil can be specified if desired but is not required.

Figure 62 shows a comparison of the calculated and measured dissolved-solids concentration for the plot with a 1 percent surface slope. The solid line is the average value for the subsurface drainage for each of the experimental runs as indicated in Table 22 of Section 6. No measurable drainage existed in the periods indicated by a dashed line. Except for the first experimental run, the agreement is considered to be very good. It is concluded that the chemistry component of the model is quite adequate for predicting the dissolved solids concentration in drainage waters.

A comparison of the composition of drainage waters as measured and calculated is shown in Table 33. The measured values in the table are the average values for each run as indicated previously in Table 22. Note that the composition of the drainage water, as calculated by the model, changes only slightly from run to run. The composition was printed out on a daily basis but was essentially identical from day-to-day. The calculated composition shown in the table is that calculated for times when drainage rates were approaching zero. Essentially no variation of composition with drainage rate was noted. The predicted concentrations of calcium and bicarbonate are consistently high and sodium is low. The magnesium and sulfate concentrations

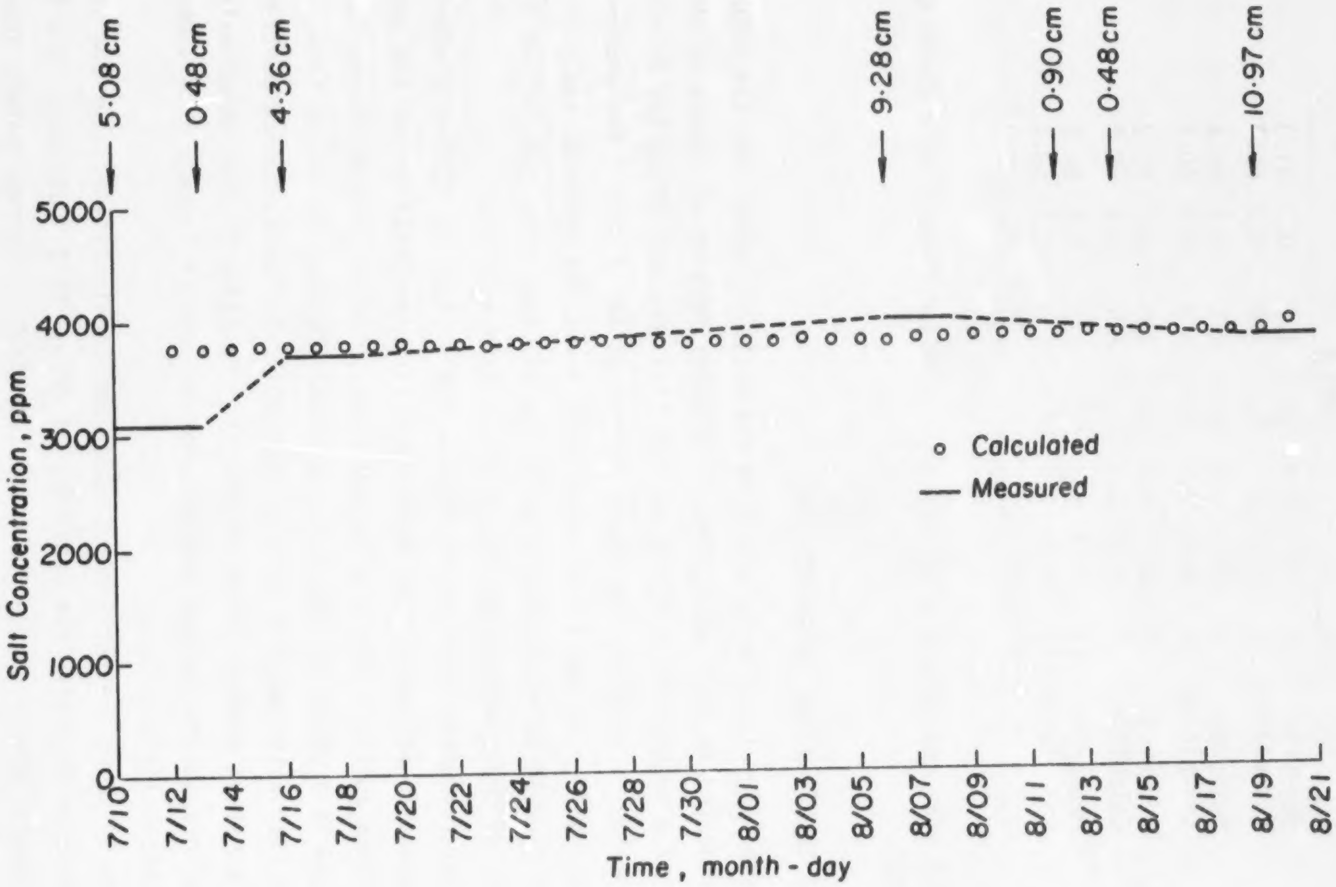

Figure 62. Comparison of calculated and measured dissolved-solids concentrations.

TABLE 33. MEASURED AND CALCULATED COMPOSITION OF DRAINAGE WATERS

	Run No.	Ca	Na	Mg	HCO_3	Cl	SO_4
				meq/l			
Measured	1	20.5	5.8	26.1	4.7	0.1	51.3
Calculated	1	33.5	1.7	30.1	3.6	0.3	50.7
Measured	2	23.2	6.5	31.7	6.1	0.1	55.4
Calculated	2	33.4	2.2	30.4	3.6	0.3	50.7
Measured	6	23.4	8.8	33.4	6.6	0.1	57.2
Calculated	6	34.0	3.2	31.2	3.6	0.3	50.5
Measured	11	21.8	6.3	32.5	7.3	0.1	54.8
Calculated	11	34.2	3.4	31.4	3.6	0.3	50.5

agreed with measured values quite closely. Similar results were observed by Ayars (1976).

EXAMPLE CALCULATION FOR SATURATED ZONE

An example application of the flow and transport model for the saturated zone is presented in this subsection. The upper portion of Figure 63 shows a plan view of a segment of confined aquifer that has been disturbed by mining. A cross-section is shown in the lower portion of the figure. The aquifer is confined everywhere except in the mined area where the specific yield (S_{ya}) is 0.1 and the hydraulic conductivity (K) is 640 m/d. The coefficient of storage (S) in the confined aquifer is 0.01 and K = 30 m/d.

The initial water table above the confining layer is 1570 m in elevation and is assumed to represent the piezometric surface elevation for the underlying confined aquifer. The piezometric head is held constant on the left boundary and is dropped to 1525 m on the right boundary to induce flow. It is assumed that water passing through the spoils in the disturbed portion reaches a constant maximum concentration (C_0) relative to that which existed in the confined aquifer before mining. No recharge or leakage is assumed to occur in this example.

Figure 64 shows the pathlines (instantaneous streamlines) for the induced flow at 360 days following the beginning of flow. At t = 360 days, the flow is approximately steady so the indicated pathlines are approximately steady-state streamlines. Note that the pathlines converge toward the disturbed

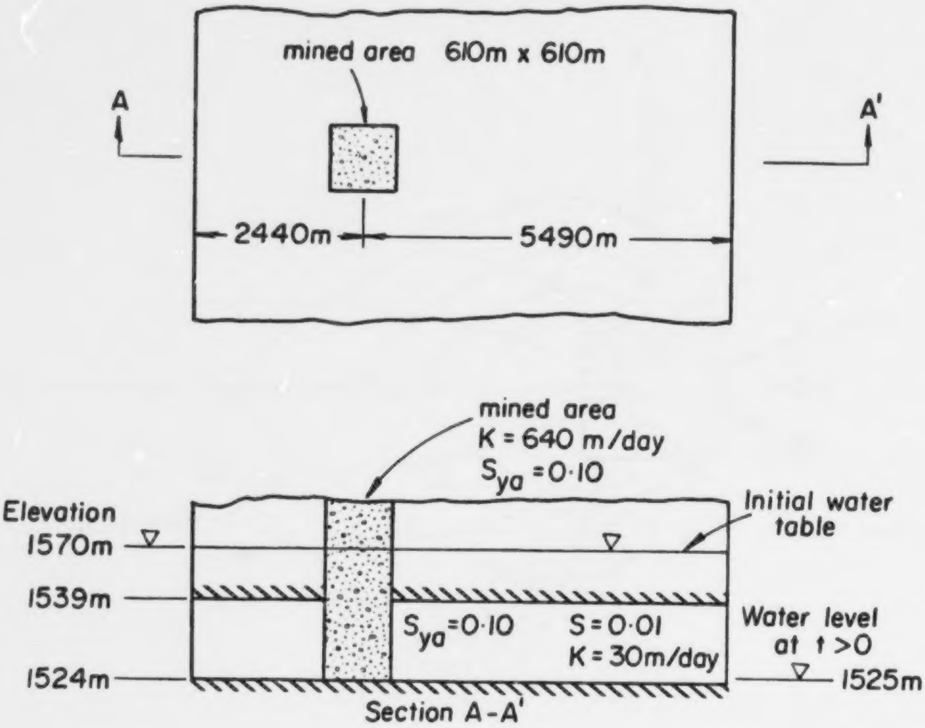
mined area 610m x 610m
A
A'
2440m
5490m
mined area
K = 640 m/day
S_{ya} = 0·10
Elevation
1570m
1539m
1524m
Initial water table
S_{ya}=0·10
S = 0·01
K = 30m/day
Water level at t > 0
1525m
Section A-A'

Figure 63. Plan and cross-section views of confined aquifer disturbed by mining.

area. This is because the hydraulic conductivity of the disturbed area is larger than that of the confined aquifer. The flow pattern is very similar to that predicted by the analytical calculations of Section 5 for a circular mined area.

Also shown are the contours of equal concentration (expressed as a fraction of C_0) at time equals 360 days. The movement of the dissolved solids is predominantly downstream from the mined area, with the largest concentrations existing in the immediate vicinity of the mine. The chemistry model can be used to predict the concentration of the ground water exiting the mined area. For example, if the spoil in the present example had the chemical characteristics contained in Table 19, then the dissolved solids concentration in water exiting the disturbed area would be 3750 mg/l.

The example selected for presentation is much less complex than others that can be analyzed with the model. For example, the mined area and the

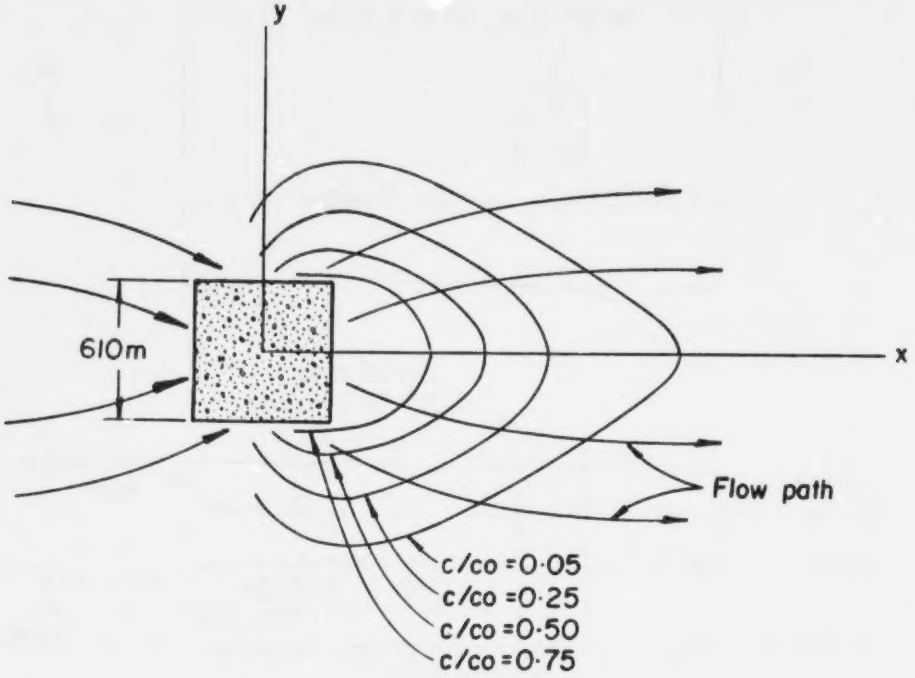

Figure 64. Induced flow streamlines 360 days after beginning of flow.

aquifer can be of any geometry, recharge in the disrupted portion can be handled, leakage through the confining layer is permissible and the aquifer and the disturbed area can be nonhomogeneous. Constant flow boundary conditions can be imposed as well.

SUMMARY COMMENTS ON WATER QUALITY MONITORING

A model for the subsurface water quality hydrology, applicable to conditions resulting from surface mining is presented. The major components of the model are a) flow in the partially saturated zone, b) equilibrium chemistry, c) flow in the saturated zone, and d) dissolved solids transport. In the current form, components a, b and c are interfaced and run as a single model. Also components c and d have been interfaced and operate as a single unit. The authors believe that it is not desirable to further interface the model components, for a number of reasons. Computer storage requirements of the total package exceed that available at most computing facilities. Furthermore, it is not necessary to formally interface the components to account for the practical interactions between the saturated and partially saturated zones. For example, the output of the combined flow and chemistry components for the partially saturated zone can be used as input to the saturated zone. The only interaction between the two zones that is not accounted for by this procedure is the effect of a fluctuating water table on the flow in the partially saturated zone. However, the effect of a fluctuating water table is negligible except when the water table is near the surface.

The combined components a, b and d were used to make a simulation run for conditions that corresponded to experimental conditions in the field. Measured and calculated results were compared. Component a accurately simulated measured infiltration but less satisfactorily simulated the subsurface drainage. The simulation was made for a case in which the water table was 183 cm from the surface; a case that provides a very critical test. In cases where the water table is a large distance below the surface, it is recommended that only the upper 2-3 m be included in the simulation and that the lower boundary condition of a unit gradient be utilized. The calculated drainage, with the unit gradient condition, is much less sensitive to the accuracy of the experimentally determined diffusivity function.

The chemistry model accurately predicted both the dissolved solids concentration and composition of subsurface drainage in this study. The combined components a, b and d predict the leaching phenomenon in the spoils and can be used to calculate the change in the quality of subsurface drainage as a function of water throughput and, therefore, as a function of time. The chemistry model can be used to estimate the pickup of dissolved solids by ground water that passes through a mined portion that has been backfilled with spoils.

Detailed user's manuals have not been prepared for the models. Flow charts and documented program listings are contained in the appendices to this report.

REFERENCES

American Public Health Association, American Water Works Association and Water Pollution Control Federation. 1971. Standard Methods for the Examination of Water and Wastewater. 13th Ed., p. 324.

American Society of Testing and Materials. 1966. Manual on Industrial Water and Industrial Waste Water. 2nd Ed., ASTM Special Publication No. 1473.

Archer, R. J., A. M. La Sala Jr., and J. C. Kammerer. 1968. Chemical Quality of Streams in the Erie-Niagra Basin, New York. State of New York Conservation Department Water Resources Commission, Basin Planning Report ENB-4.

Ayars, J. E. 1976. Salt Transport in Irrigated Soils. PhD Thesis, Department of Agricultural Engineering, Colorado State University, Fort Collins, Colorado. 228 pp.

Bass, N. W., J. B. Eby, and M. R. Campbell. 1955. Geology and Mineral Fuels of Parts of Routt and Moffat Counties, Colorado. Survey Bull. 1027-D, U. S. Geological Survey. pp. 143-177.

Brooks, R. H. and A. T. Corey. 1964. Hydraulic Properties of Porous Media. Hydrology Paper No. 3, Colorado State University, Fort Collins, Colorado. March. 27 pp.

Bubenzer, G. D. and B. A. Jones. 1971. Drop Size and Impact Velocity Effects on the Detachment of Soils Under Simulated Rainfall. Trans. Am. Soc. Agr. Engrs., Vol. 14, No. 4, pp. 625-628.

Bureau of Land Management. 1975. Resource and Potential Reclamation Evaluation, Taylor Creek Study Site, Axial Basin Coal Field. EMRIA Report No. 3-1975, U. S. Dept. of Interior, pp. 69-70.

Campbell, M. R. 1923. The Twentymile Park District of the Yampa Coal Field, Routt County, Colorado. Bull. 748, U. S. Geological Survey, pp. 4-8.

Caudill, H. M. 1973. Strip Mining: Partnership in Greed. American Forests, Vol. 79, No. 5, pp. 16-19.

Chow, V. T. 1959. Open Channel Hydraulics. McGraw-Hill Book Col, New York.

Colorado School of Mines Research Institute. 1976. Interim Progress Report for Mineralogy of Overburden as Related to Groundwater Degradation in the Strip Mining of Coal. Golden, Colorado 73 pp.

DuBoys, M. P. 1879. Le Rhone et les Rivieres a lit affouillable. Mem. Doc., Ann. Pont et Chaussees, ser. 5, Vol. XVIII.

Dutt, G. R., M. J. Shaffer, and W. J. Moore, 1972. Computer Simulation Model of Dynamic Bio-physio-chemical Processes in Soils. Technical Bull. 196, Dept. of Soils, Water and Engr., Agr. Expt. Sta., University of Arizona, Tucson, October.

Eckhardt, J. R. 1976. Simultaneous Solution for Distribution of Head in a Two Aquifer System. MS Thesis, Dept. of Civil Engr., Colorado State University, Fort Collins, Colorado, 65 pp.

Einstein, H. A. 1950. The Bed Load Function for Sediment Transportation in Open Channels. Tech. Bull. 1026, USDA.

Ekern, P. C. 1953. Problems of Raindrop Impact Erosion. Agr. Engr. Vol. 34, No. 1, pp. 23-25.

Ellison, W. D. 1946. Soil Detachment and Transportation. Soil Conservation, Vol. 11, No. 8, p. 179.

Feth, J. H., S. M. Rogers, and C. E. Roberson. 1964. Chemical Composition of Snow in the Northern Sierra Nevada and Other Areas. Water Supply Paper 1535J, U. S. Geological Survey.

Foster, G. R. and L. D. Meyer. 1972. Mathematical Simulation of Upland Erosion Using Fundamental Erosion Mechanics. Paper presented at Sediment Yield Workshop, USDA Agr. Res. Serv., Oxford, Miss., November 28-30.

Grim, E. C. and R. D. Hill. 1974. Environmental Protection in Surface Mining of Coal. National Environmental Research Center, Office of Research and Development, USEPA, Cincinnati, Ohio.

Grissinger, E. H. 1972. Laboratory Studies of the Erodibility of Cohesive Soils. Paper presented at the Mississippi Water Resources Conference, Water Resour. Res. Inst., State College, Miss.

Hem, John D. 1970. Study and Interpretation of the Chemical Characteristics of Natural Water. Water Supply Paper 1473, U. S. Geological Survey.

Hergert, G. W. 1971. Methods for Soil Characterization. CSU Soil Testing Laboratory, Colorado State University, Fort Collins, Colorado.

Irons, W. V., C. H. Hembree, and G. L. Oakland. 1965. Water Resources of the Upper Colorado River Basin. Prof. Paper 441, U. S. Geological Survey.

Laursen, E. M. 1958. The Total Sediment Load of Streams. Proc. Am. Soc. Civil Engrs., Vol. 84, No. HY 1.

Laws, J. O. and D. A. Parsons. 1943. Relation of Raindrop Size to Intensity. Trans. Am. Geophys. Union, Vol. 24, pp. 452-460.

Li, R. M. 1974. Mathematical Modeling of Response from Small Watershed. PhD Thesis, Dept. of Civil Engr., Colorado State University, Fort Collins, Colorado, 212 pp.

Li, R. M., D. B. Simons, and M. A. Stevens. 1975. Nonlinear Kinematic Wave Approximation for Water Routing. Water Res. Res., Vol. 11, No. 2, pp. 245-252, April.

Lighthill, F. R. S. and G. B. Whitman. 1955. On Kinematic Waves, 1. Flood Movement in Long Rivers. Proc. Roy. Soc. London, A. 229, pp. 281-316.

McWhorter, D. B., R. K. Skogerboe and G. V. Skogerboe. 1975. Water Quality Control in Mine Spoils, Upper Colorado River Basin. Pub. 670, Environmental Protection Technology Series, EPA.

Meyer, L. D., G. R. Foster, and M. J. M. Romkens. 1972. Source of Soil Eroded by Water From Upland Areas. Paper presented at the Interagency Sediment Yield Conference, USDA Sedimentation Laboratory, Oxford, Miss., November 28-30.

Meyer, L. D. and W. H. Wischmeier. 1969. Mathematical Simulation of the Process of Soil Erosion by Water. Trans. Am. Soc. Agr. Engrs., Vol. 12, pp. 754-758,762.

Moldenhauer, W. C. and J. C. Koswara. 1968. Effect of Initial Clod Size on Characteristics of Splash and Wash Erosion. Soil Sci. Soc. Am. Proc., Vol. 32, No. 6, pp. 875-879.

Mutchler, C. K. and R. A. Young. 1972. Soil Detachment by Raindrops. Paper presented at the Sediment Yield Workshop, USDA Agr. Res. Serv., Oxford, Miss., November 28-30.

Negev, M. 1967. A Sediment Model on a Digital Computer. Tech. Report 76, Dept. of Civil Engr., Stanford University, Stanford, Calif., 109 pp.

Onstad, C. A., C. L. Larson, L. H. Hermsmeier, and R. A. Young. 1967. A Method for Computing Soil Movement Throughout a Field. Trans. Am. Soc. Agr. Engrs., Vol. 10, No. 6, pp. 742-745.

Onstad, C. A. and W. C. Moldenhauer. 1975. Watershed Soil Detachment and Transportation Factors. J. Env. Qual., Vol. 4, No. 1, pp. 29-33.

Pinder, G. F. and J. F. Jones. 1969. Determination of the Ground Water Component of Peak Discharge From the Chemistry of Total Runoff. Water Res. Res., Vol. 5, No. 2, pp. 438-445.

Ponce, S. L. and R. H. Hawkins. 1976. Prediction of Salt Pickup by Overland Flow in the Upper Colorado River Basin. Paper given at the Hydrology Symposium of the AGU, December 8.

Richards, L. A. 1931. Capillary Conduction of Liquids Through Porous Mediums. Physics, Vol. 1, No. 5, November, p. 318-333.

Richards, L. A. 1954. Diagonsis and Improvement of Saline and Alkali Soils. Handbook 60, U. S. Dept. Agriculture, 160 pp.

Richtmyer, R. D. 1957. Difference Methods for Initial Value Problems. Interscience Publ.

Schmehl, W. R. and B. D. McCaslin. 1969. Some Properties of Spent Oil-Shale Significant to Plant Growth. Research Report to Colony Development Company, Denver, Colorado, p. 11.

Shen, H. W. and R. M. Li. 1973. Rainfall Effect on Sheet Flow Over Smooth Surface. J. Hyd. Div., ASCE, Vol. 99, No. HY 5, pp. 771-792, May.

Simons, D. B. and R. M. Li. 1976. Procedure for Estimating Model Parameters of a Mathematical Model. CER75-76DBS-RML22, 47 pp., April.

Simons, D. B., R. M. Li, and M. A. Stevens. 1975. Development of Models for Predicting Water and Sediment Routing and Yield from Storms on Small Watersheds. CER74-75DBS-RML-MAS24, 130 pp., August.

Skelly and Loy, Engineers-Consultants. 1975. Economic Engineering Analysis of U. S. Surface Coal Mines and Effective Land Reclamation. Contract Report S0241049, Bureau of Mines, Dept. of Interior, Washington, D. C.

Skogerboe, G. V., R. S. Bennett, and W. R. Walker. 1973. Selection and Installation of Cutthroat Flumes for Measuring Irrigation and Drainage Water. Colo. State Expt. Sta., Fort Collins, Tech. Bull. 120.

Su, C. and R. H. Brooks. 1975. Soil Hydraulic Properties From Infiltration Tests. In: Proc., Watershed Management Symposium, Irr. and Drainage Div., ASCA, Logan, Utah, August 11-13, pp. 516-542.

U. S. Department of Interior. 1970. Environmental Protection Agency Methods for Chemical Analysis of Waters and Wastes.

U. S. Public Health Service. 1962. Drinking Water Standards. USPHS Publ. 956.

U. S. Waterways Experiment Station. 1935. Studies of River Bed Materials and Their Movement, with Special Reference to the Lower Mississippi River. USWES, Vicksburg, Paper 17.

Visocky, A. P. 1970. Estimating the Ground Water Component to Storm Runoff by the Electrical Conductivity Method. Ground Water, Vol. 8, No. 2, pp. 5-10.

Wadleigh, C. H., H. G. Gauch, and M. Kolisch. 1951. Mineral Composition of Orchard Grass Grown on Pachappa Loam Salinized with Various Salts. Soil Science, 72:275-282.

Wentz, D. A. 1974. Effect of Mine Drainage on the Quality of Streams in Colorado, 1971072. Colorado Water Res. Circ. No. 21, Colorado Water Conservation Board.

Wischmeier, W. H. 1973. Conservation Tillage of Control Water Erosion. Paper presented at the National Conservation Tillage Conference, Des Moines, Iowa, March 28-30.

Wischmeier, W. H. and D. D. Smith. 1958. Rainfall Energy and its Relationship to Soil Loss. Trans. Am. Geophys. Union, Vol. 39, No. 2, pp. 285-291.

Young, R. A. and C. K. Mutchler. 1969. Effect of Slope Shape on Erosion and Runoff. Trans. Am. Soc. Agr. Engrs., Vol. 12, No. 2, pp. 231-233,239.

Young, R. A. and J. L. Wiersma. 1973. The Role of Rainfall Impact in Soil Detachment and Transport. Water Res. Res., Vol. 9, No. 6, pp. 1629-1636, December.

BIBLIOGRAPHY

Ahmad, M. U. 1973. Coal Mining and its Effect on Water Quality. Ground Water Pollution. In: Proceedings of Ground Water Pollution Conference, Underwater Research Institute.

Averitt, Paul. 1969. Coal Resources of the United States. Bull. 1275, U. S. Geological Survey.

Collier, C. R., R. J. Pickering, and J. J. Musser. 1970. Influence of Strip Mining on the Hydrological Environment of Parts of Beaver Creek Basin, Kentucky. Prof. Paper 427-C, U. S. Geological Survey.

Einstein, H. A. 1942. Formula for the Transporation of Bed Load. Trans. Am. Soc. Civil Engrs., Vol. 107.

Emmett, W. W. 1975. The Channels and Waters of the Upper Salmon River Area, Idaho. Prof. Paper 870-A, U. S. Geological Survey, 116 pp.

Emrich, G. H. 1969. Effects of Mine Drainage on Ground Water. Ground Water, Vol. 7, No. 3, pp. 27-33.

Federal Water Pollution Control Administration. 1969. Stream Pollution by Coal Mine Drainage in Appalachia. U. S. Department of Interior.

Gordon, Suzanne. 1973. Black Mesa, Angel of Death. John Day Co., New York.

Guy, H. P. 1969. Laboratory Theory and Methods for Sediment Analysis. In: Techniques of Water-Resources Investigations of the U. S. Geological Survey, Book 5, Chapter C1, U. S. Government Printing Office, Washington, D. C.

Kilinc, M. Y. 1972. Mechanics of Soil Erosion from Overland Flow Generated by Simulated Rainfall. PhD Thesis, Dept. of Civil Engr., Colorado State University, Fort Collins, Colorado 183 pp.

Landis, E. R. 1964. Coal. In: Mineral and Water Resources of Colorado (Report for use of U. S. Senate Committee on Interior and Insular Affairs, 88th Congress, 2nd Session), U. S. Government Printing Office, pp. 35-45.

U. S. Department of Interior. 1974. Colorado River Water Quality Improvement Program, Bureau of Reclamation Status Report, January.

Valantine, Vernon E. 1974. Impacts of Colorado River Salinity. J. Irr. and Drainage Div., ASCE, Dec., pp. 495-510.

Walker, R. E. and F. F. Hartner. 1966. Forms of Sulfur in U. S. Coals. U. S. Bureau of Mines Information Circular 8301.

Wymore, Ivan F. 1974a. Water Requirements for Stabilization of Spent Shale. PhD Thesis, Colorado State University, pp. 31-61.

Wymore, Ivan F. 1974b. Estimated Average Annual Water Balance for Piceance and Yellow Creek Watersheds. Environmental Resources Center, Technical Report Series, No. 2, Colorado State University, Fort Collins, Colorado.